INTEGRATED LIFE CYCLE FRAMEWORK FOR EVALUATING THE SUSTAINABILTIY OF EMERGING DROP-IN REPLACEMENT BIOFUELS

by

George G. Zaimes

B.S. Physics, University of Pittsburgh, 2012

Submitted to the Graduate Faculty of

Swanson School of Engineering in partial fulfillment

of the requirements for the degree of

Doctor of Philosophy

University of Pittsburgh

2016

UNIVERSITY OF PITTSBURGH

SWANSON SCHOOL OF ENGINEERING

This dissertation was presented

by

George G. Zaimes

It was defended on

June 22, 2016

and approved by

Melissa Bilec, PhD, Associate Professor, Civil and Environmental Engineering Department

Amy E. Landis, PhD, Professor, Glenn Department of Civil Engineering, Clemson University

Radisav Vidic, PhD, Professor, Civil and Environmental Engineering Department

Dissertation Director: Vikas Khanna, PhD, Assistant Professor, Civil and Environmental Engineering Department

INTEGRATED LIFE CYCLE FRAMEWORK FOR EVAULATING THE SUSTAINABILTIY OF EMERGING DROP-IN REPLACEMENT BIOFUELS

George G. Zaimes, PhD

University of Pittsburgh, 2016

Mounting concerns over energy independence and security, oil supply volatility and price, and anthropogenic-derived climate destabilization are driving the strategic development of low-carbon biofuels. Recently, second generation biofuels—fuels derived from non-food biofeedstocks including: perennial grasses, short rotation woody crops (SRWCs), and microalgae have gained significant interest from scientific and political actors due to their potential for reduced life cycle greenhouse gas (GHG) emissions relative to baseline petroleum fuels, and fungibility with existing transportation infrastructure and vehicles fleets. However, the environmental sustainability of these second generation biofuels and their capacity to meet U.S. regulatory biofuel mandates remains uncertain, and a point of scientific inquiry.

This work investigates the sustainability of emerging second-generation drop-in replacement hydrocarbon biofuels, utilizing sustainability metrics and methodologies derived from multiple disciplines including life cycle assessment, industrial ecology, statistics, thermodynamics, and process modeling. This novel interdisciplinary life cycle framework is applied to study the environmental sustainability of several distinct emerging drop-in replacement biofuel platforms including: (1) cultivation of microalgae in open raceways ponds and hydro-processing of algal-oil to renewable diesel, (2) fast pyrolysis of perennial grasses and hydro-upgrading of bio-oil to green gasoline, and (3) multistage torrefaction of SRWCs and catalytic upgrading to hydrocarbon biofuels. Traditional process-based Life Cycle Assessment

(LCA) and hybrid Ecologically-based Life Cycle Assessment (EcoLCA) models are developed to assess the degradation of ecological good and services, environmental impacts, and resource intensity of producing drop-in replacement biofuels. Rigorous process modeling and statistical analysis is performed to quantify key sustainability metrics including energy return on investment and life cycle GHG emissions for producing hydrocarbon biofuels under different combinations of biofeedstocks, fuel upgrading pathways, and coproduct scenarios, and to determine if renewable fuel(s) meet compliance with life cycle GHG emissions reductions thresholds set by U.S. federal regulatory programs. This interdisciplinary approach captures broader environmental externalities and unintended consequences of biofuel production that are outside the purview of traditional process design, and allows for holistic understanding of the potential tradeoffs, challenges, and broad-based impacts of emerging biofuels prior to their widespread commercialization—information that is pivotal for guiding the sustainable development of the nascent biofuels industry.

TABLE OF CONTENTS

NOMENCLATURE ..... **XXIII**

ACKNOWLEDGEMENTS ..... **XXVIII**

1.0 INTRODUCTION **1**

1.1.1 Policy Divers for Commercial Biofuel Production **2**

1.1.2 Comparison of Potential Feedstocks, Conversion Pathways, and Fuels **4**

1.2 LIFE CYCLE ASSESSMENT **9**

1.3 SUSTAINABILITY AND THE CHEMICAL INDUSTRY **10**

1.4 BIBLIOMETRIC ANALYSIS OF BIOFUEL LITERATURE **11**

1.5 RESEARCH OBJECTIVES **16**

1.6 ORGANIZATION OF DISSERTATION **17**

1.7 INTELLECTUAL MERIT AND BROADER IMPACTS **19**

2.0 MICROALGAL BIOMASS PRODUCTION PATHWAYS: EVALUATION OF LIFE CYCLE ENVIRONMENTAL IMPACTS **24**

2.1 CHAPTER SUMMARY **25**

2.2 INTRODUCTION **26**

2.3 METHODOLOGY AND SUSTAINABILITY METRICS **28**

2.3.1 LCA Model Overview **28**

2.3.2 Sustainability Metrics **29**

2.3.3 Algal Composition and Growth Rates **30**

2.4 PRODUCTION CHAIN OVERVIEW AND DATA SOURCES **31**

2.4.1 Production Chain Overview 31
2.4.2 Water Demands 33
2.5 RESULTS AND DISCUSSION 35
2.5.1 EROI and Life Cycle GHG Analysis 35
2.5.2 Direct Water Demands 37
2.5.3 Detailed Analysis: Phoenix, Arizona 38
2.5.4 Pure CO_2 vs. Flue Gas 39
2.5.5 Chamber Filter Press vs. Centrifugation 40
2.5.6 Natural Gas Based Drying vs. Waste Heat Drying 40
2.5.7 Sensitivity Analysis 41
2.6 CONCLUSIONS 42
3.0 ASSESSING THE CRITICAL ROLE OF ECOLOGICAL GOODS AND SERVICES IN MICROALGAL BIOFUEL LIFE CYCLES 47
3.1 CHAPTER SUMMARY 48
3.2 BACKGROUND 49
3.2.1 Ecological Goods and Services 50
3.3 HYBRID ECOLOGICALLY-BASED LCA METHODOLOGY 52
3.3.1 Process Model 54
3.3.2 EcoLCA Model 57
3.3.3 Thermodynamic Return on Investment 58
3.3.4 Thermodynamic Sustainability Metrics 62
3.4 RESULTS AND DISCUSSION 64
3.5 CONCLUSIONS 72
4.0 BIOFUELS VIA FAST PYROLYSIS OF PERENNIAL GRASSES: A LIFE CYCLE EVALUATION OF ENERGY CONSUMPTION AND GREENHOUSE GAS EMISSIONS 74

4.1 CHAPTER SUMMARY 75
4.2 BACKGROUND 76
4.3 PROCESS DESCRIPTION, DATA, AND METHODS 79
4.3.1 Agricultural Model 80
4.3.2 Fast Pyrolysis and Fuel Upgrading Model 82
4.3.3 Methodology 87
4.3.4 Sustainability Metrics 89
4.4 RESULTS AND DISCUSSION 90
4.4.1 Life Cycle Energy Analysis 90
4.4.2 Life Cycle GHG Analysis 93
4.4.3 EROI vs Life Cycle GHG Emissions 96
4.5 CONCLUSIONS 99
5.0 MULTISTAGE TORREFACTION OF BIOMASS AND IN-SITU CATALYTIC UPGRADING TO HYDROCARBON BIOFUELS: ANALYSIS OF LIFE CYCLE ENERGY USE AND GREENHOUSE GAS EMISSIONS 101
5.1 CHAPTER SUMMARY 102
5.2 BACKGROUND 103
5.3 MODEL DEVELOPMENT 107
5.3.1 Cultivation and Harvesting of SRWCs 108
5.3.2 Short Term Storage 111
5.3.3 Direct Land-use Change 112
5.3.4 Multistage Torrefaction/Pyrolysis and Catalytic Upgrading 113
5.3.5 Upgrading Chemistries 114
5.3.6 Detailed Process Description 116
5.3.7 Coproduct Scenarios 119
5.3.8 Life Cycle Assessment 120

5.3.8.1 Stochastic Simulation for Uncertainty Quantification 121
5.3.8.2 Coproduct Handling in LCA 122
5.3.9 Environmental Sustainability Metrics 122
5.3.9.1 Life Cycle GHG Emissions 122
5.3.9.1 Energy Return On Investment 123
5.4 RESULTS AND DISCUSSION 123
5.4.1 Product Distribution 123
5.4.2 Process Scale Metrics 125
5.4.3 Energy Return On Investment 126
5.4.4 Life Cycle Energy Analysis 128
5.4.5 Life Cycle GHG Emissions 129
5.4.6 Life Cycle GHG Analysis 131
5.4.7 Sensitivity Analysis 133
5.5 CONCLUSIONS 136
6.0 DESIGN OF SUSTAINABLE BIOFUEL PROCESSES AND SUPPLY CHAINS: CHALLENGES AND OPPORTUNITIES 138
6.1 CHAPTER SUMMARY 139
6.2 DESIGNING SUSTAINABLE BIOFUEL SUPPLY CHAINS 140
6.2.1 Field Trials and Laboratory Scale Experiments 143
6.2.2 Process Scale 143
6.2.3 Modeling the Supply Chain and Life Cycle 144
6.2.3.1 Process LCA 145
6.2.3.2 EIO-LCA and Hybrid LCA 147
6.2.4 Ecosystems Scale 150
6.2.5 Accounting for Multiple Objectives and Scales in Designing Sustainable Biofuel Supply Chains 153

6.2.5.1 Uncertainty and Variability 155
7.0 CONCLUSIONS AND FUTURE WORK 157
APPENDIX A 165
APPENDIX B 202
APPENDIX C 225
APPENDIX D 260
BIBLIOGRAPHY 311

LIST OF TABLES

Table 1. Themes and topics for author supplied and indexed keywords 13

Table 2. Research Questions (RQ) and corresponding thesis chapter in which they are addressed 23

Table 3. $EROI_{Fossil,}$ Net Life Cycle GHG Emissions, and Direct WD's for Examined Biomass Production Pathways and Locations 36

Table 4. Critical Parameters for Sensitivity Analysis 42

Table 5. ECEC based Sustainability Performance Metrics 63

Table 6. Comparison of ECEC thermodynamic performance metrics for microalgal renewable diesel and petroleum diesel 69

Table 7. Critical Process Design and Performance Metrics for Fast Pyrolysis HDO and Multistage Systems 126

Table 8. Electricity Generation Mix 166

Table 9. Average Solar Insolation (kWh / m^2-day) 167

Table 10. Average Monthly PAR (MJ / m^2-day) 168

Table 11. Average Pressure (kPa) 169

Table 12. Average Monthly Wind Speed (m/s) 170

Table 13. Average Monthly Temperatures (^OC) 171

Table 14. Relative Humidity (%) 172

Table 15. Monthly Average Evaporative Losses (mm / day) 174

Table 16. Average Monthly Rainfall (mm / day) 175

Table 17. Net Water Accumulation (mm / day) 176

Table 18. Fractioned Microalgal Biomass Composition 177

Table 19. Gross Microalgal Biomass Composition 177

Table 20. Photosynthetic Efficiency Terms 179

Table 21. Efficiency Terms 180

Table 22. Monthly Microalgal areal growth rates (g / m^2-day) 181

Table 23. LCI normalized per kg of biomass for MEA/CF/NGD pathways 189

Table 24. LCI normalized per kg of biomass for MEA/CF/WHD pathways 189

Table 25. LCI normalized per kg of biomass for DI/CF/NGD pathways 189

Table 26. LCI normalized per kg of biomass for DI/CF/WHD pathways 190

Table 27. LCI normalized per kg of biomass for MEA/CFP/NGD pathways 190

Table 28. LCI normalized per kg of biomass for MEA/CFP/WHD pathways 190

Table 29. LCI normalized per kg of biomass for DI/CFP/NGD pathways 191

Table 30. LCI normalized per kg of biomass for DI/CFP/WHD pathways 191

Table 31. Allocated $EROI_{Fossil}$, net life cycle GHG emissions, and direct WDs for examined production pathways 194

Table 32. Allocated $EROI_{Fossil}$, net life cycle GHG emissions, and direct WDs for examined production pathways 195

Table 33. Low Nitrogen Scenario: Allocated $EROI_{Fossil}$, net life cycle GHG emissions, and direct WDs for examined production pathways 197

Table 34. Low Nitrogen Scenario: Unallocated $EROI_{Fossil}$, net life cycle GHG emissions, and direct WDs for examined production pathways 198

Table 35. Alternate Production Scenario: Allocated $EROI_{Fossil}$, net life cycle GHG emissions, and direct WDs for examined production pathways 200

Table 36. Alternate Production Scenario: Unallocated $EROI_{Fossil}$, net life cycle GHG emissions, and direct WDs for examined production pathways 201

Table 37. Baseline and Improved Biofuel Production Pathways 202

Table 38. Process inventory for microalgal renewable diesel production 205

Table 39. Price data for economic inputs/outputs for microalgal renewable diesel production. 206

Table 40. Inflation Ratio 207

Table 41. 2002 Price data for economic inputs/outputs for microalgal renewable diesel production 208

Table 42. Economic Activity ($ 2002) for industrial sectors used in microalgal renewable diesel production 208

Table 43. Energy, ICEC, and ECEC to price ($2002) ratios for industrial sectors 209

Table 44. Energy, ICEC, and ECEC consumption obtained via EcoLCA 210

Table 45. Direct Ecological Goods and Services in Microalgal RD production 211

Table 46. Energy, Exergy, and Transformity of Direct EGS 211

Table 47. Energy, Exergy, and Emergy of direct EGS in microalgal RD production 211

Table 48. Energy, Exergy, and Transformity of Fuel and Energy Products 212

Table 49. 2002 U.S. Electricity generation mix and electricity generation conversion efficiencies 212

Table 50. Amount of each primary resource (J) required to produce 1 J of electricity based on the 2002 avg. electricity mix 213

Table 51. Direct primary energy resources consumed in the production of 1 J of electricity based on the 2002 U.S. electricity mix. Consumption is reported in terms of energy, exergy, and emergy. 213

Table 52. Use phase of energy/fuel products in miroalgal RD production 214

Table 53. Fuel Properties of Renewable Diesel and Biodiesel 215

Table 54. Thermodynamic return on investment for microalgal renewable diesel production based on energy, ICEC, and ECEC 216

Table 55. ECEC sustainability and Performance Metrics for Microalgal Renewable Diesel 218

Table 56. Process Inventory for Petroleum Diesel 220

Table 57. Economic activity ($2002) for industrial sectors used in petroleum diesel production 221

Table 58. Direct Ecological Goods and Services as well as process fuel/energy consumption in petroleum diesel production 221

Table 59. Results from EcoLCA and process analysis for the production of 4.0 x 10^6 gallons of petroleum diesel 222

Table 60. Thermodynamic Return on Investment and ECEC based performance metrics for Petroleum Diesel production..... 222

Table 61. Thermodynamic Return on Investment and ECEC based performance metrics for Microalgal Biodiesel..... 223

Table 62. Key Parameters in the calculation of EROI and Life Cycle GHG Emissions..... 227

Table 63. Reported Growth Rates for Miscanthus Feedstock 229

Table 64. Fertilizer Application Rates for Miscanthus..... 229

Table 65. Fertilizer Application Rates for Switchgrass..... 230

Table 66. Norms for diesel use in crop production (Dn) compared to values found in the referenced literature or monitored on private farms; data is representative of common farming practices..... 231

Table 67. Machinery used during cultivation of perennial grasses and resulting diesel fuel consumption..... 232

Table 68. Diesel consumption for harvesting equipment 232

Table 69. Field Efficiency (%)..... 232

Table 70. Direct Nitrogen Volatilization Rates (%) 233

Table 71. Indirect Nitrogen Volatilization Rates (%)..... 234

Table 72. Switchgrass and Miscanthus Composition 235

Table 73. Proximate and Ultimate Analysis of Switchgrass and Miscanthus biofeedstocks 235

Table 74. Composition of Switchgrass and Miscanthus Biochars produced via fast pyrolysis at 500°C 235

Table 75. Key Parameters for Grinding and Chopping of Switchgrass and Miscanthus Feedstock 236

Table 76. Primary pyrolysis product distribution resulting from hemicellulose pyrolysis at 500°C 236

Table 77. Primary pyrolysis product distribution resulting from cellulose pyrolysis at 500°C . 237

Table 78. Primary pyrolysis product distribution resulting from lignin pyrolysis at 500°C 238

Table 79. Product distribution resulting from fast pyrolysis at 500°C in increasing carbon number 239

Table 80. Hydrodeoxygenation of Bio-Oil 241

Table 81. Coke formation in hydro-upgrading of bio-oil products 242

Table 82. Overview of HDO catalysts and operating conditions 243

Table 83. Estimation of Biomass and Biochar/Ash Higher Heating Value 244

Table 84. Switchgrass: Fast Pyrolysis Production Distribution 244

Table 85. Switchgrass: HDO derived Renewable Fuels 244

Table 86. Switchgrass: HDO Renewable Fuel Product Distribution 245

Table 87. Switchgrass: Fast Pyrolysis System Flows 245

Table 88. Switchgrass: Overview Product Distribution 246

Table 89. Switchgrass: Energy Products 246

Table 90. Switchgrass: Pretreatment, Conversion, and Upgrading Utilities 246

Table 91. Miscanthus: Fast Pyrolysis Production Distribution 246

Table 92. Miscanthus: HDO derived Renewable Fuels 247

Table 93. Miscanthus: HDO Renewable Fuel Product Distribution 247

Table 94. Miscanthus: Fast Pyrolysis System Flows 248

Table 95. Miscanthus: Overview Product Distribution 248

Table 96. Miscanthus: Energy Products 249

Table 97. Miscanthus: Pretreatment, Conversion, and Upgrading Utilities 249

Table 98. Life Cycle Data Sources 250

Table 99. Overview of key parameters and probability distributions 252

Table 100. Hypothesis Testing: 1 Sample Sign Test is performed to determine if median value is statistically different from key sustainability performance thresholds. 253

Table 101. EROI and life cycle GHG emission for fast pyrolysis gasoline derived from switchgrass and miscanthus 254

Table 102. EROI and life cycle GHG emission for select 1st generation, 2nd generation, and petroleum fuels 255

Table 103. Soil Organic Carbon Stocks (SOC_{REF}) for Mineral Soils (Tonnes C ha^{-1} in 0-30 cm depth) 261

Table 104. Carbon Stock Factors For Grassland Management 261

Table 105. Above-ground and Below-ground Grassland Biomass Stocks 262

Table 106. Reported Growth Rates for Woody Biomass* 264

Table 107. Process Inventory for SRWC System 1 265

Table 108. Process Inventory for SRWC System 2 265

Table 109. Process Inventory for SRWC System 3 265

Table 110. Process Inventory for SRWC System 4 266

Table 111. Process Inventory for SRWC System 5 266

Table 112. Process Inventory for SRWC System 6 267

Table 113. Process Inventory for SRWC System 7 267

Table 114. Process Inventory for SRWC System 8 268

Table 115. Process Inventory for SRWC System 9 268

Table 116. Process Inventory for SRWC System 10 269

Table 117. Process Inventory for SRWC System 11 269

Table 118. Process Inventory for SRWC System 12 269

Table 119. Process Inventory for SRWC System 13 270

Table 120. Process Inventory for SRWC System 14 270

Table 121. Process Inventory for SRWC System 15 270

Table 122. Process Inventory for Cuttings Production 271

Table 123. Harvest Efficiency 271

Table 124. Direct Nitrogen Volatilization Rates (%) 272

Table 125. Indirect Nitrogen Volatilization Rates (%) 273

Table 126. Dry Matter Loss (%) as a function of Storage Time..... 274

Table 127. Parameters used in calculating emissions factors for storage off-gases 275

Table 128. Storage Off-Gas Concentration and Concentration Rate..... 275

Table 129. Literature Survey: Transportation of Biomass from Farm to Refinery 276

Table 130. Triangular Distribution: Transportation of Biomass from Farm to Refinery 276

Table 131. Key Parameters for Grinding and Chopping of Woody Biomass 277

Table 132. Model compound aggregation scheme based on identified compounds in the Pyroprobe chromatogram..... 279

Table 133. Model compound characterization of bio-oil produced via three-stage torrefaction and Pyrolysis system, and base-case single stage pyrolysis system. Results are presented as the mass fraction of total input ash-free dry biomass, and are based on volatile organic product yields obtained from the Pyroprobe..... 282

Table 134. Model compound characterization of bio-oil produced via three-stage torrefaction and Pyrolysis system, and base-case single stage pyrolysis system. Results are presented as the mass fraction of total input ash-free dry biomass, and are constructed based on coupling the volatile composition obtained from the Pyroprobe with analysis of NCG and water formation obtained from the micropyrolysis unit. 284

Table 135. Model compound characterization of bio-oil derived via a three-stage torrefaction and pyrolysis design, and comparison with single-stage fast pyrolysis (500 ^{O}C). Results are presented as the mass fraction (%) of total input ash-free dry biomass. 285

Table 136. Biomass and Biochar Composition..... 286

Table 137. Estimation of Biochar/Ash Higher Heating Value for Woody Biomass 287

Table 138. Ketonization Products..... 288

Table 139. Alkylation Products 289

Table 140. Hydrodeoygenation - Products 295

Table 141. Biorefinery Utilities..... 302

Table 142. Transportation of Biofuel Diesel from Refinery to Bulk Terminal 303

Table 143. Transportation of Biofuel from Bulk Terminal to Refueling Station 303

Table 144. Life cycle data sources..... 304

Table 145. Overview of key parameters and probability distributions..... 306

Table 146. Key parameters in the calculation of EROI and Life Cycle GHG Emissions..... 308

Table 147. Median EROI (MJ-Fuel/MJ-Primary Fossil Energy) for base-case Fast Pyrolysis HDO and Multistage Systems..... 309

Table 148. Median Life cycle GHG emissions (gCO_2e/MJ-Fuel) for base-case Fast Pyrolysis HDO and Multistage Systems..... 309

LIST OF FIGURES

Figure 1. Volumetric Biofuel Requirement set by Energy Independence and Security Act[11] ... 3

Figure 2. Overview of Biofeedstocks, Conversion Platforms, and Biofuels 4

Figure 3. Bibliometric network analysis of biofuel research articles published between 2000 to present. 14

Figure 4. Microalgal Biomass Production Chain and Examined Production Pathways. The microalgal concentration is reported on a weight/weight (w/w) basis for each stage in the process chain. 32

Figure 5. Life Cycle Energy Analysis for Phoenix, Arizona 38

Figure 6. Life Cycle GHG Analysis for Phoenix, Arizona 39

Figure 7. Sensitivity Analysis for Phoenix, Arizona 41

Figure 8. Hybrid EcoLCA Framework for Microalgal Biofuel Production 53

Figure 9. Microalgae-to-Fuel Process Chain 55

Figure 10. Thermodynamic Return on Investment Metrics. Error Bars for Baseline and Improved Scenarios Represent the Results for High (40% L / 50% C / 10% P) and Low Lipid (10% L / 20% C / 70% P) biomass composition. Error bars for Petroleum Diesel represent the range obtained via market and mass based allocation. 65

Figure 11. Fractional Contribution of total Energy, ICEC, ECEC by Ecological Resource for Microalgal Renewable Diesel and Petroleum Diesel 68

Figure 12. Ecological Resource Intensity of Producing Microalgal RD Relative to Petroleum Diesel. Resource Intensity ratios were developed via taking the ratio of ECEC of resources required to produce one MJ of RD to the ECEC required to produce on MJ of PD. Coproduct(s) were accounted for via system boundary expansion, i.e. ECEC from coproduct(s) were subtracted from total resources use. Some

columns are not shown due on the logarithmic graph due to negative value(s) that occur as a result of displacement. 71

Figure 13. Simplified Block Diagram: Fast Pyrolysis biofuel production chain. Scenario 1 (*Bioenergy Pathway*): Biochar is sent to a Combined Heat and Power unit for conversion to heat and electricity. Scenario 2 (*Soil Amendment Pathway*): Biochar is sent to a local farm to be applied as a soil amendment. 80

Figure 14. Energy Return On Investment for producing renewable fuels from miscanthus and switchgrass biofeedstock. Results are shown for displacement and energy-based allocation, as well as soil amendment and bioenergy coproduct scenarios. Median values (i.e., 50th percentile) are shown; error bars represent the 10th and 90th percentile. 91

Figure 15. Life cycle fossil energy analysis. Average primary energy impacts for process inputs and coproduct are normalized to 1 MJ of renewable fuel. Results for displacement methodology are provided. Net primary energy use represents the difference between primary fossil energy consumed in the supply chain and coproduct primary fossil energy credit. 93

Figure 16. Life cycle GHG emissions for producing renewable fuel from miscanthus and switchgrass biofeedsock. Results are shown for displacement and energy-based allocation, as well as soil amendment and bioenergy coproduct scenarios. Median values (i.e., 50th percentile) are shown; error bars represent the 10th and 90th percentile. 94

Figure 17. Life cycle carbon footprint analysis. Greenhouse gas emissions for material and energy inputs as well as coproduct credits are normalized to 1 MJ of renewable fuel. Results for displacement are provided. Net life cycle GHG emissions represent the difference between GHGs (direct and indirect) emitted throughout the life cycle and coproduct GHG credit. 96

Figure 18. EROI vs Life cycle GHG emissions for select 1st generation and 2nd generation biofuels. Values for EROI and GHG emissions of fast pyrolysis fuels using the displacement method are shown. Values for 1st & 2nd generation bioethanol were obtained from Wang et al. 2012 (ref [261]) and do not consider direct or indirect LUC impacts. Values for petroleum diesel were adapted based on data obtained from the 2014 GREET model (ref [269]). 98

Figure 19. Biomass-to-Fuel Process Chain..... 108

Figure 20. Detailed Process Flow Diagram. Several coproduct scenarios for the biochar is evaluated including: (1) combustion for heat and power and (2) land application as a soil amendment. 110

Figure 21. Multistage Torrefaction & Pyrolysis Systems. Several multistage design cases, consisting of different catalytic upgrading systems, are independently considered for tailored upgrading of bio-oil to hydrocarbon fuels 116

Figure 22. Model compound characterization of bio-oil derived via a three-stage torrefaction and pyrolysis design, and comparison with single-stage fast pyrolysis (500 ^{O}C). Mass flows of thermally fractionated bio-oil streams are reported based on a plant capacity of 2000 dry metric tonnes of biomass per day..... 118

Figure 23. Product Carbon Distribution Comparison: Multistage System(s) vs. Fast Pyrolysis HDO..... 124

Figure 24. Energy Return on Investment for hydrocarbon biofuels produced via multistage systems and single stage fast pyrolysis and HDO. Results for *displacement* and *energy-based allocation* are presented for both *Soil Amendment* and *Heat and Power* biochar coproduct scenarios. Median values (i.e. 50th percentile) are presented; error bars represent the 10th and 90th percentile. 127

Figure 25. Life cycle fossil energy analysis. Average primary energy impacts for process inputs and coproduct are normalized to 1 MJ of hydrocarbon biofuel. Well-to-wheel results are shown utilizing the *displacement method*. Negative values indicate primary fossil energy credit from coproducts, while positive values indicate primary fossil energy consumption for material and energy inputs. Net primary energy consumption represents the difference between primary fossil energy consumed in the supply chain and coproduct primary fossil energy credit. The error bars represent the 10th and 90th percentile..... 129

Figure 26. Life cycle GHG Emissions for hydrocarbon biofuels produced via multistage systems and single stage fast pyrolysis and HDO. Results for displacement and energy-based allocation are presented for both Soil Amendment and Heat and Power biochar coproduct scenarios. Median values (i.e. 50th percentile) are presented; error bars represent the 10th and 90th percentile. Life cycle GHG emissions for Petroleum Diesel is taken to be ~91.94 gCO2e/MJ-Diesel [337]..... 131

Figure 27. Life Cycle GHG Analysis. Average life cycle GHG impacts for process inputs and coproduct are normalized to 1 MJ of hydrocarbon biofuel. Well-to-wheel results are shown utilizing the displacement method. Negative values indicate GHG credit from coproducts, while positive values indicate life cycle GHG emissions for material and energy inputs. WTW life cycle GHG emissions represent the difference between life cycle GHG emissions throughout the supply chain and coproduct GHG credit..... 133

Figure 28. Sensitivity Analysis: Multistage Stage Design Case #3. Tornado Plots for Median EROI and Life Cycle GHG Emissions using Energy-based Allocation..... 135

Figure 29. Modular Multi-scale, Multi-objective, Biofuel Supply Chain Optimization Framework 142

Figure 30. Direct Water Demands for CFP pathways for Phoenix, Arizona..... 192

Figure 31. Thermodynamic Return on Investment (ROI) for the microalgal RD production under several coproduct scenarios for the de-oiled algal biomass..... 217

Figure 32. Ecological resource intensity of producing microalgal RD relative to petroleum diesel. Resource intensity ratios were developed via taking the ratio of ECEC of resources required to produce one mega-joule (MJ) of RD to the ECEC required to produce one MJ of PD. Coproduct(s) were accounted for via system boundary expansion, i.e. ECEC from coproduct(s) were subtracted from total resource use. Some columns are not shown on the logarithmic graph due to negative value(s) that occur as a result of displacement. 219

Figure 33. Ecological resource intensity of producing microalgal BD relative to petroleum diesel. Resource intensity ratios were developed via taking the ratio of ECEC of resources required to produce one mega-joule (MJ) of BD to the ECEC required to produce one MJ of PD. Coproduct(s) were accounted for via system boundary expansion, i.e. ECEC from coproduct(s) were subtracted from total resource use. Some columns are not shown on the logarithmic graph due to negative value(s) that occur as a result of displacement. 224

Figure 34. Tornado Plots: Median EROI, Switchgrass..... 257

Figure 35. Tornado Plots: Median Life Cycle GHG Emissions, Switchgrass..... 258

Figure 36. Tornado Plots: Median EROI, Miscanthus 258

Figure 37. Tornado Plots: Median Life Cycle GHG Emissions, Miscanthus..... 259

Figure 38. Pyroprobe Schematic..... 278

Figure 39. Quartz Sample Tube Diagram..... 278

Figure 40. Bench Scale Reactor System..... 283

Figure 41. Multistage System 1: Hot and Cold Composite Curves..... 300

Figure 42. Multistage System 2: Hot and Cold Composite Curves..... 300

Figure 43. Multistage System 3: Hot and Cold Composite Curves..... 301

Figure 44. Single Stage Fast Pyrolysis and HDO: Hot and Cold Composite Curves..... 301

Figure 45. Sensitivity Analysis: Multistage Design Case #3. Tornado Plots for median EROI and Life Cycle GHG emissions using displacement method. 310

NOMENCLATURE

AD	Anaerobic Digestion
AF	Animal Feed, Auto-flocculation
Atm	Atmosphere
BE	Bioenergy
BD	Biodiesel
C	Carbon, Carbohydrates
C-C	Carbon-Carbon
CCF	Cross Flow Filtration
CED	Cumulative Energy Demand
CF	Centrifugation, Carbon-Footprint
CFP	Chamber Filter Press
CO_2	Carbon Dioxide
CO_2e	Carbon Dioxide Equivalent
CHP	Combine Heat and Power
DI	Direct Injection
Disp.	Displacement Method
dLUC	Direct Land Use Change
DMT	Dry Metric Tones
DOE	Department of Energy
ECEC	Ecological Cumulative Exergy Consumption

EcoLCA	Ecologically-based Life Cycle Assessment
eGRID	Emissions and Generation Resource Integrated Database
EGS	Ecological Goods and Services
EISA	Energy Independence and Security Act
ELR	Environmental Loading Ratio
EmROI	Emergy Return On Investment
EPA	Environmental Protection Agency
EROI	Energy Return On Investment
$EROI_{fossil}$	Fossil Energy Return on Investment
EU	European Union
ExROI	Exergy Return On Investment
EYR	ECEC Yield Ratio
GIS	Geographic Information Systems
GHG	Greenhouse Gas
GREET	Greenhouse Gases, Regulated Emissions, & Energy Use in Transportation Model
GWP	Global Warming Potential
Ha	Hectare
HAC	High Activity Clay
HDO	Hydrodeoxygenation
HDPE	High Density Polyethylene
HHV	Higher Heating Value
ICEC	Industrial Cumulative Exergy Consumption
InVEST	Integration Valuation of Ecosystems Services and Tradeoffs

I-O	Input-Output
IPCC	Intergovernmental Panel on Climate Change
L	Lipids
LCA	Life Cycle Assessment
LCFS	Low Carbon Fuel Standard
LCI	Life Cycle Inventory
LCIA	Life Cycle Impact Assessment
LHV	Lower Heating Value
LUC	Land Use Change
MC	Moisture Content
MEA	Monoethanolamine, Millennium Ecosystems Assessment
MJ	Mega-Joule
MSC	*Miscanthus*
NCG	Non-Condensable Gas
NG	Natural Gas
NGD	Natural Gas Drying
NOAA	National Oceanic and Atmospheric Organization
NSRD	National Solar Radiation Database
NWS	National Weather Service
OAT	One-at-a-Time
ORP	Open Raceway Ponds
P	Protein
PAR	Photosynthetically Active Radiation

PBR	Photobioreactor
PD	Petroleum Diesel
PDF	Probability Distribution Function
R	Renewability Index
RD	Renewable Diesel
RDB	Residual De-oiled Biomass
RED	Renewable Energy Directive
RFS2	Renewable Fuels Standard
ROI	Return On Investment
RVP	Reid Vapor Pressure
SI	Supporting Information
SA	Soil Amendment
Sej	Solar Equivalent Joues
SOC	Soil Organic Carbon
SRWC	Short Rotation Woody Crop
SWG	Switchgrass
TES	Techno-ecological Synergy
TRACI	Tool for the Reduction and Assessment of Chemicals and Other Environmental Impacts
US	United States
USDA	United States Department of Agriculture
USLCI	United States Life Cycle Inventory
w/w	Weight per Weight

WD	Water Demands
WHD	Waste Heat Drying
WHSV	Weight Hourly Space Velocity
WWPT	Waste Water Treatment Plant
YLR	Yield to Loading Ratio

ACKNOWLEDGEMENTS

Foremost, I would like to thank my parents and family, from the bottom of my heart, for their unconditional love and encouragement—this journey would not have been possible without their unwavering support. I will be forever grateful to my thesis advisor Vikas Khanna—his guidance, wisdom, mentorship and motivation have profoundly influenced my life, and have taught me to overcome many personal challenges and to realize my dreams and aspirations.

I would like to thank my dissertation committee members for their guidance and mentorship; they have been a constant source of inspiration and encouragement throughout my time at University of Pittsburgh, and whom I greatly admire. I am deeply grateful to Melissa Bilec, Amy E. Landis, and Radisav Vidic for their technical and scientific advice, and insightful discussions.

I would like to acknowledge the Mascaro Center for Sustainable Innovation (MCSI), the U.S. Department of Agriculture (USDA), U.S. Department of Energy (DOE), and National Science Foundation (NSF) for graciously providing financial support for this research. Additionally, I want to thank my peers, friends, and staff/faculty in the Civil and Environmental Engineering Department at the University of Pittsburgh for all of the fond memories and everlasting friendships. A special thanks to Jennifer who taught me to never bale on my dreams and that life is equal parts work and horsing around. I dedicate this work to my parents, Paul Zaimes and Leigh Zaimes, my grandmother, Agnes Zaimes, and my cat, Abby.

1.0 INTRODUCTION

The dawn of the industrial era brought the rapid expansion and development of the petroleum, natural gas, and coal industries. Over the past century exploitation and consumption of fossil resources has led to widespread gains in economic development and quality of life, but have come at the expense of environmental damages and degradation of ecological goods and services (EGS) and may impair the ability of the planet to sustain future generations [1]. Further, increased global consumption of limited fossil resources—driven by exponential population growth and rapid economic expansion, has been identified as the principle contributor to rising atmospheric concentrations of greenhouse-gases and related anthropogenic-induced climate destabilization [2], and has led to heightened market instability and supply risk for fossil and petroleum resources. In totality, mounting concerns over energy independence and security, oil supply volatility and price, and global climate change are driving nation states worldwide to adopt environmentally sustainable renewable energy systems and technologies.

Global climate change is regarded as the foremost environmental problem of the 21st century. A growing body of evidence suggests that increasing concentrations of greenhouse gases, brought on by human activities, are causing harmful and long-term global climate change [3]. Direct impacts of global climate change include heightened frequency of extreme weather events as well as rising average global temperature and sea levels, while potential higher-order effects include ecosystems destruction, species extinction, irreversible loss of biodiversity,

heightened frequency of food- and water-borne illness, widespread loss of life, civil conflict, food security, environmentally induced mass migration, heightened risk and volatility in global economic markets, and loss of economic capital [4-6].

Displacing traditional transportation fuels and modes of energy production with low-carbon biofuels—fuels derived via organic matter from plant biomass and/or industrial waste with a reduced carbon footprint relative to baseline petroleum fuels, are a promising option for mitigating and curtailing potential catastrophic climate destabilization [7-9]. Accordingly, biofuels have gained widespread attention at academic, industrial, regulatory and political levels, and to some degree among the general public. Scientists have focused on identifying the most promising biofuel feedstocks and are investigating various biochemical and thermochemical conversion pathways to transform these feedstocks into useful fuel products. Research, development, and the subsequent commercial deployment of biofuels have the potential to create new jobs and provide extensive economic benefits.

1.1.1 Policy Divers for Commercial Biofuel Production

Policy makers are playing a larger role in the development and implementation of biofuels by establishing regulatory policies and mandates for renewable fuels. In 2007, the United States passed the Energy Independence and Security Act (EISA) [10], which mandates annual domestic volumetric production targets for renewable transportation fuels. EISA mandates that 36 billion gallons of biofuels be blended into the U.S. transportation fuel mix by the year 2022, and stipulates that a fraction of the total volumetric renewable fuel requirement be derived from conventional, cellulosic, biomass-based diesel, and advanced biofuels, see Figure 1.

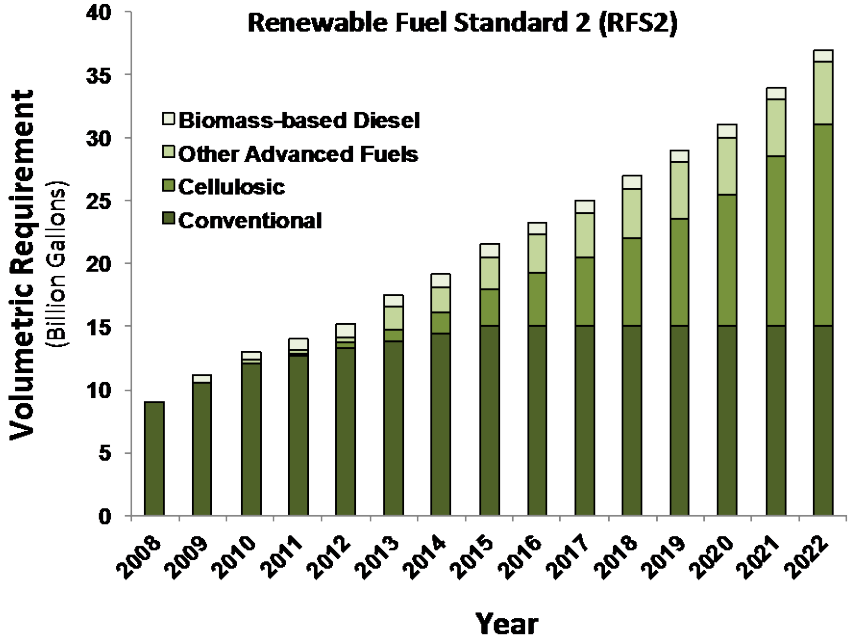

Figure 1. Volumetric Biofuel Requirement set by Energy Independence and Security Act[11]

Further, EISA mandates that biofuels have specific reduction in life cycle greenhouse gas (GHG) emissions relative to petroleum fuels. EISA defines cellulosic biofuel as any renewable fuel derived from cellulose, hemicellulose, or lignin, which reduces greenhouse gas (GHG) emissions by 60% as compared to baseline petroleum fuels. Biomass-based diesel is defined as a renewable transportation fuel, transportation fuel additive, heating oil, or jet fuel that meets the definition of either biodiesel or non-ester renewable diesel, that reduces GHG emissions by 50% or more; while advanced biofuels are defined as any renewable fuel, other than ethanol derived from corn, which reduces GHG emissions by a minimum of 50%.

Similarly, in 2009 the European Union (EU) passed the renewable energy directive (RED) [12], which requires that the EU obtain 20% of its total energy consumption from renewable sources, and derive 10% of energy consumption within the transportation sector from

renewable resources by 2020. Furthermore, the EU imposed a 5% cap on the amount of food crop-derived biofuels used to meet the EU's 2020 goal, in an effort to mitigate the potential social and economic impacts of competition between crops for food vs. fuel. The RED sets minimum life cycle GHG emission reductions targets of 35% relative to baseline petroleum fuels for the year 2010, increasing to 50% in 2017 and 60% in 2018.

1.1.2 Comparison of Potential Feedstocks, Conversion Pathways, and Fuels

Commercial biofuel production is a multifaceted issue, identifying and assessing potential biofuel feedstocks remain an arduous process as the use of some biofeedstocks raise complex ethical questions and may have unintended economic and environmental ramifications. A myriad of different biofuel conversion pathways and associated coproducts are possible, see Figure 2. In addition, the mode of biofuel production can influence the quality of the resultant fuel as well as its related economic, environmental, and energetic viability.

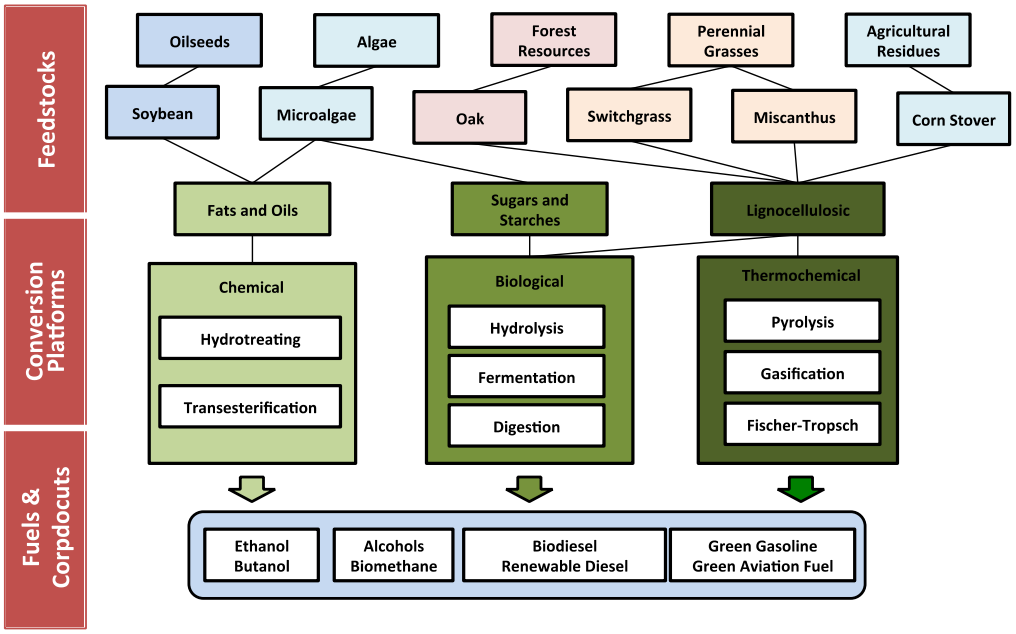

Figure 2. Overview of Biofeedstocks, Conversion Platforms, and Biofuels

First generation biofuels, also known as conventional biofuels, are fuels produced from arable crops and are derived via sugar, starch, animal fats, and plant or vegetable oils. First generation biofuels are typically produced from the fermentation of grains and crops with a high sugar or starch content, such as corn, sugarcane, sugar beets, wheat, or barley to produce bioethanol, or by transesterification of oils extracted from crops such as soybean, rapeseed, canola, mustard seed, palm, coconut, and sunflower to create biodiesel. In recent years, political and scientific actors have raised concerns that the use of first generation biofuels may result in environmental degradation [13], including potential loss of biodiversity, adverse impacts on water resources, soil erosion and depletion, accelerated deforestation, and land-use impacts [14, 15]. Existing research has also reported that direct and indirect land use change effects may possibly negate the carbon dioxide reduction potential of first generation biofuels resulting in overall higher life-cycle GHG emissions relative to baseline petroleum fuels [16, 17]. Additionally, thermodynamic and energy analyses have shown mixed results concerning the energetic viability of some first generation biofuels [13, 18, 19]. Furthermore, without government subsidies and grants, biofuels are currently not cost competitive with more established transportation fuels [13], making them an expensive option for mitigating GHGs. Additionally, there is growing concern that displacing farmland and food crops for biofuel production may lead to inflation of global food prices [20, 21], as many biofuel cultivars—including corn, soybean, and sugarcane—are primarily used for animal feed and/or human consumption. In addition, first generation biofuels require changes in the existing transportation infrastructure such as modifications to vehicle engines and fuel pipelines. For these reasons researchers have investigated producing 2nd generation biofuels—liquid transportation fuels

from nonfood-biofeedstocks, that have the potential to be fungible with existing vehicle fleets and infrastructure.

2nd generation biofuels have gained significant interest from national organizations such as the United States (US) Department Of Energy (DOE) due to their potential for lower greenhouse gas emissions relative to baseline petroleum fuels and potential to act as drop-in replacements for traditional fossil fuels. Common non-food biofeedstocks include lignocellulosic biomass, microalgae, industrial wastes, and oil-seeds. Lignocellulosic feedstocks include agricultural residues such as corn stover and forest residues; energy crops such as switchgrass, miscanthus, and poplar; and industrial/municipal solid wastes. Additionally, several non-food lipid sources including algae and jatropha are being considered for biofuel production. The 'Billion Ton Study' jointly conducted by the US Department of Energy (DOE) and the US Department of Agriculture (USDA) provides a detailed quantification of available biomass in the US for producing fuels and biobased products, and estimates that up to 1.6 billion tons of dry biomass can be produced annually in the contiguous U.S. for meeting growing energy demands without displacing critical food, fiber, or feed crops [22]. These findings are compelling as they suggest that the U.S. has the capacity to support a large-scale domestic biofuels and bioproducts market.

Several comprehensive reviews of the possible catalytic, biochemical, and thermochemical conversion pathways for the production of biofuels from biomass feedstocks are available [15, 23-25]. Traditionally, fats and oils derived from oilseed crops are converted to biodiesel via transesterification involving chemical reactions with an alcohol, such as methanol. However, biodiesel has certain undesirable properties such as poor cold flow properties, high cloud point, and roughly 10% lower energy density when compared with petroleum derived

diesel fuel. Alternatively, oils and fats can be catalytically hydrotreated and converted to renewable diesel—a renewable hydrocarbon fuel that is fungible with traditional petroleum fuels. Lignocellulosic feedstocks, such as woody biomass and agricultural residues, require acid treatments to decompose cellulose and hemicellulose into sugars, which can be subsequently reformed into hydrocarbons via microbial agents [26]. Dumesic and coworkers have unraveled an entire set of catalytic reactions that convert biomass into hydrocarbon biofuels in the gasoline, diesel, and jet range [24, 27-33]. Bond and coworkers successfully reported a strategy for converting γ–valerolactone, an intermediate produced from biomass carbohydrates, into liquid alkenes targeted for transportation fuels [34]. Their proposed integrated catalytic system eliminates the need for an external source of hydrogen.

Thermochemical conversion via pyrolysis or gasification has gained widespread attention as commercial platforms for biofuel production. Pyrolysis involves thermochemical decomposition of organic matter at 400-600 ^{o}C in absence of oxygen and produces oxygenated bio-oil as well as biochar and non-condensable gases as coproducts [35-39]. Pyrolysis oil can be catalytically converted to high-octane hydrocarbon biofuels in the gasoline and diesel range [36, 40, 41], while several uses for the bio-char including (1) a soil amendment or (2) combustion to produce electricity are actively being investigated [42-48]. Agrawal and Singh presented a conceptual design of a hydrogen bio-oil process using fast pyrolysis and hydrodeoxygenation for producing liquid transportation fuels that require only modest quantities of supplementary H2 [49]. Another promising thermochemical pathway is gasification, in which biomass is converted to synthesis gas (syngas) - a mixture containing CO, H2, CH4, N2 and CO2 by heating the input feed to high temperatures (>700 OC) and reacting with air, oxygen, and/or steam. Syngas can then be converted into liquid fuels by well-known reactions such as Fischer-Tropsch synthesis or

synthesizing methanol and subsequent conversion to gasoline. Dauenhauer and coworkers at the University of Minnesota have combined the biomass gasification, tar cleanup, and water-gas shift into a single reactor [50].

Recently, microalgae have been touted as a promising feedstock for conversion to liquid transportation fuel due to their unique ability to utilize carbon dioxide from industrial flue gas [51], high photosynthetic efficiency [52], and ability to be grown on marginal or otherwise non-arable land [53]. Algae derived biofuels do not directly displace or put market pressure on food crops, as do the production of biofuels derived from corn, soybean, or sugarcane. Furthermore, algae can be grown using different growth media including wastewater as well as brackish/saline water; the use of which has the capacity to substantially reduce the nutrient and water-footprint of microalgal fuels relative to traditional terrestrial biofeedstocks [54]. Algae can be grown in a semi-continuous to continuous manner, and thus do not require perennial harvesting such as other leading forms of biomass including poplar or perennial grasses. Brennan and Owende presented a comprehensive overview of the different technologies for microalgae cultivation, harvesting, conversion technologies, and the potential useful products including biofuels [55].

The biofuel research landscape is rapidly evolving in regards to process multiplicity, complexity, and scope. Understanding and assessing the far-reaching impacts and implications of emerging biofuels—before their widespread implementation—is critical for assuring the long-term sustainability of these biofuels systems. Failure to address the potential risks and impacts associated with biofuels may have long-standing environmental consequences, and may jeopardize the successful adoption and commercial viability of these bioresources. Sustainable commercialization of biofuel production will require simultaneously addressing multiple technical and environmental challenges that occur throughout the supply chain. Comprehensive

analysis from a systems perspective that considers the full range of impacts can address these concerns.

1.2 LIFE CYCLE ASSESSMENT

Life cycle assessment (LCA) is a technique used to quantify the environmental impacts of a product or service, and has emerged as the prevalent methodological framework for evaluating the environmental impacts of biofuel and bioenergy systems [56]. LCA considers impacts throughout all stages of the fuel life cycle-from raw materials extraction, to fuel conversion, and final use. LCA allows for a comprehensive understanding of the environmental impacts that occur at each stage of the production chain, enabling one to identify processes responsible for highest environmental burden and thus target these areas for process improvement. Furthermore, LCA can be used to quantify the anticipated impacts of a product or service prior to its widespread adoption, thus identifying and avoiding potential environmental pollutants, wastes, and environmental damages before they become embedded within the supply chain. Furthermore, LCA can used to compare the environmental performance between two products with the same functionality and thus can be used to inform environmentally conscious decision-making.

1.3 SUSTAINABILITY AND THE CHEMICAL INDUSTRY

Chemical technologies and the chemical industry provide a range of useful and valuable products for human welfare such as personal care products, health products, agrochemicals, and transportation fuels. However, the production of these products is accompanied by generation of vast quantities of wastes and a range of harmful emissions to air, water, and soil. There is increasing realization that resource consumption and anthropogenic-derived impacts can have long-standing consequences on global ecological systems, and place strain on the natural biogeochemical cycles that support human life. Published findings from the millennium ecosystem assessment (MEA)—an international collaboration designed to assess the impact and widespread consequences of environmental change for human and ecological well-being, indicate that in the second half of the 20th century anthropogenic-derived resource degradation and overconsumption of natural capital have changed ecosystems more rapidly and extensively than in any comparable period in human history [1]. Rockstrom and colleagues assessed that the Earth has transgressed planetary boundaries for climate change, biodiversity, nitrogen cycle balance and is fast approaching the limit of safe operating space for global freshwater use, land use change, ocean acidification and global phosphorous cycle balance [6, 57-59].

Traditional methods of chemical process design have primarily relied on finding the economic optimum subject to physical constraints, namely satisfying the heat and material balances under thermodynamic limitations. However, concerns over the depleting fossil energy sources, mounting regulatory compliance and the resulting push towards environmentally conscious process design are forcing designers to consider reduced environmental impact as one of the product design objectives. Business leaders have begun to realize that such a shift towards

more sustainable design practices can not only minimize the environmental impact of industrial activity but is also crucial for long term success and sustainability of their enterprises.

The emerging field of sustainability science and engineering is developing tools to recognize, quantify, and reconcile resource limitations; human needs, and optimize global and human benefit. The concept of sustainability is multifaceted; encompassing the entirety of the human enterprise, interfacing with environmental, social, political, and economic issues, and as such is highly interdisciplinary. The outstanding challenge facing the chemical industry is the incorporation of environmental and sustainability objectives along with traditional design objectives in the development of emerging chemical processes. The rapid development of biofuels as a potentially sustainable and cleaner replacement for conventional fuels represents a unique challenge for chemical industry that requires simultaneous consideration of environmental and ecological externalities that are outside the purview of traditional process design.

1.4 BIBLIOMETRIC ANALYSIS OF BIOFUEL LITERATURE

Understanding the full range of potential environmental, social, and economic impacts of biofuel production prior to its widespread commercialization and use is pivotal for avoiding unintended consequences and for guiding the sustainable development of the biofuels industry. Moreover, holistic assessment of the widespread direct and indirect effects/impacts of biofuel production requires integrating data and information across multiple research domains and rigorous analysis of peer-reviewed literature. As such, collaboration and synthesis across multiple disciplines is necessary for environmentally conscious decision-making. However, the degree to which

interdisciplinary research is occurring between biofuel research domains is often not well-understood or studied, such information is critical for determining research gaps, fragmentation between research domains, and for guiding the future trajectory of research in biofuels.

Accordingly, a bibliometric analysis is performed to (1) identify active topical areas of research in the biofuel literature and (2) quantify the relative strength of connection between various biofuels research domains via analyzing the occurrence and co-occurrence frequency of author supplied and indexed keywords from over 20,000 biofuels articles published from 2000 to present. The resulting analysis provides useful insights regarding the strength of connection and coupling between various research domains in the biofuel literature, as well as potential research gaps, i.e. research areas that may require further synthesis and integration. Keywords for over 20,700 articles were obtained using the search-term 'Biofuels' from the SCOPUS database [60]. In absence of author-supplied keywords, indexed keywords were used. This approach was leveraged over using *both* author-supplied keywords and indexed keywords, so as to avoid potential double counting. Keywords were aggregated into 36 topic areas related to 7 broad themes; see Table 1. The analysis expands on the method of identifying and aggregating keywords provided in Ridley et al. [61]. The analytic framework and bibliometric algorithm established in Van Eck and Waltman was used to detect the number of co-occurrences of select keywords [62]. The co-occurrence data is mapped via network software (ORA) [63], to visualize the dynamic interactions between select biofuel research domains. The strength of the linkage between research topics (nodes) indicates its relative co-occurrence and is proportional to the line width, while the size of the node indicates its relative occurrence.

Table 1. Themes and topics for author supplied and indexed keywords

Theme	**Topic**	**Example Keywords**
Environmental & Human Wellbeing	Food Security	Food Supply, Food Crop
	Human Health	Mortality, Asthma
	GHGs	Greenhouse Gases, Carbon Dioxide
	Air Quality (Non-GHGs)	Particulate Matter, Volatile Organic Compounds
	Soil Resources	Soil Organic Carbon, Soil Fertility
	Land Use Change	Indirect Land Use Change, Direct Land Use Change
	Water Resources	Groundwater, Water Footprint
	Biodiversity	Wildlife, Biodiversity
	Life Cycle Assessment	Life Cycle Analysis, Life Cycle Assessment
	Ecosystem Services	Ecosystem Services, Ecosystems
Economy		
	Cost of Production	Technoeconomic analysis, Infrastructure
	Market Forces	Supply and Demand, Cost Competitiveness
	Policy	RFS2, EISA, LCFS
	Trade	Import, Export, Tariff
Production Distribution, Technology, & Infrastructure		
	Feedstock Production and Agronomics	Biomass Production, Agronomics
	Feedstock Logistics	Pretreatment, Biomass transportation
	Fuel Distribution and Infrastructure	Pipeline, Fuel Storage
Biofuels		
	Aviation Fuel	Aviation Fuel, Jet Fuel
	Biodiesel	Biodiesel, Biodiesel Blend
	Ethanol	Ethanol, Lignocellulosic Ethanol
	Hydrocarbon Biofuel	Drop in replacement biofuel, Renewable Diesel
	Butanol	Butanol, Biobutanol
	Biogas	Biogas, Biomethane
Conversion Platforms		
	Pyrolysis	Fast Pyrolysis, Pyrolysis oil
	Gasification	Gasification, BTL
	Transesterification	Esterification, FAME
	Hydrolysis	Hydrolysis, Fermentation
	Anaerobic Digestion	Anaerobic Digestion, -
Feedstocks		
	Woody Biomass	Willow, Poplar
	Perennial Grasses	Switchgrass, Miscanthus
	Oil Seeds	Jatropha, Soybean, Rapeseed
	Algae	Microaglae, Macroalgae
	Agricultural Residue	Sugarcane Bagasse, Corn Stover, Forest Residue
	Industrial & Municipal Waste	Waste Cooking Oil, Vegetable Oil
	Grains & Sugar Crops	Corn, Wheat, Rye
Thermodynamics		
	N/A	Exergy, Emergy

Adapted from Ridley et al. [61]

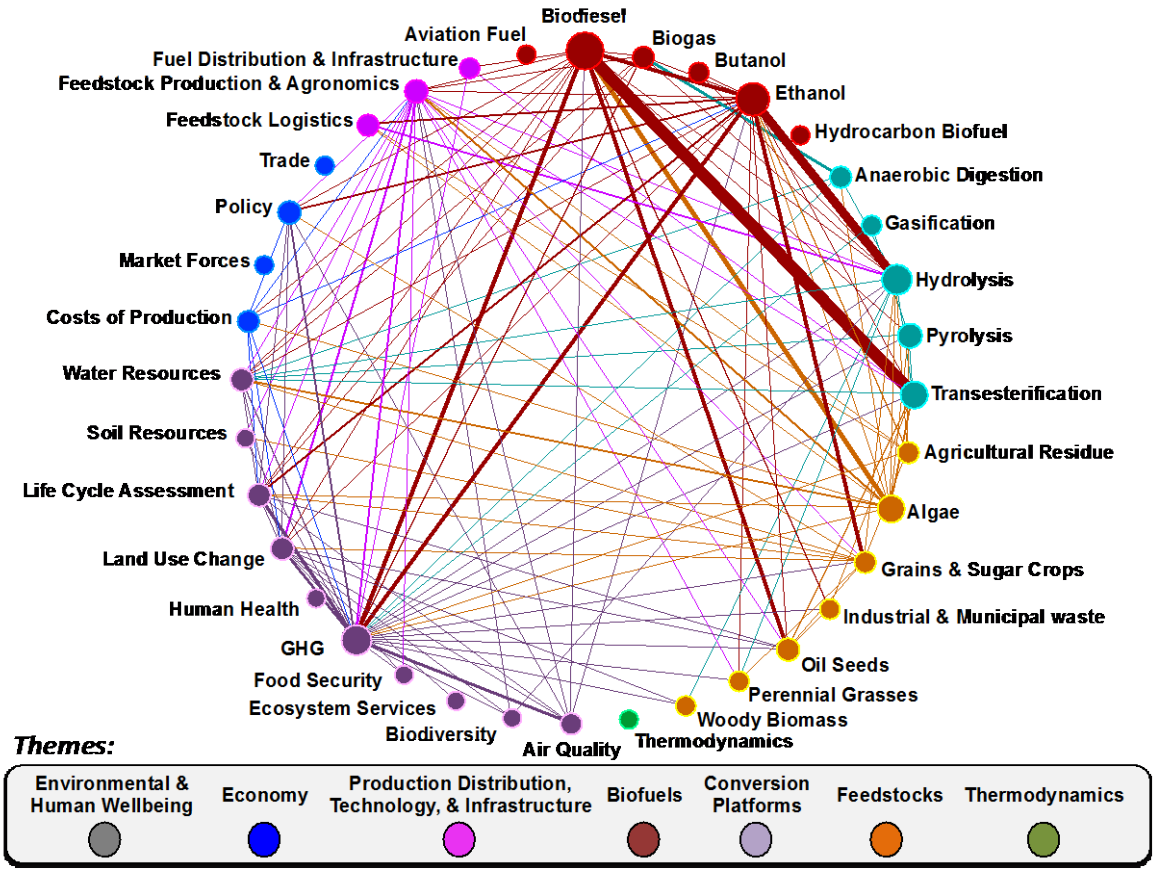

A co-occurrence cutoff value of 80 was chosen to identify significant connections between nodes in the network. As such some nodes appear to have no connections

Figure 3. Bibliometric network analysis of biofuel research articles published between 2000 to present.

Figure 3 presents a co-occurrence network graph, illustrating the connectivity between various research topics in the biofuels literature. Figure 3 reveals that greenhouse gases, biodiesel, ethanol, transesterification, and hydrolysis had the highest frequency of co-occurrence in the literature, while market forces, trade, biodiversity, ecosystems goods and services (EGS), thermodynamics, aviation fuel, and hydrocarbon biofuels were not well represented. Nodes with no connections represent research fields that lack significant collaborations with other research areas in the biofuel literature, and may be emerging or nascent topics. Figure 3 reveals that substantial research has been invested in evaluating GHG emissions related to biofuel

production, while little effort has been made to evaluate impacts on soil resources, human health, food security, biodiversity, and ecological goods and services. While GHG emissions represent an important sustainability aspect for biofuel production, other categories must also be considered so that biofuels do not inadvertently shift their impacts to other domains. Furthermore, the lack of research on ecological goods and services, biodiversity, soil resources, and water resources is alarming, as prior research has suggested that the adoption of first generation biofuels have resulted in higher rates of deforestation and soil erosion, loss of biodiversity, and increased stress on water resources [13, 64]. Hydrocarbon biofuels as well as aviation fuels were found to have marginal to no connectivity with other research domains, as these biofuels represent emerging topics and have only recently received widespread scientific inquiry. As such, further collaborative research is needed in all aspects of these emerging fuel platforms. The network diagram shows sparse scientific coverage on the market forces and/or trade aspects of biofuel production, despite consistent growth in the international trade of biomass/biofuels over the past decade. Failure to consider the broader trade and market implications of biofuel production could have significant global economic and social repercussions. This is particularly important for developing countries that are increasing biofuel exports to meet international policy mandated volumetric biofuel production and renewable energy targets, as developing nations are often highly sensitive to the potential adverse impacts of biofuel production including accelerated destruction of natural ecosystems, agricultural runoff and soil erosion, increased food insecurity and malnutrition, and global climate change.

The bibliographic analysis reveals that, to-date, little scientific converges exists regarding the potential life cycle impacts, ecological implications, and/or thermodynamics of emerging hydrocarbon biofuels derived via catalytic and/or thermochemical conversion of 2nd generation

biofeedstocks: microalgae, woody crops, or perennial grasses. Accordingly, a quantitative interdisciplinary framework is urgently needed to assess any potential dynamic interactions, feedbacks, trade-offs, and mitigate any unintended consequences that may result from the large-scale commercialization of emerging drop-in replacement hydrocarbon biofuel platforms.

1.5 RESEARCH OBJECTIVES

The principle objectives of this dissertation are to evaluate the sustainability of emerging infrastructure compatible drop-in replacement biofuels, utilizing sustainability metrics and methodologies derived from multiple disciplines including industrial ecology, systems engineering, statistics, and thermodynamics. This interdisciplinary approach allows for a broader understanding of the potential environmental implications and tradeoffs of commercial scale biofuel production, and thus allows for a holistic evaluation of the sustainability of emerging bioenergy pathways. *Specific objectives include*:

1. Construct detailed process models for the production of second-generation biofeedstocks: miscanthus, switchgrass, woody biomass, and microalgae and downstream processing to liquid transportation fuels.
2. Simulate conversion and upgrading of 2nd generation and advanced biofeedstocks via Aspen Plus and first principles of engineering to develop detailed process level material, energy, and product flows.
3. Conduct process-based Life Cycle Assessment (LCA) and hybrid Ecologically-based Life Cycle Assessment (EcoLCA) to assess the degradation and depletion of ecological

good and services, environmental impacts, and resource intensity of producing drop-in-replacement biofuels; and identify areas for process improvement in the biomass-to-fuel supply chain.

4. Perform rigorous statistical analysis to determine bounds for key sustainability metrics including energy return on investment (EROI) and life cycle GHG emissions for drop-in-replacement biofuels under different combinations of biofeedstocks, coproduct options, and fuel upgrading pathways. Determine if renewable fuel(s) meet compliance with life-cycle GHG emissions reductions thresholds set by U.S. federal regulatory programs.

1.6 ORGANIZATION OF DISSERTATION

The dissertation is organized as follows:

Chapter 2 presents the primary fossil energy consumption, life cycle greenhouse gas (GHG) emissions, and direct Water Demands (WD) for producing dried algal biomass through the cultivation of microalgae in Open Raceway Ponds (ORP) for 21 geographic locations in the contiguous United States (U.S.). For each location, comprehensive life cycle assessment (LCA) is performed for multiple microalgal biomass production pathways, consisting of a combination of cultivation and harvesting scenarios. The objective of this work is to compare the environmental profile of different technological routes and geographic locations for producing dried algal biomass to be used for as a feedstock for downstream conversion to liquid transportation fuel(s).

Chapter 3 develops a hybrid ecologically based life cycle assessment model to determine the large-scale ecological impacts of microaglal biofuel production under several coproducts

scenarios for the de-oiled algal biomass, and benchmark the results against existing petroleum fuels. This work utilizes rigorous hierarchical thermodynamic-derived performance metrics developed based on concepts of exergy and emergy to provide unique insights into the sustainability of emerging microalgal biofuel systems.

Chapter 4 presents a life cycle assessment of liquid transportation fuels derived via fast pyrolysis of perennial grasses and hydroprocessing of bio-oil, with specific focus on quantifying the life cycle GHG emissions and primary fossil energy consumption under different coproduct scenarios for the produced biochar.

Chapter 5 presents a prospective wheel-to-wheel life cycle assessment of a novel multistage torrefaction/pyrolysis and in-situ catalytic upgrading fuel platform for converting short rotation woody crops to hydrocarbon biofuels. Several critical key process design metrics and sustainability indicators including: process hydrogen consumption, liquid carbon yield, energy return on investment, and life cycle GHG emissions are utilized to compare the environmental and process performance across different design cases.

Chapter 6 discusses key research opportunities and challenges in the design of emerging biofuel supply chains, provides a high-level overview of the current ‘state of the art’ in environmental sustainability assessment of biofuel production, and proposes a novel modular multiscale and multiobjective optimization framework for the sustainable design of emerging biofuel supply chains.

Chapter 7 summarizes the main conclusions of this dissertation and provides directions for future work.

Additional information including detailed calculations and tabulated datasets are provided in the Appendices. Supporting information (S.I.) for Chapter 2 is provided in Appendix A, S.I. for Chapter 3 is provided in Appendix B, and so on and so forth for subsequent chapters.

1.7 INTELLECTUAL MERIT AND BROADER IMPACTS

The results of this dissertation aid in identifying which biofeedstocks and biofuels are best suited for U.S. domestic production; and provide a broader understanding of the environmental tradeoffs between various fuel platforms. Further, the findings of this research identify potential opportunities for process improvements throughout the biofuel supply chain and provide insights regarding the vulnerability of emerging bioenergy systems to the depletion of specific resources, environmental hazards, and the degradation of natural goods and services. This broad-based approach allows for a comprehensive examination of the potential tradeoffs, challenges, and widespread impacts of emerging biofuels—information that is pivotal for guiding the sustainable development of the biofuels industry. Additionally, this research advances the concepts and framework of sustainability via the development, utilization, and coupling of rigorous thermodynamic based sustainability metrics, probabilistic-parametric models, and detailed chemical process modeling. The body of this work takes the form of several peer-review articles, book chapters, and peer-reviewed conference proceedings that are at various stages of publication during the final writing herein:

Refereed Journal Articles

1. Zaimes, G. G.; Beck, A. W.; Janupala, R. R.; Resasco, D. E.; Crossley, S. P.; Lobban, L. L.; Khanna, V., Multistage torrefaction and in situ catalytic upgrading to hydrocarbon biofuels: analysis of life cycle energy use and greenhouse gas emissions**.** Resubmission to *Energy and Environmental Science*, November **2016**. (Chapter 5 in Thesis)
2. Montazeri, M.; Zaimes, G. G.; Khanna, V.; Eckelman, M. J., Meta-Analysis of Life Cycle Energy and Greenhouse Gas Emissions for Priority Biobased Chemicals. *ACS Sustainable Chemistry & Engineering* **2016**.
3. Zaimes, G. G.; Vora, N.; Chopra, S. S.; Landis, A. E.; Khanna, V., Design of Sustainable Biofuel Processes and Supply Chains: Challenges and Opportunities. *Processes* **2015,** *3,* (3), 634-663. (Chapter 6 in Thesis)
4. Zaimes, G. G.; Soratana, K.; Harden, C. L.; Landis, A. E.; Khanna, V., Biofuels via Fast Pyrolysis of Perennial Grasses: A Life Cycle Evaluation of Energy Consumption and Greenhouse Gas Emissions. *Environmental Science & Technology* **2015,** *49*, (16), 10007-10018. (Chapter 4 in Thesis)
5. Soratana, K.; Harden, C. L.; Zaimes, G. G.; Rasutis, D.; Antaya, C. L.; Khanna, V.; Landis, A. E., The role of sustainability and life cycle thinking in U.S. biofuels policies. *Energy Policy* **2014,** *75* (0), 316-326.
6. Zaimes, G. G.; Khanna, V., Assessing the critical role of ecological goods and services in microalgal biofuel life cycles. *RSC Advances* **2014,** *4*, (85), 44980-44990. (Chapter 3 in Thesis)

7. Zaimes, G. G.; Khanna, V., The role of allocation and coproducts in environmental evaluation of microalgal biofuels: How important? *Sustainable Energy Technologies and Assessments* **2014,** *7*, (0), 247-256.
8. Zaimes, G. G.; Khanna, V., Environmental sustainability of emerging algal biofuels: A comparative life cycle evaluation of algal biodiesel and renewable diesel. *Environmental Progress & Sustainable Energy* **2013,** *32*, (4), 926-936.
9. Zaimes, G. G.; Khanna, V., Microalgal biomass production pathways: evaluation of life cycle environmental impacts. Biotechnology for Biofuels **2013,** 6, (1), 88. (Chapter 2 in Thesis)

Book Chapters

1. Zaimes, G. G.; Khanna, V., Life cycle sustainability aspects of microalgal biofuels. In *Assessing and Measuring Environmental Impact and Sustainability*, Klemeš, J. J., Ed. Butterworth-Heinemann: Oxford, **2015**; pp 255-276.
2. Zaimes, G. G.; Borkowski, M.; Khanna, V., Life-Cycle Environmental Impacts of Biofuels and Coproducts. In *Biofuel Technologies*, Gupta, V. K.; Tuohy, M. G., Eds. Springer Berlin Heidelberg: **2013**; pp 471-499.

Peer-Reviewed Conference Proceedings

1. Harris, T. M.; Zaimes, G. G.; Khanna, V.; Landis, A. E., Sunflower Cultivation on Coal Mine Refuse Piles in Appalachia for Diesel Biofuel Production from a Life-cycle Perspective. *Procedia Engineering* **2015,** *118*, 869-878.
2. Soratana, K.; Zaimes, G. G.; Harden, C. L.; Rasutis, D.; Antaya, C. L.; Khanna, V.; Landis, A. E., Life cycle thinking in U.S. biofuel policies, American Center for Life

Cycle Assessment (ACLCA) XIV International Conference **2014,** Proceedings of the LCA XIV International Conference: pp 57-62.

3. Borkowski, M. G.; Zaimes, G. G.; Khanna, V., Integrating LCA and thermodynamic analysis for sustainability assessment of algal biofuels: comparison of renewable diesel vs. biodiesel. International Symposium on Sustainable Systems and Technology (ISSST) **2012**, IEEE: pp 1-6.
4. Zaimes, G. G.; Borkowski, M. G.; Khanna, V., Environmental Life Cycle Assessment of Open Pond Microalgae Cultivation. American Center for Life Cycle Assessment (ACLCA) XI International Conference **2011**, Proceedings of the LCA XI International Conference: pp 113-119.

Specific Research Questions (RQ) and the corresponding chapter in which they are addressed are provided in Table 2 below:

Table 2. Research Questions (RQ) and corresponding thesis chapter in which they are addressed

#	Research Question (RQ)	Paper	Chapter
1	How does the direct water footprint, primary fossil energy consumption, and life cycle GHG emission profiles for producing microalgal biomass vary under different combinations of cultivation and harvesting technologies, as well as cultivation sites across the contiguous United States?	Zaimes, G. G.; Khanna, V., Microalgal biomass production pathways: evaluation of life cycle environmental impacts. Biotechnology for Biofuels **2013,** 6, (1), 88.	**CH2**
2	What are the potential large-scale ecological impacts of microalgal biofuel production, how do these results compare with traditional petroleum fuels? What insights can thermodynamic analysis based on exergy and emergy provide regarding the energetic viability and sustainability of emerging microalgal biofuel systems?	Zaimes, G. G.; Khanna, V., Assessing the critical role of ecological goods and services in microalgal biofuel life cycles. *RSC Advances* **2014,** *4*, (85), 44980-44990.	**CH3**
3	What is the carbon footprint and primary energy consumption for producing drop-in replacement transportation fuels via fast pyrolysis of perennial grasses (switchgrass or miscanthus); and subsequent hydroprocessing of bio-oil to transportation fuel? Which unit processes are responsible for the highest environmental burdens in the supply chain, how do the results change for different combinations of allocation schemes and coproduct scenarios? How do these results benchmark against leading other biofuels as well as petrochemical fuels?	Zaimes, G. G.; Soratana, K.; Harden, C. L.; Landis, A. E.; Khanna, V., Biofuels via Fast Pyrolysis of Perennial Grasses: A Life Cycle Evaluation of Energy Consumption and Greenhouse Gas Emissions. *Environmental Science & Technology* **2015,** *49*, (16), 10007-10018.	**CH4**
4	What are the well-to-wheel life cycle energy use and greenhouse gas emissions for producing infrastructure compatible transportation fuels via a novel multistage torrefaction and in-situ catalytic upgrading fuel platform? Do renewable fuel(s) meet compliance with life-cycle GHG emissions reductions thresholds set by U.S. federal regulatory programs, as well as minimum energy return on investment (EROI) criteria under different allocation schemes and coproduct scenarios? Which unit processes are responsible for the highest environmental burdens in the supply chain? Which parameters have the largest impact on the EROI and life cycle GHG emissions profile of renewable fuels?	Zaimes, G. G.; Beck, A. W.; Janupala, R. R.; Resasco, D. E.; Crossley, S. P.; Lobban, L. L.; Khanna, V., Multistage torrefaction and in situ catalytic upgrading to hydrocarbon biofuels: analysis of life cycle energy use and greenhouse gas emissions**.** Resubmission to *Energy and Environmental Science*, November **2016**.	**CH5**
5	What is the current 'state of the art' in environmental assessment of emerging biofuel systems? Furthermore, what are the outstanding challenges and opportunities facing the biofuel industry? Can the integration of new methods and models provide better resolution and insights into the sustainability of emerging biofuel systems—does such a transition demarcate a new paradigm in the environmental sustainability assessment and design of fuel and energy systems?	Zaimes, G. G.; Vora, N.; Chopra, S. S.; Landis, A. E.; Khanna, V., Design of Sustainable Biofuel Processes and Supply Chains: Challenges and Opportunities. *Processes* **2015,** *3*, (3), 634-663.	**CH6**

2.0 MICROALGAL BIOMASS PRODUCTION PATHWAYS: EVALUATION OF LIFE CYCLE ENVIRONMENTAL IMPACTS

The following chapter is based on a peer-reviewed article published in *Biotechnology for Biofuels* with the citation:

Zaimes, G. G. and V. Khanna, *Microalgal biomass production pathways: evaluation of life cycle environmental impacts.* Biotechnology for Biofuels, 2013. **6**(1): p. 88.

2.1 CHAPTER SUMMARY

Microalgae are touted as an attractive alternative to traditional forms of biomass for biofuel production, due to high productivity, ability to be cultivated on marginal lands, and potential to utilize carbon dioxide (CO2) from industrial flue gas. This chapter examines the fossil energy return on investment ($EROI_{fossil}$), greenhouse gas (GHG) emissions, and direct Water Demands (WD) of producing dried algal biomass through the cultivation of microalgae in Open Raceway Ponds (ORP) for 21 geographic locations in the contiguous United States (U.S.). For each location, comprehensive life cycle assessment (LCA) is performed for multiple microalgal biomass production pathways, consisting of a combination of cultivation and harvesting options. Results indicate that the $EROI_{fossil}$ for microalgae biomass vary from 0.38 to 1.08 with life cycle GHG emissions of −46.2 to 48.9 (g CO2 eq/MJ-biomass) and direct WDs of 20.8 to 38.8 (Liters/MJ-biomass) over the range of scenarios analyzed. Further analysis reveals that the $EROI_{fossil}$ for production pathways is relatively location invariant, and that algae's life cycle energy balance and GHG impacts are highly dependent on cultivation and harvesting parameters. Contrarily, algae's direct water demands were found to be highly sensitive to geographic location, and thus may be a constraining factor in sustainable algal-derived biofuel production. Additionally, scenarios with promising $EROI_{fossil}$ and GHG emissions profiles are plagued with high technological uncertainty. Given the high variability in microalgae's energy and environmental performance, careful evaluation of the algae-to-fuel supply chain is necessary to ensure the long-term sustainability of emerging algal biofuel systems. Alternative production scenarios and technologies may have the potential to reduce the critical demands of biomass production, and should be considered to make algae a viable and more efficient biofuel alternative.

2.2 INTRODUCTION

Heightened global awareness of climate change and consumption of finite resources has driven research in biomass-based forms of energy production. Current fossil fuel depletion rates and related emissions have prompted development of sustainable energy alternatives that are both carbon neutral and compatible with existing infrastructure. In past years, researchers have examined various biomass feedstocks such as corn, soybean, canola, and lignocellulosic crops for their bioenergy potential. Major drawbacks to these first and second generation biofuels including land use, water footprint, and influence in global food markets have prompted research in alternative forms of biomass [15]. Accordingly, algae-to-energy systems are receiving increased attention from both academic and industrial sectors. Microalgae's promising characteristics, such as: high productivity [65], ability to be cultivated on marginal lands [66], semi-continuous to continuous harvesting, high lipid content, and potential to utilize carbon dioxide (CO_2) from industrial flue gas make it an attractive feedstock for biofuel production [53, 67-70]. In addition, microalgae production does not directly displace food crops, as do other leading biomass candidates such as corn or soybean [71]. Extraction and subsequent upgrading of microalgal biomass feedstock may provide both a liquid fuel that has the potential to be compatible with current transportation fuel infrastructure, and satisfy the Energy Independence and Security Act (EISA) mandate [10].

The prospect of utilizing microalgae for energy production is not a recent phenomenon: between 1978 and 1998 the Unites States Department of Energy's (DOE) Aquatic Species Program, a research program aimed to develop renewable transportation fuels, extensively examined the production of biodiesel from microalgae [72]. Current demand for transportation fuels, as well as technological advancements and maturation, have motivated researchers to re-

examine microalgae's potential as a fuel source [73], and in recent years have led to a host of microalgae based life cycle assessments (LCA) [51, 56, 74-94]. Prior studies have shown that different algae harvesting options, reactor configurations, culture conditions, and cultivation assumptions yield divergent results concerning algae's environmental and energy performance [74, 75, 81-83, 85, 94, 95]. As such, evaluation of the life cycle greenhouse gas (GHG) emissions, fossil energy consumption, and water demands for multiple biomass production pathways within the framework of one study can provide insight into the potential tradeoffs, environmental impacts, and technical feasibility of these pathways. As microalgal derived fuels are inherently dependent on the cultivation of microalgae feedstock, a sustainable pathway for microalgae feedstock production must be identified if algal-based fuels are to become a commercial reality. Furthermore, additional pilot testing and laboratory scale results will be necessary for validating and benchmarking theoretical process modeling [96-98]. Holistic evaluation of emerging algae-to-fuel systems that considers the resource consumption, emissions, and their impact across the entire life cycle is critical to assess the environmental sustainability of emerging algae-based energy systems.

This study examines the critical life cycle energy and environmental drivers in algae cultivation through a comprehensive analysis of a theoretical industrial algae Open Raceway Pond (ORP) facility. Prior studies have indicated that photobioreactors (PBR) have high initial capital and operating costs, which limit their commercial viability [78, 99]. For these reasons only ORPs were investigated as a means for mass cultivation of microalgae. This work focuses on a typical process chain for ORPs: cultivation followed by a series of flocculation, dewatering, and additional drying [100]. Algal drying requirements were based on soybean production, where final biomass has a solids concentration of 90% on a weight per weight basis (w/w) [94].

Process energy and material flows were constructed based on first principles of thermodynamics, peer-reviewed literature, heat and material balances, and best available engineering knowledge. Multiple cultivation locations across the United States (U.S.) as well as cultivation and harvesting options are modeled to investigate the extent to which these parameters affect the overall energy balance, GHG emissions, and direct water demand of microalgal biomass production, and identify opportunities for process improvements along the algae supply chain.

This work models the production of microalgal biomass using freshwater algae grown using synthetic fertilizers and CO_2/flue gas from an industrial power plant. The objective of this work is to compare different technological routes for producing dried algal biomass to be used for as a feedstock for conversion to liquid transportation fuel(s). It is assumed that the biomass must be dried to 90% (w/w) before further downstream processing of biomass-to-fuel is possible and is consistent with current commercially available lipid extraction technologies.

2.3 METHODOLOGY AND SUSTAINABILITY METRICS

2.3.1 LCA Model Overview

In this study, a comparative LCA of microalgae cultivation and harvesting options for ORPs was conducted. The scope of the LCA is cradle-to-gate, in which all processes upstream of dried biomass are evaluated. With the exception of PVC lining [83], previous LCA studies have shown that algae infrastructure related impacts are negligible as compared to other system processes [76], and were thus excluded from the scope of this study. The functional unit was chosen as one Megajoule (MJ) of dried algal biomass, and calculated based on the lower heating value of the produced microalgal biomass. Cultivation of microalgae was evaluated for 232

National Weather Service (NWS) sites in the continental U.S. [101]. Prior research has suggested that for ORPs, microalgae growth rates rapidly decline when exposed to average temperatures less than 15^0 C [102]. Of the 232 examined locations, 21 sites were found to have monthly average temperatures within the requisite temperature range required to support the mass cultivation of microalgae. Complete LCA was then conducted for these 21 locations, to examine if variations in regional energy mix as well as climatological and geographical parameters influence algal biomass production. For each cultivation location multiple biomass production pathways were examined, consisting of a combination of two options for CO_2 procurement (Monoethanolamine (MEA) scrubbing with injection of pure CO_2 or Direct Injection (DI) of industrial flue gas), two algal dewatering options (centrifugation (CF) or chamber filter press (CFP)), and two algal drying scenarios (natural gas based drying (NGD) or waste heat drying (WHD)).

2.3.2 Sustainability Metrics

The focus of this study was to create an LCA model to evaluate the life cycle energy balance, direct water demands (WD), and net life cycle GHG emissions for the cultivation of microalgae in ORPs. The direct WD was evaluated as the difference between the volume of freshwater required to support algae cultivation and annual regional precipitation. Net life cycle GHG emissions were calculated as the difference between CO_2 embedded in the microalgae feedstock, as carbon, to the amount of life cycle GHGs emitted throughout the biomass supply chain. As the primary motivation for microalgae production is its potential to displace fossil derived fuels, a fossil energy return on investment metric ($EROI_{fossil}$) was chosen to assess the sustainability of microalgae production. $EROI_{fossil}$, is defined as the ratio of the energy stored in algal biomass

(lower heating value x mass of biomass) to the embodied non-renewable primary fossil energy required to produce algal biomass, and is presented in equation 1.

$$EROI_{fossil} = \frac{(Lower\ Heating\ Value\ x\ Mass\ of\ Feedstock)}{\sum Nonrenewable\ Primary\ Fossil\ Energy} \quad (1)$$

Production pathways in which the $EROI_{fossil}$ are greater than 1 are desirable, as more biomass energy is produced than non-renewable fossil energy consumed in biomass production. As the cultivation, dewatering, and harvesting of microalgae is energy intensive and a major bottleneck in the algae-to-fuel production chain [98, 103, 104], identifying renewable and sustainable pathways for the cultivation of microalgae is critical for the overall advancement of microalgal derived fuels. To reduce the complexity and dimensionality of the data, as well as to allow ease of comparison between different studies, this chapter provides a detailed analysis and comparison of the net life cycle GHG emissions, direct water demands, and $EROI_{fossil}$ for biomass production pathways for Phoenix, AZ. Detailed tables for $EROI_{fossil}$, direct WD, and GHG emissions for all examined production pathways and locations are provided in Appendix A.

2.3.3 Algal Composition and Growth Rates

An algal growth model was constructed to evaluate microalgal growth rates for ORPs in the continental U.S. Theoretical microalgae photosynthetic yields were constructed based on solar insolation values averaged over a thirty-year period (1961-1990), obtained from the National Solar Radiation Database (NSRD) [105], and efficiency factors determined by pond design and characteristics of the algal culture [52, 106]. The fractionated composition of the algae was

assumed to be 20% lipids, 25% carbohydrates, 50% proteins, and 5% other organic material and is consistent with previous studies [51, 107]. The composition of algae was calculated to be 517 grams (g) C, 81.2 g N, 17.6 g P, and 14.5 g K per kilogram (kg) biomass. The lower heating value (LHV) of the biomass was computed to be 18.66 MJ/kg-biomass.

2.4 PRODUCTION CHAIN OVERVIEW AND DATA SOURCES

2.4.1 Production Chain Overview

Figure 4 shows the microalgal biomass production chain and examined production pathways. Cultivation of the freshwater algae strain, *Chlorella vulgaris*, was modeled in a 1000-hectare (ha) virtual algae production facility, in which 500 ha are allocated for algae cultivation and 500 for infrastructure related demands. This virtual facility was assumed to be colocated with natural gas (NG) fired power plants, and would operate for eight months out of the year, from March to October. *Comprehensive LCA was performed on 21 cultivation locations, spanning seven states: (AL, AZ, CA, FL, GA, LA, & TX).* In each of these locations, biomass production was based on cultivating algae in ORPs. Data concerning the regional electricity mix for the cultivation locations was gathered from the EPA's "Power Profiler", based off the 2007 Emissions and Generation Resource Integrated Database (eGRID) [108].

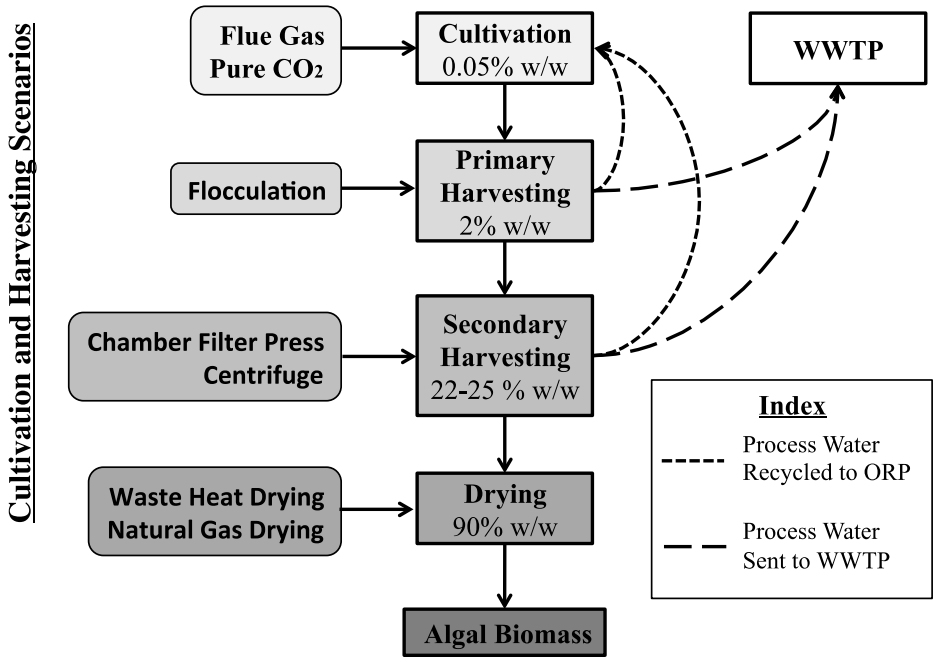

Figure 4. Microalgal Biomass Production Chain and Examined Production Pathways. The microalgal concentration is reported on a weight/weight (w/w) basis for each stage in the process chain.

The algal cultivation area is comprised of individual 1-ha ORPs, with a pond depth of 0.3 meters, and operating at an algal concentration of 0.05% (w/w) [77, 94]. The algal growth medium circulates at a mixing velocity of 15 cm/second via paddlewheels [100]. A 0.75 mm thick PVC membrane lines the cultivation area [83], with an assumed average lifetime of 5 years [83]. Nutrient and fertilizer requirements were estimated based on algal growth rates and composition of the algal culture. Prior studies have differing assumptions regarding the quantity of nutrients required for algae growth, ranging from approximately one [94] to two [76] times the stoichiometric requirement. In this study a 75% nutrient use-efficiency is assumed, with nitrogen provided by synthetic urea, potassium by potassium chloride, and phosphate by superphosphate. Nutrients and fertilizers are pumped into the ponds with freshwater so that no additional mixing

is required. CO_2 is supplied from a nearby NG fired power plant either by the direct injection of flue gas, or by separating flue gas into pure CO_2 via MEA scrubbing and delivering pure CO_2 into the algae ponds [109]. Post cultivation, microalgae are sent to holding tanks, wherein a chemical flocculent, aluminum sulfate, is added to the algal culture to agglomerate the algal biomass so that it can be efficiently separated from the water matrix [110]. The flocculated algae are then sent to either an industrial centrifuge or chamber filter press to concentrate the algae by dewatering. Medium from both flocculation and dewatering stages are recycled back into the ponds to minimize the overall water demands. After dewatering, the microalgae slurry undergoes additional drying. Two scenarios were examined for algal drying. In the first scenario, microalgae are sent to an industrial boiler, in which natural gas is burned to concentrate the algae slurry. The second scenario utilizes waste heat from a co-located power plant as a means of drying the algal biomass. Life cycle data for aluminum sulfate, fertilizers, PVC, and wastewater were taken from the Ecoinvent database [111]. Life cycle data concerning electricity generation and natural gas were taken from the United States Life Cycle Inventory (USLCI) database [112]. Further information regarding algal growth rates, composition, and detailed LCI for all modeled production pathways is available in Appendix A.

2.4.2 Water Demands

The production of biofuels has been shown to be water intensive [113-117]. Quantifying the direct component of the WD can help determine the impacts of biofuel production on regional water resources, and therefore is an important criterion for evaluating optimal locations for algal cultivation. In this study, the direct WD was calculated as the difference between the volume of freshwater required to support algae cultivation and annual precipitation. It is assumed that ORPs

are drained and treated at a wastewater treatment facility once every four months to avoid build-up of bacteria and invasive microbes. Additionally, freshwater is required to be pumped into the ponds due to water loss from pond leaking, evaporation, blowdown, photosynthetic requirements, water lost during the harvesting process, algal drying, and water contained within the final biomass slurry that is transported offsite. Water lost due to leaking from the open ponds was evaluated at a rate of 0.27 m^3/m^2-year [80]. Evaporative losses were estimated based on the Penman equation [118]. Data for wind speed (m/s), average temperature (^{0}C), and relative humidity (%) averaged over a thirty year period (1961-1990) was obtained from the NSRD [101]. Data concerning average rainfall for the various locations was taken from the National Oceanic and Atmospheric Administration (NOAA) [119]. To avoid excess mineral and salt build-up, and to regulate the pH of the culture medium, a portion of the algal growth medium must be removed from the ponds and replaced with an equivalent amount of freshwater [120]. This process is known as “blowdown”, and it was assumed that onsite evaporation ponds would be used for blowdown disposal. The chemical process of photosynthesis consumes water as a reactant; therefore freshwater that is consumed by photosynthesis in the cultivation ponds must be replaced. During the harvesting stage, process water from both flocculation and dewatering stages are recycled back into the ponds. It was assumed that only 90% [86] of the water recycled from these stages would be returned to the ponds, the remaining 10% must be treated at a wastewater treatment plant (WWTP). Therefore, freshwater must be supplied to the ORPs to offset water that is lost during the harvesting process. Furthermore, freshwater is required to makeup the volume of water that is contained in the final algae slurry that is transported off-site.

2.5 RESULTS AND DISCUSSION

2.5.1 EROI and Life Cycle GHG Analysis

Table 3 presents the direct WDs, $EROI_{fossil}$, and net life cycle GHG emissions for all examined biomass production pathways (denoted as A-H) and locations. Table 3 reveals that the net energy balance is negative for a majority of the scenarios analyzed. This indicates that more fossil energy is consumed than bioenergy produced during biomass production. Only one out of the eight examined production pathways, (scenario H), was found to yield an $EROI_{fossil}$ greater than 1. Furthermore, scenario H was found to have a barely positive energy balance and is plagued with high technological uncertainty. Additionally, the results reveal that net life cycle GHG emissions are negative for various biomass production pathways, indicating that microalgae sequester more GHGs than are emitted during biomass production via these pathways.

Table 3. $EROI_{Fossil,}$ Net Life Cycle GHG Emissions, and Direct WD's for Examined Biomass Production Pathways and Locations

Scenarios	**A***	**B***	**C***	**D***	**E***	**F***	**G***	**H***	**WD[1]**	
Location	MEA/CF/NGD	MEA/CFP/NGD	DI/CF/ NGD	DI/CFP/NGD	MEA/CF/WHD	MEA/CFP/WHD	DI/CF/WHD	DI/CFP/WHD	CFP	CF
Mobile, AL	0.40 (44.2)	0.46 (22.5)	0.49 (18.9)	0.59 (-2.8)	0.60 (-0.4)	0.68 (-15.1)	0.86 (-25.7)	1.04 (-40.4)	22.1	22.3
Phoenix, AZ	0.38 (48.9)	0.43 (28.4)	0.47 (23.5)	0.56 (3.0)	0.57 (4.2)	0.64 (-9.2)	0.79 (-21.2)	0.94 (-34.6)	38.6	38.8
San Diego, CA	0.41 (32.0)	0.46 (16.0)	0.51 (6.3)	0.60 (-9.6)	0.63 (-12.6)	0.69 (-21.5)	0.91 (-38.3)	1.06 (-47.2)	32.8	33.0
Daytona Beach, FL	0.38 (43.0)	0.44 (22.7)	0.47 (17.5)	0.57 (-2.7)	0.58 (-1.6)	0.66 (-14.8)	0.81 (-27.1)	0.97 (-40.2)	24.1	24.3
Jacksonville, FL	0.38 (43.1)	0.44 (22.8)	0.47 (17.7)	0.57 (-2.6)	0.58 (-1.5)	0.66 (-14.7)	0.81 (-27.0)	0.97 (-40.1)	22.6	22.9
Key West, FL	0.38 (43.6)	0.44 (23.4)	0.47 (18.2)	0.57 (-2.1)	0.57 (-1.0)	0.65 (-14.2)	0.80 (-26.4)	0.97 (-39.6)	28.4	28.6
Miami, FL	0.38 (42.7)	0.44 (22.5)	0.48 (17.3)	0.57 (-3.0)	0.58 (-1.9)	0.66 (-15.1)	0.81 (-27.3)	0.98 (-40.5)	22.1	22.4
Tallahassee, FL	0.39 (42.4)	0.44 (22.2)	0.48 (17.0)	0.57 (-3.2)	0.58 (-2.2)	0.66 (-15.4)	0.82 (-27.6)	0.98 (-40.8)	20.8	21.1
Tampa, FL	0.38 (43.2)	0.44 (23.0)	0.47 (17.8)	0.57 (-2.5)	0.58 (-1.4)	0.65 (-14.6)	0.81 (-26.8)	0.97 (-40.0)	25.1	25.4
West Palm Beach, FL	0.38 (43.0)	0.44 (22.7)	0.47 (17.6)	0.57 (-2.7)	0.58 (-1.6)	0.66 (-14.8)	0.81 (-27.0)	0.97 (-40.2)	22.9	23.1
Savannah, GA	0.39 (45.0)	0.45 (23.2)	0.49 (19.7)	0.59 (-2.1)	0.60 (0.4)	0.68 (-14.3)	0.86 (-24.9)	1.03 (-39.6)	24.1	24.4
Baton Rouge, LA	0.39 (39.2)	0.45 (20.8)	0.49 (13.6)	0.58 (-4.7)	0.60 (-5.4)	0.67 (-16.8)	0.86 (-31.0)	1.01 (-42.3)	22.6	22.8
Lake Charles, LA	0.39 (39.0)	0.45 (20.6)	0.49 (13.5)	0.58 (-4.9)	0.60 (-5.6)	0.67 (-16.9)	0.86 (-31.1)	1.02 (-42.4)	23.0	23.2
New Orleans, LA	0.40 (38.9)	0.45 (20.5)	0.49 (13.4)	0.58 (-5.0)	0.60 (-5.7)	0.67 (-17.0)	0.86 (-31.2)	1.02 (-42.5)	22.1	22.3
Austin, TX	0.39 (41.5)	0.45 (20.6)	0.49 (16.1)	0.59 (-4.8)	0.59 (-3.1)	0.68 (-16.9)	0.85 (-28.5)	1.03 (-42.3)	29.8	30.0
Brownsville, TX	0.39 (41.8)	0.45 (20.9)	0.49 (16.4)	0.58 (-4.5)	0.59 (-2.8)	0.68 (-16.6)	0.84 (-28.2)	1.02 (-42.0)	30.6	30.8
Corpus Christi, TX	0.39 (42.1)	0.45 (21.3)	0.48 (16.8)	0.58 (-4.1)	0.59 (-2.5)	0.67 (-16.3)	0.84 (-27.8)	1.02 (-41.7)	29.7	29.9
Houston, TX	0.39 (42.0)	0.45 (21.1)	0.49 (16.7)	0.58 (-4.2)	0.59 (-2.6)	0.67 (-16.4)	0.84 (-27.9)	1.02 (-41.8)	25.6	25.8
Lufkin, TX	0.39 (41.5)	0.45 (20.6)	0.49 (16.1)	0.59 (-4.8)	0.59 (-3.1)	0.68 (-16.9)	0.85 (-28.5)	1.03 (-42.3)	26.1	26.3
Port Arthur, TX	0.40 (35.2)	0.46 (16.9)	0.51 (9.7)	0.60 (-8.6)	0.62 (-9.4)	0.70 (-20.6)	0.91 (-34.9)	1.08 (-46.2)	22.8	23.0
San Antonio, TX	0.39 (41.3)	0.45 (20.4)	0.49 (16.0)	0.59 (-4.9)	0.60 (-3.3)	0.68 (-17.1)	0.85 (-28.6)	1.03 (-42.5)	29.9	30.1
Victoria, TX	0.39 (41.9)	0.45 (21.0)	0.49 (16.5)	0.58 (-4.4)	0.59 (-2.7)	0.68 (-16.5)	0.84 (-28.1)	1.02 (-41.9)	27.4	27.7

MEA- monoethanolamine; DI- direct injection; CF- centrifuge; CFP- chamber filter press; NGD- natural gas drying; WHD- waste heat drying

* Values in parentheses represent Net Life Cycle GHG Emissions expressed in unit of (g CO_2 eq/MJ-Biomass). Values outside of parentheses represent $EROI_{fossil}$. The last two columns represent water demand (WD).

[1] The results for the WD are presented in units of (liters/MJ-biomass).

A particularly noteworthy observation from Table 3 is that $EROI_{fossil}$ values are relatively location invariant, indicating that changes in regional electricity mix and climatological factors are negligible as compared to other fossil energy intensive processes such as algal biomass drying. Although cultivation locations, such as Arizona, have significantly higher algal growth rates as compared to other examined locations, the energy and GHG impact of producing microalgal feedstock on a per MJ basis for a given production pathway is not significantly different amongst examined locations. However, locations with high aerial biomass productivity may be preferable for algae cultivation as they are capable of generating a greater amount of microalgal biomass feedstock per unit surface area, thus reducing potential land use impacts.

2.5.2 Direct Water Demands

Table 3 provides direct WDs for the examined cultivation locations. The results from Table 3 indicate that the WDs of algae cultivation are highly sensitive to geographic location. Moreover, variation in production pathway has negligible effects upon the direct WDs, a trend directly opposite to that observed for $EROI_{fossil}$ and net life cycle GHG emissions. Further analysis indicates that evaporative losses and process water lost during the harvesting stage accounts for the majority of the direct WDs. Additionally, the large variance observed in the direct WDs is primarily due to the large variation in location specific rates of evaporation and precipitation. Additional details on various contributors to water demand for Phoenix, AZ is available in Appendix A.

2.5.3 Detailed Analysis: Phoenix, Arizona

Figure 5 presents the fossil energy inputs normalized per unit of biomass energy output for biomass production pathways for Phoenix, Arizona. For each production pathway, *input* indicates the amount of primary fossil energy consumed for the production of one MJ of biomass energy, *output*. The results highlight that CO_2 procurement, drying, and fertilizer inputs constitute the largest share of the fossil energy consumption in algal biomass production. In addition these parameters were also found to comprise a high percentage of total life cycle GHG emissions in biomass production as indicated in Figure 6.

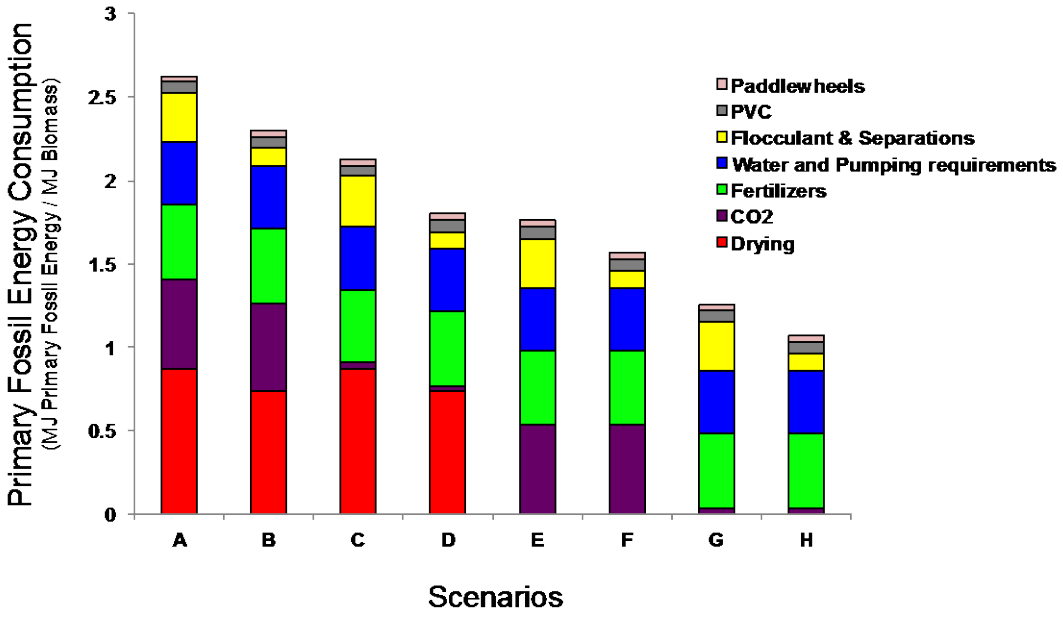

Figure 5. Life Cycle Energy Analysis for Phoenix, Arizona

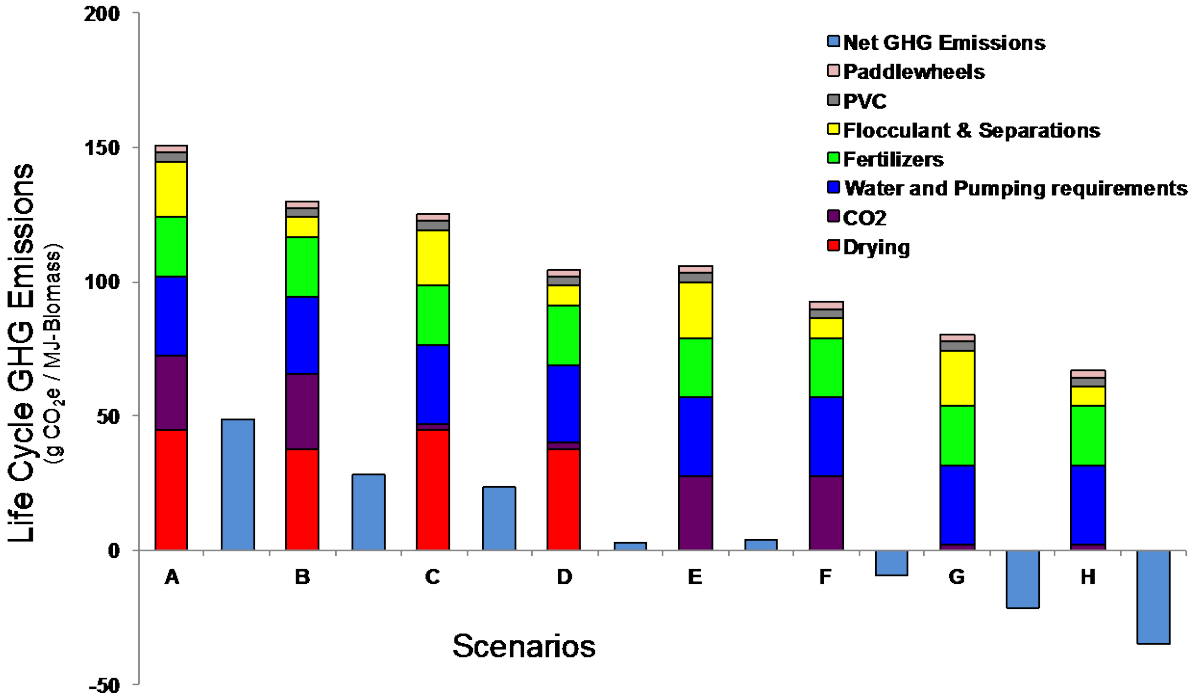

Figure 6. Life Cycle GHG Analysis for Phoenix, Arizona

2.5.4 Pure CO_2 vs. Flue Gas

The results indicate that the use of MEA-based CO_2 capture to purify industrial flue gas is energy intensive, primarily due to the high steam requirements for the MEA process. For Phoenix AZ, the primary energy required for the direct injection of industrial flue gas is equivalent to 3.3% of total produced bioenergy. Additionally, life cycle GHG emissions for the direct injection of flue gas were determined to be 2.31 g CO_2 eq./MJ-biomass. While microalgae's potential to utilize flue gas as a source of CO_2 has been extensively cited in the literature [121, 122], it remains uncertain if the presence of flue gas will have detrimental effects upon the algae culture [123, 124]. There is potential concern that industrial flue gases may contain heavy metals, which may pose serious problems in downstream algal biomass upgrading to transportation fuels. Furthermore, industrial scale operational logistics for the direct injection of flue gas have yet to be evaluated. Therefore, while the utilization of industrial flue gas has the potential to decrease

the high energy and environmental cost associated with CO_2 procurement, the feasibility of direct injection of flue gas on an industrial scale remains questionable, and its effects upon the algal culture are highly uncertain.

2.5.5 Chamber Filter Press vs. Centrifugation

Chamber filter presses were found to be a more energy efficient method of dewatering, producing a higher concentration biomass (w/w) at a lower energy and environmental cost as compared to centrifugation. For Phoenix, Arizona, switching from centrifugation to chamber filter presses was found to decrease the primary energy consumption of dewatering from approximately 21.4% to 2.4% of total produced bioenergy and decrease related life cycle GHG emissions from 15.0 to 1.65 g CO_2 eq/MJ-biomass, respectively.

2.5.6 Natural Gas Based Drying vs. Waste Heat Drying

Natural gas based drying of microalgae was determined to be a critical energy and GHG burden in biomass production. For scenarios utilizing chamber filer presses, the primary energy required for natural gas drying of the microalgae is equivalent to 73% of total produced bioenergy, resulting in life cycle GHG emissions of 37.55 g CO_2 eq./MJ-biomass. For centrifugation-based pathways the primary energy required for natural gas drying is approximately 87% of total produced bioenergy, with corresponding life cycle GHG emissions of 44.62 g CO_2 eq./MJ-biomass. Given the high energy and environmental impacts of natural gas based drying, alternate and effective dewatering and drying strategies must be realized. Prior studies have suggested that utilizing waste heat from flue gas streams emanating from co-located power plants could be used to offset algal drying requirements. While the use of this waste heat could considerably decrease

algae's environmental and energy impacts, the technical feasibility and practicality of such a system remains uncertain. Additionally, the quality of the waste heat, and thus its ability to do useful work, are important parameters that may constrain the effectiveness of this approach.

2.5.7 Sensitivity Analysis

A sensitivity analysis was conducted to examine how variations in model parameters influence net life cycle GHG emissions and $EROI_{fossil}$ for algal biomass production. Figure 7 presents tornado plots for $EROI_{fossil}$ values and net life cycle GHG emissions for Phoenix, Arizona. The results in Figure 7 reveal the relative importance and sensitivity of $EROI_{fossil}$ and life cycle GHG emissions to system parameters, and confirm that the cultivation and harvesting of microalgae is highly sensitive to algal composition, CO_2 procurement, algal growth rates, and drying method. Furthermore, the results suggest that improvements in algae-to-energy production are likely to occur via greater control over algal compositional inputs and advancements in algal drying technologies. Model parameters for sensitivity analysis are provided in Table 4.

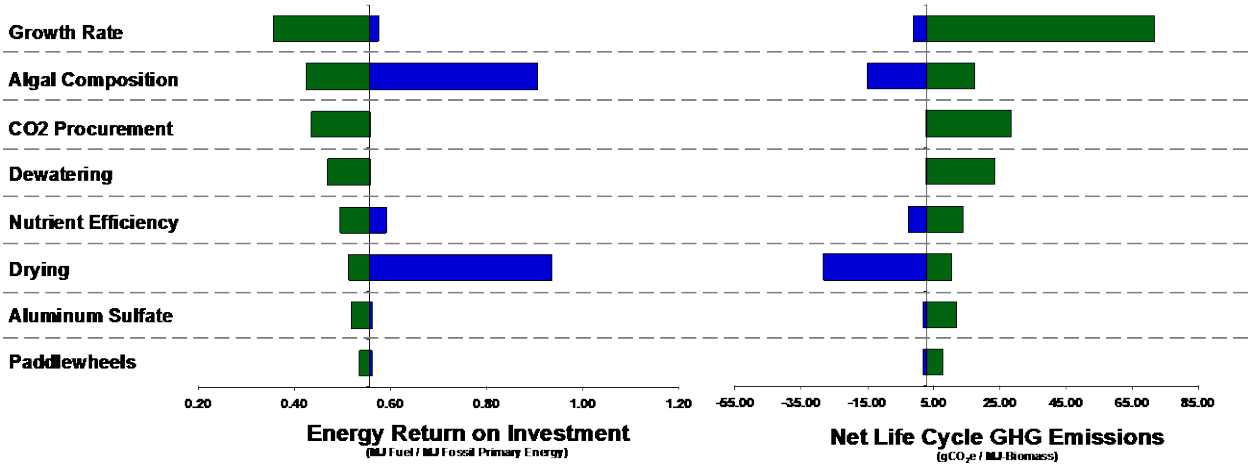

Figure 7. Sensitivity Analysis for Phoenix, Arizona

Table 4. Critical Parameters for Sensitivity Analysis

Sensitivity Analysis			
Parameters	**Low Impact**	**Baseline**	**High Impact**
Algal Composition [% Lipid/Carb/Protein]	50/40/5	20/25/50	5/20/70
Aluminum Sulfate [g/m^3]	80	100	250
CO_2 Procurement [N/A]	Flue gas (DI) [-20% CO_2 injected]	Flue gas (DI)	Pure CO_2 (MEA)
Dewatering [N/A]	CFP [-20% electricity utility]	CFP	CF
Drying [N/A]	WHD	NGD	NGD [+20% NG consumption]
Growth Rate [g/m^2-day]	35	25	5
Nutrient Uptake [%]	100	75	50
Paddlewheels [MJ/m^2-day]	36	65	180

2.6 CONCLUSIONS

The results of this chapter indicate that the life cycle energy and GHG performance of algal biomass production is highly dependent on the production pathway. Analysis reveals that 5 out of the 8 examined production pathways have positive net GHG emissions, while only 1 out of the 8 scenarios have a positive energy balance. Generally, the production of microalgae biomass is energy intensive (reflected in the low EROI), however, the process may be net GHG negative. Furthermore, the life cycle energy balance is found to be relatively location invariant. Contrarily, microalgae's direct WDs were found to be highly sensitive to geographic location, primarily due to differences in annual precipitation and evaporation. Although regions with high biomass productivity are often touted as optimal locations for microalgae cultivation, they are characteristically found in arid regions with low-freshwater availability. Therefore, quantifying and evaluating the economic and environmental impacts of large scale algae production upon

water resources at both the regional and global level is a critical issue that needs to be addressed if algae is to be a commercial source of sustainable bioenergy. Issues of water scarcity, land use change, and land availability may prove to be the constraining factors in commercial bioenergy production. While the direct WD, $EROI_{fossil}$, and net life cycle GHG emissions are important criteria for evaluating biomass feedstocks and biofuels, other sustainability indicators must also be considered to ensure that microalgal derived biofuels do not shift the environmental impacts across their life cycle from one impact category to another.

Thermodynamic constraints dictate that downstream processing and conversion of biomass feedstocks into fuels may only result in further reduction of $EROI_{fossil}$. Therefore, the $EROI_{fossil}$ values for biomass feedstocks may represent an upper bound, or maximum $EROI_{fossil}$ value, for fuels generated via these feedstocks. This chapter found that the majority of examined microalgal biomass production pathways had a negative energy balance. Subsequently, only one production pathway (H) yielded an $EROI_{fossil}$ value greater than 1, and was found to be only marginally energy positive and plagued with high technological uncertainty, and thus is an indicator that a different approach is necessary. An alternate technological route utilizing auto-flocculation [125], cross flow filtration [126], chamber filter press, as well as natural gas based drying and waste heat drying for producing dried algal biomass was evaluated. Recent studies have suggested that cross flow filtration (CFF) is a low-energy intensive technology that can be used to dewater the algae culture [126], and has many advantages over conventional centrifugation, dissolved air and/or froth flotation [127], and pressure filtration. This technological route may be favorable, as it does not rely on a coagulant for biomass production and uses low-energy dewatering strategies. The $EROI_{fossil}$ and life cycle GHG emissions for this pathway are comparable to scenario (H), detailed results are provided in Appendix A.

Improvements in dewatering technologies represent one avenue to decrease microalgae's high energy burden. In recent years, geo-synthetic membranes designed for containment and dewatering of various industrial wastes, have seen commercial application in both wastewater treatment and other industrial processes [128, 129]. As these geosynthetic membranes can provide both a low energy and low cost method for dewatering, they may have significant application in algae cultivation. In addition, after use, these geo-synthetic textiles can be recycled and may have a variety of applications in both construction and other industries.

Researchers have suggested coupling wastewater treatment with algae cultivation to reduce the nutrient and freshwater inputs required for algal biomass production and resource inputs necessary for wastewater treatment [76, 130, 131]. While the use of wastewater for algal biomass cultivation could help minimize algal nutrient requirements, as well as decrease algae's water footprint [86], studies suggest that waste streams may have relatively low concentrations of both nitrogen and phosphate and thus provide only minor fertilizer offsets [75]. Therefore, the potential of wastewater effluent to offset fertilizer requirements needs further evaluation and validation. Research has suggested that the use of saltwater algae cultures may mitigate algae's water footprint, however; further research is needed to understand and quantify the potential tradeoffs between sourcing saltwater, land availability, proximity to CO_2 source, etc. Coupling Geographical Information Systems (GIS) with systems analysis for a realistic evaluation of potential synergies between available land and waste streams (flue gas, wastewater, saltwater) can shed light on the feasibility of large-scale microalgal biomass production [132].

Anaerobic digestion of residual de-oiled biomass (post lipid extraction) has also been suggested as a means of increasing the energy performance of the algae-to-energy system [94, 133]. A downfall in this process configuration is that lipid extraction of microalgae feedstock

with present-day commercial technology (dry extraction) requires algae to be dried to approximately 90% (w/w), and therefore may be constrained by the energy considerations presented in this study. While the allure of algae based energy is its potential to act as a replacement for traditional transportation fuels, natural gas production via anaerobic digestion of the entire algal biomass may have the potential for higher energy yields [134]. One unique advantage of anaerobic digestion is its ability to process wet input streams, and therefore is not limited by algal drying requirements. In addition, recycling of anaerobic digestate may offset a portion of algal nutrient requirements. However, further investigation of the life cycle environmental impacts and benefits of such a system is necessary before a statement can be issued.

This chapter highlights the importance of systems analysis of emerging algal technologies. Although the need for systems analysis is understood, it receives little attention at early stages of research, often leading to unfounded technological exuberance and optimism. A systems approach with life cycle thinking can test, ground the claims, and assess the environmental sustainability of emerging technologies. Furthermore, systems analysis can aid in identifying technological bottlenecks and sources of process inefficiencies along the supply chain before they become embedded. While industrial symbiosis via the use of wastewater or industrial flue gas and various other synergies have the potential to offset algae's high cultivation and harvesting costs, with each additional interdependent synergistic technology comes a level of complication that may challenge the performance, reliability, resilience, and viability of the system. The most efficient theoretical system in the end may not provide a practical solution. High-level evaluation of these synergistic opportunities and logistics must be performed in order to assess the commercial viability of algal biofuel systems. As an emerging field, there are many

opportunities to enhance the potential of microalgae as an energy source. Alternative production scenarios and technologies may have the potential to reduce the critical demands of microalgal biomass production, and should be considered to make algae a viable and more efficient biofuel alternative.

3.0 ASSESSING THE CRITICAL ROLE OF ECOLOGICAL GOODS AND SERVICES IN MICROALGAL BIOFUEL LIFE CYCLES

The following chapter is based on a peer-reviewed article published in *RSC Advances* with the citation:

Zaimes, G. G. and V. Khanna, *Assessing the critical role of ecological goods and services in microalgal biofuel life cycles.* RSC Advances, 2014. **4**(85): p. 44980-44990.

3.1 CHAPTER SUMMARY

Microalgae bioenergy systems are gaining attention as a commercial biotechnical platform for producing renewable transportation fuels. In recent years, process-based LCA has been extensively applied to understand the life cycle environmental impacts of emerging microalgal biofuel systems. However, conventional process-based LCA fails to account for the role of ecological goods and services within fuel and product life cycles. Additionally, traditional life cycle energy analysis suffers from several limitations such as ignoring the difference in quality and substitutability of resources, and accounting for only the first law of thermodynamics. To address these shortcomings, a hybrid Ecologically based-LCA (EcoLCA) model is developed to quantify the contribution of ecological resources within the algae-to-fuel supply chain and to compare the resource intensity of producing microalgal derived renewable diesel (RD) to that of petroleum diesel (PD). Multiple thermodynamic ROI metrics and performance indicators are used to quantify the consumption of ecological goods and services, environmental impacts, and resource intensity of producing microalgal RD. Results indicate that the quality corrected thermodynamic return on investment and renewability index for microalgal RD ranges from 0.17 to 0.44 and 3.51% to 6.36% respectively, depending on the choice of coproduct options and processing technologies. This work reveals that algae-to-fuel systems are highly dependent on non-renewable ecological resources reflected in their low renewability index; have a low quality corrected thermodynamic ROI (<1) and thus are not energetically viable; and are more ecologically resource intensive as compared to their petroleum equivalent—potentially negating their environmental benefits.

3.2 BACKGROUND

Emerging issues of global climate change, domestic energy security concerns, and regulatory renewable fuel mandates are driving the production of low carbon biofuels [11]. However, there is concern that the production of first generation biofuels—fuels derived from arable crops such as corn or soybean may displace or compete with cropland, potentially reducing the quantity of food crops available for human/livestock consumption. This could have major economic consequences including food shortages and inflation of global food prices [21, 135]. Previous analysis has also shown that first generation biofuels have marginal energy returns [135] and provide limited greenhouse gas (GHG) emissions reductions relative to petroleum fuels [16, 17, 136, 137]. Additionally, the production of first generation biofuels may result in increased ecosystems degradation including impacts on biodiversity, water, soil and forest resources [13, 14]. Recently, liquid transportation fuels derived from microalgae have generated significant interest from leaders in academia, government, and industry [138]. Microalgae are considered a promising feedstock for conversion to liquid fuels due to their ability to capture waste carbon dioxide from industrial flue gas streams [139], high photosynthetic yield and lipid content [52], ability to be grown on marginal and non-arable land [53], and potential for achieving policy mandated volumetric renewable fuel targets aimed at mitigating anthropogenic derived climate change and increasing U.S. energy independence and security.

In recent years, LCA has emerged as the preferential method for modeling the energy and environmental performance of biomass-to-fuel systems, and has been extensively applied to emerging microalgal biofuel and bioenergy systems [81, 84, 92-94, 140-143]. Existing LCA of microalgae biofuel production have focused on quantifying the life-cycle greenhouse gas (GHG) emissions and life cycle energy balance for different microalgal growth configurations and fuel

conversion pathways [56, 74, 75, 78, 83, 89, 144, 145]. Additionally, prior work has investigated the impact of microalgal biofuels on nutrient and water resources [80, 86, 146], and quantified the geospatial constraints and related impacts on microalgal fuel production [132, 147-149]. However, traditional energy analysis suffers from several limitations such as ignoring the difference in quality and substitutability of different resources, and accounting for only the first law of thermodynamics [150-154]. Hierarchical thermodynamic based approaches and metrics have been suggested to address the limitations of traditional energy analysis while concurrently providing a methodological framework for quantifying ecological resource consumption from a life-cycle perspective [155-158]. However, these have not yet been applied to study emerging microalgal biofuels. Additionally, existing sustainability assessments have ignored the contribution of ecological goods and services (EGS) or natural capital within the algal biofuel supply chain. Natural capital extends the economic notion of capital to include goods and services provided by ecosystems and the natural environment, which are essential to sustaining human and ecological life—such as: timber, food, water, energy resources, clean air, minerals and ores, purification of air and water resources, flood and drought mitigation, pollination of crops and vegetation, maintenance of global biodiversity, as well as climate and disease regulation. Despite the critical importance of EGS to human and global welfare, most existing measures of sustainability do not account for the role/consumption of EGS within product or fuel life cycles [151, 155, 156].

3.2.1 Ecological Goods and Services

Pre-industrial revolution, the paradigm of environmental awareness operated under the assumption that the global ecosphere would be able to absorb the totality of anthropogenic-

derived pollution and resource degradation without widespread negative consequences for human life or the environment. However, in recent decades research has reported accelerated degradation of numerous ecosystem goods and services as a direct consequence of economic development and human activity [159]. There is increasing realization that anthropogenic-derived environmental impacts can cause irreparable damage to the world's ecosystems and strain the natural ecological functions that support human life [160].

In 2001, the United Nations (UN) initiated the millennium ecosystem assessment (MEA)—an international collaboration designed to assess the impact and widespread consequences of environmental change for human and ecological well-being. The MEA developed a scientifically rigorous framework for assessing the impacts of environmental change in coupled dynamic socio-ecological systems, and provided guidelines for policy measures and human action required for the conservation and long-term sustainability of the earths biosphere [1]. Published in 2005, the findings of the MEA indicate that in the second half of the 20th century anthropogenic-derived resource degradation and overconsumption of natural capital have changed ecosystems more rapidly and extensively than in any comparable period in human history [1]. Results from the MEA study indicate that 6 out of the 11 global ecological provisioning services, 7 out of the 10 ecological regulating services, and 2 out of the examined 3 ecological cultural services have been severely degraded over the past 50 years. Furthermore, the results of the MEA indicate that anthropogenic derived environmental impacts have resulted in loss of global biodiversity, and may impair the ability of the planet's ecosystems to sustain human life. Clearly, it is imperative that sustainability assessments consider the consumption of ecological goods and services within biofuel life cycles at early stages of research and development, so as to avoid or mitigate any potential widespread negative impacts for human

and global ecological welfare that may result as a consequence of full-scale commercialization of these fuels.

3.3 HYBRID ECOLOGICALLY-BASED LCA METHODOLOGY

EcoLCA is an environmentally extended input-output model capable of accounting for the consumption/role of ecosystem goods and services in a life cycle framework [150, 153, 161]. This work extends the EcoLCA framework developed by Bakshi and colleagues to study the environmental sustainability of emerging microalgal biofuel systems [155, 156]. The hybrid framework developed in this study utilizes the 2002 EcoLCA model to quantify ecosystem/economy wide impacts, while a detail process inventory is used to assess direct material, energy, and ecological impacts of biofuel production. By integrating process and EcoLCA models, we quantify the total life cycle impacts of microalgal biofuel production. Figure 8 presents an overview of the hybrid EcoLCA framework utilized in the present study.

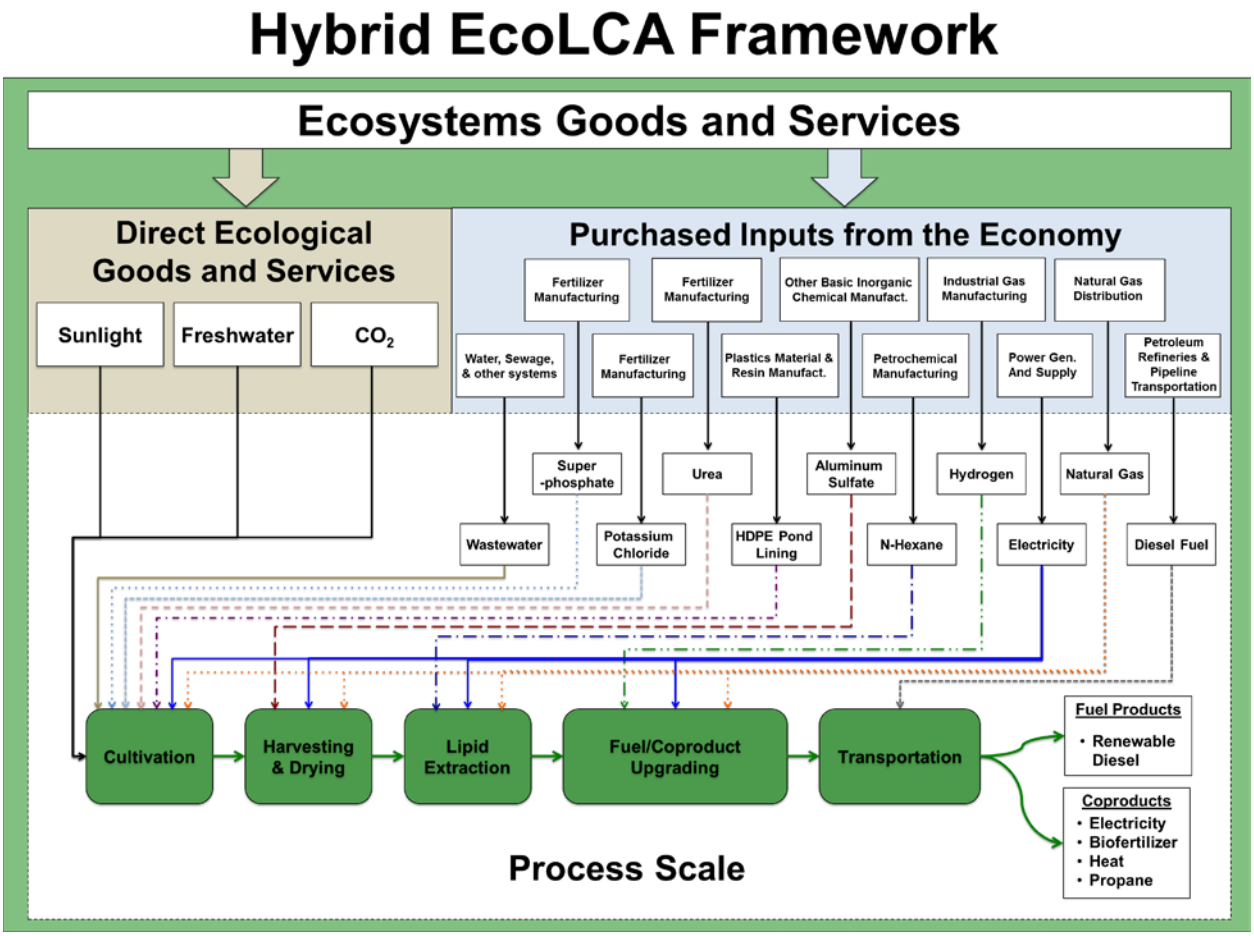

Figure 8. Hybrid EcoLCA Framework for Microalgal Biofuel Production

In this chapter, a hybrid EcoLCA model is developed to quantify the contribution of ecological resources within the algae-to-fuel life cycle, and to compare the resource intensity of producing microalgal derived renewable diesel and biodiesel to that of traditional petroleum diesel. Furthermore, a host of hierarchical thermodynamic metrics is utilized to address the shortcomings of existing life cycle energy analysis and provide novel insights into the environmental performance and sustainability of emerging microalgal biofuel systems. Renewable diesel also known as “green diesel” is an infrastructure compatible biofuel produced via hydrotreating of algal lipids. RD is attractive as a fuel product because of its high energy density, cetane number, and storage stability [162]. Furthermore, RD is fungible with petroleum

diesel and as such can be used in current commercial vehicle fleets and fuel infrastructure. This chapter provides an in-depth analysis of microalgal derived RD; results for microalgal biodiesel are provided in Appendix B.

3.3.1 Process Model

A detailed process model was developed to quantify the direct material, energy, and ecological inputs for producing algal derived renewable diesel and biodiesel via a theoretical integrated open raceway pond (ORP) biorefinery operating in Phoenix, AZ [144, 147]. Two technological routes, baseline and improved scenarios, spanning a large feasibility space were evaluated for biofuel production. Baseline scenarios represent current commercial day refining and processing technologies, while improved scenarios represent technological options which have undergone pilot scale experimentation but whose feasibility on a commercial scale has yet to be determined.

Algal growth rates were developed based on monthly average meteorological and climate parameters obtained from the NSRD [101] and NOAA [163] as well as biomass composition and photosynthetic efficiency terms [52, 70, 147]. The fractional composition of the algal biomass was assumed to be 25% lipids (L), 28% carbohydrates (C), and 47% proteins (P) [70]. The molecular composition of the biomass fractions was constructed based on the work of Lardon et al. 2009 [94]. It was assumed that the integrated ORP biorefinery operates for eight months out of the calendar year. Furthermore, the biorefinery is constructed on a 1000 hectare plot of land in which 500 hectares are allocated for open raceways ponds and 500 hectares for infrastructure requirements.

The modeled biomass-to-biofuel production chain consists of the following sub-modules: cultivation, CO_2 procurement, primary harvesting, secondary harvesting, drying, lipid extraction,

coproduct and fuel conversion, and transportation. An overview of the biomass-to-fuel process chain along with technological routes examined in this work is provided in Figure 9.

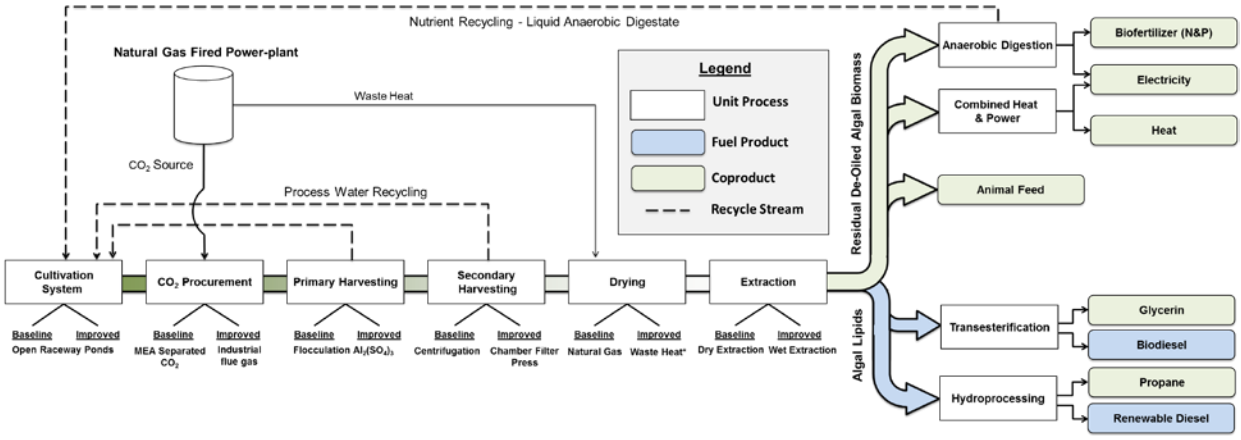

Figure 9. Microalgae-to-Fuel Process Chain

It was assumed that the algal biorefinery would be co-located with a natural gas (NG) fired power plant, which would provide industrial flue gas as a carbon source for algal growth. In the biomass-to-biofuel model, two process options are evaluated for CO_2 procurement. In the baseline scenario(s) industrial flue gas is separated into pure CO_2 via monoethanolamine scrubbing, this pure CO_2 is then compressed and injected into the algae ponds. In the improved scenario(s) industrial flue gas is directly compressed from the NG fired powerplant and pumped into the ORP via low-pressure blowers. Process energy requirements for flue gas/CO_2 compression and transportation were constructed based on the work of Kadam 2002 [109]. While the use of industrial flue gas may reduce the high resource and energy demands associated with CO_2 procurement, there is high technological uncertainty regarding the feasibility of direct injection of industrial flue gas and its effects on the microalgal culture [123, 164, 165].

Inputs for the cultivation of microalgae include: sunlight, freshwater, high density polyethylene (HDPE) pond liner, urea (N-fertilizer), super phosphate (P-fertilizer), potassium chloride (K-fertilizer), industrial flue gas, and electricity required for pumping and water

movement as well as for the compression and transportation of industrial flue gas/CO_2. It was assumed that a HDPE pond liner would be used to line the ORP [80], and paddlewheels are utilized for circulating the algal growth medium. Energy requirements for sourcing ground/surface water were developed based on the 2008 Farm and Ranch Irrigation Survey [166]. Energy requirements for circulation of pond medium and pumping between various system components was developed based on the Darcy-Weisbach equation. Additionally, factors such as water loss due to evaporation, pond leaking, pond blowdown, as well as the embodied impacts of the HDPE pond liner are also considered in the algae-to-fuel model [147].

After cultivation, the algal biomass undergoes chemical flocculation via the addition of aluminum sulfate. In the baseline scenario the flocculated algae is further dewatered via a decanter centrifuge, resulting in a solids content of 22% (w/w). In the improved scenarios chamber filter presses are utilized as a means of dewatering the biomass; resulting in a final solids content of 25% weight by weight (w/w). It was assumed that the environmental impacts for the membrane replacement/regeneration are negligible as compared to operating costs, and thus was not considered in the analysis. Process requirements for the harvesting stage were developed based on prior pilot scale tests as well as peer-reviewed and technical literature [167-169]. Post harvesting, in the base-case scenario thermal dewatering via combustion of natural gas is performed to dry the algal slurry to a 90% solids content [94]. Hexane extraction is then utilized to separate the non-lipid and lipid fraction(s) of the algal biomass. In the improved scenario(s), liquid-liquid (wet) extraction via countercurrent circulation of n-hexane is utilized to separate the lipid and non-lipid fractions of the biomass [144, 170]. In both technological routes, the extracted lipids are either hydrotreated using hydrogen to produce algal derived renewable diesel as well as coproduct propane or transesterified to produce algal biodiesel and coproduct

glycerin. Three process options are considered for the non-lipid fraction of the algal biomass: (1) use as an animal feed, (2) anaerobic digestion of residual de-oiled biomass (RDB) to produce bioelectricity as well as biofertilizer, and (3) cogeneration of RDB via combined heat and power (CHP) to produce bioelectricity and heat. Efficiencies were considered at each stage in the algae-to-fuel process chain including: 75% nutrient uptake efficiency [147], 70% CO_2 utilization efficiency [83], 5% harvesting product loss for centrifugation and chamber filter presses [56], 90% process medium recycling for 1st and 2nd stage harvesting [86], 95% lipid extraction and conversion efficiency for wet extraction pathways [170] and 97% lipid extraction and conversion efficiency for dry extraction pathways [171], 5% nitrogen volatilization for recycling of liquid anaerobic digestate [170], and a 25% electrical and 56.3% heat conversion efficiency for combustion of RDB in a combined heat and power plant [172]. Detailed process level inventory and model parameters are provided in Appendix B.

3.3.2 EcoLCA Model

The EcoLCA model is constructed based on the 2002 input-output (IO) model of the U.S. economy[155, 156]. Input-output models, first developed by Nobel laureate Wassily Leontief, provide a mathematical framework for quantifying the inter-industry transactions between different sectors in an economy or a region. The EcoLCA model extends the I-O framework to quantify the direct and indirect environmental impacts that result from economic activities via translating the monetary flows of purchased inputs from the economy to ecological and natural resource consumption, emissions, land-use, and other environmental impact categories via the use of monetary to resource use or emission ratios for industrial sectors [173]. As such, information regarding sector-wide economic activity is required to run the EcoLCA model. The

economic activity for specific industrial sectors was calculated by translating the resource flows as developed in the process inventory with their corresponding 2002 producer price and aggregating the results. If the 2002 producer price was not available a price inflator was used to convert to the 2002 price equivalent [174]. Additionally, EcoLCA does not consider the use phase of purchased inputs from the economy as well as direct ecological good and services that are consumed at the process scale [150]. Therefore, economy wide environmental impacts obtained from EcoLCA must be integrated with environmental burdens at the process scale to obtain data on a life-cycle basis. Price data for inputs, as well as detailed material and energy flows are provided in Appendix B.

3.3.3 Thermodynamic Return on Investment

A host of metrics has been utilized in LCA to quantify and compare the energy intensity of producing transportation fuel(s) from petroleum and biomass feedstocks [85, 175, 176]. Traditional energy metrics, such as EROI, compare the quantity of primary energy required to produce a functional unit of transportation fuel energy—evaluated over the life cycle [19, 177, 178]. As the primary function of biofuels lies in their utility to displace petroleum-derived liquid fuels, a fossil-based EROI metric is relevant for measuring and benchmarking the performance and sustainability of emerging microalgal biofuel systems. In this chapter, $EROI_{fossil}$ is defined as the ratio of output fuel energy to the non-renewable primary energy required for its production, and is provided in equation 2.

$$EROI_{fossil} = \frac{(Lower\ Heating\ Value\ x\ Mass\ of\ Biofuel)}{\sum Nonrenewable\ Primary\ Energy} \quad (2)$$

Common energy metrics such as EROI and variants are often used due to their intuitive appeal and ease of comparison with existing studies. However, these traditional energy metrics implicitly assume that all forms of primary energy are fungible, i.e. the heating value of different primary energy resources such as crude oil, coal, natural gas, uranium, solar, wind, tidal, biomass, and geothermal are perfectly substitutable, have the same work-potential, and thus may be added together and represented via a single aggregate metric [179]. This traditional aggregation of different primary energy sources has several limitations including: (1) accounting for only the first law of thermodynamics, (2) assuming perfect substitutability between resources, and (3) failing to account for resource quality; and thus has led some researchers to question the utility of the resulting metrics and their ability for informing decision making [179].

Exergy analysis has been proposed and utilized to address some of these shortcomings [152]. Exergy represents the maximum amount of useful work that can be extracted from a system (or resource) when it is brought into thermodynamic equilibrium with the surrounding environment or reference state [152]. The presence of exergy destruction in a system indicates the possibility of a thermodynamic improvement; thus exergy analysis has been widely used in process engineering for optimizing industrial operations and commercial processes [152]. Exergy is appealing from a methodological standpoint since it considers both the first and second law of thermodynamics, and can aggregate material and energy resources using a common denominator (joules). As such, aggregating primary energy sources based on *exergy* provides a better representation of the ability of these resources to produce useful work—as compared to *energy*. The quantity of exergy consumed throughout the industrial supply chain is defined as the Industrial Cumulative Exergy Consumption (ICEC)[151, 152, 173]. Analogous to $EROI_{fossil}$, the fossil exergy return on investment ($ExROI_{fossil}$) for a fuel is defined as the ratio of output exergy

of the fuel product to the non-renewable ICEC required for its production and is provided in equation 3:

$$ExROI_{Fossil} = \frac{Exergy\ of\ Biofuel}{\sum Nonrenewable\ ICEC} \quad (3)$$

While traditional exergy analysis overcomes many of the shortcomings of energy analysis, it does not account for the quality of different energy or material resources, nor does it consider the contribution of ecosystems in making ecological goods and services available for human and industrial activities. As natural capital provides the basis for human made capital, quantifying the consumption of ecological goods and services across the life cycle is critical for determining the sustainability of emerging microalgal biofuels.

Odum developed a methodological framework built upon principles and concepts from thermodynamics, general systems theory, and systems ecology to understand the dynamic transformation of energy and resource flows within human-ecological systems, in what is formally known today as *emergy* [180]. Odum observed that, in regards to the 'global energy budget', incident solar exergy becomes concentrated in as it flows through human-ecological systems. Analogous to energy pyramids commonly used in traditional ecological and food-chain modeling, emergy analysis posits that a hierarchical energy structure exists in human-ecological systems in which dilute sunlight is converted to plant matter, from plant matter to coal, from coal to oil, to electricity and other products, and finally to human made goods and services [181]. Therefore, the utility of a resource as well as the ability of an energy carrier to provide useful work are measured in respect to both quantity (MJ, kWh, BTU, kg, etc.) and quality—the amount of available energy of one kind of a lower grade required to develop the higher grade [181]. Emergy is formally defined as "the amount of available energy of one kind that is used up

in transformations directly and indirectly to generate a product or service", and is typically expressed in terms of solar equivalent joules (sej) [180]. Emergy analysis provides an objective basis for comparing energy and material resources by assessing the direct and indirect past solar energy required for their production. The ratio of emergy input to exergy output of a product or service is defined as transformity, expressed in equation 4.

$$\text{Transformity} = \frac{\text{Emergy Input}}{\text{Exergy Output}} \tag{4}$$

By definition transformity evaluates the amount of emergy required to create a unit of available energy (*exergy*) of another form. As such, transformity provides a quantitative measure for determining and ranking the quality of different energy and material resources. The amount of past solar exergy that is consumed throughout the ecological and industrial supply chain is referred to as ecological cumulative exergy consumption (ECEC), and is equivalent to emergy if the same system boundary and accounting procedures are chosen [151]. Furthermore, a fuels emergy return on investment (EmROI), analogous to the prior return on investment (ROI) metrics, is defined below in equation 5.

$$\text{EmROI} = \frac{(\text{Exergy of Biofuel}) \times \tau_{max}}{\sum \text{ECEC}} \tag{5}$$

Where τ_{max} is the maximum transformity for fuels with the same functionality or usefulness, and is used to adjust for the quality of the output fuel exergy so that it is comparable to other products within the same functional group or class [153]. In this study, the transformity

of petroleum diesel is used for τ_{max}. EmROI represents the amount of quality-adjusted thermodynamic work potential generated per unit work (sej) invested via the economy.

While the emergy methodology has distinct advantages over traditional energy and exergy analysis, uncertainty in reported transformity values and misperception regarding emergy accounting has limited its widespread adoption [182]. Nevertheless, emergy intrinsically considers differences in the quality and substitutability of resources, and provides a consistent, scientifically rigorous, and eco-centric framework for valuing the contribution of ecological processes and natural capital [183]. However, as energy, exergy, and emergy analysis all offer unique insights regarding the sustainability of a product or service, a hierarchy of sustainability and performance indicators based on these thermodynamic metrics may be preferable.

3.3.4 Thermodynamic Sustainability Metrics

In this chapter a variety of thermodynamic return on investment metrics, sustainability indicators, and renewability indices based off of energy, exergy and emergy analysis are used to quantify the consumption of ecological goods and services, environmental impacts, and resource intensity of producing microalgal derived fuels. Several performance metrics based on ECEC analysis including: ECEC Yield Ratio (EYR), Environmental Loading Ratio (ELR), Yield-to-Loading Ratio (YLR), and Renewability Index (R) are used to assess the sustainability of transportation fuel production and are formally defined and summarized in Table 5.

Table 5. ECEC based Sustainability Performance Metrics

Performance Metrics	Formula	Definition and Implications
Direct Inputs (DI)		ECEC of direct inputs from nature. For microalgal biofuel systems direct inputs include: sunlight, water, and photosynthetic CO_2.
Indirect Inputs (II)		ECEC of purchased inputs from the economy. For microalgal biofuel systems purchased inputs from the economy includes fertilizers, electricity, natural gas, wastewater treatment, hexane, hydrogen, diesel, HDPE pond liner, and other material and energy products considered in the biomass-to-fuel process chain.
Inputs from Non-Renewable Resources (NR)		ECEC of direct and purchased inputs from non-renewable resources. Includes direct and indirect ECEC consumed via metallic ores: Fe, Cu, Cr, Au, Pb, Zn, Ag, Mo, Ti, Al; sand and stone; non-metallic ores: apatite, clay, gypsum, feldspar, garnet, potash, salt, soda ash, diatomite, barite, talc, pumice, perlite, mica, quick lime, and other non-metallic ores; and non-renewable energy: nuclear, coal, natural gas, and crude oil.
Inputs from Renewable Resources (REN)		ECEC of direct and purchased inputs from renewable resources. Includes direct and indirect ECEC consumed via ecological regulation and maintenance services: detrital matter, photosynthetic CO_2, pollination, nitrogen and phosphorous mineralization, nitrogen deposition from the atmosphere; ecological provisioning services: wood, fish, soil, grass, water; and renewable energy: hydropower, wind, geothermal, and sunlight.
Yield (Y)		Sum of ECEC consumed from purchased inputs from the economy and ECEC of direct inputs from nature. Yield is equivalent to the sum of direct and indirect renewable and non-renewable ECEC consumed in the ecological supply chain.
ECEC Yield Ratio (EYR)		Ratio of total ECEC to ECEC embodied in purchased inputs from the economy. The EYR indicates how much work is invested by the economy in converting natural resources into goods and services. A large EYR (>1) indicates that less ECEC is provided via purchased inputs from the economy relative to direct inputs from the nature in the production of a good or service.
Environmental Loading Ratio (ELR)		Ratio of ECEC of inputs from non-renewable resources to ECEC of inputs from renewable resources. ELR provides a measure of the stress on the environment due to a transformation or process. Values for ELR greater than unity indicate there is a higher reliance on non-renewable resources as compared to renewable resources. Thus, an ELR less than one is desired as it indicates that a product or services is more dependent on renewable resources.
Yield-to-Loading Ratio (YLR)		Ratio of ECEC yield ratio to environmental loading ratio. The ratio of the yield ratio to environmental loading ratio has been suggested as an index for determining the sustainability of a product or service. YLR considers the contribution of a resource or process to the economy per unit of environmental loading, thus an YLR value greater than one is preferred.
Renewability Index % (R)		Ratio of renewable ECEC to Yield. Renewability Index provides a measure of the relative contribution of renewable ecological resources in the production of a product or service.

3.4 RESULTS AND DISCUSSION

Figure 10 presents thermodynamic return on investment metrics for the production of microalgal RD via current day commercial technologies (baseline scenarios) and optimistic future technologies (improved scenarios) under several coproduct scenarios, and compares the results with petroleum diesel. For $EROI_{fossil}$, $ExROI_{fossil}$, or EmROI a value greater than one is desirable as it indicates that more work is produced per functional unit via the fuel system relative to the work invested for its production. Comparison of these thermodynamic metrics across multiple microalgal biofuel processing technologies and coproduct options provides unique perspectives on the performance and environmental sustainability of current and future microalgal biofuel systems at both the industrial and coupled industrial-ecological scale.

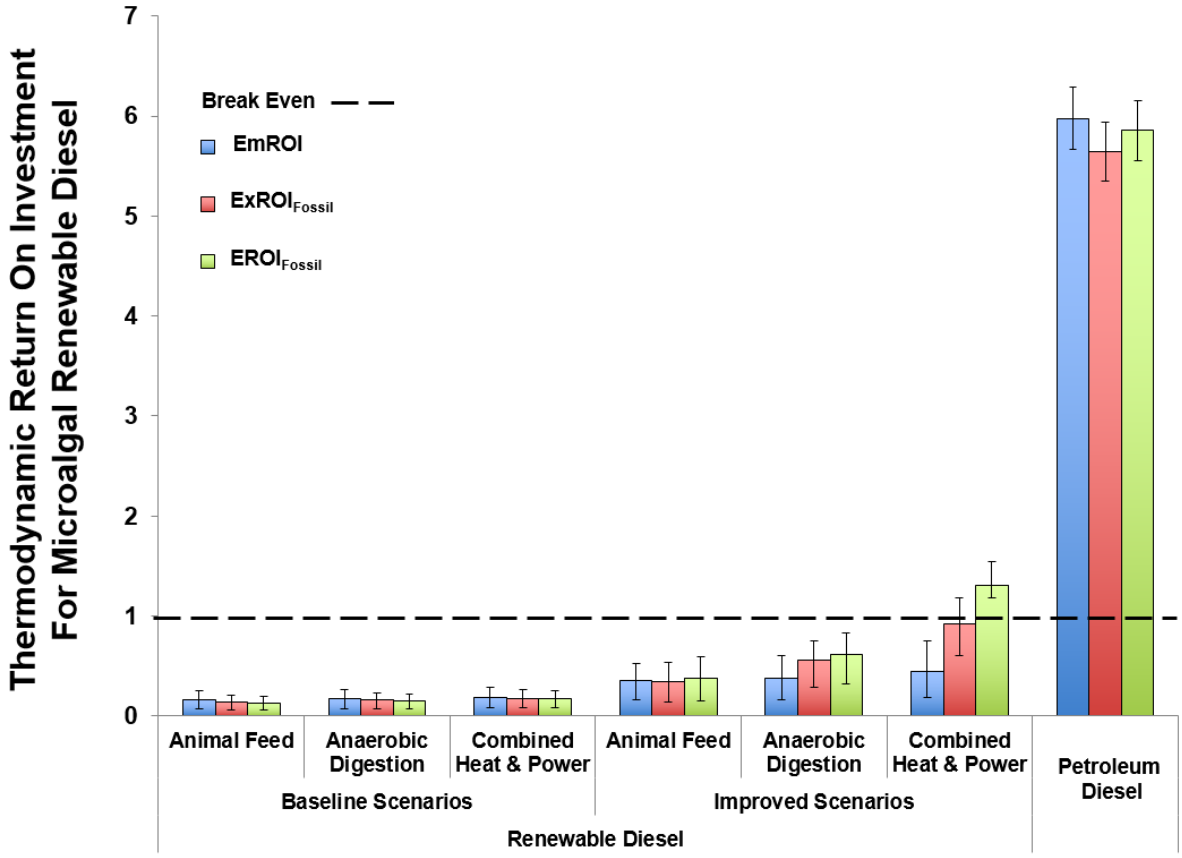

Figure 10. Thermodynamic Return on Investment Metrics. Error Bars for Baseline and Improved Scenarios Represent the Results for High (40% L / 50% C / 10% P) and Low Lipid (10% L / 20% C / 70% P) biomass composition. Error bars for Petroleum Diesel represent the range obtained via market and mass based allocation.

The results reveal that current day microalgal RD production has a low return on investment (ROI<1) for all examined thermodynamic metrics and coproduct scenarios, and is a consequence of the exceedingly resource intensive stages in the algae-to-fuel process chain: including the high energy requirements for water circulation and pumping in the ORP system [80], dewatering and harvesting operations [184], high upstream impacts of synthetic fertilizers

[76], CO2 procurement [147], and drying. Future and optimistic processing technologies (improved scenarios) offer superior ROI but are plagued with high technological uncertainty as these scenarios have yet to be effectively demonstrated at a commercial scale. Error bars for baseline and improved scenarios represent the results for high (40% L / 50% C / 10% P) and low lipid (10% L / 20% C / 70% P) biomass composition, while error bars for petroleum diesel represent the range obtained via market and mass based allocation. The results from Figure 10 indicate only one of the evaluated RD production pathways yields an $EROI_{fossil}$ greater than one (improved scenarios utilizing CHP). However, analysis reveals that by correcting for the availability of the energy (i.e. ExROIfossil) the resulting ROI is less than unity. This value is further lowered when correcting for the quality of resources (i.e. EmROI). These results are compelling as they suggest that after accounting for the quality of resources, more useful work is invested via the economy in producing microalgal fuels than useful work generated from these fuels.

Although traditional energy metrics such as EROI are commonly used in the fuel and energy literature, this work has shown that these metrics fail to accurately measure the amount of useful work generated via microalgal biofuel systems as well as adequately quantify the amount of past ecological work required for their production, thus producing misleading and erroneous results regarding the environmental sustainability and performance of these fuel systems. These findings are significant, as traditional energy metrics such as EROI are frequently utilized to guide the course of fuel and energy policy and the sustainable adoption of fuel and energy resources.

The results from Figure 10 reveal that petroleum diesel is thermodynamically superior to microalgal RD as indicated by its high ROI across all thermodynamic metrics relative to

microalgal fuels. The high ROI for petroleum diesel is a direct consequence of the fact that nature has performed most of the past work in making these resources available for human consumption. The low ROI for microalgae biofuels reflects the highly engineered and resource intensive nature of microalgal fuel production and has broad sustainability implications, as the large scale adoption of alternative fuels with lower ROI relative to petroleum transportation fuels could have long-standing societal consequences [95, 185] as a greater portion of useful work must be diverted from the economy for fuel production and thus cannot be used to sustain other economic activities.

Figure 11 plots the fractional contribution of energy, ICEC, and ECEC by ecological resource type for microalgal RD production under different coproduct options and compares the results to petroleum diesel. Figure 11 shows that natural gas, coal, sunlight, and crude oil contribute the majority of total energy consumption in the algae-to-fuel supply chain, with similar trends found across the evaluated coproduct scenarios. ICEC analysis expands upon traditional energy analysis to consider both energy and material inputs; this is evident from the contribution of metallic and non-metallic ores, water, and other material inputs to overall resource consumption. However, the contribution of these resources is still small relative to other ecological resources (such as natural gas, coal, etc). As shown in Figure 11, the contribution of 'low-quality' resources such as sunlight have a significant impact on overall resource contribution in traditional energy and exergy analysis. This is a direct consequence of the fact that low quality resources are weighted equitably with other energy and natural resources in traditional energy and exergy analysis. However, emergy analysis corrects for the quality of resources by comparing them in terms of their solar equivalence. As such, their contribution is minimal when evaluated from an emergy perspective. Furthermore, resources of higher quality

(high transformity) such as metallic and non-metallic ores are found to comprise a larger fraction of total ecological resource contribution when evaluated via ECEC analysis. The results from Figure 11 show that crude oil constitutes over 85% of total resource consumption in energy, ICEC, and ECEC analysis of petroleum diesel production. As such, petroleum diesel requires less work from the economy for conversion to transportation fuel compared to microalgal biofuels, as the majority of past work has been provided by nature via the formation of crude oil. Consequently, this results in a higher ROI for petroleum diesel relative to microalgal renewable diesel.

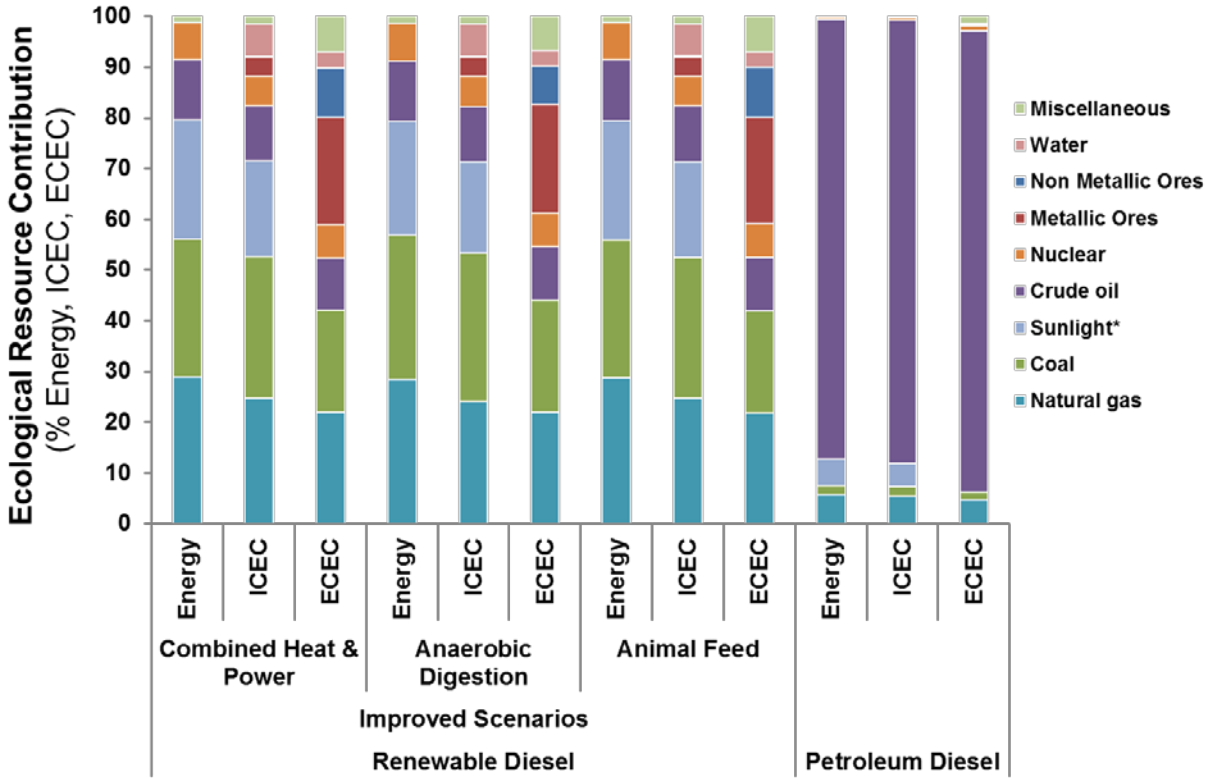

Figure 11. Fractional Contribution of total Energy, ICEC, ECEC by Ecological Resource for Microalgal Renewable Diesel and Petroleum Diesel

Table 6 provides an overview of the ECEC sustainability and thermodynamic performance metrics for the scenarios considered in this work. The results show that petroleum

diesel has a high ECEC yield ratio as a larger amount of past work has been performed by nature in producing crude oil as compared to the direct and indirect solar exergy of purchased inputs from the economy required for its extraction, refining, etc. However, microalgal biofuels require substantial material and energy inputs from the economy, and a comparatively minimal amount of past work from direct ecological good and services (direct sunlight, freshwater, and photosynthetic CO_2). As such, the EYR for petroleum diesel is larger than that of microalgal derived renewable diesel. The results from Table 6 reveal that petroleum diesel has a low renewability index and low YLR, indicating that these fuels are not sustainable in the long-term. Additionally, the results indicate that production of microalgal biofuels is highly dependent on non-renewable ecological resources reflected in the low renewability index and YLR, and high ELR. The high ELR for microalgal derived RD (ELR>1 for all examined production pathways) indicates that more non-renewable ECEC is utilized in the algal-to-fuel supply chain as compared to renewable ECEC. Additional results for microalgal-derived biodiesel are provided in Appendix B.

Table 6. Comparison of ECEC thermodynamic performance metrics for microalgal renewable diesel and petroleum diesel

Transportation Fuel	**Petroleum Diesel**	**Microalgal RD (Baseline)**			**Microalgal RD (Improved)**		
Coproduct Scenarios	N/A	AF	AD	CHP	AF	AD	CHP
Renewability Index (%)	0.13	3.62	3.51	3.63	6.34	6.23	6.36
ECEC Yield Ratio	6.34	1.02	1.02	1.02	1.04	1.04	1.04
Environmental Loading Ratio	760.19	26.62	27.53	26.57	14.78	15.06	14.72
Yield-to-Load Ratio	0.01	0.04	0.04	0.04	0.07	0.07	0.07

Animal Feed (AF); Anaerobic Digestion (AD); Combined Heat and Power (CHP)

Figure 12 plots the ratio of ecological resource intensity of producing microalgal renewable diesel relative to petroleum diesel for a common functional unit, 1 mega-joule (MJ).

The results indicate that microalgal RD consumes significantly more metallic/non-metallic ores and water resources, and generally have higher ecological resource intensity as compared to petroleum diesel on a functional unit basis. For animal feed pathways microalgal RD provides benefits in the following ecological resources categories: crude oil, crushed ore, grass, sunlight, phosphorus and nitrogen mineralization, nitrogen deposition, detrital matter, soil erosion, fish, relative to petroleum diesel. For anaerobic (AD) and combined heat and power (CHP) coproduct scenarios, microalgal derived renewable diesel has higher ecological resource consumption relative to petroleum diesel across all resource categories except for crude oil and natural gas. These findings are startling and suggest that the large-scale adoption of microalgae biofuels could result in heightened ecosystem degradation, potentially negating the environmental benefits of these fuels. It is important to note that ECEC analysis considers energy and resource flows in complex coupled industrial-ecological systems, and thus has a high degree of uncertainty relative to traditional energy and exergy analysis. Coupling the results obtained via EcoLCA with dynamic ecological modelling [186] can provide a spatially and temporally explicit framework for quantifying the contribution of ecosystems goods, and potentially reduce uncertainty in the quantification of direct ecological goods and services. However, such an analysis is beyond the scope of this present study. Methods such as economic valuation of natural capital provide an alternative basis for valuing the contribution of EGS [187]. However, economic valuation is sensitive to market distortions and price volatility, and may not capture environmental externalities. Furthermore, economic valuation intrinsically considers the value added via a service or resource in regards to its utility for mankind. This anthro-centric framework is diametrically opposed to the eco-centric framework utilized in ECEC or emergy analysis.

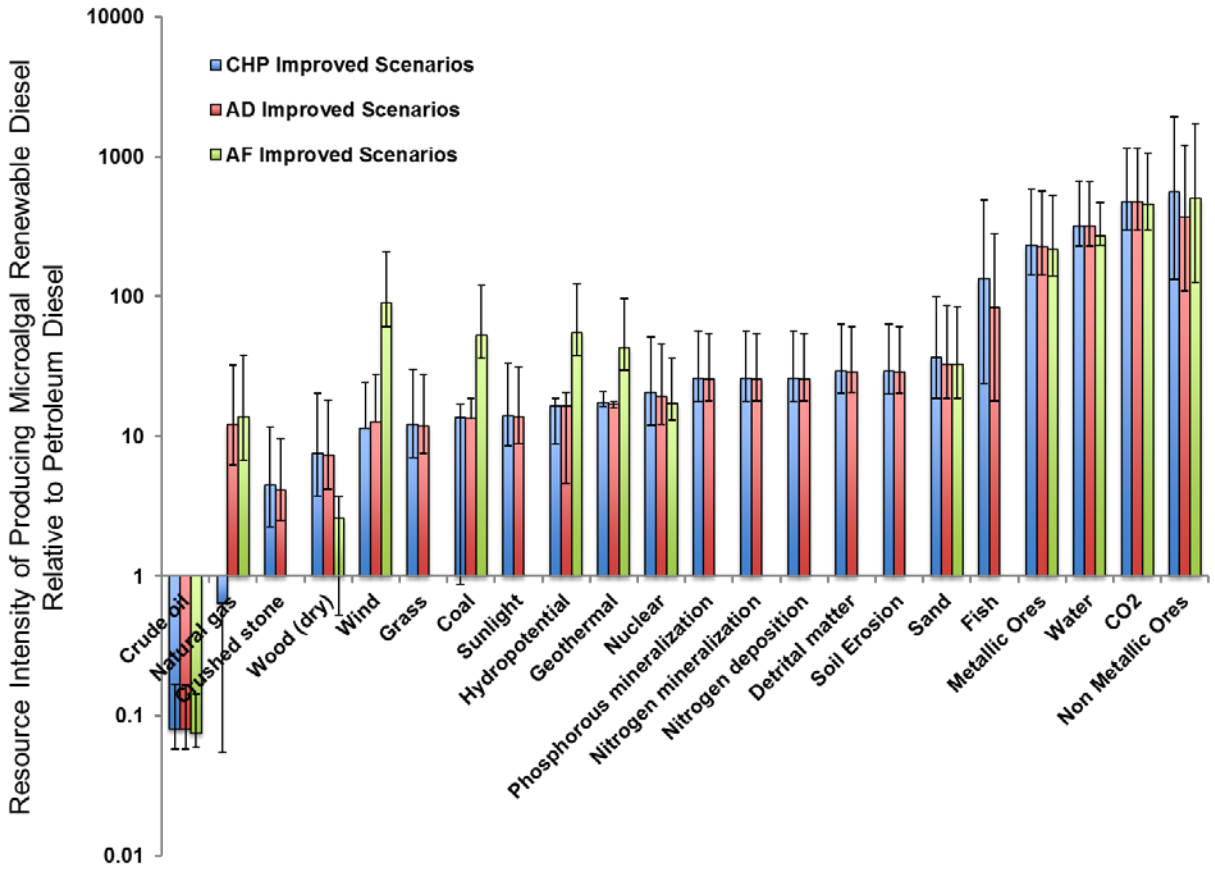

Figure 12. Ecological Resource Intensity of Producing Microalgal RD Relative to Petroleum Diesel.

Resource Intensity ratios were developed via taking the ratio of ECEC of resources required to produce one MJ of RD to the ECEC required to produce on MJ of PD. Coproduct(s) were accounted for via system boundary expansion, i.e. ECEC from coproduct(s) were subtracted from total resources use. Some columns are not shown due on the logarithmic graph due to negative value(s) that occur as a result of displacement.

Two strategies exist to enhance the performance and sustainability of microalgal biofuels: (1) reduce the amount of purchased inputs from the economy required for microalgal fuel production, or (2) leverage natural ecological processes to increase the amount of past work provided by nature in making microalgal biofuels available for human consumption. The first option can be met with increases in technological maturation and commercial optimization of algae-to-fuel conversion processes. Multiple strategies such as genetic modification [188],

hydrothermal liquefaction [189, 190], cross flow and membrane based filtration/separations [126], and industrial symbiosis [82] via the use of wastewater [191, 192] and other synergies are being explored for increasing the performance of emerging microalgal biofuel systems. However, it is important to recognize that microalgae biofuel production is ultimately constrained via the 2nd law efficiency, i.e. the minimum thermodynamic work required for fuel production [193]. For the second option, it is possible to envision a scenario in which microalgae are consumed via predators at a higher trophic level in the ecological food chain (such as fish). Assuming that the lipid fraction of the microalgae be absorbed and retained via these predators, it may be possible to harvest and utilize these organisms for conversion to liquid transportation fuels [194], effectively allowing nature to perform the work traditionally required via energy intensive dewatering and conversion processes. Additionally, alternate microalgal processing options such as solar drying of the biomass may reduce the amount of human made work required for biofuel production. However, the high land-use requirements for solar drying may limit its commercial applicability.

3.5 CONCLUSIONS

Failure to consider the impacts of emerging technologies on ecological goods and services before their widespread adoption and use could result in unsustainable choices and dramatic consequences for the earth's ecosphere including heightened depletion and degradation of the global ecological resource base, potentially straining the ecological functions that support human life. Thermodynamic analysis based on exergy and emergy provides a scientifically rigorous approach for valuing the contribution of ecological goods and services in product life cycles, and

concurrently addresses several existing problems in traditional energy analysis including accounting for the quality, substitutability, and useful work provided via material and energy resources. This chapter highlights the misconceptions of traditional energy analysis, and shows that exergy and emergy analysis can provide valuable insights into the sustainability and performance of emerging microalgal biofuel systems. This work has shown that in the best-case scenario microalgal fuel systems are marginally energy positive, and more ecologically resource intensive as compared to their petroleum equivalent on a functional unit basis. However, technological maturation and optimization of the algae-to-fuel production chain as well as coupling microalgal biofuel production with ecological processes have the potential for reducing the amount of human made work required for biofuel production while concurrently increasing the sustainability of these emerging fuel systems. The hierarchical thermodynamic-based resource aggregation scheme utilized in this work can be extended to other nascent fuel and energy platforms and thus help guide the sustainable development and adoption of next-generation biofuels.

4.0 BIOFUELS VIA FAST PYROLYSIS OF PERENNIAL GRASSES: A LIFE CYCLE EVALUATION OF ENERGY CONSUMPTION AND GREENHOUSE GAS EMISSIONS

The following chapter is based on a peer-reviewed article published in *Environmental Science & Technology* with the citation:

Zaimes, G. G.; Soratana, K.; Harden, C. L.; Landis, A. E.; Khanna, V., *Biofuels via Fast Pyrolysis of Perennial Grasses: A Life Cycle Evaluation of Energy Consumption and Greenhouse Gas Emissions.* Environmental Science & Technology, 2015. **49**(16): p. 10007-10018.

4.1 CHAPTER SUMMARY

A Well-to-Wheel (WTW) life cycle assessment (LCA) model is developed to evaluate the environmental profile of producing liquid transportation fuels via fast pyrolysis of perennial grasses: switchgrass and miscanthus. The framework established in this study consists of: (1) an agricultural model used to determine biomass growth rates, agrochemical application rates, and other key parameters in the production of miscanthus and switchgrass biofeedstock; (2) an ASPEN model utilized to simulate thermochemical conversion via fast pyrolysis and catalytic upgrading of bio-oil to renewable transportation fuel. Monte Carlo analysis is performed to determine statistical bounds for key sustainability and performance measures including life cycle GHG emissions and EROI. The results of this work reveal that the EROI and GHG emissions (gCO_2e/MJ-fuel) for fast pyrolysis derived fuels range from 1.52 to 2.56 and 22.5 to 61.0 respectively, over the eight scenarios evaluated. Further analysis reveals that the energetic performance and GHG reduction potential of fast pyrolysis-derived fuels are highly sensitive to the choice of coproduct scenario and LCA allocation scheme, and in select cases can change the life cycle carbon balance from meeting to exceeding the renewable fuel standard emissions reduction threshold for cellulosic biofuels.

4.2 BACKGROUND

The threat of climate change is considered to be one of the most critical and far-reaching global challenges facing the U.S. and the world. Fuels derived from biomass resources represent a promising option for mitigating anthropogenic carbon emissions and related climate change impacts, while concurrently providing a potential large-scale domestic source of renewable transportation fuel and energy [22]. Subsequently, this has prompted the development of U.S. regulatory programs designed to increase domestic energy independence and security as well as mitigate GHG emissions from the transportation sector via establishing mandatory volumetric production targets and carbon reduction criteria for transportation fuels derived from biomass. In 2007 the U.S. congress passed the Energy Independence and Security Act (EISA), this legislation mandates the production of 36 billion gallons of renewable fuels by the year 2022, and stipulates that a percentage must be derived from conventional, cellulosic biofuel, biomass-based diesel, and advanced biofuels [11]. Additionally, EISA sets minimum life cycle GHG reduction standards for biofuels relative to baseline-petroleum fuels. Currently, corn based ethanol and soybean biodiesel are the most widely produced and utilized biofuels in the US [195]. However, critical concerns have been raised about the potential of corn ethanol and other first generation biofuels in mitigating climate change and reducing dependence on fossil fuels. Previous work has reported that the direct and indirect land use change (LUC) effects may possibly negate the carbon dioxide reduction potential of first generation biofuels [16, 17, 136]. Accordingly, the production of liquid fuels derived from non-food biofeedstocks such as forest and agricultural residues, industrial wastes, herbaceous crops, and microalgae [144, 147, 196, 197] has garnered widespread attention [9]. Fast growing perennial grasses such as miscanthus and switchgrass are considered an ideal candidate for conversion to biofuel/bioenergy due to

their high growth rates over a variety of soil conditions/types, ability to be cultivated and harvested utilizing conventional farming practices, and minimal nutrient requirements relative to other leading biofeedstocks [198, 199].

Substantial research and development has been invested in developing next generation hydrocarbon bio-refineries capable of converting lignocellulosic biomass into infrastructure-compatible liquid transportation fuels, i.e. biomass derived fuels that can act as drop-in replacements for petroleum-based gasoline, diesel, and jet fuels [7, 91, 200]. Recently, fast pyrolysis has emerged as a promising technological route for converting cellulosic biomass [201] into liquid transportation fuel and value-added products [37, 202, 203]. Fast pyrolysis is the process of thermal decomposition of organic matter in the absence of oxygen, at elevated temperatures [204] and short residence times [205]. Fast pyrolysis converts biomass into three main intermediate products: bio-oil, biochar, and non-condensable gases (NCGs). Bio-oil generated via fast pyrolysis can be upgraded using established refining technologies into renewable transportation fuel(s) [206] that are compatible with current fuel infrastructure and vehicle fleets [35]; while biochar can be co-generated via combined heat and power (CHP) to produce heat and electricity to be utilized internally in the fuel conversion system, or exported and used as a soil amendment for agricultural lands. As such, renewable fuel(s) derived via the fast pyrolysis of perennial grasses may be a favorable option for achieving policy mandated renewable energy/fuel targets focused on mitigating anthropogenic GHG emissions including the U.S. RFS2 [207], California Low Carbon Fuel Standard (LCFS) [208], and the EU's RED [209].

Prior work has investigated various sustainability aspects of fast pyrolysis of lignocellulosic biomass. Techno-economic analysis has shown that fast pyrolysis is competitive with other lignocellulosic fuel conversion platforms, and may be economically viable at a

commercial scale [37]. Several recent studies have evaluated the environmental impacts of producing liquid fuels by fast pyrolysis of microalgae [210], corn stover [201, 211], and woody biomass [203, 212-214] using LCA, and have shown that fast pyrolysis derived fuels may provide life cycle GHG reductions relative to petroleum fuels. However, little emphasis has been placed on environmental systems analysis of drop-in replacement biofuels derived via fast pyrolysis of perennial grasses. Additionally, the effect of different coproduct scenarios, allocation schemes, as well as uncertainty in the LCA results, is widely understudied in the literature.

This study performs a comparative life cycle assessment of renewable fuels derived via fast pyrolysis of perennial grasses switchgrass and miscanthus. Data for the agricultural production of perennial grasses is based on peer-reviewed literature and technical reports from field trails. Additionally, this work develops an ASPEN model to simulate the thermochemical conversion of lignocellulosic biomass to fuel and utilizes Monte-Carlo simulation to account for uncertainty and variability in key LCA metrics. The main objectives of this study are to (1) quantify the EROI and life cycle GHG emissions for renewable fuels derived via fast pyrolysis of miscanthus and switchgrass biofeedstock and catalytic upgrading of resultant bio-oil; (2) investigate the sensitivity of the results to various LCA allocation schemes as well as several coproduct scenarios for biochar including: direct application as a soil amendment and co-generation to produce heat and electricity; (3) identify combinations of feedstock and biofuel pathways that meet the life cycle GHG reduction threshold as set by the RFS2; (4) identify areas for process improvement in the biomass-to-fuel supply chain; (5) compare the environmental performance of fast pyrolysis derived fuels to the production of other leading biofuels. These insights are pivotal for guiding the sustainable adoption of biofeedstocks for fuel conversion, and

for benchmarking the performance and environmental sustainability of emerging fast-pyrolysis thermochemical fuel platforms.

4.3 PROCESS DESCRIPTION, DATA, AND METHODS

Process inventories for the production of miscanthus and switchgrass feedstock were developed based on peer-reviewed literature; while data for fast pyrolysis and fuel upgrading were constructed based on a combination of detailed ASPEN simulation, experimental data, and best available engineering knowledge. An overview of the biomass-to-fuel process is provided in Figure 13.

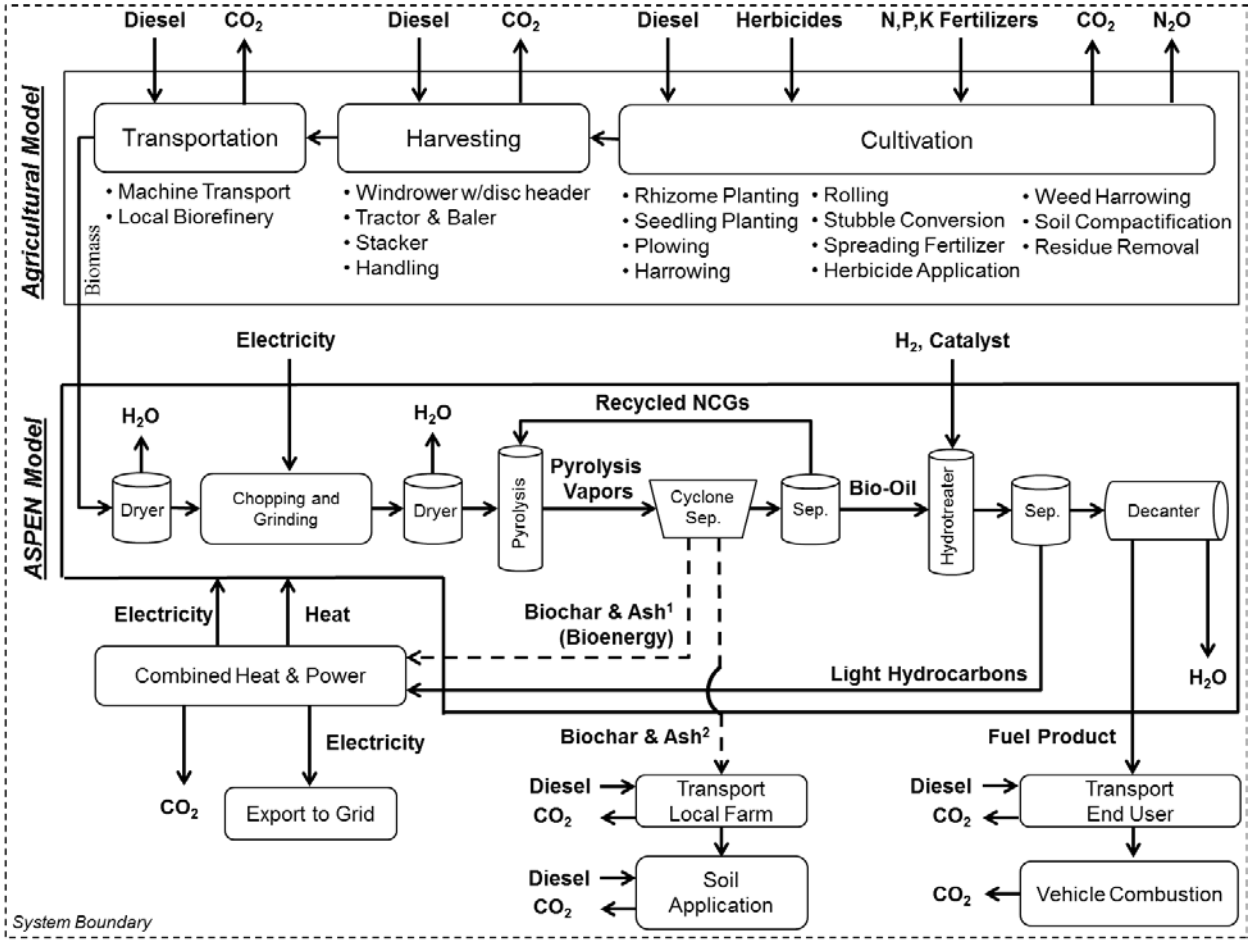

Figure 13. Simplified Block Diagram: Fast Pyrolysis biofuel production chain. Scenario 1 (*Bioenergy Pathway*): Biochar is sent to a Combined Heat and Power unit for conversion to heat and electricity. Scenario 2 (*Soil Amendment Pathway*): Biochar is sent to a local farm to be applied as a soil amendment.

4.3.1 Agricultural Model

Production of miscanthus and switchgrass feedstock is modeled assuming a 10 and 15-year stand life [215], respectively. Perennial grasses require an initial establishment year, and approximately 3 years until optimal crops yields are achieved [216]. In the initial establishment period, several land/farm preparations are performed including plowing, harrowing, rolling, herbicide application, soil compactification, and rhizome/seedling planting. For miscanthus feedstock, it is assumed that rhizomes from mature perennial grasses are planted directly in the

field [216], thus avoiding the high energetic costs of producing plantlets via greenhouses. Herbicides are applied during the first and second year of establishment to control and mitigate the growth of invasive plant species [217]. Herbicides are not required post third year, as weed interference is effectively suppressed once the perennial grass achieves maturity. Additionally, fertilizers are not applied during the first two years of establishment as they are subject to large losses/high runoff rates and encourage the growth of other unwanted weeds and grasses. Furthermore, irrigation is not required due to the low economic value of the produced biomass [218]. Post-3rd year of establishment, it is assumed that fertilizers are applied annually (once per harvest cycle) to mitigate soil nutrient depletion and maintain overall soil quality [215]. However, it is important to note that numerous field trails have shown that perennial grasses have limited to no yield response to heighten N-fertilizer application [219-222], and it is possible that these crops require marginal synthetic fertilizer for growth. As such, the assumptions in this study represent a conservative estimate for fertilizers required for biofuel production.

Miscanthus and switchgrass feedstock(s) are harvested once per year during the late fall via a windrower and baler, each with an average field efficiency of 80% [223]. Late (*delayed)* harvest lowers total dry matter yield relative to peak harvest; however, it substantially decreases the moisture content (MC) of the harvested biomass [224, 225]. This is favorable as it reduces the amount of energy required for feedstock drying prior to fuel conversion. Post harvesting, baled biomass is transported to a local biorefinery via lorries. Densification and/or long-storage of biomass is not considered in the present work, but due to logistic and geographic constraints may be required for commercial biofuel production. The average round trip distance from farm to refinery is assumed to be 100 km, with 2500 metric tons of biomass delivered to the biorefinery at a moisture content of 20% weight/weight (w/w) [226].

Probability distribution functions (PDFs) for switchgrass yields were developed based on the Global Switchgrass database [227], which contains over 1190 observations from 39 field trials conducted across the United States [228-243]. Distributions for miscanthus yields were estimated based on values reported in peer-reviewed studies and field trials [207, 217, 219-222, 244-246]. Average switchgrass and miscanthus yield is estimated at 11.04 dry metric tons per hectare (t/ha) and 15.29 t/ha, respectively. PDFs for direct volatilization of N fertilizer (N_2O conversion rates) were estimated based on 59 trials conducted on various agricultural lands. Indirect N volatilization is developed based on estimates of soil nitrogen leaching and run-off rates as well as conversion rates of soil N to N_2O as reported by the Intergovernmental Panel for Climate Change (IPCC) [247]. PDFs for diesel use in farming practices including: plowing, soil compactification, harrowing, rolling, stubble conversion, spreading fertilizer, and weed harrowing were constructed based on a survey of published literature reported in Dalgaard et al [248]. Point estimates were used for diesel use in rhizome/seedling planting, windrower harvesting, baling, stacking, and handling. Summary information for distribution types as well as a detailed summary of all inventory data is provided in Appendix C.

4.3.2 Fast Pyrolysis and Fuel Upgrading Model

An ASPEN process model is developed using Aspen Plus version V8.6 software to simulate the thermochemical conversion of cellulosic biomass to bio-oil, and catalytic upgrading of resultant bio-oil to renewable transportation fuel. The developed ASPEN model provides a scientifically rigorous basis for determining the utility requirements as well as material and energy flows for conversion of cellulosic biomass to liquid transportation fuel. Furthermore, the fuel upgrading and conversion model provides important details such as the liquid carbon yield, product

distribution, and hydrogen consumption for fast pyrolysis conversion of cellulosic feedstock to renewable transportation fuel. The primary stages in the fuel conversion and upgrading model consist of pretreatment, thermochemical conversion of biomass via fast pyrolysis, hydroprocessing of bio-oil to renewable fuel, coproduct integration/use, and fuel/coproduct transportation.

This work models a theoretical stand-alone biorefinery operating at a throughput of 2000 dry metric ton-biomass/day, consistent with the design case provided in Jones et al. [249] and Wright et al. [37] Biomass received by the refinery is dried to a moisture content of 15% w/w and subsequently chopped/ground via a hammer mill and screened until the exiting mass has a particle size diameter of 3mm [250]. Reduction in particle size increases total heat transfer area, resulting in high heat transfers rates. Energy requirements for chopping/grinding of switchgrass and miscanthus were developed based on empirical correlations provided in Miao et al. [251] After chopping/grinding, biomass is dried to a moisture content of 7% w/w and sent to a fast pyrolysis reactor operating at 1 atmosphere (atm) and 500 ^{o}C. Product distribution for fast pyrolysis was constructed based on experimental results for pure (dry, ash-free) hemicellulose, cellulose, and lignin provided in Patwardhan [38, 39]. Feedstock specific product characterization is obtained via weighting the product distribution based on the fractional cellulose, hemicellulose, and lignin content of the input biofeedstock. It is important to note that trace minerals in biomass can act as catalysts during thermochemical conversion of biomass to fuel, and thus alter the resulting product distribution. However, the effect of differing mineral concentrations on the product distribution of fast pyrolysis derived fuels is beyond the scope of this work, and thus is not considered. The study by Patwardhan captured/identified 84.3-92.9% of the input feed mass in their spectrometric analysis of the products of fast pyrolysis, and

speculated that the unaccounted mass is primarily in the form of water vapor and other light molecular compounds [38, 39]. In this work, to satisfy overall mass and elemental balances, an optimization routine is performed to determine the composition of the unaccounted mass via minimizing the Gibbs free energy of formation of several light hydrocarbons as well as gaseous compounds including: CO, CO_2, H_2O, H_2, C_2H_6, C_3H_6, and C_3H_8. Analysis indicates that the product distribution for fast pyrolysis ranges from 44.56-53.1% bio-oil (dry basis), 12.0-17.5% biochar and ash, 24.4-27.2% non-condensable gases, and 10.5-10.8% water on a mass basis for the two feedstocks considered in this work. The resultant product stream is sent to a cyclone separator to separate biochar/ash from pyrolysis vapors and NCGs.

Two coproduct scenarios were considered for biochar formed via fast pyrolysis, denoted as Bioenergy (BE) and Soil Amendment (SA) pathways. In the first scenario biochar is sent to a combined heat and power unit for conversion to electricity and heat. Coproduct heat generated via CHP is used to offset processing heating requirements, while excess heat is discarded. Coproduct electricity is utilized internally in the fuel conversion system, while any surplus electricity is exported to the grid. The higher heating value (HHV) of biochar/ash is estimated based off of its fractional element composition (% C,H,O,N,S, & Ash) via correlations provided in Channiwala and Parikh [252], and is estimated to be 23.81 MJ/kg for miscanthus and 24.22 MJ/kg-biochar for switchgrass. CHP conversion efficiencies for electricity and heat were assumed to range from 20% to 35% and 44% to 52%, respectively [253]. In the second scenario, biochar is transported to a local farm to be applied as a soil amendment [254]. The use of biochar as a soil amendment may provide many benefits to local farms/agricultural land [48, 255] including: reduction of N_2O emissions and leaching of nitrogen into groundwater[256], improved soil fertility, moderating soil pH [46], heightened retention of soil nutrients and water [44], and

increased number of beneficial soil microbes [43]. Due to lack of data regarding the bioavailability of the nutrient content of the biochar it is assumed that the application of biochar does not displace synthetic fertilizer (N, P, K) requirements. Additionally, this works assumes that up to 20% of the carbon content of the biochar is released to the atmosphere as carbon dioxide [257]. Energy use for machinery required to spread/apply biochar to farmland is estimated based on diesel use for spreading and loading manure.

Post cyclone separation pyrolysis vapors are cooled and separated from NCGs via a quench, while NCGs are recycled back to the pyrolysis reactor to act as a fluidizing agent and are flared and vented onsite. Bio-oil is highly oxygenated and must be hydrotreated prior to use in commercial vehicle engines. As such, bio-oil produced via fast pyrolysis is sent to a hydrotreating unit utilizing a catalyst bed operating at 400 ^{o}C and 2000 psig [258, 259], wherein it is catalytically hydrodeoxygenated (HDO) [260]. Hydrogen requirements for HDO were constructed based on stoichiometry, i.e. the amount of hydrogen necessary for complete removal of oxygen from bio-oil compounds and hydrogen required for saturation of carbon compounds. Furthermore, it is assumed that all hydrogen is externally sourced and produced via steam methane reforming. The high efficiency and low cost of fossil hydrogen production via steam methane reforming relative to other renewable hydrogen producing platforms such as hydrogen from steam reforming biomass or electrolyzing water using wind or solar energy sources, make it attractive as a commercial source of hydrogen for biofuel production. However, future work should investigate the economic and environmental tradeoffs of catalytic steam reforming the aqueous fraction of fast pyrolysis bio-oil to produce hydrogen for subsequent use in downstream conversion of bio-oil to renewable fuel. The mass of hydrogen consumed relative to input bio-oil

feed is approximately 8.16 and 8.23% on a dry basis or 6.57 and 6.87% on a wet basis for switchgrass and miscanthus respectively.

After hydrotreating, light hydrocarbons (C1-C4 molecular species) are separated from the fuel pool via distillation and are sent to an onsite CHP unit to be combusted to produce heat and electricity. Higher carbon chain molecular species (C5+) are then separated from water via a decanter centrifuge, and transported to a regional fuel facility assuming an average round trip distance of 100 km. Combustion of biofuel and bioenergy products was modeled based on stoichiometry, under the assumption that that all carbon is converted to CO_2. Final renewable fuel is comprised of carbon compounds ranging from C5 to C11 in carbon number, and is chemically similar to petroleum gasoline. In the absence of biofuel loss due to coking, the fraction of carbon in final fuel and coproducts relative to carbon in the input biomass feed ranges from 37.0 to 44.1% in the liquid transportation fuel, 9.39 to 9.42% in light hydrocarbons (C1-C4 molecular species), 18.0 to 24.7% in ash and biochar, and 28.6 to 28.8% in NCGs for the different biofeedstocks. The ASPEN energy analyzer module is utilized to optimize heat integration for the fuel conversion/upgrading system, and estimate net heating and cooling requirements. The results show that after heat integration, the heating requirements for fuel conversion and upgrading range from 1.22 to 1.25 MJ heat/kg-dry biomass. Total electricity requirements for pretreatment, fuel conversion, and upgrading including: chopping/grinding, compression, and pumping requirements are approximately ~ 0.63 MJ electricity/kg-dry biomass for either switchgrass or miscanthus. PDFs were developed for several key parameters in the fuel conversion and upgrading module including: catalyst lifetime, CHP heat and electricity conversion efficiency, biochar carbon sequestration, loss of biofuel due to coking, weight hourly

space velocity (WHSV), and transportation distance. Summary information for distribution types as well as a detailed summary of all inventory data is provided in Appendix C.

4.3.3 Methodology

The scope of the LCA is well-to-wheel and the functional unit is chosen as 1 MJ of renewable fuel. As such, carbon dioxide absorption (i.e. *Biogenic* CO_2) and combustion emissions are considered in the analysis. It is important to note that the functional unit considered in this work does not account for vehicle fuel use efficiency, and was selected so that the results are comparable to prior published literature [261]. The developed LCA model translates process data including material, energy, emissions, and heat flows into specific impacts on energy and the environment. In this work the Intergovernmental Panel for Climate Change (IPCC) 100-year Global Warming Potential (GWP) characterization factors [262] are utilized to quantify the life cycle GHG emissions for biofuel production while the Cumulative Energy Demand (CED) methodology [263] is utilized to determine primary energy consumption. Life cycle data is obtained from the ecoinvent database [111]. Infrastructure related environmental impacts, as well as direct and indirect land use change impacts, are not considered in this study. Thus, changes in the above and below-ground soil organic carbon (SOC) dynamics and carbon balances are beyond the scope of this work and thus not considered in the analysis. However, past research has shown that the LUC impacts can play an important role in the carbon balance for the production of biofuels [264].

In this study, probability distribution functions (PDFs) are developed for key parameters in the cultivation, harvesting, and transportation of switchgrass and miscanthus feedstock as well as the upgrading and conversion of bio-oil to renewable transportation fuel. Anderson-Darling

statistical tests are performed to determine the distribution type and parameters that best fit the sample data. All physically relevant and/or possible families of distributions are considered including: normal, triangular, lognormal, weibull, gamma, extreme value, exponential, and loglogistic. These probability distribution functions are randomly sampled via Monte Carlo simulation (10,000 trials) to capture uncertainty in the life cycle inventory (LCI). Uncertainty in the life cycle impact assessment (LCIA) is captured via the use of Monte Carlo simulation (10,000 trials) to randomly sample from statistical distributions for environmental impact factors obtained from the Ecoinvent database. Addressing uncertainty in a stochastic manner, at both the process and life cycle-scale, allows for a broader understanding of the expected range for key life cycle sustainability and performance metrics. Summary information for distribution types as well as a detailed summary of all inventory data is provided in the supporting information (SI).

Two LCA schemes were considered for dealing with coproducts in this work: (i) energy-based allocation and (ii) displacement method (Disp.). In energy-based allocation, environmental burdens are partitioned between final renewable fuel and coproducts (bioelectricity, useable heat) based on their fraction of total energy flow. For the displacement method, coproducts generated via a process/system are assumed to displace an existing product; the system is then credited with the avoided life cycle energy use and environmental burdens of the displaced product(s). In this work it is assumed that heat generated via CHP would displace heat derived via combustion of natural gas, while electricity generated via CHP displaces the U.S. average electricity mix. Only useable heat (i.e. heat used to meet system-wide heat duty requirements) generated via CHP are considered in energy allocation and displacement calculations. For soil amendment (SA) scenarios, carbon sequestered via biochar is subtracted from total life cycle GHG emissions. It is important to note that energy based allocation is the preferred method of the EU

in determining fuels eligible for the RED, while displacement is the favored method of the U.S. Environmental Protection Agency (EPA) for determining fuels eligible for the renewable fuel standard (RFS2). Additionally, economic- and/or exergy-based allocation provide a method for adjusting for the difference in quality of energy and material resources and thus overcome many of the limitations of traditional energy allocation. However, economic and exergy-based allocation are beyond the scope and goal of the current work, but should be considered in future analysis.

4.3.4 Sustainability Metrics

Energy return on investment and life cycle GHG emissions have been extensively used to quantify and compare the energy intensity and GHG reduction potential of producing transportation fuel(s) derived from biomass feedstocks [19, 144, 265]. Net life cycle GHG emissions are calculated based on the quantity of life cycle GHGs emitted throughout the biomass supply chain as well as carbon credit and/or impacts allocated to coproducts, and is contingent on the choice of LCA scheme utilized for dealing with coproducts. This work identifies biofuel pathways that meet the US EPA Renewable Fuel Standard for cellulosic biofuels, i.e. 60% reduction in overall life cycle GHG emissions relative to baseline petroleum fuels (~92 gCO_2e/MJ-fuel).

EROI quantifies the amount of primary energy required to produce a functional unit of transportation fuel energy evaluated over the entire supply chain. As the primary motivation for biofuel production is its potential to displace fossil derived fuels, a fossil energy return on investment metric is chosen to assess the sustainability of biofuel production. In this work, EROI is defined as the ratio of output biofuel energy to the embodied primary fossil energy required for

its production, and is presented in equation 6. Output biofuel energy is calculated based on the mass flow of fuel compounds (pentane, hexane, etc.) and their respective lower heating value (LHV).

$$EROI = \frac{\sum(Fuel\ compound)*(LHV)}{Biofuel\ Share\ of\ Primary\ Fossil\ Energy\ Invested} \quad (6)$$

EROI values greater than 1 are desirable, as more energy is provided by the biofuel as compared to the primary fossil energy required for its production. Recent studies have proposed that a liquid fuel must have a minimum EROI of 3 in order to support the U.S. transportation system [178]; and, failure to meet such criteria could have significant economic and societal implications [266, 267]. As such, it is critical to identify biofuel pathways that achieve life cycle GHG reductions targets as set by the RFS2 and have favorable EROI profiles, i.e. comparable to petroleum fuels and leading first generation biofuels.

4.4 RESULTS AND DISCUSSION

4.4.1 Life Cycle Energy Analysis

Figure 14 plots the median EROI for producing renewable fuels from miscanthus and switchgrass biofeedstocks, error bars represent the 10^{th} and 90^{th} percentile. Median values are presented instead of average values, as the distributions for EROI are highly skewed and non-symmetric. For each feedstock two allocation scenarios (displacement and energy allocation) as well as two biochar coproduct scenarios (use as a soil amendment or cogeneration to produce bioenergy) were evaluated. The results reveal that the median EROI for fast pyrolysis derived

fuels range from 1.52 to 2.56 over the host of pathways evaluated, with similar trends found for switchgrass and miscanthus. For BE scenarios, the EROI using displacement is significantly higher as compared to energy allocation and is a consequence of the avoided high upstream impacts of electricity generation—producing a large coproduct credit in displacement scenarios. As shown in Figure 14, the combination of coproduct scenario and allocation scheme can have a dramatic impact on the environmental performance of fast pyrolysis derived fuels. Additionally, the results reveal that the EROI is greater than unity for all examined biofuel pathways, indicating that these systems are net energy positive. However, none of the examined pathways meet the minimum EROI criteria of 3 as advocated by Hall and co-workers [178].

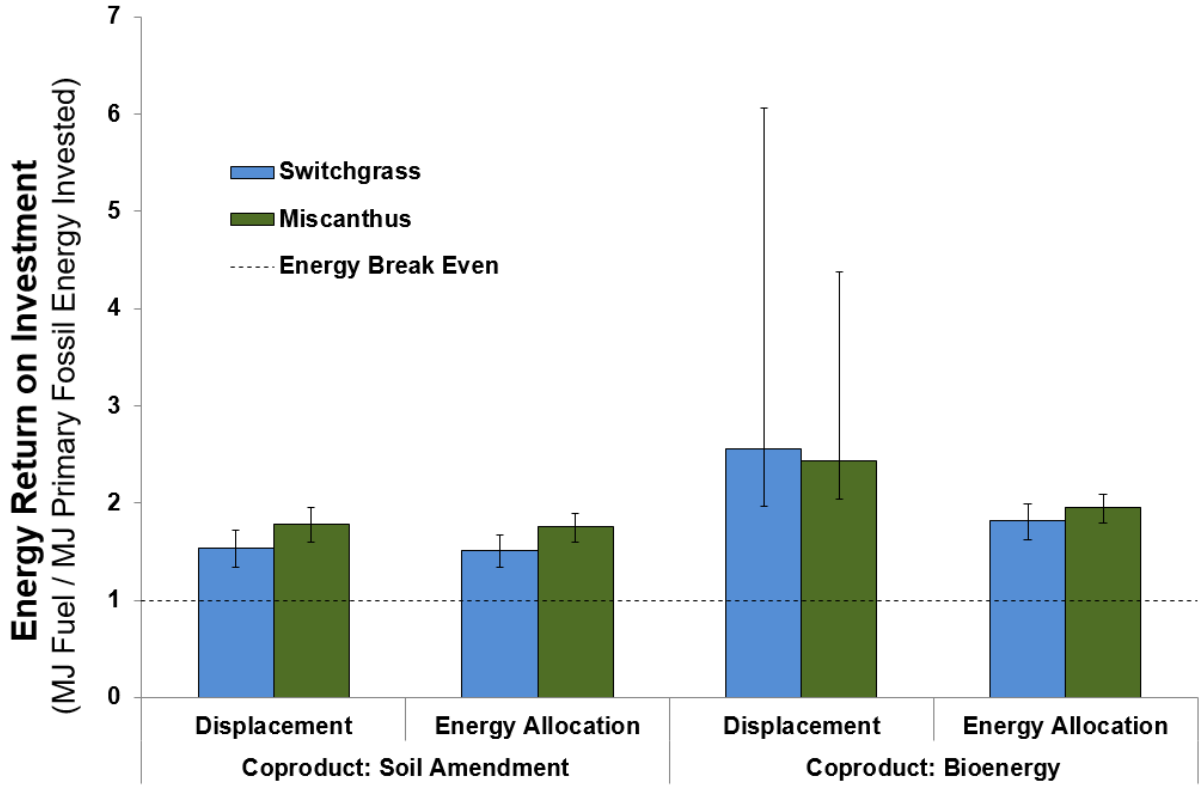

Figure 14. Energy Return On Investment for producing renewable fuels from miscanthus and switchgrass biofeedstock. Results are shown for displacement and energy-based allocation, as well as soil amendment and bioenergy coproduct scenarios. Median values (i.e., 50th percentile) are shown; error bars represent the 10th and 90th percentile.

Figure 15 presents the average fossil life cycle energy consumed by process input, normalized per MJ renewable fuel output. Results are shown utilizing the displacement methodology; negative values represent primary fossil energy credit(s) received from coproducts. The results from Figure 15 indicate that hydrogen and electricity requirements constitute the largest energy burdens in the biomass-to-fuel supply chain. Primary energy consumption for hydrogen is ~0.38 MJ primary fossil energy/MJ-Fuel for either biofeedstock; while electricity requirements account for 0.16 to 0.20 MJ primary fossil energy/MJ-Fuel for miscanthus and switchgrass respectively. Additionally, the combustion of light hydrocarbons and/or biochar to produce heat and bioelectricity results in a significant coproduct credit, up to -0.79 MJ primary energy/MJ-Fuel for switchgrass bioenergy scenarios. Further analysis reveals that fuel conversion and upgrading stages constitute over 75% of total fossil life cycle energy consumption in the biomass to fuel supply chain. As such, minimizing the quantity of hydrogen and electricity required for fuel conversion will be crucial for increasing the energetic performance of fast pyrolysis derived biofuels. The findings of the present work compare favorably with those reported in prior studies [212, 268].

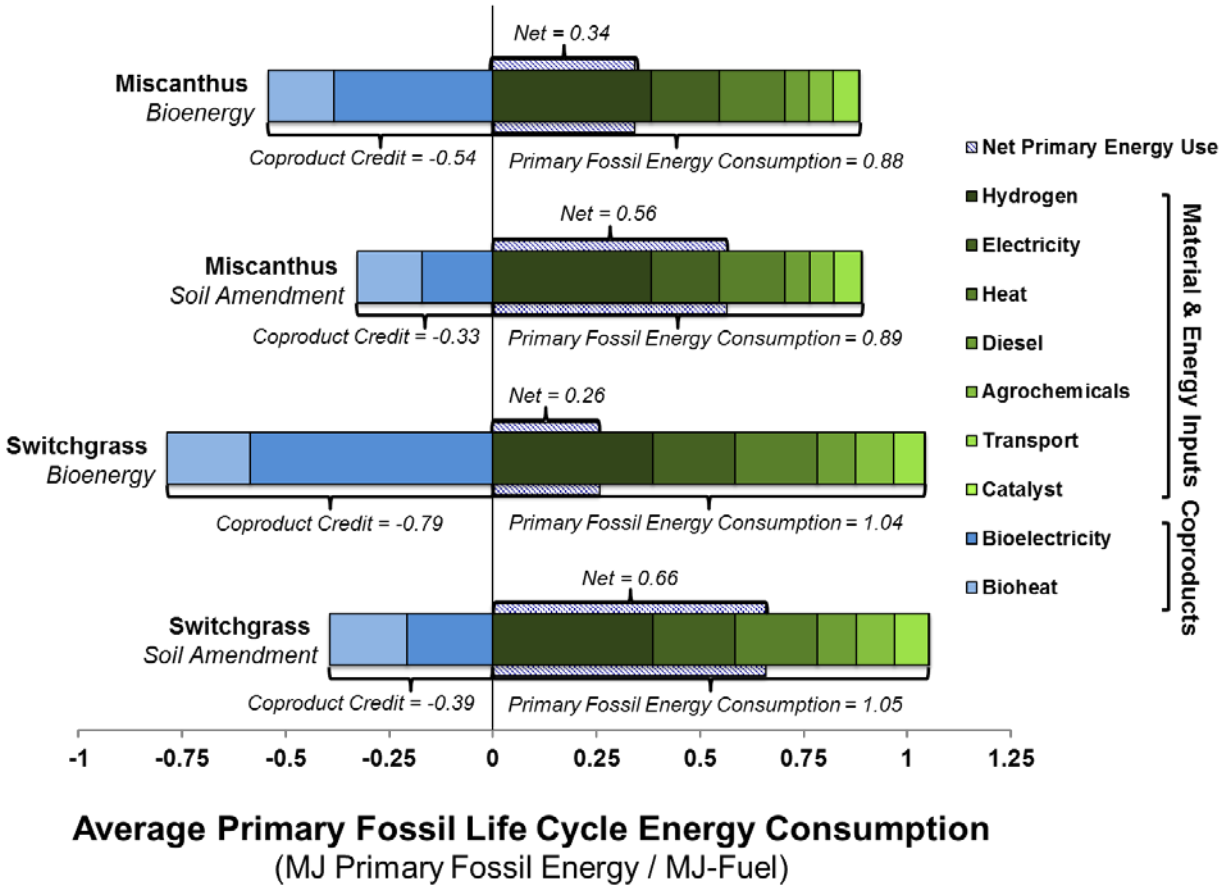

Figure 15. Life cycle fossil energy analysis. Average primary energy impacts for process inputs and coproduct are normalized to 1 MJ of renewable fuel. Results for displacement methodology are provided. Net primary energy use represents the difference between primary fossil energy consumed in the supply chain and coproduct primary fossil energy credit.

4.4.2 Life Cycle GHG Analysis

Figure 16 presents the median life cycle GHG emissions for producing renewable fuels from miscanthus and switchgrass biofeedstocks. The results reveal that the life cycle GHG emissions for fast pyrolysis derived fuels range from 22.5 to 61.0 gCO_2e/MJ-fuel. The choice of displacement or energy allocation has a significant impact on the LCA results; with miscanthus

and switchgrass meeting the RFS2 GHG reduction threshold under soil amendment (SA) pathways, but exceeding the threshold for bioenergy (BE) pathways. These results are significant as they indicate that the choice of biofeedstock, coproduct scenario, and allocation scheme can change the life cycle GHG emission profile of fuels derived via perennial grasses from *meeting* to *exceeding* the GHG reduction threshold as established by the RFS2.

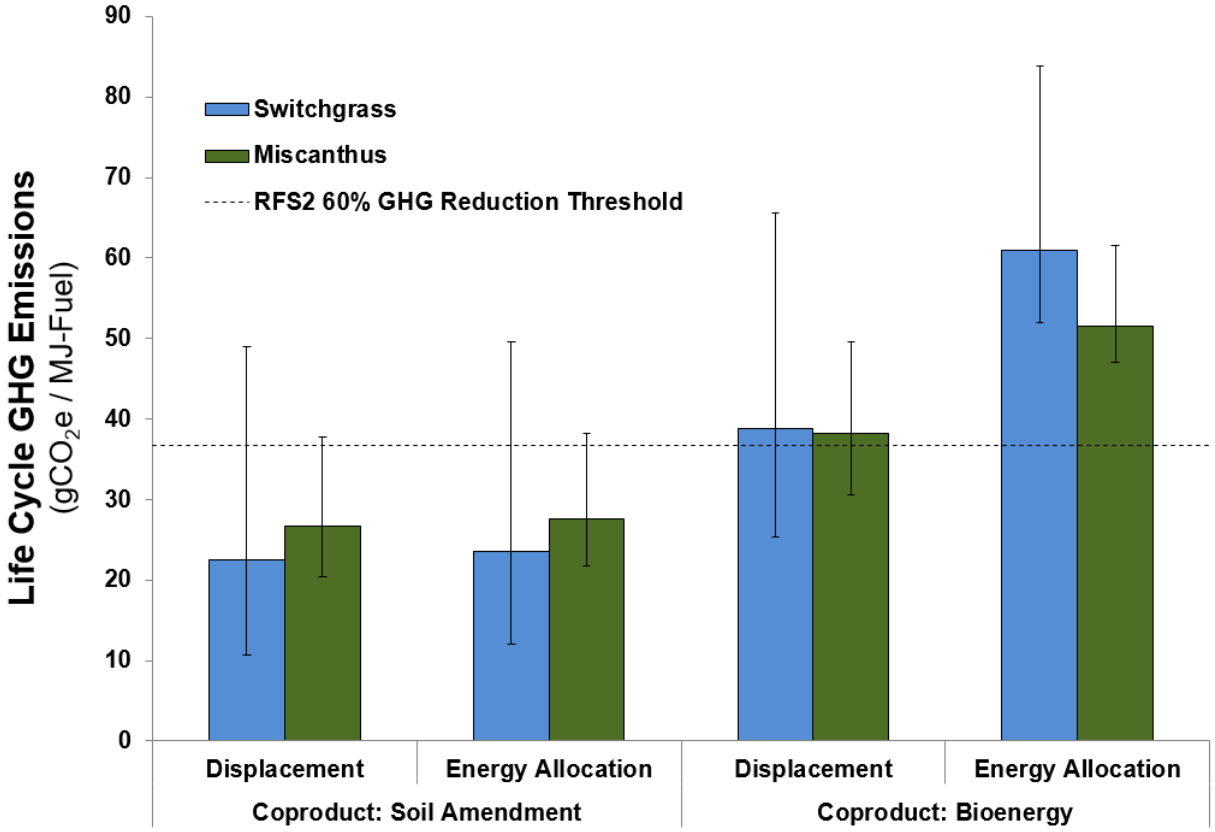

Figure 16. Life cycle GHG emissions for producing renewable fuel from miscanthus and switchgrass biofeedsock. Results are shown for displacement and energy-based allocation, as well as soil amendment and bioenergy coproduct scenarios. Median values (i.e., 50th percentile) are shown; error bars represent the 10th and 90th percentile.

The average life cycle GHG emissions by process input normalized per unit fuel energy output are presented in Figure 17. Results for displacement methodology are shown, negative values represent life cycle GHG credit(s) received from coproducts. The results from Figure 17

indicate that hydrogen, agrochemicals, and electricity requirements have the largest global warming potential impacts in the biomass-to-fuel supply chain. Figure 17 reveals that hydrogen impacts account for approximately 38.7 gCO_2e/MJ-fuel for switchgrass and 38.2 gCO_2e/MJ-fuel for miscanthus feedstocks, agrochemical impacts account for over 26.5 gCO_2e/MJ-fuel for switchgrass and 11.9 gCO_2e/MJ-fuel for miscanthus feedstocks, while electricity requirements account for 16.8 gCO_2e/MJ-fuel for switchgrass and 13.9 gCO_2e/MJ-fuel for miscanthus feedstock. Additionally, the results from Figure 17 show that biochar sequesters, on average, 49.0 gCO_2e/MJ-fuel for switchgrass and 29.7 gCO_2e/MJ-fuel for miscanthus. The GHG reductions for biochar are significantly higher for switchgrass as compared to miscanthus, due to increased rate of biochar formation as a result of higher lignin content.

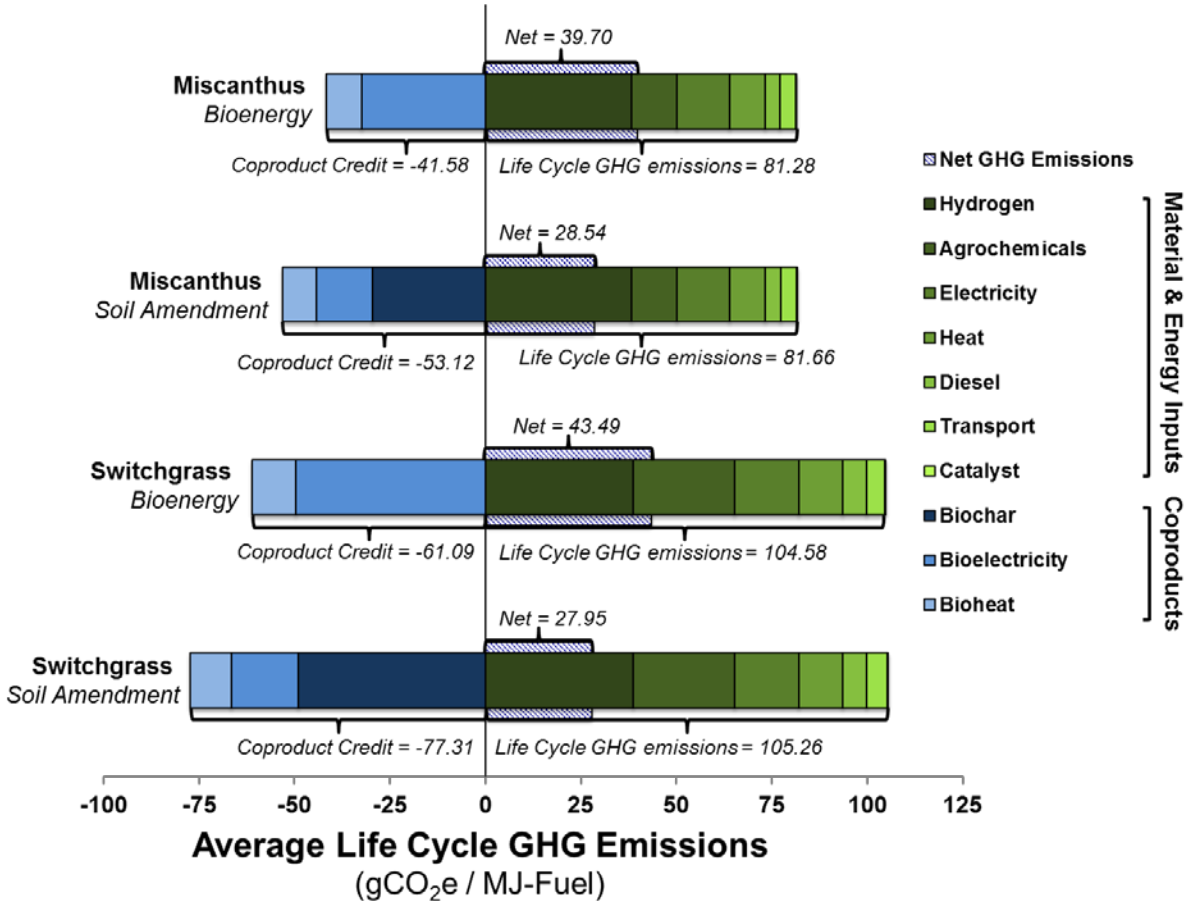

Figure 17. Life cycle carbon footprint analysis. Greenhouse gas emissions for material and energy inputs as well as coproduct credits are normalized to 1 MJ of renewable fuel. Results for displacement are provided. Net life cycle GHG emissions represent the difference between GHGs (direct and indirect) emitted throughout the life cycle and coproduct GHG credit.

4.4.3 EROI vs Life Cycle GHG Emissions

Figure 18 presents a comparison of EROI vs life cycle GHG emissions for fast pyrolysis-derived biofuels against select first generation, second-generation (i.e. cellulosic ethanol), and petroleum fuels. As shown in Figure 18, 1st generation biofuels such as corn and sugarcane ethanol are found to have higher GHG emissions relative to 2nd generation fuel derived from corn stover, miscanthus, or switchgrass. Additionally, the results reveal that sugarcane ethanol has a high

EROI (~4.3) exceeding the EROI performance threshold of 3, while corn ethanol has a marginally positive energy balance. Figure 18 reveals a weak clustering of 2nd generation bioethanol derived from corn stover, switchgrass, and miscanthus, and shows that bioethanol generated via 2nd generation feedstocks are near carbon neutral and have a correspondingly high EROI (i.e. greater than 3). Fast pyrolysis derived gasoline is found to have significantly lower EROI and higher overall life cycle GHG emissions as compared to 2nd generation bioethanol derived via miscanthus or switchgrass. Fossil hydrogen consumption and process electricity requirements are primarily responsible for the low environmental performance of pyrolysis gasoline relative to other 1st generation and 2nd generation biofuels. It is important to note that bioethanol must be blended with existing transportation fuel prior to use in vehicle engines, while pyrolysis gasoline can be used as a drop-in replacement for existing hydrocarbon fuels. Petroleum diesel is found to have a high EROI (~4.8), yet have correspondingly high fossil GHG emissions (~92 gCO_2e/MJ-Fuel). These results highlight the challenge of producing liquid transportation fuel from biomass that is simultaneously carbon neutral over its life cycle, chemically similar to traditional hydrocarbon fuels, and energetically competitive with existing petroleum resources.

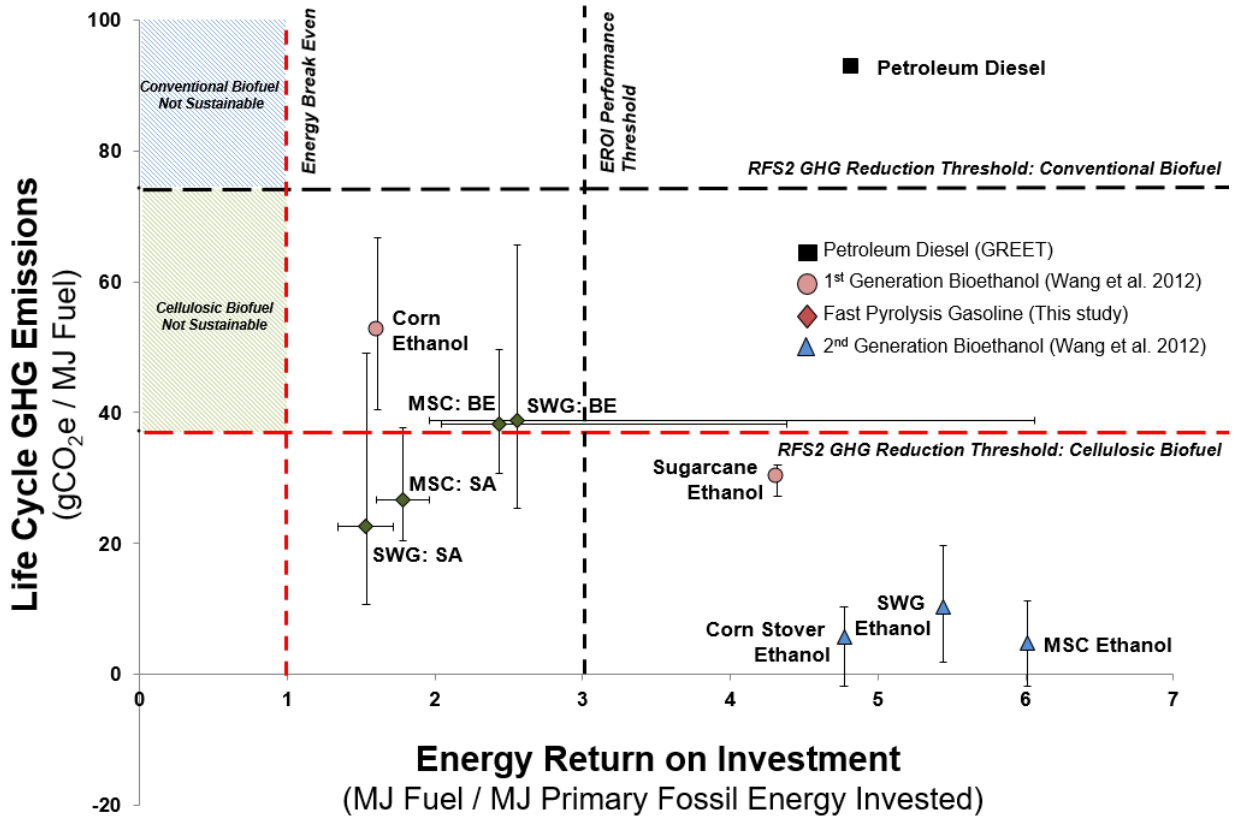

SWG: Switchgrass; **MSC**: Miscanthus; **SA**: Soil amendment; **BE**: Bioenergy

Figure 18. EROI vs Life cycle GHG emissions for select 1st generation and 2nd generation biofuels. Values for EROI and GHG emissions of fast pyrolysis fuels using the displacement method are shown. Values for 1st & 2nd generation bioethanol were obtained from Wang et al. 2012 (ref [261]) and do not consider direct or indirect LUC impacts. Values for petroleum diesel were adapted based on data obtained from the 2014 GREET model (ref [269]).

Direct and indirect land use change induced global warming impacts are not considered in this work. Estimates of LUC impacts for miscanthus and switchgrass derived ethanol range from -10 to -2.1 gCO_2e/MJ-miscanthus ethanol and 2.7 to 19 gCO_2e/MJ-switchgrass ethanol depending on the choice of domestic/international emissions modeling scenarios and model parameter(s) settings [270, 271]. Negative values for LUC impacts are due to changes in soil organic carbon (SOC) dynamics. This suggests that while LUC impacts may increase the carbon

footprint of switchgrass fuels, it has the potential to lower that of miscanthus derived fuels; and thus merits further investigation.

4.5 CONCLUSIONS

Further work is needed at the process level, such as determining ideal catalyst(s) for fuel conversion, effect of bio-oil on catalyst coking, and catalyst lifetime. High-level biomass/biofuel logistical and geospatial modeling [272] as well as economic evaluation should be concurrently considered to ensure that biofuel production is technically feasible and economically viable. The results of this work indicate that single-stage fast pyrolysis and hydroprocessing system have several limitations including: high hydrogen consumption, high production of light hydrocarbons, and low liquid carbon yield. A one-at-a-time (OAT) sensitivity analysis was performed to show how variations in individual parameters affect the LCA results (see Appendix C) Analysis reveals that the EROI and GHG emissions for single-stage fast pyrolysis systems are highly sensitive to bio-oil yield as well as hydrogen consumption. Alternative reactor configurations, process options, and chemical conversion pathways have the potential to reduce the hydrogen requirements for fuel conversion and upgrading while simultaneously increasing the liquid carbon yield, and thus increase the environmental sustainability of emerging thermochemical fuel platforms [32, 273], and should be considered in future environmental sustainability analysis of pyrolysis derived biofuels. Furthermore, additional research is required to determine the far-reaching environmental implications and feasibility of commercial scale biofuel production and related coproduct scenarios. For example, while biochar scenarios show merit for reducing life cycle GHG emissions for fuel production, past research has suggested that

the application of biochar could have severe environmental ramifications, as a fraction of biochar may be lost to wind and seepage and thus pose an environmental hazard to local waterways and groundwater aquifers [45]. Accordingly, while energy return on investment and life cycle GHG emissions are important criteria for screening potential biofuel pathways for commercial use, other environmental criteria such as impacts on water and air quality, biodiversity, etc. must also be considered so that biofuel production does not generate adverse impacts on ecological and human welfare [274, 275].

5.0 MULTISTAGE TORREFACTION OF BIOMASS AND IN-SITU CATALYTIC UPGRADING TO HYDROCARBON BIOFUELS: ANALYSIS OF LIFE CYCLE ENERGY USE AND GREENHOUSE GAS EMISSIONS

The following chapter is based on an article currently pending submission to *Energy and Environmental Science* with the citation:

Zaimes, G. G., Beck, A. W.; Janupala, R. R.; Resasco, D. E.; Crossley, S. P.; Lobban, L. L.; Khanna, V., *Multistage Torrefaction of Biomass and in-situ Catalytic Upgrading to Hydrocarbon Biofuels: analysis of life cycle energy use and greenhouse gas emissions.* Resubmission to Energy and Environmental Science, November 2016.

5.1 CHAPTER SUMMARY

A well-to-wheel life cycle assessment (LCA) model is developed to characterize the life cycle energy consumption and greenhouse gas emissions profiles of a series of novel multistage torrefaction and pyrolysis systems for targeted thermochemical conversion of short rotation woody crops to bio-oil and in situ catalytic upgrading to hydrocarbon transportation fuels, and benchmark the results against a base-case fast pyrolysis and hydrodeoxygenation (HDO) platform. Multistage systems utilize a staged thermal gradient to fractionate bio-oil into product streams consisting of distinct functional groups, and multi-step chemical synthesis for downstream processing of bio-oil fractions to hydrocarbon fuels. Results at the process scale reveal that multistage system(s) have several advantages over the base-case including: (1) ~40% reduction in process hydrogen consumption and (2) the product distribution for multistage systems are skewed towards longer carbon chain compounds that are fungible with diesel-range fuels. LCA reveals that the median Energy Return On Investment (EROI) and life cycle greenhouse gas (GHG) emissions for multistage systems range from 1.32 to 3.76 MJ-Fuel/MJ-Primary Fossil Energy and 17.1 to 52.8 gCO2e/MJ-Fuel respectively, over the host of co-product scenarios and allocation schemes analyzed, with fossil-derived hydrogen constituting the principle GHG and primary energy burden across all systems. These results are compelling and indicate that multistage systems exhibit comparatively higher gasoline/diesel-range fuel yield relative to current technology and produce a high quality infrastructure compatible hydrocarbon

transportation fuel capable of achieving over 80% reduction in life cycle GHG relative to baseline petroleum diesel.

5.2 BACKGROUND

Anthropogenic derived climate change threatens to destabilize and damage the global stocks of economic, social, and ecological capital—the keystones of modern civilization, and thus is considered to be one of the most urgent, ubiquitous, and long-standing challenges facing humanity [4-6]. Carbon dioxide emissions resulting from fossil fuel use and industrial processes are the largest contributor to global greenhouse (GHG) gas emissions, constituting over 65% of total GHGs in 2010 [3]. Moreover, in 2013 energy production and use accounted for over 84% of total United States (U.S.) GHG emissions on a carbon dioxide equivalent (CO2e) basis [276]. Subsequently this has spurred worldwide efforts to transition to renewable, low-carbon, and sustainable energy technologies in an attempt to mitigate and curtail potential catastrophic climate destabilization, as evident by the historic 2015 Paris Agreement [277]. Furthermore, nation-states have enacted legislation that mandate annual renewable energy and volumetric fuel production targets, such as the Renewable Fuel Standard (RFS2) in the U.S. [11] and the Renewable Energy Directive (RED) in the European Union (EU) [278], that require renewable energy systems achieve life cycle GHG reduction thresholds relative to baseline fossil technologies.

Over the past decade, biomass-derived hydrocarbon transportation fuels have gained prominence as a potential low-carbon and sustainable solution to the global energy crisis [7-9].

Recently, thermochemical conversion of lignocellulosic biomass via pyrolysis and catalytic upgrading of bio-oil has garnered traction as a commercial platform for producing renewable fuel(s) and value-added coproducts [279, 280]. Pyrolysis is the process of thermal decomposition of organic matter at elevated temperatures (450-600 OC) in the absence of oxygen, and produces three main products: pyrolysis-vapors, biochar, and non-condensable gases (NCGs). Pyrolytic-vapors condense to form a highly oxygenated synthetic bio-oil that can be catalytically hydroprocessed for use as a petroleum fuel substitute [40, 280, 281], while residual biochar can be applied to agriculturally degraded lands for concurrent carbon abatement and soil reclamation and has also gained notoriety as a sustainable replacement for coal [48, 255, 282].

Agronomic-pyrolytic fuel platforms using lignocellulosic biomass exhibit several unique advantages over existing first- and second-generation biofuels systems. Biofuels produced via pyrolysis of lignocellulosic biomass do not directly compete with food supply, as do leading first generation biofuels such as corn ethanol and soybean biodiesel, and can be produced from a host of novel feedstocks including short rotation woody crops (SRWC), perennial grasses, agricultural and forest residues, and industrial wastes [135, 283]. Pyrolysis oil can be upgraded via traditional petroleum refining and hydroprocessing technologies into transportation fuels that are compatible with current vehicle fleets and infrastructure [284], and thus do not suffer from issues such as the ‘blend wall’, i.e. the maximum percentage of ethanol that can be blended with gasoline/diesel, or require modifications to vehicle fleets which constrain large-scale ethanol production[285]. Further, several catalytic routes have been demonstrated to convert bio-oil into high quality transportation [24, 32, 34] and aviation-fuels [33], as well as value-added platform and specialty chemicals [286]—providing a potential secondary market for an emerging biochemical and bioplastics industry. Recent techno-economic analysis has identified fast

pyrolysis and hydroprocessing [287] as the most economically viable cellulosic fuel platform compared to cellulosic ethanol [288] and gasification with Fischer-Tropsch synthesis [289], and suggest that pyrolysis-derived biofuels are cost-competitive with current petroleum fuels. Life cycle assessment has shown that pyrolysis biofuel systems have the capacity for GHG reductions relative to baseline petroleum fuels [212, 290], but are sensitive to the choice of coproduct scenario for the produced biochar [226, 291, 292].

While pyrolytic fuel systems hold promise for reducing GHG emissions from the energy and transportation sector, several technical barriers including high hydrogen consumption, thermal instability and corrosiveness of produced bio-oil, high formation of light (C1-C5) alkanes, and low liquid carbon yield hinder their environmental performance [291]. Several strategies including pre-treatment via torrefaction (mild pyrolysis) [293, 294], catalytic upgrading [7], and sequential hydroprocessing [258] stages have been proposed as a means to increase the stability of the intermediate bio-oil as well as carbon chain length of the resultant biofuel. However, bio-oil is a highly complex synthetic oil containing multiple chemical functionalities, making selective stabilization and upgrading problematic [295]. This work explores an innovative new design strategy in which a staged thermal gradient, consisting of a series of sequential torrefaction stages followed by pyrolysis, is utilized for targeted thermal decomposition of the hemicellulose, cellulose, and lignin fractions of the biomass respectively. Multistage thermal decomposition produces several fractionated bio-oil streams comprised primarily of carboxylic acids, light oxygenates, furan derivatives, aromatics, and phenolic species. This modular multistage design strategy permits tailored catalytic upgrading of the fractionated bio-oil streams to produce high-quality infrastructure compatible fuels with minimal process hydrogen consumption. Furthermore, the proposed 3-stage fractionated catalytic

upgrading design has the capacity to increase the ratio of carbon yield to desired products—a major technological bottleneck of traditional pyrolytic systems [296], and thus shows merit for substantial improvement over the current industrial design case.

In this chapter, a prospective well-to-wheel life cycle assessment (LCA) model is developed to characterize the life cycle energy use and greenhouse emissions profiles of a series of novel multistage torrefaction and pyrolysis systems for targeted thermochemical conversion of short rotation woody crops to bio-oil and in situ catalytic upgrading to hydrocarbon transportation fuels, and benchmark the results against a base-case fast pyrolysis and hydrodeoxygenation (HDO) platform. Several multistage conversion and upgrading design cases of varying process complexity are considered, with the goal of selectively upgrading bio-oil via catalytic routes to increase the carbon chain length and gasoline/diesel range fuel yield (C6 to C21) of the fuel pool, while simultaneously reducing hydrogen consumption. The primary objectives of this study are to (1) assess the process viability of several multistage design cases via quantification of multiple process design metrics including hydrogen consumption, gasoline- and diesel-range fuel yield, liquid carbon efficiency, and process complexity—and benchmark against a base-case fast pyrolysis and hydroprocessesing system. (2) Characterize the environmental profile of multistage systems via comparison across several sustainability indicators including Energy Return on Investment (EROI) and Life Cycle Greenhouse Gas (GHG) emissions. (3) Examine the influence of different LCA allocation schemes and coproduct scenarios for the biochar on key LCA sustainability metrics.

5.3 MODEL DEVELOPMENT

This work models a ‘theoretical’ centralized biorefinery utilizing a multistage torrefaction and catalytic upgrading design to convert short rotation woody crops to hydrocarbon biofuels. As no such commercial facilities currently exist, this work performs a prospective analysis, extrapolating experimental and laboratory scale data as a surrogate for process flows for a ‘theoretical’ commercial plant. Further, biofuel production is considered over a broad technological space, thus the results presented in this work are optimistic and indicative of how these systems may perform in the medium-to-long term. Such *Prospective LCA* (also known as *Anticipatory LCA*) allows for the quantification of the anticipated environmental impacts of a product or service, identification of the environmental hotspots within the supply chain, and for environmental performance comparison with existing technologies [297]. Incorporating LCA at early stages of research and development (R&D) is touted as an “essential tool for the rational development of sustainable chemical processes” [298]. The analytic framework established in this study is consistent with the protocol used in several prior studies of emerging pyrolytic biofuel platforms conducted by the National Renewable Energy Laboratory (NREL) [37] and Pacific Northwest National Laboratory (PNNL) [250], and consists of several sub-models: (1) an agricultural model is developed to determine the biomass growth rates, direct land-use change impacts, agrochemical application rates, and other key parameters in the cultivation, harvesting, and short-term storage of SRWCs. (2) An Aspen Plus process model is constructed to determine the product distribution, utility requirements, and material/emissions flows for thermochemical conversion of biomass to bio-oil and catalytic upgrading to hydrocarbon fuels. Scenario analysis is carried out to determine the impact of different end-uses for the biochar on the environmental profile of hydrocarbon biofuels. Monte-Carlo analysis is performed to quantify uncertainty in

key environmental sustainability metrics. Model parameters and data are constructed based on reported field trials, national databases, peer-reviewed literature, laboratory and experimental data, technical reports, stoichiometry, first principles, and best engineering knowledge. An overview of the principle stages in the biomass-to-fuel process chain is provided in Figure 19.

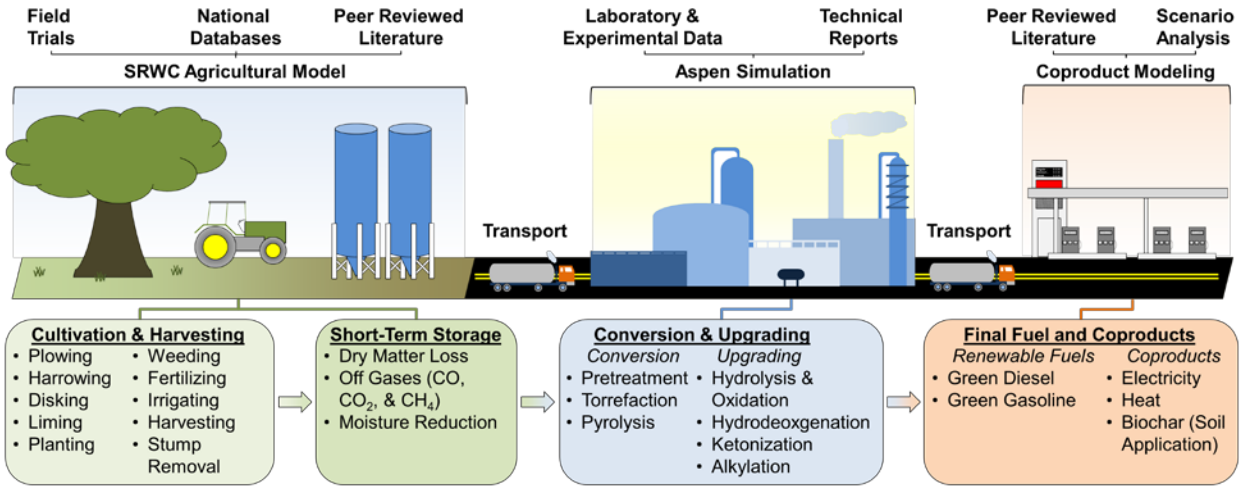

Figure 19. Biomass-to-Fuel Process Chain

5.3.1 Cultivation and Harvesting of SRWCs

Short rotation woody crops are considered an attractive feedstock for thermochemical conversion to transportation fuel owing to their unique biophysical characteristics including low ash content [299] and comparatively greater bio-oil yields relative to other lignocellulosic energy crops [300]. Unlike perennial energy crops, purpose-grown woody biomass can be harvested year-round, reducing large-scale storage infrastructure, holding time, and associated dry matter losses. SRWCs flexible harvest schedule mitigates risk of yield loss due to drought, pests, disease, etc., and enables growers to adjust to biofuel/bioenergy market supply and demand dynamics [301]. SRWC production is evaluated across fifteen separate management systems that span both extensive (i.e. minimal use of agrochemicals and/or machinery) and intensive practices (i.e. use

of synthetic fertilizers, irrigation, etc.), and vary in regards to harvesting frequency, fertilizer and agrochemical application rates, dry matter yield, etc. Process flows for SRWC systems are constructed based on harmonized field trials reported in Djomo et al. 2015 [302], and is provided in Appendix D. The main unit operations considered in SRWC production include cuttings production, plowing, harrowing, disking, liming, planting, weeding, fertilizing, irrigation, harvesting, and stump removal; however, each SRWC system may only include a subset of said unit operations depending on management practice (intensive or extensive), see Figure 20 for a detailed overview. Life cycle inventories for woody biomass production are evaluated stochastically via statistical bootstrapping, in which process inventories for SRWC management systems are randomly sampled with replacements.

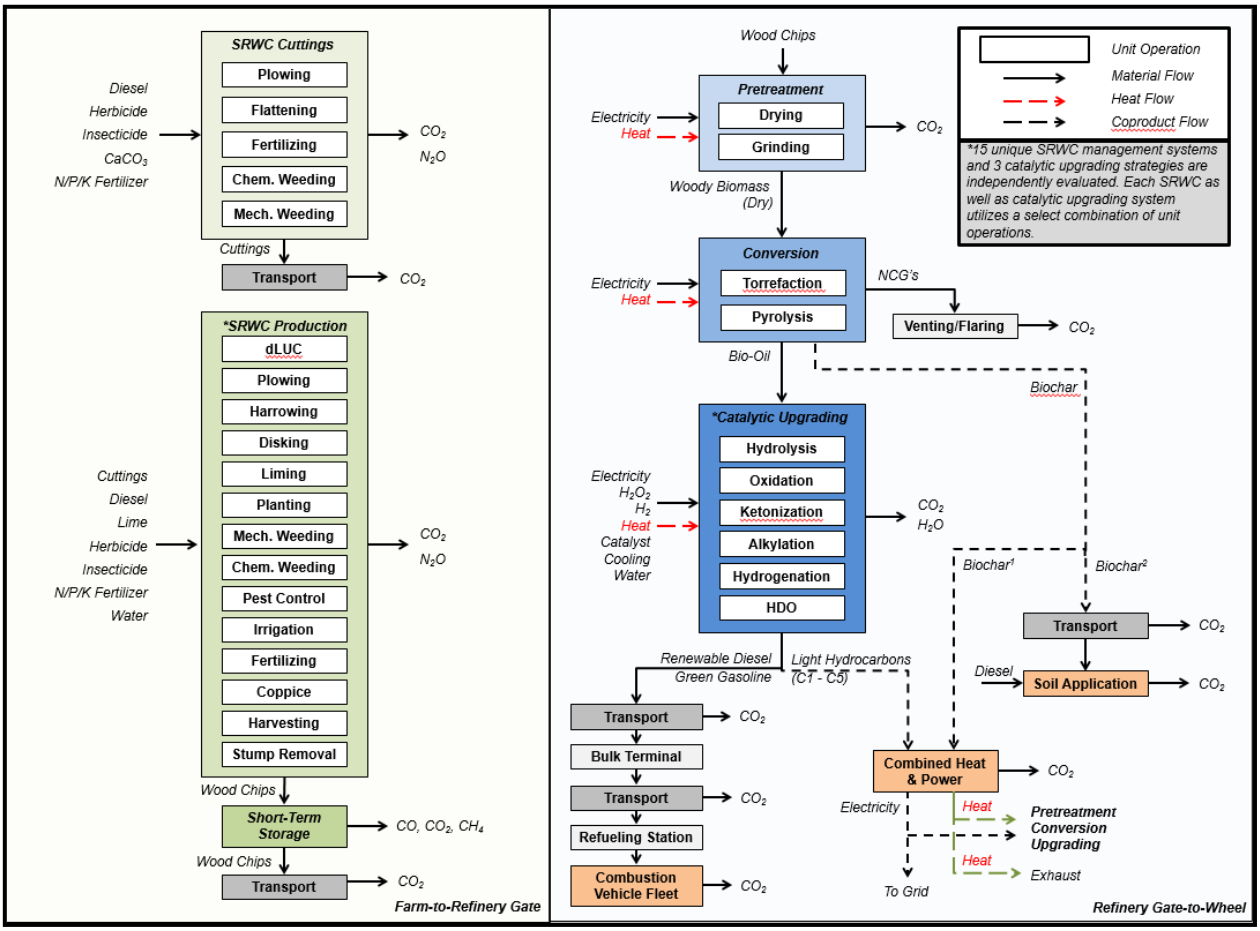

Figure 20. Detailed Process Flow Diagram. Several coproduct scenarios for the biochar is evaluated including: (1) combustion for heat and power and (2) land application as a soil amendment.

Pre-cultivation, several land preparations including plowing, harrowing, and disking, are performed to aerate the soil and make it conducive for crop production. Lime application may be necessary to moderate soil-pH, depending on soil quality and type. Cuttings are subsequently transplanted into the soil and a series of weeding (chemical & mechanical), fertilizing, and irrigation processes are implemented to mitigate the growth of weeds and invasive plant species, reduce pests and disease, and promote higher biomass yields. Coppicing, the process of pruning via repetitive felling of the same stump (near to ground level), may be employed to stimulate growth and allows for continual harvesting of woody biomass. Average SRWC annual yields

across management systems is ~9.87 (dry metrics tonnes ha^{-1} $year^{-1}$); it is assumed that current technology is able to harvest between 77.4% to 94.5% of annual dry matter yield [303]. Upon harvest SRWCs are chipped to produce wood chips with a moisture content of 50% weight per weight (w/w), and are transported to a regional storage facility for short-term holding of the biomass. At end of stand-life SRWC stumps and root systems are removed.

Direct volatilization rates of N to N_2O from 59 field trials spanning various land-types reported from peer-reviewed literature, are randomly sampled with replacements via statistical bootstrapping. Intergovernmental Panel for Climate Change (IPCC) methodology [247] is used to estimate direct CO_2 emissions resulting from land application of N-fertilizer and lime, as well as indirect N_2O emissions resulting from soil nitrogen leaching, runoff, and conversion of soil N to N_2O. Data for the production of cuttings is taken from Djomo et al. 2013 [304], a detailed summary of all inventory data and distributions used in the analysis is provided in Appendix D.

5.3.2 Short Term Storage

The ability to store biomass, without significant loss of quality and/or decomposition, is critical to the supply chains of emerging lignocellulosic biorefineries [305]. Sufficient storage of biomass is necessary to offset seasonal variation in productivity, ensuring a continual supply to producers. Due to SRWCs flexible harvest schedule, it is assumed that only short-term storage (30 to 60 days) of the biomass is required. Linear regression is utilized to determine the rate of biodegradation (i.e. dry matter loss) and off-gas concentration (CO, CO2, and CH4) as a function of storage time (days), based on experimental data provided in Bonner et al. [306] and Tumuluru et al. [307] respectively. Details of the linear regression model are provided in Appendix D. Additionally, it is assumed that storage reduces biomass moisture content to 25% w/w, due to

self-heating that occurs over the holding period[308]. Post-storage, wood-chips are transported to a regional biorefinery via lorries for subsequent downstream processing to transportation fuel. Transportation distance from farm-to-refinery was modeled via a triangular distribution, assuming one-way transport via lorries. A minimum one-way transportation distance of 50 km, most likely value of 100 km, and maximum of 150 km were selected, and capture a broad range of values reported via prior published literaturec

5.3.3 Direct Land-use Change

Prior research has suggested that direct land use change (dLUC) effects—i.e. GHG emissions (or reductions) resulting from changes in the carbon stocks of above and belowground biomass as well as changes in soil organic carbon (SOC) concentrations and other carbon pools as a result of the direct transformation or conversion of land, may jeopardize the carbon neutrality of biofuels [17, 309]. Failure to consider dLUC effects may inadvertently overestimate the climate benefit of biofuels, and thus should be included in LCAs of biofuel production [271]. In this work, estimates for dLUC are developed based on guidelines provided via the IPCC Tier 1 methodology. Several broad-based assumptions are made regarding the calculation of dLUC: (1) grasslands would exclusively be targeted for conversion to SRWC plantations, (2) the soil type and climate zone for converted lands are high activity clays (HAC) and temperate [310] (cold, moist) respectively, and (3) IPCC defined *Forestlands* can act as a proxy for the SOC concentrations for SRWC plantations. Direct land use change impacts are normalized over the 20-year [250] lifespan of the biorefinery. It is important to note that indirect LUC impacts are not considered in the scope of this work. Further details regarding the calculation of dLUC are provided in Appendix D.

5.3.4 Multistage Torrefaction/Pyrolysis and Catalytic Upgrading

Multistage thermochemical conversion of biomass and catalytic upgrading of bio-oil is modeled using Aspen Plus V8.8[311], using the UNIQUAC thermodynamic property set. Pyrolysis oil is a highly complex synthetic fuel containing myriad compounds, thus detailed modeling of bio-oil is computationally taxing and prohibitive. To manage the complexity and dimensionality, a model compound approach is used for characterizing bio-oil. In this methodology, bio-oil compounds are broadly aggregated based on chemistry/functionality and assigned a representative a model compound, this protocol is consistent with prior published literature[295, 312, 313]. Seven major families of compounds are considered: carboxylic acids (acetic acid), light oxygenates (acetol), furanics (furan, furfural), anhydrosugars (levoglucosan), aromatics (toluene), multifunctional phenolics (guaiacol), and alkylated phenolics (m-cresol). Furthermore, in this study the oligomeric content (i.e. pyrolytic lignin) is assumed to be upgradable and is evenly distributed among the organic compounds on a mass basis. Additional details regarding the experimental setup, data acquisition, and model compound methodology is provided in Appendix D.

A combination of experimental data and model-compound studies performed at the University of Oklahoma is used to parameterize design blocks in the Aspen Plus simulation, and guide process model development [314]. Process yields for catalytic upgrading strategies were estimated via equilibrium reactors blocks in ASPEN. This approach allows for a robust assessment that is likely to be achieved under steady state operating conditions, and accounts for the propensity of select chemical reactionary pathways to proceed based on underlying thermodynamic data. Details regarding the reaction stoichiometry considered for each catalytic upgrading strategy are provided in Appendix D. Biomass and biochar are defined in the Aspen

Plus simulation as non-conventional products, based on their Proximal, Ultanal, and Sulfanal analysis. Thermodynamic property data for model compounds is obtained using commercial ASPEN databases. In cases where thermodynamic data is not available, thermodynamic properties for these compounds is estimated via the National Institute of Science and Technology ThermoData Engine (NIST-TDE) based on chemical structure and bond connectivity. Pinch analysis is utilized to estimate optimal heat integration strategies and system-wide heating and cooling duties. Additional information regarding biorefinery utilities is provided in Appendix D.

5.3.5 Upgrading Chemistries

Multistage system(s) utilize a staged thermal gradient to fractionate bio-oil into product streams comprised of distinct functional groups that can be selectively catalytically upgraded via a host of upgrading chemistries including ketonization, alkylation, hydrolysis and oxidation, hydrogenation, and hydrodeoxygenation to produce high-quality transportation fuel(s) as well as fuel additives, details of the design cases are provided in Figure 21. Catalytic upgrading strategies can be broadly classified into Carbon-Carbon (C-C) coupling or hydroprocessing reactions. *Ketonization*, also known as ketonic decarboxylation, is a chemical reaction wherein two carboxylic acids are converted into a ketone, producing carbon dioxide and water as by-products. Ketonization has gained attention as a promising strategy for upgrading oxygenated bio-oil compounds, due to its ability to convert corrosive, unstable, and highly abundant carboxylic acids into higher carbon-chain length and stable bio-oil intermediates and fuel precursors [273]. *Alkylation,* the addition or substitution of an alkyl group has been widely employed in petrochemical refining for converting isobutane and low-molecular weight alkenes (i.e. propene) into high-quality gasoline. Recently, alkylation and derivatives (i.e.

hydroalkylation, hydroxyalkylation, etc.) have seen application in biofuel production as these carbon-carbon coupling reactions can convert otherwise undesirable low molecular weight bio-oil compounds into longer carbon chain length compounds that can be hydroprocessed into transportation fuels that are fungible with current diesel [315, 316] and aviation blendstocks [317]. *Hydrolysis and oxidation* uses an oxidizing agent to convert bio-oil compounds into carboxylic acids, and has been demonstrated to be a promising option for converting levoglucosan into glucionic acid with high purity and selectivity [318]. Carboxylic acids produced in this manner, can be converted to long carbon chain ketones via ketonization. *Hydroprocessing* via hydrogenation or hydrodeoxygenation utilize a high-pressure, hydrogen rich environment to remove oxygen from bio-oil compounds, to make them suitable for combustion in vehicle engines and industrial use [280]. Mild hydrotreating via hydrogenation can convert bio-oil into stable compounds, and desirable intermediates for further downstream upgrading. Hydrodeoxygenation utilizes severe hydroprocessing conditions to remove oxygen from bio-oil compounds and saturate carbon rings, forming water as a byproduct.

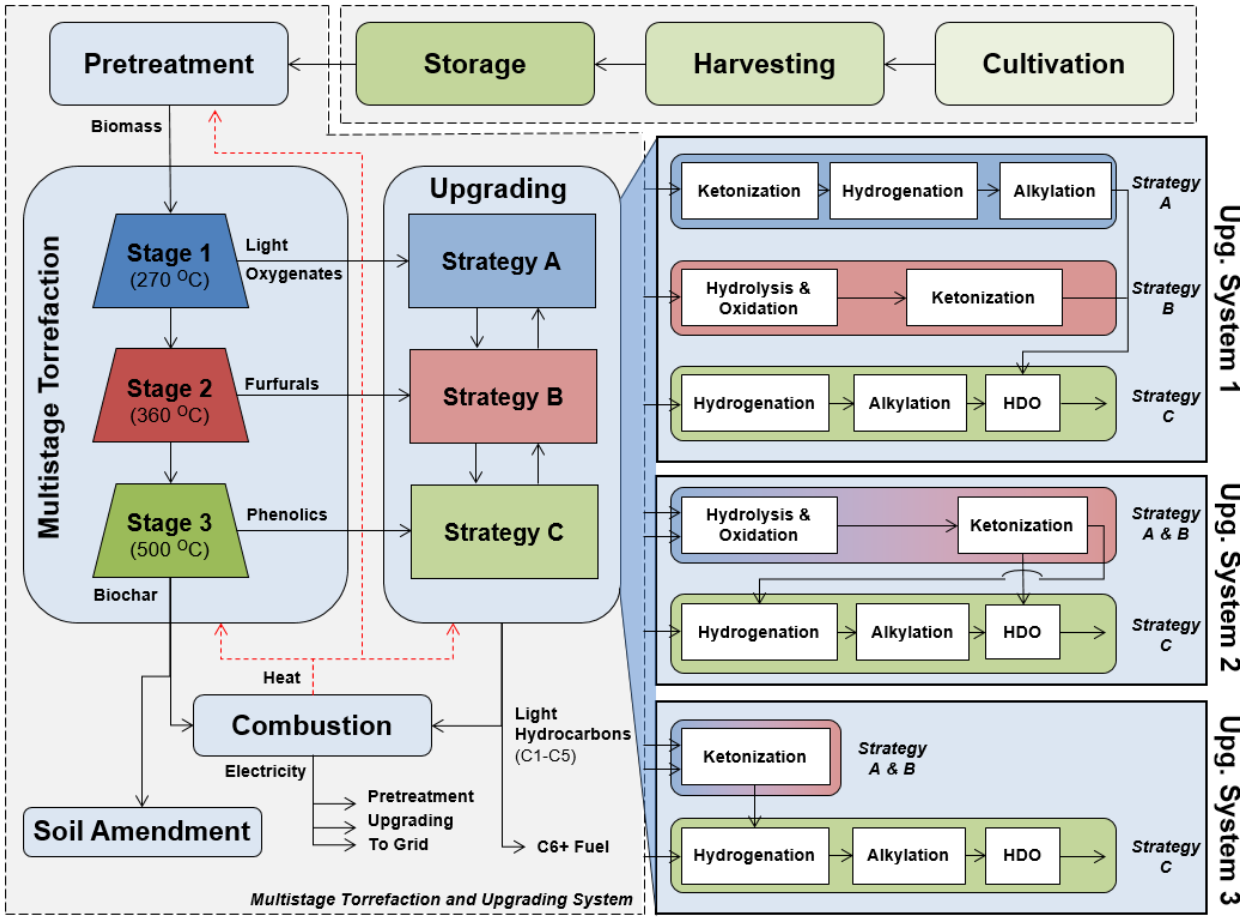

Upgrading strategies A, B, and C represent catalytic approaches for targeted upgrading of stage 1, stage 2, and stage 3 bio-oil respectively. Integration and coupling of thermally fractioned bio-oil streams and upgrading strategies (A,B,C) can occur, denoted by the connecting arrows. Multistage system "X" refers to thermochemical conversion of biomass to bio-oil via multistage torrefaction and catalytic upgrading via upgrading system "X". For example, multistage system 1 denotes the use of upgrading system 1 to convert fractionated bio-oil to hydrocarbon fuels.

Figure 21. Multistage Torrefaction & Pyrolysis Systems. Several multistage design cases, consisting of different catalytic upgrading systems, are independently considered for tailored upgrading of bio-oil to hydrocarbon fuels

5.3.6 Detailed Process Description

This work models a 'theoretical' biorefinery operating at 2,000 dry metric tonnes (DMT) of biomass per day, consistent with the design case provided in Jones et al. [249] and Wright et al. [37] Input feed received by the biorefinery undergoes an initial pretreatment phase, in which biomass is chopped/ground via a hammer-mill to a particle size diameter of 3mm [250], and

subsequently dried to remove any remaining moisture content. Energy requirements for chopping/grinding were constructed based on empirical correlations provided in Miao et al. 2011 [251]. Pretreated biomass is sent to a multistage torrefaction and pyrolysis reactor to produce thermally fractionated bio-oil, biochar, and non-condensable gases. Product yields for multistage torrefaction and pyrolysis are 46.3% bio-oil (dry basis), 27.2% NCGs, 10.5% biochar, and 16% water on an ash-free mass basis, based on laboratory-scale experiments conducted at the University of Oklahoma. Comparatively, product yields for single-stage fast pyrolysis (500 ^{O}C) are 53.5% bio-oil, 24.3% NCGs, 9.01% biochar, and 13.2% water on an ash-free dry mass basis—based on experimental data from University of Oklahoma. Composition of the NCGs is estimated using an optimization routine that minimizes the Gibbs free energy of formation of several light hydrocarbons and gaseous products including CO, CO_2, CH_4, C_2H_6, C_3H_6, C_3H_8, H_2, and H_2O. Mass flows for thermally fractionated bio-oil streams are provided in Figure 22, a comparison with bio-oil produced via single stage fast pyrolysis (500 ^{O}C) of woody biomass, obtained from University of Oklahoma, is provided for reference. Post thermochemical conversion, biochar/ash is separated from bio-oil and NCGs via a cyclone separator and subsequently cogenerated on-site via a combined heat and power (CHP) unit to produce heat and electricity or transported off-site for use as a soil amendment. Torrefaction and pyrolysis vapors are cooled via a quench, and condense to form bio-oil. NCGs are separated from bio-oil via flash separation and subsequently flared to CO_2 and vented onsite. Energy requirements for flaring are assumed to be minimal and thus not considered in this work. Several multistage design cases of varying process complexity are investigated for tailored upgrading of bio-oil fractions to transportation fuel. *Multistage system 1* upgrades bio-oil fractions independently, targeting promising catalytic pathways based on the composition of each stream. *Multistage system 2*

employs an integrated strategy, upgrading stage 1 & 2 bio-oil concurrently. *Multistage system 2* focuses extensively on oxidation of bio-oil to carboxylic acids and subsequent ketonization, as a catalytic pathway to produce gasoline and diesel range fuel precursors. *Multistage system 3* adopts an integrated minimalist approach, utilizing a minimal number of design blocks to upgrade bio-oil to hydrocarbon fuels. This design strategy converts unstable, corrosive, and highly abundant acetic acid into ketones (acetone) via ketonization. Ketones and bio-oil intermediates are then hydrogenated to produce light alcohols, which are subsequently used as alkylating agents to upgrade furanics and phenolics.

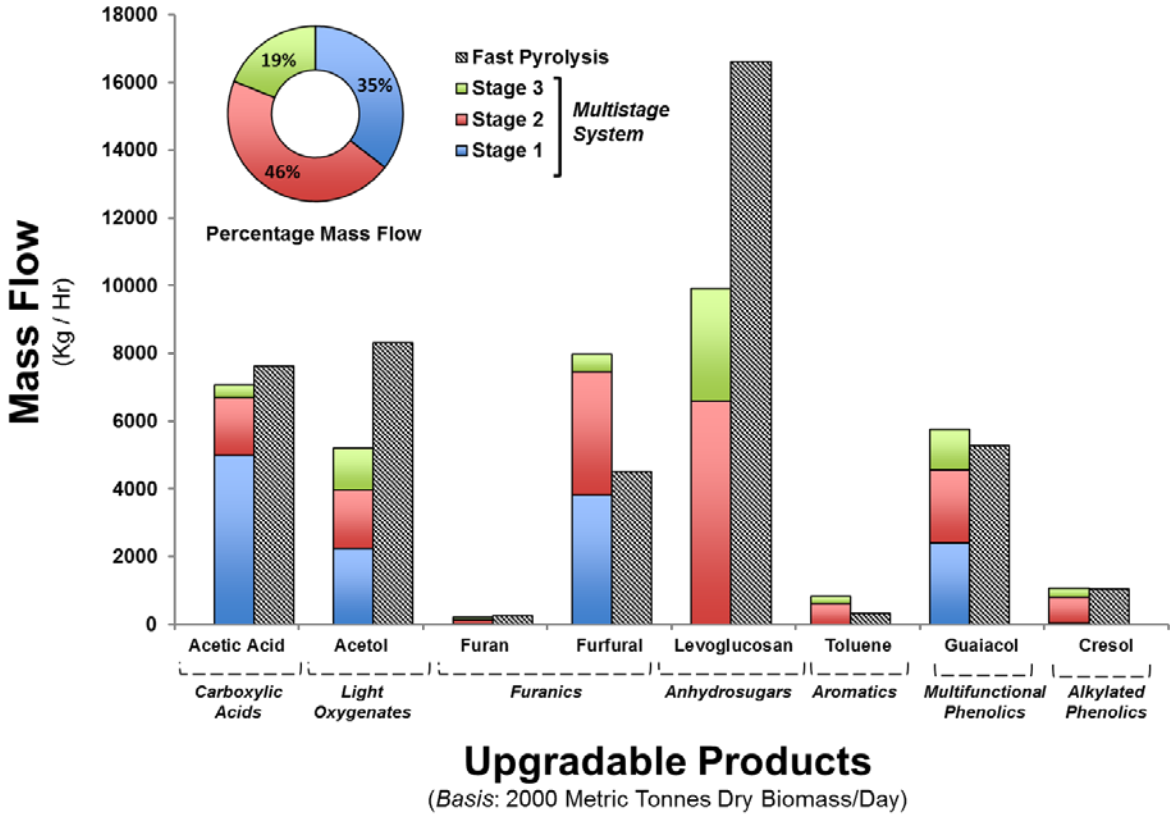

Figure 22. Model compound characterization of bio-oil derived via a three-stage torrefaction and pyrolysis design, and comparison with single-stage fast pyrolysis (500 ^{O}C). Mass flows of thermally fractionated bio-oil streams are reported based on a plant capacity of 2000 dry metric tonnes of biomass per day.

Hydrodeoxygenation of alkylated furanics is assumed to produce linear-chain alkanes due to ring opening that occurs during hydroprocessing, while HDO of alkylated phenolics produces branched hydrocarbons. Due to high hydrogen partial pressure used in the reactor(s), no coking of the catalyst is assumed to occur during hydroprocessing. Furthermore, it is assumed that external hydrogen is produced via steam methane reforming of natural gas and supplied at a discharge pressure of 27 atm. Due to issues of Reid vapor pressure (RVP), only fuel compounds with a carbon chain length of C6 or greater are assumed to meet the requisite standards for transportation fuel. As such, light hydrocarbons (C1-C5) are separated from the fuel pool and sent to an onsite CHP unit to produce heat and power. Transportation of biomass-based diesel from the refinery-to-pump is based on the 2016 GREET model [269]. It is assumed that biomass-based diesel is transported from refinery to bulk terminal assuming a transportation mix of 8% by barge, 29% by rail, 63% by heavy duty truck (on a mass basis) and a corresponding average transportation distance of 520 miles, 800 miles, and 50 miles respectively. Biomass-based diesel is subsequently transported from bulk terminal to refueling station via heavy-duty trucks assuming a one-way transportation distance of 30 miles.

5.3.7 Coproduct Scenarios

Several coproduct scenarios are considered for the produced biochar including (i) application as a soil-amendment and (ii) cogeneration via CHP to produce heat and electricity. Application of biochar as a soil amendment has been touted for its beneficial properties such as reduction in N_2O emissions and leaching of nitrogen into groundwater [319], improved soil quality/fertility [320, 321] and crop yield [43, 46], heightened retention and bioavailability of soil nutrients and water [322], moderating soil pH, and increased biodiversity of beneficial soil microbes [323,

324]. For land application scenarios it is assumed that up to 20% of the carbon content of the biochar is emitted to the atmosphere as CO_2 over a 100-year time horizon [257]. Due to lack of data regarding the bio-availability of nutrients in the biochar it is assumed that land application of biochar does not offset synthetic N,P,K fertilizers. Elemental composition of the biochar (C,H,O) is based on values reported in Enders et al. [325]. Diesel use for spreading and loading manure is used as a proxy to estimate the energy consumption and GHG emissions for land application of biochar, and are taken from Dalgaard et al. [248].

In the second scenario, biochar is combusted via CHP to produce heat and electricity to be used internally within the biorefinery and/or exported to the grid. Cogeneration of biochar and/or light hydrocarbons via CHP is modeled outside of the ASPEN simulation, and is constructed based on the higher heating value (HHV) of solid and liquid fuels as well as CHP conversion efficiencies [253]. The higher heating value for biochar and select model compounds is estimated based on the percentage carbon, hydrogen, oxygen, and ash content via correlations provided in Channiwala and Parikh [252]. Heat and power derived via combustion of biochar and/or light hydrocarbons is used to offset process utilities, excess electricity is sent to the grid while excess heat is discarded.

5.3.8 Life Cycle Assessment

The scope of the LCA is well-to-wheel and the functional unit is chosen as 1 MJ of renewable fuel. It is important to note that the functional unit used in this study does not account for vehicle-use efficiency (i.e. combustion efficiency), so that the results from this work can be compared against prior published literature. Prior biofuel LCA studies have shown that capital equipment and infrastructure have a negligible contribution to overall environmental impacts

[225, 308, 326-329], and thus are commonly excluded from the life cycle boundary [330]. As such, capital equipment and infrastructure related environmental impacts are assumed to be marginal and thus not considered in the analysis. Intergovernmental Panel for Climate Change (IPCC) 100-year global warming potential (GWP) [331] and Cumulative Energy Demand (CED) [332] characterization factors are used to quantify the life cycle GHG emissions and primary fossil energy consumption for biofuel production. Life cycle data is obtained from several sources including: United States Life Cycle Inventory (USLCI) [333], Ecoinvent Database [334], and industry data. Due to the proprietary nature of catalyst production, limited life cycle data is available for commercial catalysts. Life cycle impacts for catalysts are estimated via a zeolite product in the Ecoinvent database (Zeolite Powder), consistent with several prior studies [203, 268].

5.3.8.1 Stochastic Simulation for Uncertainty Quantification

In this study, probability distribution functions (PDF) are developed for select key parameters in the biomass-to-fuel supply chain. Stochastic simulation (10,000 trials) is performed via (i) randomly sampling from PDFs and (ii) a method of statistical bootstrapping in which data is randomly sampled with replacements. Uncertainty in the life cycle impact assessment (LCIA) is captured via the use of Monte Carlo simulation (10,000 trials) to randomly sample from statistical distributions for GWP and CED characterization factors. The statistical approach used in this analysis captures variability at both the process and life cycle scale, and thus provides a holistic understanding of uncertainty in key sustainability and performance metrics. Summary information for distribution types as well as a detailed summary of all inventory data is provided in Appendix D.

5.3.8.2 Coproduct Handling in LCA

Two LCA schemes were considered for dealing with coproducts in this work: (i) energy-based allocation and (ii) displacement method. In energy-based allocation, environmental burdens are partitioned between final renewable fuel (C6+) and exported bioelectricity based on their fraction of total energy flow (MJ). In the displacement method, exported electricity is assumed to displace the U.S. average grid mix, and the biofuel system is thus accredited with the 'avoided' environmental impacts of electricity production. Heat and electricity recycled internally within the biorefinery is not subject to allocation or displacement, as these flows are used to offset process utility requirements and thus do not leave the product system. For soil amendment coproduct scenarios, GHG abatement credits from land-application are subtracted from total life cycle GHG emissions prior to allocation procedures or displacement method.

5.3.9 Environmental Sustainability Metrics

5.3.9.1 Life Cycle GHG Emissions

Life cycle GHG emissions are defined as the sum of direct and indirect GHG emissions that occur throughout all stages of the fuel life cycle. Life cycle GHG emissions are calculated over a specific time horizon and measured in units of carbon dioxide equivalents (CO_2e). This work considers a 100-year time horizon and CO_2e emissions from all fossil sources as well as select biogenic sources including: (1) biogenic CO_2 emissions (or reductions) from direct land-use change, (2) biogenic GHG emissions from storage-off gases, and (3) GHG abatement from land application of biochar. In the carbon-accounting scheme used in this work, no carbon-sequestration credit is given to carbon dioxide stored in SRWC via photosynthesis. Consequently, CO_2 emissions resulting from storage-off gases, flaring of NCGs, combustion of

light hydrocarbons (C1-C5), catalytic upgrading, combustion of biochar, and vehicle combustion of transportation fuel (C6+ fuel) is considered to be carbon-neutral, as it re-releases atmospheric carbon dioxide that is captured via SRWCs in the carbon cycle. In this framework a negative GHG credit is given to carbon sequestered via soil application of biochar, however volatilization and re-release of biochar-carbon as CO_2 is carbon neutral (i.e. a 100-year GWP of O kg CO_2e).

5.3.9.1 Energy Return On Investment

Energy return on investment has been widely used in the literature to assess the energetic viability of fuel and energy systems [19, 144, 147, 153, 177], and is defined as the ratio of fuel energy (MJ) to the primary fossil energy required for its production (MJ), shown in equation 7.

$$EROI = \frac{Fuel\ Energy\ (MJ)}{Primary\ Fossil\ Energy\ Invested\ (MJ)} \quad (7)$$

Fuel energy is defined as the sum of the product of model compounds (e.g. hexane, heptane, octane, etc.) and their respective lower heating values (LHV). Biofuel systems with EROI values greater than 1 are desirable, as more fuel energy is produced than fossil primary energy required for its production over the life cycle.

5.4 RESULTS AND DISCUSSION

5.4.1 Product Distribution

The product distribution for multistage design cases is plotted in Figure 23, and compared against a base-case fast-pyrolysis HDO fuel platform. Results reveal that the product-distribution

for the fast pyrolysis and HDO system range from C2-C7 in carbon number, with lower carbon chain length fuels (i.e. C2-C5) constituting the majority of the carbon in the fuel pool. The high formation of light hydrocarbons is due to: (i) abundance of light oxygenates and furanics in bio-oil that are converted to low molecular weight alkanes during HDO, and (ii) conversion of levoglucosan, which constitutes ~38% of the bio-oil via fast pyrolysis on a mass basis, to C2, C3, and C4 hydrocarbons during hydroprocessing [335]. Thus, for fast pyrolysis HDO systems, only a small fraction of the total carbon in the fuel pool is retained in C6+ liquid products. Comparatively, the product distributions for multistage systems are skewed towards longer carbon chain length compounds in the gasoline and diesel-range. Multistage system 3 exhibits the most promising product profile of the examined design cases, with the majority of fuel products with a carbon number of C6 or greater, thus making it an excellent candidate for targeted production of gasoline and diesel-range fuels.

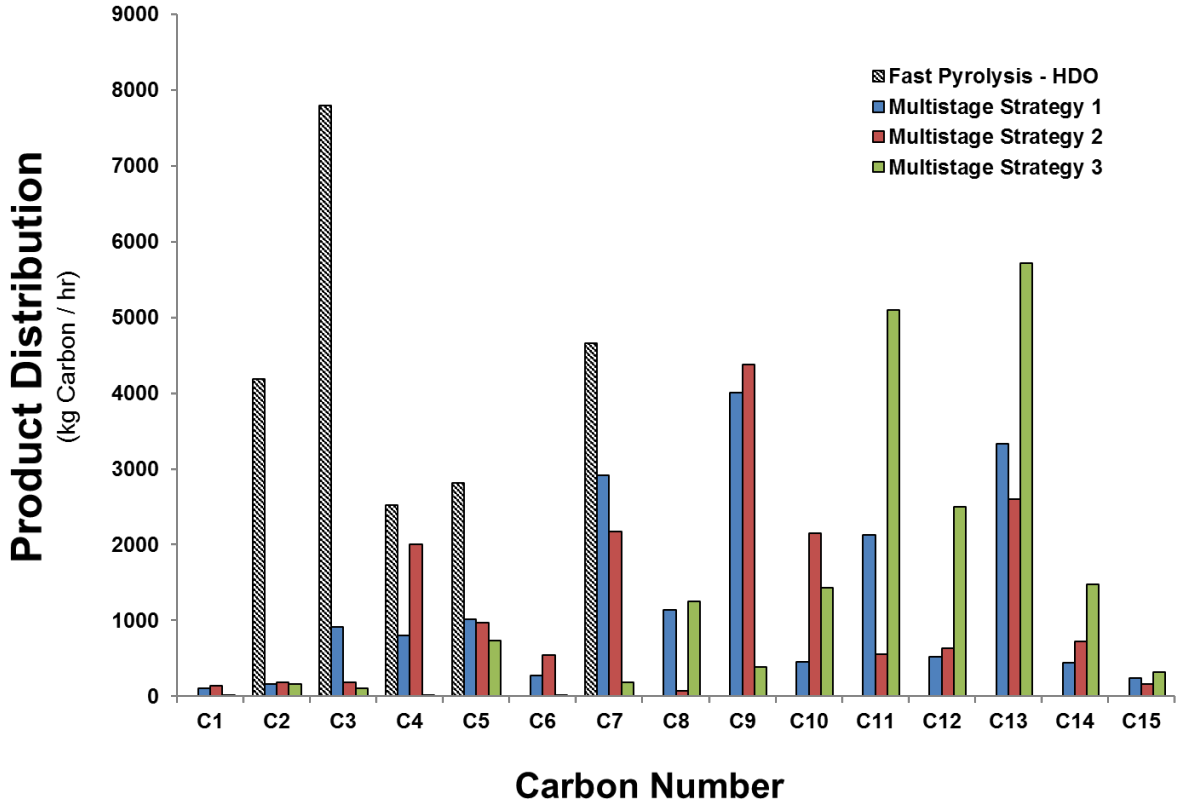

Figure 23. Product Carbon Distribution Comparison: Multistage System(s) vs. Fast Pyrolysis HDO

5.4.2 Process Scale Metrics

Several process scale metrics are used to compare the performance of multistage systems and benchmark against a fast pyrolysis and HDO fuel platform, see Table 7. Results reveal that the base-case fast pyrolysis and HDO system has the highest absolute fuel yield (kg C / hr) of all examined biofuel systems, due to higher bio-oil yields obtained via fast pyrolysis, as well as loss of carbon (as CO_2) that occurs during ketonization in multistage systems. However, the base-case fast pyrolysis and HDO system has high process hydrogen consumption, and despite heightened absolute fuel yield—exhibits the lowest C6+ liquid carbon yield and C6+ carbon efficiency of all examined design cases, with only ~12% of the carbon in the initial biomass retained in C6+ liquid products. Further, for fast pyrolysis and HDO systems the ratio of C6+ fuel (C / hr) to hydrogen consumption (kg H_2 / hr) is marginally greater than unity, indicating that these systems are grossly inefficient. Comparatively, multistage systems are found to lower process hydrogen consumption by ~40% relative to the base-case fast pyrolysis and HDO system, across all examined design cases. Further, multistage systems are able to retain a significant fraction of carbon in C6+ liquid products, with C6+ carbon efficiency and C6+ fuel-to-hydrogen consumption ranging from 36% to ~47% and 6.4 to 8.0 (kg C / H_2), respectively, across design cases. Multistage system 3 is found to have the highest performance across all design metrics and lowest process complexity relative to other multistage designs, and produces over four times the C6+ liquid carbon yield compared to fast pyrolysis and HDO systems.

Table 7. Critical Process Design and Performance Metrics for Fast Pyrolysis HDO and Multistage Systems

Process Design Parameters & Performance Metrics	***Fast Pyrolysis HDO***	***Multistage System 1***	***Multistage System 2***	***Multistage System 3***
Absolute Fuel Yield [kg $Fuel_{Carbon}$ / hr]	21981	18451	17461	19358
C6+ Liquid Carbon Yield [kg C6+ $Fuel_{Carbon}$ / hr]	4659	15448	13981	18350
Hydrogen Consumption [kg H_2 / hr]	3875	2339	2195	2295
C6+ Fuel to Hydrogen Consumption [kg C6+ $Fuel_{carbon}$ / kg H_2]	1.2	6.6	6.4	8.0
C6+ Carbon Efficiency [C6+ $Fuel_{Carbon}$ / $Biomass_{Carbon}$) x 100]	12.1	40.1	36.3	47.6
Process Complexity [# Decomposition, Upgrading Blocks]	(1,1)	(3,8)	(3,5)	(3,4)

5.4.3 Energy Return On Investment

Figure 24 plots the median EROI for hydrocarbon fuels produced via multistage systems, and benchmarks the results against a base-case fast pyrolysis and HDO fuel platform. Median values are presented instead of average values, as the distributions for sustainability metrics (i.e. EROI and life GHG Emissions) are non-symmetric and skewed. In fast pyrolysis and HDO systems, the displacement method generates highly distorted results due to the substantial coproduct credit received from exported electricity. In such circumstances EROI lacks meaningful interpretation, and indicates that displacement is not an appropriate method for accounting for coproduct flows and an alternate allocation procedure should be chosen [336]. Accordingly, for the base-case fast pyrolysis and HDO system only results obtained via energy-based allocation are presented in this work. The results from Figure 24 reveal that the median EROI for multistage systems range from 1.32 to 3.76 MJ-fuel/MJ-primary fossil energy over the host of design cases analyzed. For fast pyrolysis and HDO the median EROI is near unity for either coproduct scenario for the biochar, indicating that these systems are not energetically viable over the life cycle. For all design cases, combustion of biochar via CHP results in higher overall EROI as compared to soil-amendment

scenarios—due to reduced process utility requirements and higher quantities of exported coproduct electricity. Moreover, biochar-CHP scenarios utilizing displacement produce higher EROI relative to energy-based allocation across all design cases, due to the large coproduct credit received for 'displaced' electricity. For multistage systems in which biochar is used as a soil amendment, all coproduct electricity and heat is consumed internally within the biorefinery; consequentially, the results are invariant to the choice of displacement method or energy-based allocation. Multistage system 3 exhibits the highest median EROI (~3.76 MJ/MJ-Primary Fossil Energy) out of all examined systems, and shows substantial improvement over the base-case fast pyrolysis and HDO fuel platform.

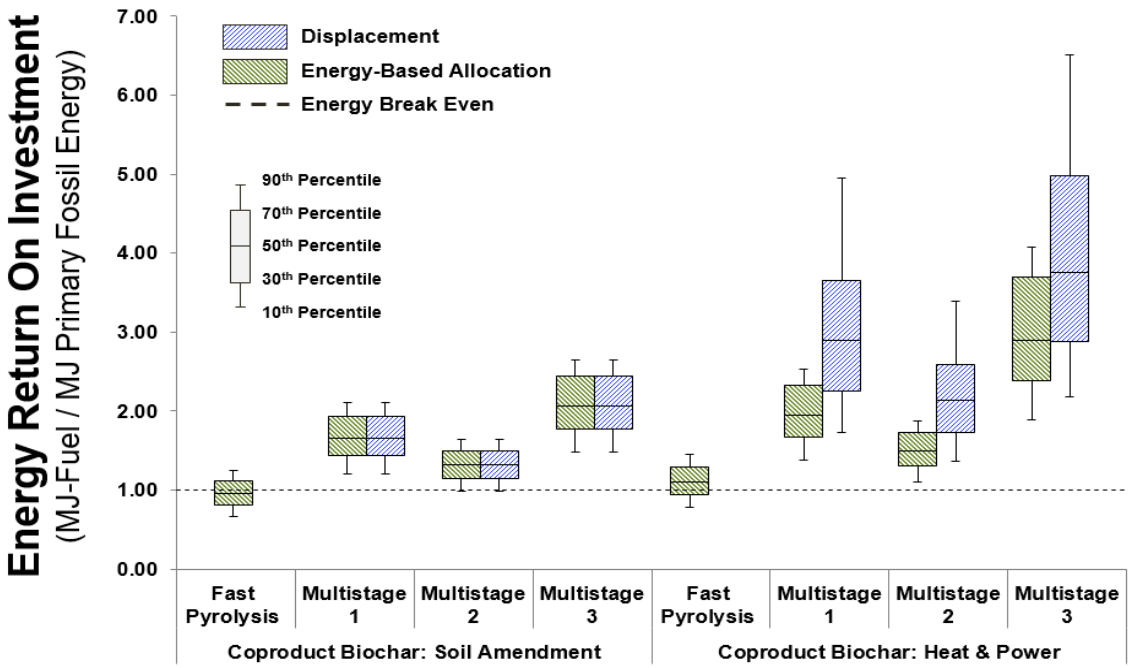

Figure 24. Energy Return on Investment for hydrocarbon biofuels produced via multistage systems and single stage fast pyrolysis and HDO. Results for *displacement* and *energy-based allocation* are presented for both *Soil Amendment* and *Heat and Power* biochar coproduct scenarios. Median values (i.e. 50th percentile) are presented; error bars represent the 10th and 90th percentile.

5.4.4 Life Cycle Energy Analysis

Figure 25 presents the average primary fossil energy consumption by process input, normalized per MJ of fuel (C6+) output. The results from Figure 25 indicate that external hydrogen consumption constitutes the principle burden across all three systems, ranging from ~0.18 to 0.24 MJ-Primary Fossil Energy/MJ-Fuel. For multistage systems 1 and 2 the use of H_2O_2 as an oxidizing agent during hydrolysis and oxidation results in high primary fossil-energy consumption, primarily driven by the high upstream impacts of hydrogen peroxide production, and suggests that an alternative-oxidizing agent may enhance the environmental performance of these systems. Net electricity utility constitutes a large primary fossil energy impact for soil-amendment pathways, due to the high electricity requirement for biomass pretreatment as well as for hydrogen compression. For biochar-CHP scenarios, all process utilities are met with heat and electricity-produced onsite. Agrochemicals constitute a significant energy burden across all design cases and coproduct scenarios, ranging from ~0.08 to 0.11 MJ-Primary Fossil Energy/MJ-Fuel, due to high upstream impacts of N-fertilizer production. Primary fossil-energy consumption for diesel use as well as transportation were found to be marginal as compared to other fossil-intensive material and energy inputs (i.e. hydrogen consumption).

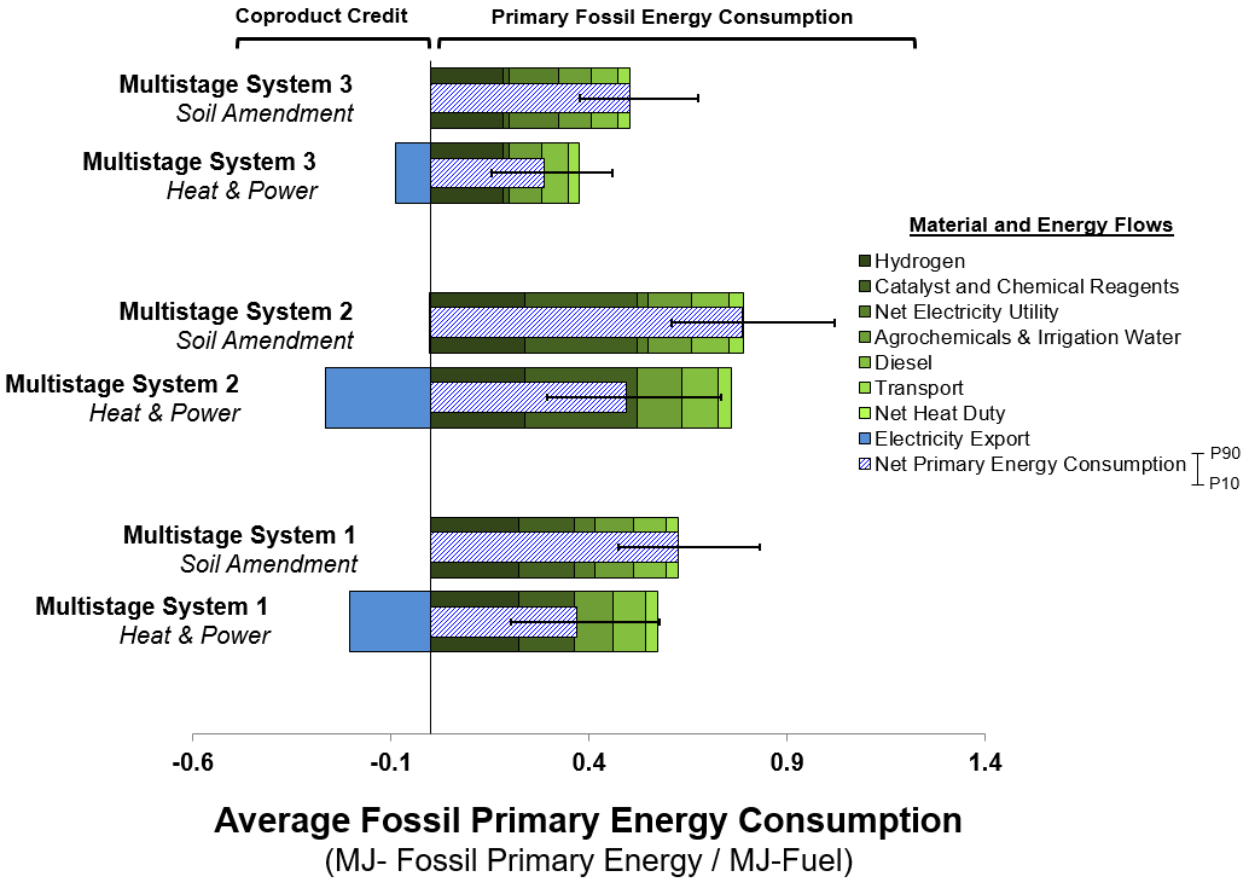

Figure 25. Life cycle fossil energy analysis. Average primary energy impacts for process inputs and coproduct are normalized to 1 MJ of hydrocarbon biofuel. Well-to-wheel results are shown utilizing the *displacement method*. Negative values indicate primary fossil energy credit from coproducts, while positive values indicate primary fossil energy consumption for material and energy inputs. Net primary energy consumption represents the difference between primary fossil energy consumed in the supply chain and coproduct primary fossil energy credit. The error bars represent the 10th and 90th percentile.

5.4.5 Life Cycle GHG Emissions

Figure 26 plots the median life cycle GHG emissions for multistage and base-case systems, and compares the results against the U.S. Environmental Protection Agencies (EPA) renewable fuels standard (RFS2) 50% GHG reduction threshold relative to petroleum diesel. Results reveal that

the median life cycle GHG emissions for fast pyrolysis and HDO systems range from 52 to 87 gCO_2e/MJ-Fuel for biochar -soil amendment and -CHP scenarios, respectively. These results are startling and suggest that the life cycle GHG emissions for fast pyrolysis and HDO systems may be comparable to baseline petroleum fuels (~91.94 gCO_2e/MJ-Petroleum Diesel [337]). Conversely, life cycle GHG emissions profiles for multistage systems range from 17.1 to 52.8 across design cases, corresponding to life cycle GHG emissions reductions of 42.5 to 81.5% relative to baseline petroleum fuels. For multistage systems, land application of biochar results in lower GHG emissions relative to combustion via CHP and meets the RFS2 50% GHG reduction threshold for bio-based diesel across all examined multistage design cases. For biochar-CHP coproduct scenarios, with the exception of multistage system 2 using energy based-allocation, all combinations of multistage systems and allocation schemes are able to achieve sufficient median GHG reductions to qualify for the RFS2 mandate. Further, for a fixed coproduct scenario or allocation scheme the results reveal that multistage system 3 has the lowest overall GHG emissions across all examined systems, and thus holds promise as a commercial platform for next-generation biofuels.

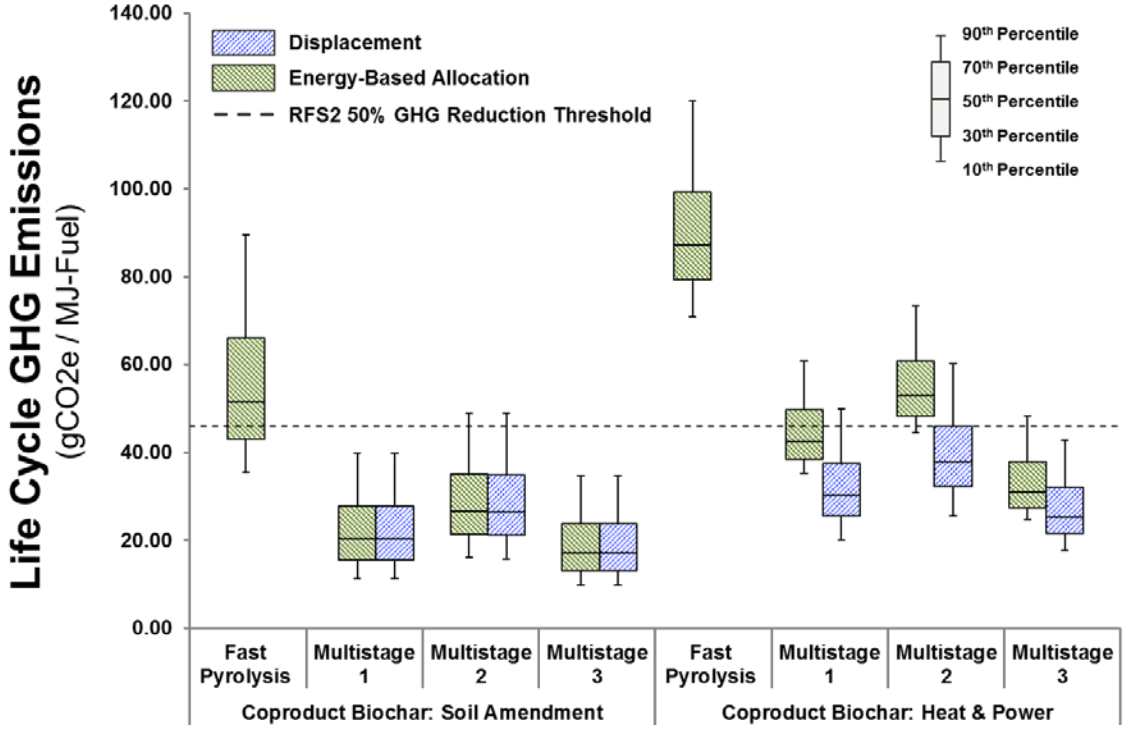

Figure 26. Life cycle GHG Emissions for hydrocarbon biofuels produced via multistage systems and single stage fast pyrolysis and HDO. Results for displacement and energy-based allocation are presented for both Soil Amendment and Heat and Power biochar coproduct scenarios. Median values (i.e. 50th percentile) are presented; error bars represent the 10th and 90th percentile. Life cycle GHG emissions for Petroleum Diesel is taken to be ~91.94 gCO2e/MJ-Diesel [337].

5.4.6 Life Cycle GHG Analysis

Figure 27 presents the average life cycle GHG emissions by process input, normalized per MJ of fuel (C6+) output. The results from Figure 27 indicate that external fossil hydrogen supply, agrochemicals, catalysts and chemical reagents, and net electricity utility constitute the majority of GHG emissions over the fuel life cycle. External fossil hydrogen consumption is the largest GHG burden across all three systems, ranging from ~20.2 to 26.1 gCO2e/MJ-Fuel, due to the

high life cycle GHG intensity of H2 production via steam-methane reforming of natural gas. The use of agrochemicals results in high overall GHG emissions across all design cases and coproduct scenarios, ranging from ~9.2 to 11.3 gCO2e/MJ-Fuel, due to high upstream impacts of N-Fertilizer production as well as N2O emissions as a result of direct/indirect N volatilization. Application of biochar as a soil amendment results in a large GHG sequestration credit ranging from approximately -25.3 to -34.2 gCO2e/MJ-Fuel across designs. Production of SRWCs was found to increase overall SOC concentrations relative to grassland land-type, resulting in carbon abatement. After accounting for removal of above and belowground biomass during land conversion, as well as changes to the SOC concentration, average dLUC impacts are found to be marginally carbon negative—ranging from approximately -2.3 to -3.1 gCO2e/MJ-Fuel across design cases.

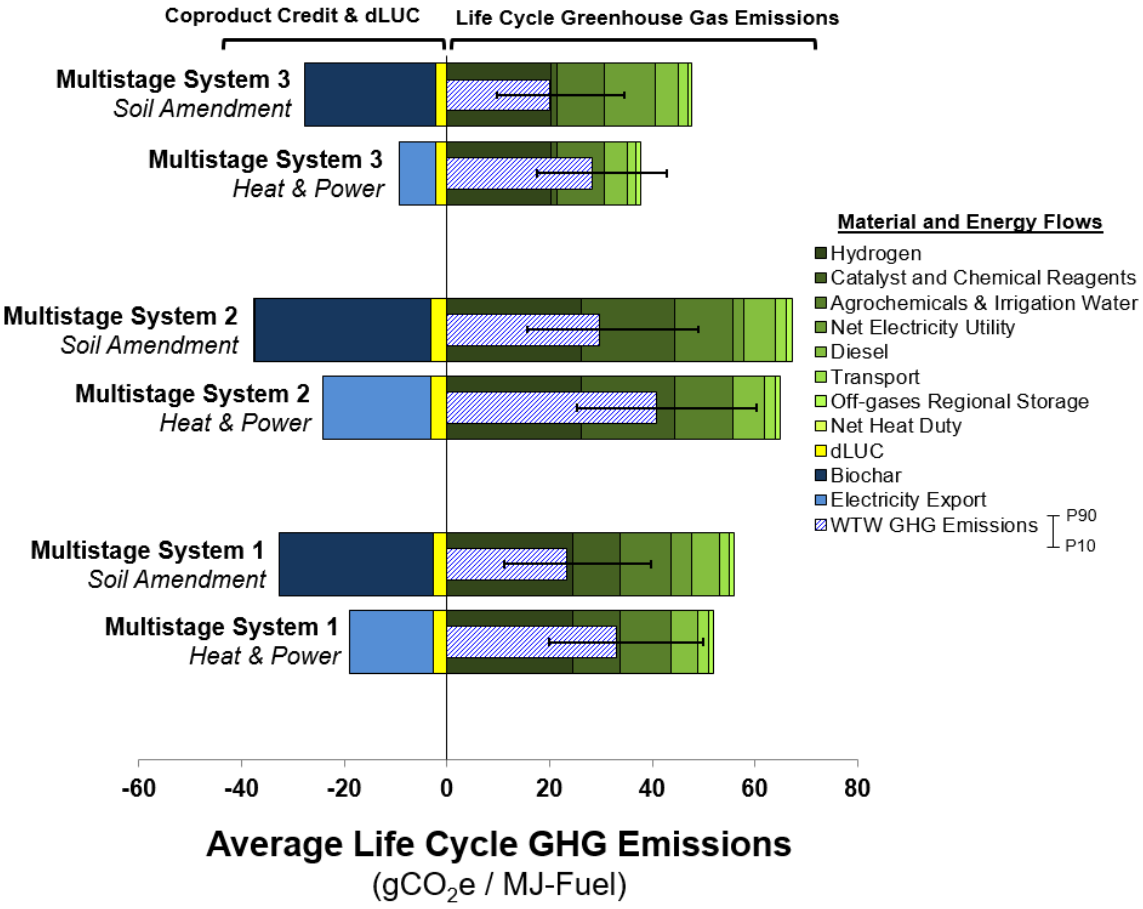

Figure 27. Life Cycle GHG Analysis. Average life cycle GHG impacts for process inputs and coproduct are normalized to 1 MJ of hydrocarbon biofuel. Well-to-wheel results are shown utilizing the displacement method. Negative values indicate GHG credit from coproducts, while positive values indicate life cycle GHG emissions for material and energy inputs. WTW life cycle GHG emissions represent the difference between life cycle GHG emissions throughout the supply chain and coproduct GHG credit.

5.4.7 Sensitivity Analysis

Sensitivity analysis was conducted to determine how variation in model parameters influence key sustainability metrics under different coproduct scenarios and allocation schemes. Figure 28

presents a series of tornado plots for life-cycle GHG emissions and EROI for multistage system 3 using energy-based allocation, Results using the displacement method are provided in Appendix D. Results reveal that key sustainability metrics are highly sensitive to liquid fuel yield, hydrogen consumption, and biochar yield. These findings highlight the utility of catalytic strategies for improving the environmental profile of biofuel systems, i.e. via increasing the liquid carbon fuel yield through C-C coupling reactions while simultaneously reducing hydrogen consumption, and are reflected in the large differential in observed environmental performance (i.e. EROI and life cycle GHG emissions) between multistage and base-case systems. Past research has suggested that the environmental performance of biofuel systems could be increased via converting the aqueous fraction of the bio-oil to bio-hydrogen [338]. However, given the high sensitivity of the results to liquid fuel yield, the findings from Figure 28 suggest that it is more advantageous to convert light molecular weight bio-oil compounds to hydrocarbon fuels via catalytic routes, as compared to conversion to bio-hydrogen, as it results in higher median EROI and lower life cycle GHG emissions.

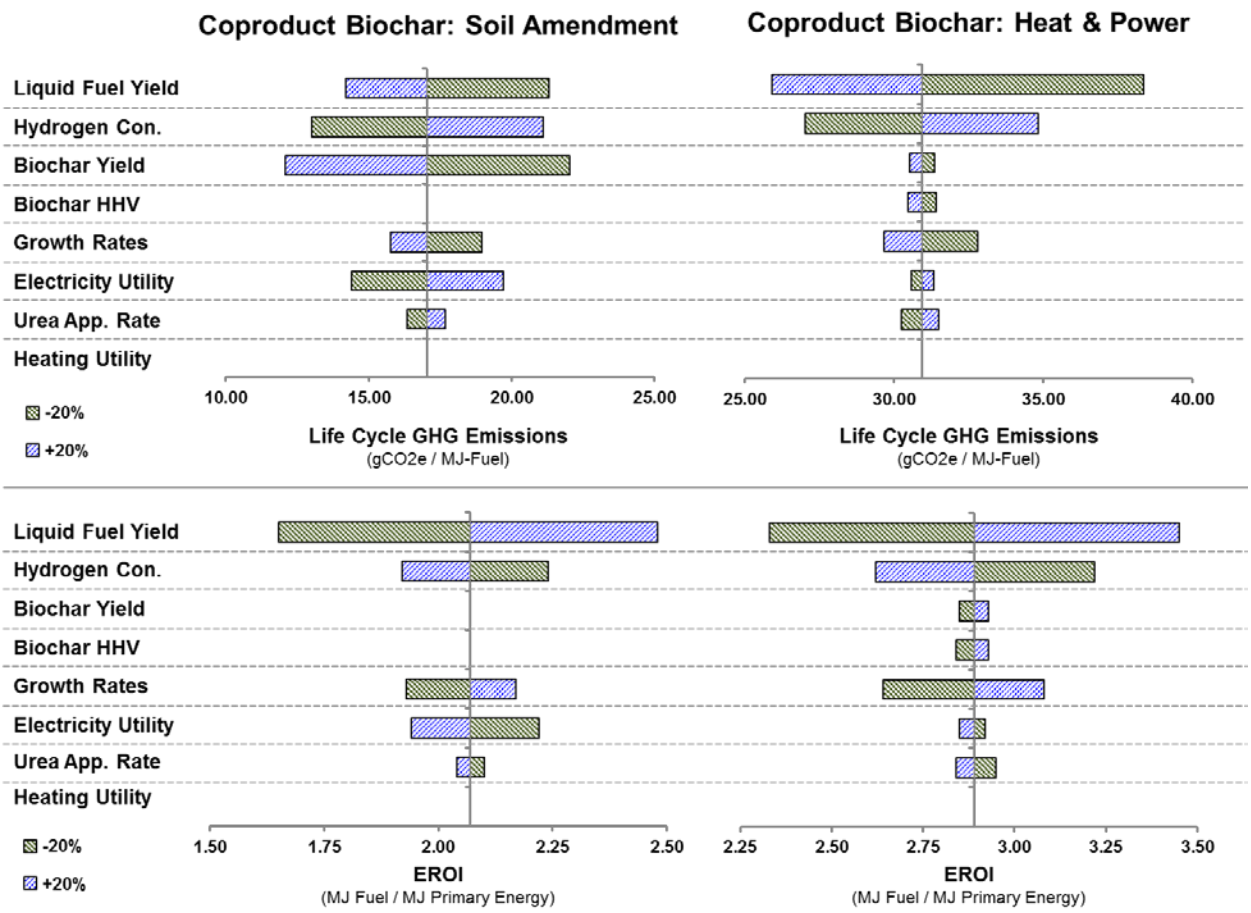

Figure 28. Sensitivity Analysis: Multistage Stage Design Case #3. Tornado Plots for Median EROI and Life Cycle GHG Emissions using Energy-based Allocation.

5.5 CONCLUSIONS

This work is *proof of concept* that multistage torrefaction/pyrolysis and *in-situ* catalytic upgrading is an environmentally sustainable and promising platform for producing hydrocarbon transportation fuels. The results of this work have shown that multistage system 3 has the highest environmental performance of the examined design cases, and suggest that reduction in overall process complexity can be achieved via collapsing the two torrefaction stages (i.e. stage 1 and stage 2) into a single reactor. Furthermore, the results of this work have shown that hydrocarbon biofuels produced via multistage systems have promising EROI and GHG emissions profiles, with over 80% reduction in life cycle GHG emissions relative to baseline petroleum fuels, but are sensitive to the choice of LCA allocation scheme and coproduct scenario for the produced biochar. Fossil-derived hydrogen was found to constitute the principle GHG and primary energy burden across all systems. Additionally, while primary energy consumption and life cycle GHG emissions are two important metrics for benchmarking and screening the sustainability of emerging fuel pathways, single-metric analysis fails to capture broader environmental externalities and unintended consequences that may compromise the long-term sustainability of these systems [339]. Accordingly, additional criteria such as process economics, impacts on water and air quality, biodiversity, human health, ecological wellbeing [197], etc. must be considered so that biofuel production does not inadvertently shift environment impacts across domains or outside the analytic boundary. While outside the scope of this study, techno-economic analysis is to necessary to determine the economic and commercial viability of hydrocarbon fuels produced via multistage torrefaction and catalytic upgrading. Further, concurrent production of hydrocarbon biofuels and high-value bio-based chemicals via lignocellulosic biorefineries has received attention from national actors such as the U.S.

Department of Energy for their potential for mitigating risk, improving process economics, and reducing environmental impacts across the life cycle [340-343]. Multistage torrefaction and pyrolysis systems unique thermal fractionation and catalytic upgrading design show merit for the coproduction and valorization of platform/specialty chemicals and hydrocarbon biofuels, and should be considered in future environmental sustainability assessments.

6.0 DESIGN OF SUSTAINABLE BIOFUEL PROCESSES AND SUPPLY CHAINS: CHALLENGES AND OPPORTUNITIES

The following chapter is based on a peer-reviewed article published in *Processes* with the citation:

Zaimes, G. G., Vora, N.; Chopra, S. S.; Landis, A. E.; Khanna, V., *Design of Sustainable Biofuel Processes and Supply Chains: Challenges and Opportunities.* Processes, 2015. **3**(3): p. 634-663.

6.1 CHAPTER SUMMARY

The current methodological approach for developing sustainable biofuel processes and supply chains is flawed. Life cycle principles are often retrospectively incorporated in the design phase resulting in incremental environmental improvement rather than *a priori* selection of fuel pathways that minimize environmental impacts across the life cycle. Further, designing sustainable biofuel supply chains requires joint consideration of economic, environmental, and social factors that span multiple spatial and temporal scales. However, traditional life cycle assessment (LCA) ignores economic aspects and the role of ecological goods and services in supply chains, and hence is limited in its ability for guiding decision-making among alternatives—often resulting in sub-optimal solutions. Simultaneously incorporating economic and environment objectives in the design and optimization of emerging biofuel supply chains requires a radical new paradigm. This work discusses key research opportunities and challenges in the design of emerging biofuel supply chains and provides a high-level overview of the current "state of the art" in environmental sustainability assessment of biofuel production and proposes a novel modular multiscale and multiobjective optimization framework for the sustainable design of emerging biofuel supply chains.

6.2 DESIGNING SUSTAINABLE BIOFUEL SUPPLY CHAINS

Recent interest in biofuels has led to the development and use of models and computational tools at multiple scales including large-scale crop models, detailed chemical process design simulations, life cycle assessment models, and mathematical optimization tools. While these computational methods each provide unique and novel insights into the sustainability of emerging biofuels, these tools are often used in isolation and thus are limited in their ability for guiding decision-making. Synthesis of these models and tools into a unified framework is required to provide a broader understanding of the sustainability of emerging biomass-to-fuel supply chains. Accordingly, this work discusses a modular multi-scale and multi-objective optimization framework spanning from the field/lab scale, to the detailed process scale, the life cycle scale, and finally the ecosystems scale for holistic sustainability assessment of biofuel production; see Figure 29. The envisioned multi-scale approach evaluates the process in a hierarchical fashion, starting from the field/lab scale and expanding the system boundaries as successive scales are added. Information from lab/field trials such as reactor kinetic studies, pilot-scale biomass growth trials, and experimental trials on biofuel yields are used to parameterize design blocks and crop models used at the process level. Information such as liquid product distribution and operating plant utility requirements obtained via the process level is subsequently utilized to model unit processes in the supply chain. Information at the supply chain is coupled with the larger economy and ecosystems via the use of environmentally extended economic models. Such an approach is conceptually attractive since it facilitates the evaluation procedure starting with simple systems and increasing complexity gradually as successive information layers are added. This approach can allow for screening out bad alternatives, for example, those with a negative economic potential early in the design stage thus

saving computational time and providing a range of alternatives to the decision maker while avoiding arbitrary combinations. Further, the proposed framework considers multi-objective optimization over the broader superstructure to identify supply chain configurations that optimize ecological and economic performance while simultaneous achieving minimum threshold sustainability criteria. Design opportunities and challenges for each scale of analysis are discussed in the following sections.

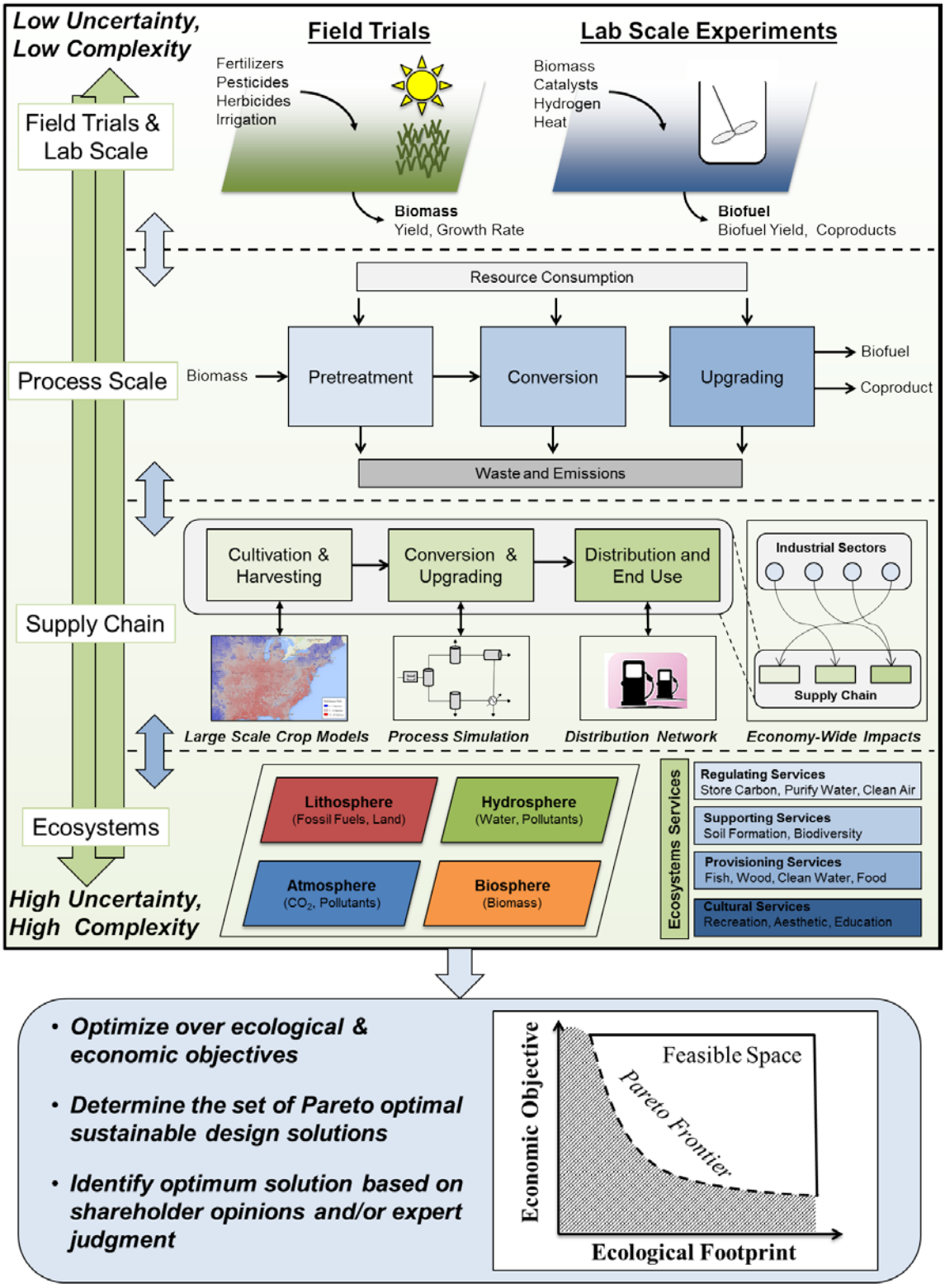

Figure 29. Modular Multi-scale, Multi-objective, Biofuel Supply Chain Optimization Framework

6.2.1 Field Trials and Laboratory Scale Experiments

The first level of analysis involves field trials and laboratory scale experiments such as model compound studies [312, 313], effects of catalysts and reactor conditions on product streams [273], estimation of fuel properties [344], reactor kinetic studies [345, 346], pilot-scale biomass growth trials [215], and the effect of varying fertilizer and management practice on biomass yield [243, 347]. This research is often focused on understanding the mechanism or principles underlying experimental observation, or determining the technically feasibility of an emerging technology. Factorial designs are often implemented to study the effect of each effect factor on the response variable (i.e. biofuel yield), as well as the effect of interactions between factors on the response variable [348]. Further, data at the field/lab scale typically has low uncertainty, and is often used for calibration and parameterization in process models.

6.2.2 Process Scale

The next tier of analysis involves the use of agricultural crop models as well as traditional process design analysis. A variety of large-scale crop models have been developed to simulate bioenergy crop production including herbaceous crops (EPIC, ALMANAC, MISCANMOD, MISCANFOR, WIMOVAC, Agro-IBIS, Agro-BGC, APSIM, AUSCANE, LPJmL, CANEGRO), woody bioenergy crops (3PG, SECRETS), and crassulacean acid metabolism crops (EPI) [349]. These models simulate biomass yield, nutrient cycling, water requirements, carbon flux, and other key parameters under different crop management practices. Recent efforts have been made to integrate these models with Geographic Information Systems (GIS) to create spatially explicit large-scale crop models [350]. Conversion of biomass to fuel can be modeled using conventional process simulators such as Aspen Plus, ChemCAD, or SuperPro [351]. Inputs

to the biorefinery generally include the raw materials and utilities such as biomass, steam, electricity, and cooling water. Similarly, the final products typically include biofuel, coproducts, waste, and emissions. Process simulators provide a scientifically rigorous method for determining the utility requirements as well as material and energy flows for conversion of biomass to renewable transportation fuel. Information at this scale of analysis is often used for developing technoeconomic models [37, 352], with the primary objective of maximizing material and energy efficiency while concurrently minimizing operating costs. Life cycle considerations such as the *embodied impacts* of material and energy inputs are not considered within the scope of analysis at this scale, thus decision-making based solely on information at the *process scale* could result in unsustainable design choices. For example, analysis based solely on the process scale could result in selection of high quality resources (i.e. fossil fuels) for maximizing plant performance and economics; however, these resources often have high upstream environmental or human health impacts.

6.2.3 Modeling the Supply Chain and Life Cycle

The third level of analysis extends the analytic boundary to consider the material, energy, and emissions flows throughout the entire supply chain. This holistic systems approach captures environmental impacts that are outside the purview of the traditional process design boundary. Life cycle Assessment (LCA) is one of the most common approaches for evaluating the environmental impact of a product or a process over its entire life cycle, and in recent years has emerged as the predominant method for analyzing the environmental sustainability of emerging biofuel platforms [56, 75, 91, 144, 147, 208, 211, 261]. LCA considers impacts throughout all stages of the fuel life cycle—from raw material acquisition, to fuel conversion, and final use.

LCA allows for a comprehensive understanding of the environmental impacts that occur at each stage of the supply chain, enabling the LCA practitioner to identify processes responsible for highest environmental burden and thus target these areas for process improvement. LCA can be used to quantify the anticipated impacts of a product or service prior to its widespread adoption, thus identifying and avoiding potential environmental pollutants, wastes, and environmental damages before they become embedded within the supply chain. Further, LCA can be used to compare the environmental performance between two products with the same functionality and can inform environmentally conscious decision-making. Garcia and You reviewed major challenges and opportunities in supply chain design and optimization—identifying several key technical challenges including (i) multiscale challenges, (ii) multiobjective and sustainability challenges, and (iii) multi-player challenges [353].

6.2.3.1 Process LCA

LCA is a data intensive approach and has been extensively applied to study biofuel systems over the past decade. Several different LCA modeling methods have been developed; the most widely used LCA approach (*i.e.*, Process-LCA) defines a finite boundary by selecting the most important processes in a life cycle [95]. Data concerning the resource consumption and emissions for these processes are developed and compiled to generate a life cycle inventory (LCI). The life cycle impact assessment (LCIA) phase translates the energy, resource, and emissions flows identified in the LCI into their potential consequences for human health and the environment, and consists of a two-step process of impact classification and quantitative characterization. The classification step links each LCI flow with its related impacts on resource use, human health, and the environment. The characterization step calculates the magnitude of the associated impacts in terms of a reference unit for each category via multiplying the related

resource, material, or energy flows with their respective impact factors. Translating the environmental impacts to a reference unit provides a common basis or measure for the generated impact, so that different emissions and resources can be compared and aggregated using a common unit. Data required for LCA can be obtained via commercial life cycle databases (e.g., ecoinvent [96]), publicly available life cycle data (e.g., OpenLCA [97], USLCI [98], GREET [99]), information from the open literature, or proprietary information.

Although widely used, process LCA suffers from many limitations including the use of an arbitrary life cycle boundary, combining data in disparate units and at multiple spatial and temporal scales, dealing with high dimensionality data involving varying degrees of uncertainty, and dealing with processes having a range of emissions [11]. Furthermore, for a system that simultaneously produces multiple products and coproducts these is no universally accepted method as to how to apportion the environmental impacts amongst said products. This is particularly important for biofuel systems in which non-fuel coproducts represent a significant fraction of total market value, mass, or energy flow as the choice of allocation procedure can often yield divergent results concerning the sustainability of these systems [100,101]. Additionally, biofuel LCAs often utilize differing functional units, system boundaries, allocation schemes, impact assessment methods, and report different sustainability metrics. Consequently, it is not unusual for LCA practitioners to obtain contradictory LCA results for the same system; this discrepancy has led to several harmonization and meta-analysis studies in the biofuels literature [102,103]. Data used in process LCA is at an intermediate scale since it is typically averaged to represent manufacturing processes, thus making it of limited use for making environmentally conscious engineering decisions about an individual process or equipment,

which are at a finer scale, or for evaluating the effect on the macro economy, which is at a coarser scale.

6.2.3.2 EIO-LCA and Hybrid LCA

Input-output (IO) models, first developed by Nobel Prize winning economist Wassily Leontief, provide a mathematical framework for quantifying the inter-industrial connections and economic flows between different industrial sectors in the economy [104]. The traditional IO framework can be extended to consider the environmental impacts, emissions, and resource use for industrial sectors in the economy; and thus be utilized to perform LCA at the economy scale. This approach, known as Economic Input-Output LCA (EIO-LCA) [105], does not suffer from the challenge of defining a finite life cycle boundary as does Process LCA. Further, EIO-LCA uses a relatively complete network, but at a coarse scale of resolution. Data at this scale often do not include the use phase of the life cycle. Recently, Bakshi and colleagues have developed Ecologically-based Life Cycle Assessment (EcoLCA), an environmentally extended input-output life cycle model capable of accounting for the consumption/role of ecosystem goods and services in a life cycle framework [106,107]. The EcoLCA model extends the traditional I-O framework to consider the direct and indirect environmental impacts that result from economic activities; including ecological and natural resource consumption, emissions, land-use, and other environmental impact categories [108–110]. EcoLCA quantifies ecological resource consumption using a hierarchy of thermodynamic metrics including energy, industrial cumulative exergy consumption (ICEC), and ecological cumulative exergy consumption (ECEC), as well as mass flow. However, while exergy-based methods for thermodynamic aggregation of natural resource consumption may provide useful insights, these methods have their own limitations and are debated in the literature [111–118]. Research on combining the best

advantages of Process LCA and EIO-LCA has also resulted in Hybrid LCA approaches, which combine the details of Process LCA with the greater completeness of EIOLCA [119,120]. Hybrid LCA attempts to balance computational tractability, completeness, and the use of detailed information.

LCA models may also differ in the approach employed to address the material and energy flows in the system under investigation. The attributional LCA (ALCA) methodology, which has been utilized for a vast majority of the LCA studies, attempts to quantify the flow of resources and emissions from a product system and its subsystems. Emissions and their impact are attributed to the final product by one of the several available methods (allocation or system expansion). However, researchers have argued that it is not fully possible to draw conclusions on future changes by using only ALCA [121,122]. In contrast, consequential LCA (CLCA) methodology, aims to explain how the physical flows to and from the technosphere may change in response to a change in the life cycle of the product or service [123]. CLCAs attempt to consider a much broader system boundary. The most commonly employed form of a CLCA considers the use of economic models that track monetary, material, and energy flows across economic systems. This is generally accomplished using marginal data and is accounted for on the basis of price elasticity of supply and demand [124–126].

The US Environmental Protection Agency (US EPA) has used a multi-market multi-region partial equilibrium model to determine land use change emissions in biofuel lifecycles. Several dynamic general/partial equilibrium models have been used to predict the implications of biofuel policy and commercialization on land use, international/domestic trade, and GHG fluxes and commodity markets within the agricultural sector including the Global Trade Analysis Project (GTAP), the Market Allocation Model, the Forestry and Agricultural Sector

Optimization Model (FASOM), and the Food and Agricultural Policy Research Institute model, LEI-TAP model, and Modular Applied General Equilibrium Tool, Center for Agricultural and Rural Development model, International Model for Policy Analysis of Agricultural Commodities and Trade model, Common Agricultural Policy Regional Impact Analysis model, the Worldwide Agribusiness Linkage Program and Commodity Simulation Model, and the Modeling International Relationships in Applied General Equilibrium model [127–132]. However, lack of model transparency and high complexity often limit the utility of these approaches. Furthermore, these models often vary in regards to data requirements, scope, and model resolution. For example, models such as FASOM have high resolution for the United States but lack information regarding international trade; while models such as GTAP can provide estimates for domestic and international land-use change but at a low level resolution. Synthesis and coupling these dynamic economic models with biophysical land-use models such as the Integrated Model to Assess the Greenhouse Effect, Conversion of Land Use and its Effects as well as energy models such as the PRIMES Energy System Model can help support informed decision making [133,134]. However, it is important to note that that economic systems exhibit structural inconstancy (*i.e.*, change in individual behavior in response to a policy change), and coupling economic and biophysical models will increase overall model uncertainty [135]. Plevin *et al.* pair an economic-computable general equilibrium model with a CO_2 emissions estimation model and conclude that due to parametric uncertainties, the results obtained should be used for developing a range of possible results for comparison purposes rather than as deterministic estimates of land use change emissions [136].

LCAs of emerging technologies are difficult to conduct due to lack of technology specific data, dynamic and rapidly evolving systems, and isolation of environmental research from

technical developments [137]. Prospective LCAs involve estimating environmental impacts of possible future scenarios and are affected by the choice of time horizon, complexity of the system, and extent of stakeholder engagement. Studies have used approaches such as scenario analysis [138,139], participatory methods involving expert elicitations and stakeholder opinions [137] and modeling of economic transactions to understand market-mediated effects [140]. Many of the challenges associated with prospective LCA can be overcome with inclusion of life cycle thinking at an early stage in research and development (R&D) via a collaborative dialogue between industry experts, stakeholders, and LCA practitioners.

Analysis at this scale is often focused on improving efficiency and reducing environmental impacts across the life cycle, utilizing methods and metrics such as eco-efficiency, life cycle GHG emissions, net energy analysis, water footprint, and others. However, these methods fail to capture the impact of biofuel life cycles on ecological goods and services, i.e. the fundamental goods and services provided by nature that sustain human life and are the fodder for all man-made capital and industrial activity [354]. Consequently, decisions based on these methods could result in unsustainable choices including heightened depletion and degradation of natural capital and ecosystems [153, 355, 356].

6.2.4 Ecosystems Scale

The final tier of analysis extends the analytic scope to consider the role of ecological goods and services throughout the supply chain. As ecological goods and services play a fundamental role in sustaining industrial activity, it is paramount to account for their role in evaluating the impact and sustainability of emerging biofuel platforms. Examples of ecological goods and services include: timber, food, water, energy resources, clean air, minerals and ores, purification of air

and water resources, flood and drought mitigation, pollination of crops and vegetation, maintenance of global biodiversity, as well as climate and disease regulation [357-359]. Since it is computationally intractable to model the complete supply chain by including each process as done at the life cycle level of analysis, the approach leveraged at this scale of analysis is closely related to existing hybrid (tiered) LCA methods in which a process level model is used to determine *process level* consumption of ecological goods and services while economy wide-impacts are incorporated using EcoLCA [151, 155, 156, 173, 183].

Process level flows of ecological goods and services can be modeled using a host of computational models. Detailed models such as Century, EPIC, APEX, and SWAT can be used to simulate the effects of land management decisions on soil, water, nutrients and watersheds; however, these tools are data intensive and suffer from high model complexity [360-362]. The Integrated Valuation of Ecosystems Services and Tradeoffs (InVEST) modeling suite can be used to quantify and map a variety of regional ecosystems goods services as well as biodiversity for both terrestrial and marine environments including crop pollination, habitat quality, habitat risk assessment, managed timber production, managed fish aquaculture, marine water quality, sediment retention, water purification, carbon sequestration, and others [363]. Further, InVEST model(s) are open-source, generally simpler, more transparent, and user friendly as compared to the aforementioned approaches. Integrating these computational models with EcoLCA can provide a holistic understanding of the potential impacts and tradeoffs of biofuel production on ecological resources and biodiversity. Although this tier of analysis is the most comprehensive it often has high uncertainty due to (i) variability that is propagated and compounded at each preceding level of analysis (i.e. from lab/field scale, to process scale, to supply chain), and (ii) high uncertainty in the modeling approaches used to quantify ecological goods and services.

Bakshi and colleagues have developed and applied a hybrid EcoLCA framework to investigate the sustainability of petroleum transportation fuels as well as select first and second-generation biofuels [150, 153]. More recently, this framework has been applied to study emerging microalgal biofuel systems [197]. The results of these studies reveal that biofuels have high renewability but typically have low thermodynamic return on investment relative to baseline petroleum fuels. The low energy return on investment for biofuels is concerning as prior studies have suggested that a liquid technical fuel must achieve minimum threshold energy return on investment (EROI) values to sustain society, failure to meet this minimum EROI criterion could result in widespread economic and social ramifications as more useful work must be expended by society for fuel production and thus cannot sustain other economic activities [178, 266]. Recently, Bakshi and colleagues have developed a conceptual framework for designing technological and ecological systems that encourages synergy between human activity and nature [364, 365]. The proposed techno-ecological synergy (TES) framework considers the demand of ecological goods and services from technological systems at multiple spatial scales ranging from the individual process scale, to supply chains and life cycles, as well as the supply of ecological good and services from ecological systems ranging from regional, to watershed, to global. The TES framework aims to reduce overconsumption of natural capital, and promotes technological systems to operate within safe ecological boundaries at multiple analytic scales. Application of the TES framework can provide unique insights into the sustainability of emerging biofuel supply chains.

6.2.5 Accounting for Multiple Objectives and Scales in Designing Sustainable Biofuel Supply Chains

Environmentally conscious development of emerging biofuel pathways requires addressing alternatives that exist at each step along the life cycle with the possibility of a multitude of useful coproducts and waste streams. As such, decisions based on optimizing a single criterion (such as carbon footprint, EROI, or economic potential) can lead to the unintended consequence of trading one environmental problem for another. Many studies have focused on evaluating bioenergy potential encompassing several criteria—economic performance, environmental and social impact and have developed several tools that quantify these indicators [157]. For example, the SCORE Model developed by Krajnc and Domac uses a mix of qualitative and quantitative indicators such as contribution to forest management, impact of regional unemployment, CO_2 emissions, and percentage of self-sufficiency in electricity production, to analyze the sustainability of woody biomass production [158].

Studies often employ various optimization techniques to design an optimal biomass supply chain based on multiple criteria [159,160]. Formulating the design problem as a mathematical optimization task has been a common approach for analyzing technological systems. The design problem is generally formulated as either a mixed integer linear or non-linear optimization problem [161,162]. Research efforts have also resulted in coupling the design problem with LCA by quantifying the life cycle impacts of process alternatives. This could be accomplished using either single objective or multi-objective optimization (MOP) resulting in designs or options that represent the best compromise between the selected design criteria [163,164] Several studies have utilized MOP for the strategic design and implementation of biofuel systems. Zamboni *et al.* developed a spatially explicitly mixed integer linear program (MILP) optimization model for bioethanol production systems that simultaneously considers

supply chain costs and life cycle GHG emissions [165,166]. De Meyer *et al.* developed a generalized mathematical model, OPTIMASS, that optimizes over strategic and tactical decisions, and can be used to investigate the potential effect of policy changes, emerging biofeedstocks, technological adoption/evolution, and logistics on the environmental sustainability of biofuel supply chains [167]. Čuček *et al.* coupled MOP with a regional biomass supply chain model [168].Mele *et al.* developed a MILP optimization model to optimize economic and environmental objectives of the biofuel production chain, and applied the model to the sugarcane industry in Argentina [169]. More recently, Yue *et al.* developed a multi-objective life cycle optimization framework and applied it to study emerging hydrocarbon biofuel production [170]. MOP can be used to identify design solutions that optimize economic, environmental, and ecological dimensions of biofuel production; this set of optimal points constitutes a Pareto frontier in the design-solution space. Moreover, solutions that do not lie on the Pareto frontier are either infeasible or are sub-optimal. The Pareto frontier is particularly useful in MOP problems since by restricting attention to the set of choices that are Pareto efficient, a designer can evaluate tradeoffs within this set, rather than considering the full range of every parameter. Further, MOP can be used to identify the optimal mix of useful coproducts satisfying the selected set of life cycle environmental constraints. An alternative to mathematical programing is a heuristic approach that employs algorithms based on artificial intelligence to obtain a satisfactory local optimal solution, when a global optimal solution is not possible. Studies have employed various algorithms such as particle swarm optimization, genetic algorithms or honeybee foraging algorithms to identify a range of optimal solutions for various aspects of the biomass supply chain [171–173]. These approaches are expected to lead to the

identification of synergies between feedstock production, processing methods, and the final mix of fuels and coproducts for the sustainable design of biorefineries [170,174,175].

6.2.5.1 Uncertainty and Variability

Emerging hydrocarbon biofuel platforms have a high degree of uncertainty [176], due to lack of commercialization, climatic variability, technological evolution, material and energy price volatility, variability in supply and demand dynamics, dynamic effects in ecosystems, and changes in biofuel incentives and legislation over time. Further, sources of modeling uncertainty generally include: (i) parameter uncertainty; (ii) technological uncertainty; (iii) random error; (iv) systematic uncertainty; (v) methodological uncertainty; (vi) parametric variability; (vii) structural uncertainty; (viii) algorithmic/interpolation uncertainty; and (ix) policy uncertainty. These sources of uncertainty introduce variability at each stage of the analysis, which are compounded and propagated with subsequent modeling scales and the use of higher complexity models. Several commons approaches are often utilized to quantify uncertainty in environmental sustainability analysis including stochastic modeling and one-at-a-time (OAT) sensitivity analysis [177–179]. It is important to note that the primary utility of environmental sustainability analysis is to identify potential environmental impacts or damages of emerging technologies at early stages of R&D. However, recommendations at the design/conceptual phase typically have high uncertainty, which is often only reduced after large investments and progress in R&D have been made. As such, environmental sustainability analysis of emerging technologies inherently faces a tradeoff between utility and uncertainty. Additionally, for biofuel production uncertainty in upstream processes can translate into heightened risk downstream. For example, farmers are often reluctant to grow second generation biofeedstocks due to their high fixed cost of production, long establishment period, and uncertainty regarding the demand for these crops. However, the

lack of large-scale agricultural production of second generation biofeedstocks generates heightened risk for developing next generation biorefineries, thus potentially limiting the demand for second-generation biofeedstocks.

7.0 CONCLUSIONS AND FUTURE WORK

In its inception, first generation biofuels were touted as a revolutionary new renewable and *sustainable* fuel source. Technological exuberance and naivety lead to their large-scale commercialization without proper consideration of the potential widespread consequences for industry and the environment. Since then, a multitude of studies have shown that the production and use of first generation biofuels has resulted in detrimental impacts on the ecosphere, environment, economy, and social welfare [64, 366]. As biofuel production is inherently interconnected with various critical sectors of the economy (i.e. agriculture, transportation, etc), it is crucial to understand the potential widespread impact of emerging 2nd generation biofuels on economics, environment, and human welfare prior to their widespread adoption and commercialization. To date, the scientific consensus is inconclusive on several pivotal questions within the sustainability and fuel/energy discourse, including: (I) What are the potential environmental impacts and ecological resource consumption for large-scale 2nd generation biofuel production, (II) how do different technological and coproduct scenarios as well as LCA allocation schemes effect the environmental profile of nascent biofuel pathways, (III) do biofuel(s) met compliance with life-cycle GHG emissions reductions thresholds set by U.S. federal regulatory programs and/or select key sustainability criteria (such as critical EROI performance thresholds), and (IV) what are the tradeoffs between various combinations of

biofeedstocks and fuels platforms—which provide the greatest potential benefits? This work sought to answer these questions piecewise using a case-study approach.

Chapter 2 investigated the environmental impacts of producing dried algal biomass through the cultivation of microalgae in Open Raceway Ponds (ORP) for 21 geographic locations in the contiguous United States (RQ #1). The results indicate that microalgal biomass has a marginally positive energy balance and is plagued with high technological uncertainty, but has potential for GHG reductions via synergies with industrial processes. EROI & GHG emissions for microalgal biomass were found to be highly dependent on technological route, but are relatively location invariant. Contrarily, the direct water-footprint for microalgal biomass production is highly dependent on cultivation location. The critical parameters in biomass production were determined to be natural gas required for biomass drying and MEA scrubbing, electricity required for freshwater supply and circulation, and nitrogen fertilizer demands. Alterative approaches involving hydrothermal [64] and solvothermal processes [65] and the use of supercritical fluids such as methanol or CO_2 for lipid extraction from wet algal biomass have emerged as promising solutions for eliminating algal drying requirements, and are actively being investigated [69–74]. Developments in algal species selection [75], increased control over algal composition and growth parameters, and genetic engineering [76,77] may provide a means of maximizing algae's lipid content while concurrently minimizing fertilizer requirements. Researchers are investigating other synergies such as the use of wastewater as a source of nitrogen and phosphorus for algal growth [78–84]. However, high-level evaluation of these industrial symbiotic opportunities is required in order to determine their technical feasibility and commercial applicability. Additionally, while regions such as AZ are often touted as favorable locations for biofuel production due to their high aerial growth rates, these locations are

characteristically found in arid climates with low freshwater availability, and thus may limit their commercial viability and merits further investigation.

Chapter 3 developed a hybrid Ecologically based-LCA (EcoLCA) model to quantify the contribution of ecological resources within the algae-to-fuel supply chain and to compare the resource intensity of producing microalgal derived renewable diesel (RD) to that of petroleum diesel (PD) (RQ #2). This work revealed that algae-to-fuel systems are highly dependent on non-renewable ecological resources reflected in their low renewability index; have a low quality corrected thermodynamic ROI (<1) and thus are not energetically viable; and are more ecologically resource intensive as compared to their petroleum equivalent—potentially negating their environmental benefits. Thermodynamic analysis based on exergy and emergy were found to provide a scientifically rigorous approach for valuing the contribution of ecological goods and services in product life cycles, while concurrently addresses several existing problems in traditional energy analysis including accounting for the quality, substitutability, and useful work provided via material and energy resources. This work highlighted the fallacies of traditional energy analysis, and showed that exergy and emergy analysis can provide valuable insights into the sustainability and performance of emerging microalgal biofuel systems. Additionally, this work has shown that in the best-case scenario microalgal fuel systems are marginally energy positive, and more ecologically resource intensive as compared to their petroleum equivalent on a functional unit basis. However, technological maturation and optimization of the algae-to-fuel production chain as well as coupling microaglal biofuel production with ecological processes have the potential for reducing the amount of human made work required for biofuel production while concurrently increasing the sustainability of these emerging fuel systems.

Chapter 4 presented a life cycle assessment of liquid transportation fuels derived via fast pyrolysis of perennial grasses and hydroprocessing of bio-oil (RQ #3). The results of this work indicate that single-stage fast pyrolysis and hydroprocessing system have several limitations including: high hydrogen consumption, high production of light hydrocarbons, and low liquid carbon yield. Analysis reveals that the EROI and GHG emissions for single-stage fast pyrolysis systems are highly sensitive to bio-oil yield as well as hydrogen consumption, with exogenous fossil hydrogen consumption the primary energy burden and GHG in the supply chain. Further analysis reveals that the energetic performance and GHG reduction potential of fast pyrolysis-derived fuels are dependent on the choice of coproduct scenario for the biochar and LCA allocation scheme, and in select cases can change the life cycle carbon balance from meeting to exceeding the renewable fuel standard emissions reduction threshold for cellulosic biofuels. Alternative reactor configurations, process options, and chemical conversion pathways including pre-treatment via torrefaction (mild pyrolysis) [293, 294], catalytic upgrading strategies [7], and sequential hydroprocessing [258] stages have the potential to reduce the hydrogen requirements for fuel conversion and upgrading while simultaneously increasing the liquid carbon yield, and thus increase the environmental sustainability of emerging thermochemical fuel platforms [32, 273], and should be considered in future environmental sustainability analysis of pyrolysis derived biofuels.

Chapter 5 presented a prospective wheel-to-wheel life cycle assessment of a series of novel multistage torrefaction/pyrolysis and in-situ catalytic upgrading fuel platforms for converting short rotation woody crops to hydrocarbon biofuels (RQ #4). This work revealed that multistage system(s) have several advantages over current industrial practice (*base-case*) including: (1) the product distribution for multistage systems are skewed towards longer carbon

chain compounds that are fungible with diesel-range fuels and (2) multistage systems use up to ~38% less hydrogen as compared to the base-case. Multistage thermal fractionation and selective catalytic upgrading systems were found to have promising EROI & GHG emissions profiles, with up to 76% reduction in GHG emissions relative to petroleum diesel. Fossil-derived hydrogen was found to constitute the principle GHG and primary energy burden across all systems. Additionally, multistage torrefaction and pyrolysis systems unique thermal fractionation and catalytic upgrading design show merit for the coproduction and valorization of platform/specialty chemicals and hydrocarbon biofuels, and thus should be considered in future environmental sustainability assessments.

Chapter 6 discussed key research opportunities and challenges in the design of emerging biofuel supply chains, and proposed a novel modular multiscale and multiobjective optimization framework for the sustainable design of emerging biofuel supply chains (RQ #5). The proposed multiscale and multiobjective framework outlined in this chapter has multiple features that make it conceptually attractive; however, the approach faces several challenges: (I) Interdisciplinary research requires effective communication, transfer, and synthesis of domain specific knowledge and data across research fields. This requires that collaborators become proficient in the colloquial terminology commonly used in said research fields, so that domain specific modeling results and technical information can be exchanged efficiently and information is not lost at the interface of research fields. (II) The long timeframe required for laboratory/field trials as well as the development and implementation of modeling tools may limit the effectiveness of this approach, as the “state of the art” may have changed or the technical system evolved from its prior conception at the start of the analysis. However, this issue can be addressed via several means. Streamlined models and methods can help reduce the computation time necessary for

model development and implementation. Further, open source databases and the use of "big data" may help reduce the time required for data acquisition. Additionally, the modeling approach should be iterative; models should be configured to use the most robust, accurate and up-to-date data, with modeling tiers providing feedback-loops to inform the strategic design and development of biofuel processes and supply chains. (III) Differing models/tools may have contrasting assumptions, conflicting theoretical premises, and may report the results using disparate metrics. Additionally, the results may be subjective and have high degree of uncertainty. For these reasons, results should not be considered deterministic outcomes, but probabilistic measures to be used for comparative purposes [180]. While process-scale analysis is the most reductionist and is commonly employed in engineering analysis and traditional process design, this narrowly focused approach fails to capture broader environmental externalities; such shortsightedness could jeopardize the sustainability of emerging biofuel systems. The conceptual multiscale and multiobjective optimization framework presented in this chapter addresses these limitations by optimizing economic and environmental objectives over the field/lab scale, process scale, supply chain, and ecosystems scale. This broad-based interdisciplinary approach is critical for guiding the sustainable development of the biofuels industry and for mitigating and avoiding any unintended consequences. Further, the results of the bibliographic analysis support the need for such a collaborative framework. As such, next generation biofuels represent a promising opportunity for the chemical industry and sustainability engineers to work hand in hand, and transform the traditional paradigm from "end of pipe" solutions to innovative, state of the art, and sustainable design solutions.

In spite of the 'perceived' environmental benefits of biofuels, this body of work suggests that emerging biofuel systems offer only limited solutions to the prevailing energy crisis,

anthropogenic-derived climate change, and destruction of natural capital associated with fossil resources. While biofuels are often touted as an environmental panacea, this work has shown that the choice of biofeedstock, conversion platform, and subjective choice of LCA allocation scheme can yield divergent results regarding the sustainability of biofuel systems and in select cases can result in higher overall environmental and/or ecological impacts relative to baseline petroleum fuels. As such, the benefits of emerging biofuels have been shown to be neither comprehensive nor are biofuels inherently sustainable in the long-term.

This dissertation has shown that biofuels have the capacity for GHG abatement relative to baseline petroleum fuels; however, in the best-case scenario hydrocarbon biofuels are marginally able to achieve the minimum EROI performance threshold (EROI=3) as set by Hall and coworkers [178]—which is considerably less than that of current petroleum diesel (~5). This indicates that broad advances in biotechnologies are required if biofuels are to be energetically competitive with established petroleum fuels. However, it is important to recognize that the formation of crude oil occurs over large geologic time-frames, and that the heat, energy, and material inputs required for the formation of crude oil is provided by nature, that is, earth's natural biogeochemical processes. Additionally, the petrochemical industry is a highly mature field, utilizing petroleum extraction and refining processes and technologies that have undergone continual optimization for more than a century. Conversely, the production of biofuel is highly energy intensive and requires substantial energy and material inputs from the economy. Furthermore, next-generation biomass cultivation, harvesting, and biofuel conversion technologies are emerging fields, which in part explains why the return on investment for biofuels are lower than that of conventional petroleum fuels. However, the differential in EROI between petroleum and hydrocarbon biofuels is expected to decrease over time and ultimately

reach an inflection point, as biofuel processing and conversion efficiencies continue to improve, while finite hydrocarbon resources become more costly to recover. In the near-term, concurrent production of hydrocarbon biofuels and high-value bio-based chemicals via lignocellulosic biorefineries show merit for mitigating risk, improving process economics, and reducing environmental impacts across the life cycle, and represent a promising route to successful commercialization of biofuels and bioproducts.

APPENDIX A

SUPPORTING INFORMATION FOR MICROALGAL BIOMASS PRODUCTION PATHWAYS: EVAULATION OF LIFE CYCLE ENVIRONMETAL IMPACTS

A.1 ELECTRICITY MIX

Data concerning the regional electricity mix for the examined cultivation locations was gathered from the EPA's "Power Profiler", based off the 2007 Emissions and Generation Resource Integrated Database (eGRID), and is presented in Table 8 [108]. Life cycle impact factors for regional electricity generation were constructed based on data available in eGRID database. Existing USLCI data for electricity generation was modified for each location based on the electricity generation mix (% Coal, Gas, Oil, Nuclear, Hydro, Renewables, etc). Impact factors for regional electricity generation were constructed using the Tool for the Reduction and Assessment of Chemical and other environmental Impacts (TRACI) and cumulative energy demand (CED) methods, and account for transmission distribution losses.

Table 8. Electricity Generation Mix

		Resource Mix (%)					
State	**City**	**Coal**	**Gas**	**Oil**	**Nuclear**	**Hydro**	**Non-Hydro Renewables**
AL	Mobile	52.2	22.3	0.3	18.1	4.1	2.9
AZ	Phoenix	38.6	35.7	0.1	16.5	6.1	3.1
CA	San Diego	7.3	53	1.4	14.9	12.7	10.1
FL	Daytona Beach	23.7	54.8	4.4	14	0	1.7
FL	Jacksonville	23.7	54.8	4.4	14	0	1.7
FL	Key West	23.7	54.8	4.4	14	0	1.7
FL	Miami	23.7	54.8	4.4	14	0	1.7
FL	Tallahassee	23.7	54.8	4.4	14	0	1.7
FL	Tampa	23.7	54.8	4.4	14	0	1.7
FL	West Palm Beach	23.7	54.8	4.4	14	0	1.7
GA	Savannah	52.2	22.3	0.3	18.1	4.1	2.9
LA	Baton Rouge	22.7	45.1	1.5	26	1.7	1.9
LA	Lake Charles	22.7	45.1	1.5	26	1.7	1.9
LA	New Orleans	22.7	45.1	1.5	26	1.7	1.9
TX	Austin	33	47.8	1.1	12.3	0.2	5.5
TX	Brownsville	33	47.8	1.1	12.3	0.2	5.5
TX	Corpus Christi	33	47.8	1.1	12.3	0.2	5.5
TX	Houston	33	47.8	1.1	12.3	0.2	5.5
TX	Lufkin	33	47.8	1.1	12.3	0.2	5.5
TX	Port Arthur	22.7	45.1	1.5	26	1.7	1.9
TX	San Antonio	33	47.8	1.1	12.3	0.2	5.5
TX	Victoria	33	47.8	1.1	12.3	0.2	5.5

A.2 SOLAR INSOLATION

A.2.1 Solar Insolation

Data concerning solar insolation for the cultivation locations was gathered from the National Solar Radiation Database (NSRD). This data set contains the average values of solar insolation over a thirty-year period (1961-1990) [105], and is provided Table 9.

Table 9. Average Solar Insolation (kWh / m^2-day)

State	City	March	April	May	June	July	Aug	Sept	Oct	Average
AL	Mobile	4.4	5.4	5.9	5.9	5.6	5.2	4.7	4.2	5.2
AZ	Phoenix	5.5	7.1	8.0	8.4	7.6	7.1	6.1	4.9	6.8
CA	San Diego	4.9	6.1	6.3	6.5	6.9	6.5	5.4	4.4	5.9
FL	Daytona Beach	5.0	6.2	6.4	6.1	6.0	5.7	4.9	4.2	5.6
FL	Jacksonville	4.7	5.9	6.1	6.0	5.8	5.4	4.6	4.0	5.3
FL	Key West	5.5	6.3	6.3	6.1	6.1	5.8	5.2	4.6	5.7
FL	Miami	5.2	6.0	6.0	5.6	5.8	5.6	4.9	4.4	5.4
FL	Tallahassee	4.7	5.9	6.3	6.1	5.8	5.5	4.9	4.3	5.4
FL	Tampa	5.1	6.2	6.4	6.1	5.8	5.5	4.9	4.4	5.6
FL	West Palm Beach	5.0	5.9	6.0	5.7	5.9	5.6	4.8	4.2	5.4
GA	Savannah	4.7	5.8	6.2	6.3	6.1	5.5	4.7	4.1	5.4
LA	Baton Rouge	4.4	5.4	5.9	6.0	5.7	5.4	4.8	4.3	5.2
LA	Lake Charles	4.5	5.4	6.0	6.3	6.0	5.6	5.0	4.3	5.4
LA	New Orleans	4.5	5.5	6.1	6.1	5.7	5.5	4.9	4.3	5.3
TX	Austin	4.7	5.4	5.9	6.6	6.8	6.3	5.2	4.4	5.7
TX	Brownsville	4.6	5.3	5.8	6.4	6.5	6.0	5.2	4.5	5.5
TX	Corpus Christi	4.4	5.0	5.5	6.1	6.3	5.8	5.0	4.3	5.3
TX	Houston	4.2	5.0	5.6	6.0	5.9	5.6	4.9	4.2	5.2
TX	Lufkin	4.5	5.3	5.9	6.4	6.4	6.0	5.1	4.3	5.5
TX	Port Arthur	4.3	5.2	5.8	6.3	6.1	5.7	5.0	4.3	5.3
TX	San Antonio	4.8	5.5	6.0	6.7	6.9	6.4	5.4	4.5	5.8
TX	Victoria	4.4	5.1	5.7	6.2	6.2	5.8	5.0	4.3	5.3

A.2.2 Photosynthetically Active Radiation (PAR)

The fraction of solar energy that can be utilized in photosynthesis relative to the full spectrum solar energy is defined as the percent Photosynthetically Active Radiation (% PAR). In this work the % PAR is assumed to be a constant (46%), consistent with previous studies [52], and is assumed to be the same across all examined cultivation locations. Average monthly PAR values (MJ / m^2) are developed via multiplying values in Table 9 by the % PAR and are provided in Table 10.

Table 10. Average Monthly PAR (MJ / m^2-day)

State	City	March	April	May	June	July	Aug	Sept	Oct	Average
AL	Mobile	7.3	8.9	9.8	9.8	9.3	8.6	7.8	7.0	8.5
AZ	Phoenix	9.1	11.8	13.2	13.9	12.6	11.8	10.1	8.1	11.3
CA	San Diego	8.1	10.1	10.4	10.8	11.4	10.8	8.9	7.3	9.7
FL	Daytona Beach	8.3	10.3	10.6	10.1	9.9	9.4	8.1	7.0	9.2
FL	Jacksonville	7.8	9.8	10.1	9.9	9.6	8.9	7.6	6.6	8.8
FL	Key West	9.1	10.4	10.4	10.1	10.1	9.6	8.6	7.6	9.5
FL	Miami	8.6	9.9	9.9	9.3	9.6	9.3	8.1	7.3	9.0
FL	Tallahassee	7.8	9.8	10.4	10.1	9.6	9.1	8.1	7.1	9.0
FL	Tampa	8.4	10.3	10.6	10.1	9.6	9.1	8.1	7.3	9.2
FL	West Palm Beach	8.3	9.8	9.9	9.4	9.8	9.3	7.9	7.0	8.9
GA	Savannah	7.8	9.6	10.3	10.4	10.1	9.1	7.8	6.8	9.0
LA	Baton Rouge	7.3	8.9	9.8	9.9	9.4	8.9	7.9	7.1	8.7
LA	Lake Charles	7.5	8.9	9.9	10.4	9.9	9.3	8.3	7.1	8.9
LA	New Orleans	7.5	9.1	10.1	10.1	9.4	9.1	8.1	7.1	8.8
TX	Austin	7.8	8.9	9.8	10.9	11.3	10.4	8.6	7.3	9.4
TX	Brownsville	7.6	8.8	9.6	10.6	10.8	9.9	8.6	7.5	9.2
TX	Corpus Christi	7.3	8.3	9.1	10.1	10.4	9.6	8.3	7.1	8.8
TX	Houston	7.0	8.3	9.3	9.9	9.8	9.3	8.1	7.0	8.6
TX	Lufkin	7.5	8.8	9.8	10.6	10.6	9.9	8.4	7.1	9.1
TX	Port Arthur	7.1	8.6	9.6	10.4	10.1	9.4	8.3	7.1	8.8
TX	San Antonio	7.9	9.1	9.9	11.1	11.4	10.6	8.9	7.5	9.6
TX	Victoria	7.3	8.4	9.4	10.3	10.3	9.6	8.3	7.1	8.8

A.3 CLIMATOLOGICAL PARAMETERS

Site specific data for average wind speed (meters/second), average temperature (^{O}C), average pressure (kPa), and relative humidity (%) was gathered from the National Solar Radiation Database (NSRD) [105], and is presented in Table 11 through Table 14.

Table 11. Average Pressure (kPa)

State	City	Pressure (mb)	Pressure (kPa)
AL	Mobile	1010	101
AZ	Phoenix	974	97.4
CA	San Diego	1014	101.4
FL	Daytona Beach	1017	101.7
FL	Jacksonville	1017	101.7
FL	Key West	1016	101.6
FL	Miami	1017	101.7
FL	Tallahassee	1016	101.6
FL	Tampa	1018	101.8
FL	West Palm Beach	1017	101.7
GA	Savannah	1017	101.7
LA	Baton Rouge	1015	101.5
LA	Lake Charles	1016	101.6
LA	New Orleans	1017	101.7
TX	Austin	994	99.4
TX	Brownsville	1015	101.5
TX	Corpus Christi	1014	101.4
TX	Houston	1014	101.4
TX	Lufkin	1006	100.6
TX	Port Arthur	1017	101.7
TX	San Antonio	988	98.8
TX	Victoria	1012	101.2

Table 12. Average Monthly Wind Speed (m/s)

State	City	Mar	Apr	May	Jun	Jul	Aug	Sep	Oct	Average
AL	Mobile	4.7	4.6	3.9	3.4	3	2.9	3.4	3.6	3.7
AZ	Phoenix	3.2	3.4	3.4	3.2	3.4	3.2	3	2.8	3.2
CA	San Diego	3.5	3.7	3.7	3.6	3.5	3.5	3.4	3.1	3.5
FL	Daytona Beach	4.2	4.1	3.8	3.4	3.2	3	3.5	4	3.7
FL	Jacksonville	3.9	3.7	3.4	3.2	3	2.8	3.1	3.4	3.3
FL	Key West	5.5	5.3	4.8	4.5	4.3	4.1	4.3	5.2	4.8
FL	Miami	4.9	4.8	4.4	3.8	3.7	3.7	3.8	4.4	4.2
FL	Tallahassee	3.4	3.2	2.9	2.5	2.3	2.3	2.7	2.9	2.8
FL	Tampa	4.2	4.1	3.9	3.6	3.3	3.1	3.4	3.8	3.7
FL	West Palm Beach	5.1	4.9	4.6	3.9	3.7	3.7	3.9	4.8	4.3
GA	Savannah	4.1	3.9	3.4	3.3	3.2	2.9	3.2	3.3	3.4
LA	Baton Rouge	4.1	3.9	3.4	2.9	2.6	2.4	2.9	2.9	3.1
LA	Lake Charles	4.6	4.5	3.9	3.4	2.9	2.7	3.2	3.4	3.6
LA	New Orleans	4.2	4.1	3.6	3	2.6	2.6	3.1	3.3	3.3
TX	Austin	4.7	4.5	4.2	3.8	3.5	3.4	3.5	3.5	3.9
TX	Brownsville	5.9	6	5.7	5.1	5	4.6	4.2	4.1	5.1
TX	Corpus Christi	6.4	6.4	5.7	5	5.1	5	4.9	4.8	5.4
TX	Houston	4.4	4.4	3.9	3.6	3.2	3	3.3	3.4	3.7
TX	Lufkin	3.6	3.5	3.1	2.6	2.4	2.4	2.6	2.6	2.9
TX	Port Arthur	5	5.1	4.4	3.8	3.2	3.1	3.6	3.8	4.0
TX	San Antonio	4.5	4.4	4.4	4.3	4.2	3.8	3.8	3.8	4.2
TX	Victoria	5.3	5.2	4.9	4.3	4.1	3.8	4	4.1	4.5

Table 13. Average Monthly Temperatures (^{O}C)

State	City	Mar	Apr	May	Jun	Jul	Aug	Sep	Oct	Average
AL	Mobile	15.8	19.9	23.6	26.9	27.9	27.7	25.5	20.2	23.4
AZ	Phoenix	16.8	21.1	26.0	31.2	34.2	33.1	29.8	23.6	27.0
CA	San Diego	15.3	16.7	17.8	19.3	21.7	22.6	21.9	19.8	19.4
FL	Daytona Beach	17.9	20.7	23.7	26.3	27.3	27.2	26.3	23.0	24.1
FL	Jacksonville	16.2	19.4	23.0	26.2	27.6	27.3	25.6	21.0	23.3
FL	Key West	23.2	25.0	27.0	28.4	29.1	29.1	28.5	26.7	27.1
FL	Miami	22.1	24.0	25.9	27.4	28.1	28.2	27.7	25.7	26.1
FL	Tallahassee	15.7	19.1	23.1	26.4	27.4	27.4	25.7	20.4	23.2
FL	Tampa	19.1	21.8	25.1	27.2	27.8	27.8	27.2	23.8	25.0
FL	West Palm Beach	21.1	23.0	25.3	27.0	27.9	28.1	27.6	25.4	25.7
GA	Savannah	15.1	18.9	23.1	26.2	27.7	27.2	24.8	19.6	22.8
LA	Baton Rouge	16.3	20.5	24.1	26.9	27.9	27.7	25.6	20.3	23.7
LA	Lake Charles	15.9	20.2	23.8	26.8	27.9	27.7	25.4	20.6	23.5
LA	New Orleans	16.4	20.3	23.8	26.7	27.7	27.5	25.6	20.6	23.6
TX	Austin	16.4	20.9	24.2	27.4	29.2	29.3	26.8	21.7	24.5
TX	Brownsville	20.4	24.1	26.6	28.3	29.2	29.2	27.7	24.3	26.2
TX	Corpus Christi	18.7	22.5	25.5	27.7	28.9	29.0	27.2	23.3	25.4
TX	Houston	15.9	20.2	23.6	26.9	28.1	27.9	25.7	20.9	23.7
TX	Lufkin	15.3	19.7	23.3	26.6	28.2	28.1	25.2	19.8	23.3
TX	Port Arthur	16.3	20.5	24.0	27.1	28.2	28.1	25.9	20.9	23.9
TX	San Antonio	16.5	20.7	24.2	27.9	29.4	29.4	26.3	21.2	24.5
TX	Victoria	17.4	21.4	24.8	27.6	28.9	28.9	26.4	22.1	24.7

Table 14. Relative Humidity (%)

State	City	Mar	Apr	May	Jun	Jul	Aug	Sep	Oct	Average
AL	Mobile	71	70	71	73	76	78	75	71	73
AZ	Phoenix	39	28	22	19	32	36	36	37	31
CA	San Diego	67	67	71	74	75	74	73	69	71
FL	Daytona Beach	71	69	72	77	78	80	79	75	75
FL	Jacksonville	71	69	73	77	78	80	81	79	76
FL	Key West	73	70	72	74	72	73	75	75	73
FL	Miami	69	67	72	76	75	76	78	75	74
FL	Tallahassee	72	70	72	76	80	81	78	74	75
FL	Tampa	72	69	70	74	77	78	77	74	74
FL	West Palm Beach	70	67	71	77	77	76	77	74	74
GA	Savannah	67	65	70	74	76	79	78	73	73
LA	Baton Rouge	70	71	72	74	77	78	77	73	74
LA	Lake Charles	76	76	77	78	80	80	79	76	78
LA	New Orleans	73	73	74	76	79	79	78	75	76
TX	Austin	64	66	71	69	65	64	68	68	67
TX	Brownsville	75	75	77	75	73	74	76	75	75
TX	Corpus Christi	74	77	79	78	75	75	76	75	76
TX	Houston	73	74	75	75	75	75	76	74	75
TX	Lufkin	70	72	75	75	74	73	75	73	73
TX	Port Arthur	76	77	79	79	81	80	79	77	79
TX	San Antonio	63	66	71	69	65	65	68	67	67
TX	Victoria	72	74	76	76	74	74	76	74	75

A.4 EVAPORATION

Evaporative loss was constructed based on the Penman Equation [118], provided in equation 8:

$$E_{mass} = \frac{m*R_n+\gamma*6.43*(1+0.563*U_m)*\delta e}{\lambda_v*(m+\gamma)} \quad (8)$$

E_{mass} Evaporation rate (mm day^{-1})
m Slope of the saturation vapor pressure curve (kPa K^{-1})
R_{n} Net Solar radiation (MJ m^{-2} day^{-1})
γ psychometric constant (kPa K^{-1})
U_m Wind speed (m s^{-1})
δe Vapor pressure deficit (kPa)

λ_v Latent heat of vaporization (MJ kg^{-1})

Net solar radiation R_n in units of (MJ/m^2-day) is computed using equation 9 [76] provided below.

$$R_n = \left(I_{avg} * \left(\frac{63}{100}\right) - 40\right) * \left(\frac{24}{1000}\right) \quad (9)$$

The latent heat of vaporization ($MJ*kg^{-1}$) is given by equation 10, where $Tavg_c$ is the average temperature in Celsius [118].

$$\lambda_v = (2.501 - 0.002361 * Tavg_c) \quad (10)$$

The slopes of the saturation vapor pressure curve in units of (kPa K^{-1}) are computed via equation 11, where $Tavg_k$ is the average temperature in Kelvin.

$$\boldsymbol{m = \frac{711.5}{Tavg_k^2} * \exp(21.07 - \frac{5336}{Tavg_k})} \quad (11)$$

The psychometric constant in units of (kPa K^{-1}) is computed via equation 12 [118], where: $Pavg_{kPa}$ is the mean pressure for the given location in units of kPa.

$$\gamma = \frac{.0016286 * Pavg_{kPa}}{\lambda_v} \quad (12)$$

The vapor pressure deficit in units of (kPa), denoted δe, is provided in equation 13, where e_s is the saturated vapor pressure of air (kPa), e_a is the vapor pressure of free flowing air (kPa), relative humidity (%).

$$\boldsymbol{\delta e = (e_s - e_a) = (1 - relative\ humidity) * e_s} \quad (13)$$

The saturation vapor pressure of air in units of (kPa), denoted e_s, is approximated using equation 14 [367].

$$e_s = \frac{1}{7.5} * \exp(21.07 - \frac{5336}{Tavg_k}) \quad (14)$$

Monthly average evaporative losses in units of (mm / day) are presented in Table 15.

Table 15. Monthly Average Evaporative Losses (mm / day)

State	City	Mar	Apr	May	Jun	Jul	Aug	Sep	Oct	Average
AL	Mobile	3.5	4.5	4.9	4.9	4.4	4.0	3.8	3.4	4.2
AZ	Phoenix	5.4	7.7	9.5	10.6	9.7	8.7	7.4	5.6	8.1
CA	San Diego	3.6	4.5	4.5	4.6	5.0	4.9	4.1	3.5	4.3
FL	Daytona Beach	3.9	5.0	5.2	4.7	4.6	4.2	3.8	3.5	4.4
FL	Jacksonville	3.5	4.6	4.7	4.6	4.4	3.9	3.3	2.8	4.0
FL	Key West	5.0	5.9	5.7	5.5	5.6	5.2	4.7	4.4	5.2
FL	Miami	4.8	5.6	5.3	4.6	4.9	4.7	4.0	3.9	4.7
FL	Tallahassee	3.3	4.3	4.7	4.5	4.1	3.8	3.6	3.1	3.9
FL	Tampa	4.0	5.1	5.5	5.0	4.6	4.2	3.9	3.7	4.5
FL	West Palm Beach	4.6	5.5	5.4	4.6	4.8	4.7	4.0	4.0	4.7
GA	Savannah	3.7	4.8	5.0	5.0	4.8	4.1	3.5	3.1	4.2
LA	Baton Rouge	3.4	4.3	4.7	4.7	4.3	4.0	3.6	3.2	4.0
LA	Lake Charles	3.2	4.1	4.6	4.8	4.4	4.1	3.7	3.2	4.0
LA	New Orleans	3.4	4.3	4.8	4.7	4.2	4.0	3.7	3.2	4.0
TX	Austin	4.2	4.9	5.1	5.8	6.3	6.0	4.7	3.8	5.1
TX	Brownsville	4.1	4.9	5.2	5.8	6.1	5.5	4.5	3.8	5.0
TX	Corpus Christi	4.0	4.5	4.7	5.2	5.8	5.4	4.5	3.8	4.7
TX	Houston	3.2	4.0	4.4	4.9	4.8	4.5	3.9	3.2	4.1
TX	Lufkin	3.3	4.0	4.4	4.8	4.9	4.7	3.8	3.0	4.1
TX	Port Arthur	3.2	4.1	4.5	4.9	4.5	4.3	3.8	3.2	4.1
TX	San Antonio	4.2	4.9	5.2	6.1	6.7	6.2	4.9	4.0	5.3
TX	Victoria	3.7	4.4	4.8	5.2	5.4	5.0	4.2	3.6	4.6

A.5 PRECIPITATION

Data concerning average rainfall for the various locations was taken from the National Oceanic and Atmospheric Administration (NOAA) [119], average rainfall (mm/day) for the examined cultivation locations is presented in Table 16.

Table 16. Average Monthly Rainfall (mm / day)

State	City	Mar	Apr	May	Jun	Jul	Aug	Sep	Oct	Average
AL	Mobile	5.9	4.1	5.0	4.1	5.4	5.1	4.9	2.7	4.6
AZ	Phoenix	0.9	0.2	0.1	0.1	0.8	0.8	0.6	0.6	0.5
CA	San Diego	1.9	0.6	0.2	0.1	0.0	0.1	0.2	0.4	0.4
FL	Daytona Beach	3.1	2.1	2.7	4.7	4.2	5.0	5.4	3.7	3.9
FL	Jacksonville	3.2	2.6	2.9	4.4	4.9	5.6	6.5	3.2	4.2
FL	Key West	1.5	1.7	2.9	3.7	2.7	4.4	4.5	3.6	3.1
FL	Miami	2.1	2.8	4.5	7.0	4.7	7.1	6.9	5.1	5.0
FL	Tallahassee	5.3	2.9	4.1	5.7	6.6	5.8	4.1	2.7	4.6
FL	Tampa	2.3	1.5	2.3	4.5	5.3	6.2	5.4	1.9	3.7
FL	West Palm Beach	3.0	2.9	4.4	6.2	4.9	5.4	6.6	4.5	4.8
GA	Savannah	3.0	2.7	3.0	4.5	4.9	5.9	4.2	2.6	3.8
LA	Baton Rouge	4.2	4.6	4.4	4.4	4.9	4.8	4.0	3.1	4.3
LA	Lake Charles	2.9	3.0	5.0	5.0	4.2	4.0	4.9	3.2	4.0
LA	New Orleans	4.3	4.1	3.8	5.6	5.1	5.0	4.5	2.5	4.4
TX	Austin	1.8	2.1	4.1	3.1	1.6	1.9	2.4	3.3	2.5
TX	Brownsville	0.8	1.6	2.0	2.4	1.5	2.4	4.4	3.1	2.3
TX	Corpus Christi	1.4	1.7	2.9	2.9	1.6	2.9	4.1	3.2	2.6
TX	Houston	2.8	2.9	4.2	4.4	2.6	3.1	3.5	3.7	3.4
TX	Lufkin	3.0	3.2	4.0	3.1	2.6	2.5	2.8	2.7	3.0
TX	Port Arthur	3.1	3.1	4.8	5.4	4.3	4.0	5.0	3.8	4.2
TX	San Antonio	1.5	2.1	3.9	3.5	1.7	2.1	2.5	3.2	2.6
TX	Victoria	1.8	2.4	4.2	4.1	2.4	2.5	4.1	3.5	3.1

A.6 NET WATER ACCUMULATION

The net water accumulation (mm/day) was calculated as the difference between the average rainfall (mm/day) and evaporative losses (mm/day). Negative values signify a net loss of water, indicating that additional water must be pumped into the ORPs. The values for net water accumulation for the examined cultivation locations are provided in Table 17.

Table 17. Net Water Accumulation (mm / day)

State	City	Mar	Apr	May	Jun	Jul	Aug	Sep	Oct	Average
AL	Mobile	2.4	-0.2	0.1	-0.6	0.9	1.1	1.3	-0.7	0.5
AZ	Phoenix	-4.5	-7.5	-9.4	-10.5	-8.9	-8.0	-6.8	-5.0	-7.6
CA	San Diego	-1.8	-3.9	-4.4	-4.5	-5.0	-4.8	-4.0	-3.1	-3.9
FL	Daytona Beach	-0.8	-2.9	-2.5	0.1	-0.4	0.8	1.8	0.2	-0.4
FL	Jacksonville	-0.3	-1.9	-1.8	0.0	0.5	1.7	3.4	0.3	0.2
FL	Key West	-3.5	-4.2	-2.9	-1.6	-2.9	-0.8	-0.1	-0.8	-2.1
FL	Miami	-2.7	-2.8	-0.8	2.6	-0.1	2.4	3.1	1.1	0.4
FL	Tallahassee	2.0	-1.3	-0.7	1.4	2.5	1.9	0.7	-0.4	0.8
FL	Tampa	-1.7	-3.6	-3.1	-0.4	0.7	2.0	1.6	-1.8	-0.8
FL	West Palm Beach	-1.5	-2.5	-1.0	1.8	0.1	0.8	2.8	0.5	0.1
GA	Savannah	-0.7	-2.0	-2.0	-0.4	0.1	1.8	0.8	-0.5	-0.4
LA	Baton Rouge	0.7	0.4	-0.3	-0.2	0.6	0.8	0.5	0.0	0.3
LA	Lake Charles	-0.3	-1.0	0.4	0.3	-0.2	-0.1	1.3	0.1	0.1
LA	New Orleans	0.9	0.0	-1.0	1.1	0.9	1.0	1.0	-0.7	0.4
TX	Austin	-2.4	-2.7	-0.9	-2.6	-4.7	-4.1	-2.3	-0.5	-2.5
TX	Brownsville	-3.3	-3.2	-3.2	-3.3	-4.6	-3.0	0.0	-0.7	-2.7
TX	Corpus Christi	-2.6	-2.7	-1.9	-2.2	-4.1	-2.5	-0.3	-0.6	-2.1
TX	Houston	-0.4	-0.9	-0.2	-0.4	-2.2	-1.3	-0.2	0.5	-0.6
TX	Lufkin	-0.2	-0.7	-0.4	-1.6	-2.3	-2.2	-0.9	-0.3	-1.1
TX	Port Arthur	-0.2	-0.8	0.3	0.7	-0.2	-0.3	1.3	0.6	0.2
TX	San Antonio	-2.7	-2.7	-1.3	-2.5	-5.0	-4.0	-2.4	-0.8	-2.7
TX	Victoria	-1.9	-1.9	-0.6	-1.0	-3.0	-2.5	0.0	-0.1	-1.4

A.7 MICROALGAL BIOMASS COMPOSITION

The composition and net calorific value of the microalgal biomass fractions (Proteins, Carbohydrates, Lipids) were taken from Lardon et al. 2009 [94], and are presented in Table 18.

Table 18. Fractioned Microalgal Biomass Composition

Fraction	Composition	Molar Mass ($g*mole^{-1}$)	Net Calorific Value (MJ/g- biomass)
Protein	$C_{4.43}H_7O_{1.44}N_{1.16}$	100.1	$15.5*10^{-3}$
Carbohydrate	$C_6H_{12}O_6$	180	$13*10^{-3}$
Lipid	$C_{40}H_{74}O_5$	634	$38.3*10^{-3}$

The algae composition was assumed to be 50% proteins, 25% carbohydrates, 20% lipids, and 5% other organic material, which correlates with previous studies [51, 107]. It was assumed that the values of P, K, Mg, and S vary linearly with the protein content. A proportionality constant was constructed based on a reference composition of Chlorella vulgaris, obtained from Lardon et al. 2009 [94]. The algae compositional parameters are provided in Table 19.

Table 19. Gross Microalgal Biomass Composition

Parameters	Reference Composition (g/kg-biomass)	Composition assumed in this study (g/kg-biomass)
Protein	282	500
Carbohydrate	495	250
Lipid	175	200
C	480	517
N	46	81.2
P	9.9	17.6
K	8.2	14.5
Mg	3.8	6.7
S	2.2	3.9

The Lower heating value (LHV) of the algae (MJ/kg-biomass) calculated as the sum of the individual biomass fractions (g/kg biomass) multiplied by their respective energetic content (MJ/g). The gross biomass Lower Heating Value (LHV) was computed to be 18.66 MJ/kg-biomass.

A.8 MICROALGAL GROWTH RATES

Algae growth rates are calculated based on the amount of PAR energy (MJ / m^2) a region receives as well as efficiency factors determined by both pond design and characteristics of the algae culture.

A.8.1 Efficiency Factors

Photosynthetic Efficiency (PE): accounts for the efficiency of converting solar energy into chemical energy by the process of photosynthesis, see equation 15. The photosynthetic efficiency is determined by the quantum requirement, average photon energy, and carbohydrate energy content, see equation 16. Values for quantum requirement, average photon energy, and carbohydrate energy content were taken from Weyer et al. 2010 [52].

$$CO_2 + H_2O + 8\,photons \rightarrow CH_2O + O_2 \tag{15}$$

Quantum Requirement (Mole Photons / Mole CH_2O): represents the number of photons needed to produce a photosynthetic reaction, this value was assumed to be 8 moles of photons per mole of CH_2O. [52] *Average Photon Energy* (MJ / Mole Photons): corresponds to the

average photonic energy of solar radiation, this value was assumed to be 225.3 x 10^{-3} MJ per mole of photons. [52] *Carbohydrate Energy Content* (MJ / Mole CH_2O): represents the energetic content of CH_2O formed in photosynthesis, this value was taken to be 482.5 x 10^{-3} MJ per mole of CH_2O. [52]

$$PE\ (\%) = \left(\frac{Carbohydrate\ Enery\ Content}{Average\ Photon\ Energy\ x\ Quantum\ Requirement}\right) x100 \quad (16)$$

Values for photosynthetic efficiency, quantum requirement, average photon energy, and carbohydrate energy content are presented in Table 20.

Table 20. Photosynthetic Efficiency Terms

Term	Value
Photosynthetic Efficiency (%)	26.8
Quantum Requirement (Moles Photons/Moles CH_2O):	8
Average Photon Energy (MJ/Mole Photons):	225. x 10^{-3}
Carbohydrate Energy Content (MJ/Mole CH_2O):	482.5 x 10^{-3}

Losses due to Reflection accounts for solar radiation reflected off of the pond surface. For the months of March through October, and for regions between 20-30 degrees latitude, the percent of solar radiation reflected off of the pond surface ranges between 6-8% [368]. This corresponds to an average efficiency value of 93%. *Losses due to sub-optimal environmental conditions* accounts for losses in photon absorption due to temperature and environmental conditions, this value was taken to be 95% [52]. *Photon Utilization Efficiency* accounts for losses in photon absorption in the algal culture due to high or low light levels. For low light levels, photon utilization typically varies between 50-90%, for high light levels 10-30% [106]. For the

open pond system, the photon utilization efficiency was taken to be 25%. *Biomass accumulation efficiency,* energy that is available to the algae culture will be used either in cellular respiration or will be stored as biomass. The biomass accumulation efficiency is the ratio of the amount of energy stored in the biomass to the total energy available to the algal culture, and thus shows the efficiency at which algae convert available energy into biomass, this value was taken to be 72% [369]. The values for the efficiency terms are provided in Table 21. Let α denote the product of the five efficiency factors, as shown in equation 17

Table 21. Efficiency Terms

Efficiency Factors	Value (%)
Photosynthetic efficiency:	26.8
Losses due to reflection:	93
Losses due to sub-optimal environmental conditions:	95
Photon utilization efficiency:	25
Biomass accumulation efficiency:	72

$$\alpha = \prod Efficiency\ Factors = 4.2\% \tag{17}$$

A.8.2 Microalgal Growth Rates

Microalgal growth rates in units of (g / m^2-day) are computed based on the average PAR energy (MJ / m^2-day), efficiency factors, and biomass lower heating value, see equation 18.

$$Growth\ Rates_{\ avg} = \frac{PAR_{avg} \times \alpha}{LHV_{Biomass}} \tag{18}$$

Monthly average microalgal growth rates for all examined locations are presented in Table 22.

Table 22. Monthly Microalgal areal growth rates (g / m^2-day)

State	City	Mar	Apr	May	Jun	Jul	Aug	Sep	Oct	Average
AL	Mobile	16.6	20.4	22.3	22.3	21.2	19.6	17.8	15.9	19.5
AZ	Phoenix	20.8	26.8	30.2	31.7	28.7	26.8	23.0	18.5	25.8
CA	San Diego	18.5	23.0	23.8	24.6	26.1	24.6	20.4	16.6	22.2
FL	Daytona Beach	18.9	23.4	24.2	23.0	22.7	21.5	18.5	15.9	21.0
FL	Jacksonville	17.8	22.3	23.0	22.7	21.9	20.4	17.4	15.1	20.1
FL	Key West	20.8	23.8	23.8	23.0	23.0	21.9	19.6	17.4	21.7
FL	Miami	19.6	22.7	22.7	21.2	21.9	21.2	18.5	16.6	20.5
FL	Tallahassee	17.8	22.3	23.8	23.0	21.9	20.8	18.5	16.2	20.5
FL	Tampa	19.3	23.4	24.2	23.0	21.9	20.8	18.5	16.6	21.0
FL	West Palm Beach	18.9	22.3	22.7	21.5	22.3	21.2	18.1	15.9	20.4
GA	Savannah	17.8	21.9	23.4	23.8	23.0	20.8	17.8	15.5	20.5
LA	Baton Rouge	16.6	20.4	22.3	22.7	21.5	20.4	18.1	16.2	19.8
LA	Lake Charles	17.0	20.4	22.7	23.8	22.7	21.2	18.9	16.2	20.4
LA	New Orleans	17.0	20.8	23.0	23.0	21.5	20.8	18.5	16.2	20.1
TX	Austin	17.8	20.4	22.3	24.9	25.7	23.8	19.6	16.6	21.4
TX	Brownsville	17.4	20.0	21.9	24.2	24.6	22.7	19.6	17.0	20.9
TX	Corpus Christi	16.6	18.9	20.8	23.0	23.8	21.9	18.9	16.2	20.0
TX	Houston	15.9	18.9	21.2	22.7	22.3	21.2	18.5	15.9	19.6
TX	Lufkin	17.0	20.0	22.3	24.2	24.2	22.7	19.3	16.2	20.7
TX	Port Arthur	16.2	19.6	21.9	23.8	23.0	21.5	18.9	16.2	20.2
TX	San Antonio	18.1	20.8	22.7	25.3	26.1	24.2	20.4	17.0	21.8
TX	Victoria	16.6	19.3	21.5	23.4	23.4	21.9	18.9	16.2	20.2

A.9 CULTIVATION OF MICROALGAL BIOMASS

A.9.1 CO_2 Procurement

CO_2 from a nearby natural gas fired power plant is supplied to the ponds in two ways: i) Flue gas is transported via lower pressure blowers and delivered to the algae ponds, evaluated at 22.2 x 10^{-3} kilowatt hours (kWh) per kg CO_2 [109]. While microalgae's potential to utilize flue gas as a source of CO_2 has been extensively cited in the literature [121, 122], it remains uncertain if the presence of flue gas will have detrimental effects upon the algae culture [123, 124]. More so, there is potential concern that industrial flue gases may contain heavy metals, which may decrease the quality of algal derived fuels. In this study, it is assumed that the Direct Injection (DI) of flue gas has no negative impacts upon the algae culture. While the utilization of industrial flue gas has the potential to decrease the high energetic cost associated with CO_2, the feasibility of direct injection of flue gas on an industrial scale remains questionable. (ii) Flue gas is separated into pure CO_2 via Monoethanolamine (MEA) scrubbing; this pure CO_2 is then delivered to the ponds via low-pressure blowers. Kadam et al. 2002 estimated that 1 kg of CO_2 from MEA extraction would require approximately 2.01 kg of steam and 32.65 x 10^{-3} kWh of electricity [109]. The energy required to transform water to steam was based on the enthalpy of steam, evaluated at 2.6 MJ/kg-steam. It was assumed that natural gas would be burned to generate steam; the energetic content of natural gas was taken to be 39 MJ/m^3-natural gas with a boiler efficiency of 80% [79]. While MEA scrubbing is the more energy intensive of the two options, it insures that the algal culture does not experience the possible negative effects as associated with the direct injection of flue gas. It this study, it was assumed that the microalgae culture captures only 70% of the injected CO_2 [83].

A.9.2 Paddlewheels

During cultivation, the algal growth medium is circulated by paddlewheels, consistent with current reactor configurations [76, 77, 100]. While other medium circulation configurations have been proposed, paddlewheels are a proven technology, and appear to be the most effective method of circulating the algal growth medium. For a mixing velocity of 15 cm/second and a pond depth of 0.3 m, the energetic cost of the paddlewheels was evaluated at 18 kWh/ha-day [100]. Existing studies have produced a wide range of values for paddlewheel energetic consumption [76, 77, 79, 83], due to variations in pond depth, mixing velocity, and process assumptions. Deviations in paddlewheel energetic consumption were included as a parameter in the sensitivity analysis.

A.9.3 PVC Liner

A 0.75 mm thick PVC membrane was assumed to line the ORPs with an average lifetime of 5 years [83]. The mass of PVC required to line the ORPs was calculated as the product of the surface area, thickness of the PVC membrane, and density of the PVC liner. The required surface area of the PVC liner was assumed to be 120% times the surface area of the cultivation ponds (500 ha) [80]. The density of the PVC membrane was taken to be 950 kg/m3. The impacts of the PVC liner were normalized over the total amount of biomass produced over the lifetime of the PVC liner.

A.9.4 Freshwater Sourcing

The energy required to source freshwater to the ORPs was evaluated based off of conventional crop irrigation. It was assumed that electric pumps would bring surface and groundwater to the ORPs. The amount of energy required to source ground and surface water was based off of the 2008 Farm and ranch Irrigation survey [370], and the cost of electricity was assumed to be $0.10 kWh [80]

A.10 HARVESTING OF MICROALGAL BIOMASS

A.10.1 Flocculation

Algae are pumped into post-cultivation holding tanks in which a coagulant, aluminum sulfate, is injected at a rate of 100 g/m^3 [169]. Aluminum sulfate was chosen for this study because it has been shown to be an effective coagulant for Chlorella algae [371]. Flocculation was assumed to concentrate the algal culture to a concentration of 2% (w/w). It was assumed that 90% of the medium from flocculation is recycled back to the cultivation ponds.

A.10.2 Pumping Energy Consumption

Pumping power requirements (kWh/day) were constructed based on pipe flowrate (l/s), pipe diameter (m), pipe length (m), pipeline roughness (m), fluid velocity (m/s), pipe head-loss (m), Reynolds number (unit-less), and pump and motor efficiency (%). The power requirement for

pond pumping (J/s) is dependent on: g the gravitational acceleration (m/s^2), total lift (m), flow rate (m^3/s), density of fluid (kg/m^3), and motor efficiency (%) and is presented in equation 19.

$$Power_{pump} = \frac{g*(Total\ Lift)*(Flowrate)*(density\ of\ fluid)}{Motor\ Efficiency} \quad (19)$$

The Total Lift (m) is calculated as the sum of the Static Lift (m) and Pipe Head loss (m). Pipe head loss was based on the Darcy–Weisbach equation and is presented in equation 20.

$$\frac{f*L*V^2}{2*g*D} = h_f \quad (20)$$

Where h_f is head loss due to friction (m), L is the length of the pipe (m), V is the mean velocity of the flow (m/s), g is the acceleration due to gravity (m/s^2), D is the pipe diameter (m), and f is the Darcy-Weisbach friction factor. The Swamee–Jain equation is used to solve for the Darcy-Weisbach friction factor *f*, and is presented in equation 21 [372].

$$f = \frac{0.25}{[Log_{10}(\frac{\varepsilon}{3.7*D}+\frac{5.74}{Re^{0.9}})]^2} \quad (21)$$

Where ε is the pipeline roughness (m), Re is the Reynolds number for fluid flow in a pipe (unitless), and D is the diameter of the pipe (m).The Reynolds number (Re) for fluid flow in a pipe is defined in equation 22, wherein Q is the volumetric flowrate (m^3/s), D_H is the hydraulic diameter of the pipe (m), A is the pipe cross sectional area (m^2), and ν is the kinematic viscosity (m^2/s).

$$Re = \frac{Q*D_H}{A*\nu} \quad (22)$$

The mean velocity of the flow (m/s) is expressed in equation 23, where A is the pipe cross sectional area (m^2), and Q is the volumetric flow rate (m^3/s).

$$V = \frac{Q}{A} \tag{23}$$

A.10.3 Centrifugation

After flocculation, algae are pumped to an industrial Centrifuge (CF) for dewatering. Decanter centrifuges were chosen as a means to concentrate the algae culture, as they are both a proven and reliable technology, and have the ability to significantly increase the concentration (% w/w) of the culture as compared to other centrifuge types. For centrifugation, the electrical consumption was evaluated at 8 kWh/m^3 consistent with centrifuges of this type [110]. Centrifugation was assumed to increase the algal concentration to 22% (w/w) [110]. In addition, it was assumed that 5% of the input culture would be lost during centrifugation, and that 90% of process medium would be recycled back into the ponds.

A.10.4 Chamber Filter Press

For Chamber Filter Presses (CFP), the electrical consumption per unit throughput was evaluated at 0.88 kWh/m^3 [110]. It was assumed that the chamber filter press would increase the algal concentration to 25% (w/w) [110]. It was assumed that 5% of the input culture would be lost during dewatering, and that 90% of the process medium would be recycled back into the ponds. The energetic and environmental costs associated with replacing the filter press membranes were not considered in this study.

A.10.5 Algal Drying

After dewatering, algae must undergo additional drying to achieve a final concentration of 90% (w/w). Two production scenarios were examined for drying: (i) natural gas based drying and (ii) waste heat drying. In scenario (i) algae from the dewatering stage are sent to an industrial boiler in which natural gas is burned to dry the biomass. The amount of heat energy needed to dry the algae was based on the amount of water extracted from the system, latent heat of evaporation of water, and boiler efficiency. The boiler efficiency was assumed to be 75%, and it was assumed that 5% of the input algal biomass would be lost in the process. The energy (kJ) required for Natural Gas based Drying (NGD) is dependent on: m the mass of water needed to be extracted from the system (kg), Cw the latent heat of evaporation of water (kJ/kg), Cv the specific heat of water (kJ/kg-C), ΔT the change in temperature of the water (C), and boiler efficiency ε_{NG} (%), expressed in equation 24.

$$\boldsymbol{Energy_{heat} = m * (Cw + Cv * \Delta T)} \quad (24)$$

(ii): Studies have suggested that it may be possible to recover waste heat contained in the exhaust gases from power plants, and therefore utilize these exhaust streams to offset a portion of the energy required to dry the algal biomass [75]. Prior studies have estimated that a 500 MW power plant could generate up to 4.4 $x10^9$ MJ of "waste" heat energy per year [75], which greatly exceeds the heat energy required to dry the biomass. For Waste Heat Dying (WHD) scenarios it was assumed that all of the heat energy required to dry the biomass could be met using waste heat from a co-located power plant.

A.11 LIFE CYCLE INVENTORY

The Life Cycle Inventory [LCI], normalized to 1 kg of biomass, for all production pathways are provided in the subsequent tables. To avoid redundancy, the LCI of the following cultivation locations are provided: Mobile AL; Phoenix, AZ; San Diego, CA; Tallahassee, FL; Savannah, GA; Baton Rouge, LA; Brownsville, TX. In the following life cycle inventory tables these specific cultibation locations are referred to by state only.

Table 23. LCI normalized per kg of biomass for MEA/CF/NGD pathways

State	Freshwater (m^3)	Wastewater Treatment (m^3)	CO2 Injected (kg)	PVC (kg)	Paddlewheels (MJ)	Urea (kg)	SSP (kg)	KCL (kg)	Flocculation (kg)	MEA (MJ)	MEA (m^3 NG)	Pumping (MJ)	CF (MJ)	NGD (m^3 NG)
AL	0.42	0.36	3.00	0.03	0.37	0.26	0.10	0.04	0.25	0.35	0.50	1.34	1.56	0.38
AZ	0.72	0.33	3.00	0.02	0.28	0.26	0.10	0.04	0.25	0.35	0.50	2.42	1.56	0.38
CA	0.62	0.34	3.00	0.03	0.32	0.26	0.10	0.04	0.25	0.35	0.50	1.85	1.56	0.38
FL	0.39	0.35	3.00	0.03	0.35	0.26	0.10	0.04	0.25	0.35	0.50	1.61	1.56	0.38
GA	0.45	0.35	3.00	0.03	0.35	0.26	0.10	0.04	0.25	0.35	0.50	1.46	1.56	0.38
LA	0.43	0.36	3.00	0.03	0.36	0.26	0.10	0.04	0.25	0.35	0.50	1.77	1.56	0.38
TX	0.58	0.35	3.00	0.03	0.34	0.26	0.10	0.04	0.25	0.35	0.50	1.38	1.56	0.38

Table 24. LCI normalized per kg of biomass for MEA/CF/WHD pathways

State	Freshwater (m^3)	Wastewater Treatment (m^3)	CO2 Injected (kg)	PVC (kg)	Paddlewheels (MJ)	Urea (kg)	SSP (kg)	KCL (kg)	Flocculation (kg)	MEA (MJ)	MEA (m^3 NG)	Pumping (MJ)	CF (MJ)	WHD (m^3 NG)
AL	0.42	0.36	3.00	0.03	0.37	0.26	0.10	0.04	0.25	0.35	0.50	1.34	1.56	0
AZ	0.72	0.33	3.00	0.02	0.28	0.26	0.10	0.04	0.25	0.35	0.50	2.42	1.56	0
CA	0.62	0.34	3.00	0.03	0.32	0.26	0.10	0.04	0.25	0.35	0.50	1.85	1.56	0
FL	0.39	0.35	3.00	0.03	0.35	0.26	0.10	0.04	0.25	0.35	0.50	1.61	1.56	0
GA	0.45	0.35	3.00	0.03	0.35	0.26	0.10	0.04	0.25	0.35	0.50	1.46	1.56	0
LA	0.43	0.36	3.00	0.03	0.36	0.26	0.10	0.04	0.25	0.35	0.50	1.77	1.56	0
TX	0.58	0.35	3.00	0.03	0.34	0.26	0.10	0.04	0.25	0.35	0.50	1.38	1.56	0

Table 25. LCI normalized per kg of biomass for DI/CF/NGD pathways

State	Freshwater (m^3)	Wastewater Treatment (m^3)	CO2 Injected (kg)	PVC (kg)	Paddlewheels (MJ)	Urea (kg)	SSP (kg)	KCL (kg)	Flocculation (kg)	DI (MJ)	Pumping (MJ)	CF (MJ)	NGD (m^3 NG)
AL	0.42	0.36	3.00	0.03	0.37	0.26	0.10	0.04	0.25	0.24	1.34	1.56	0.38
AZ	0.72	0.33	3.00	0.02	0.28	0.26	0.10	0.04	0.25	0.24	2.42	1.56	0.38
CA	0.62	0.34	3.00	0.03	0.32	0.26	0.10	0.04	0.25	0.24	1.85	1.56	0.38
FL	0.39	0.35	3.00	0.03	0.35	0.26	0.10	0.04	0.25	0.24	1.61	1.56	0.38
GA	0.45	0.35	3.00	0.03	0.35	0.26	0.10	0.04	0.25	0.24	1.46	1.56	0.38
LA	0.43	0.36	3.00	0.03	0.36	0.26	0.10	0.04	0.25	0.24	1.77	1.56	0.38
TX	0.58	0.35	3.00	0.03	0.34	0.26	0.10	0.04	0.25	0.24	1.38	1.56	0.38

Table 26. LCI normalized per kg of biomass for DI/CF/WHD pathways

State	Freshwater (m^3)	Wastewater Treatment (m^3)	CO2 Injected (kg)	PVC (kg)	Paddlewheels (MJ)	Urea (kg)	SSP (kg)	KCL (kg)	Flocculation (kg)	DI (MJ)	Pumping (MJ)	CF (MJ)	WHD (m^3 NG)
AL	0.42	0.36	3.00	0.03	0.37	0.26	0.10	0.04	0.25	0.24	1.34	1.56	0
AZ	0.72	0.33	3.00	0.02	0.28	0.26	0.10	0.04	0.25	0.24	2.42	1.56	0
CA	0.62	0.34	3.00	0.03	0.32	0.26	0.10	0.04	0.25	0.24	1.85	1.56	0
FL	0.39	0.35	3.00	0.03	0.35	0.26	0.10	0.04	0.25	0.24	1.61	1.56	0
GA	0.45	0.35	3.00	0.03	0.35	0.26	0.10	0.04	0.25	0.24	1.46	1.56	0
LA	0.43	0.36	3.00	0.03	0.36	0.26	0.10	0.04	0.25	0.24	1.77	1.56	0
TX	0.58	0.35	3.00	0.03	0.34	0.26	0.10	0.04	0.25	0.24	1.38	1.56	0

Table 27. LCI normalized per kg of biomass for MEA/CFP/NGD pathways

State	Freshwater (m^3)	Wastewater Treatment (m^3)	CO2 Injected (kg)	PVC (kg)	Paddlewheels (MJ)	Urea (kg)	SSP (kg)	KCL (kg)	Flocculation (kg)	MEA (MJ)	MEA (m3 NG)	Pumping (MJ)	CF (MJ)	NGD (m^3 NG)
AL	0.41	0.36	3.00	0.03	0.37	0.26	0.10	0.04	0.25	0.35	0.50	1.34	0.17	0.32
AZ	0.72	0.33	3.00	0.02	0.28	0.26	0.10	0.04	0.25	0.35	0.50	2.42	0.17	0.32
CA	0.61	0.34	3.00	0.03	0.32	0.26	0.10	0.04	0.25	0.35	0.50	1.85	0.17	0.32
FL	0.39	0.35	3.00	0.03	0.35	0.26	0.10	0.04	0.25	0.35	0.50	1.61	0.17	0.32
GA	0.45	0.35	3.00	0.03	0.35	0.26	0.10	0.04	0.25	0.35	0.50	1.46	0.17	0.32
LA	0.42	0.36	3.00	0.03	0.36	0.26	0.10	0.04	0.25	0.35	0.50	1.77	0.17	0.32
TX	0.57	0.35	3.00	0.03	0.34	0.26	0.10	0.04	0.25	0.35	0.50	1.38	0.17	0.32

Table 28. LCI normalized per kg of biomass for MEA/CFP/WHD pathways

State	Freshwater (m^3)	Wastewater Treatment (m^3)	CO2 Injected (kg)	PVC (kg)	Paddlewheels (MJ)	Urea (kg)	SSP (kg)	KCL (kg)	Flocculation (kg)	MEA (MJ)	MEA (m3 NG)	Pumping (MJ)	CF (MJ)	WHD (m^3 NG)
AL	0.41	0.36	3.00	0.03	0.37	0.26	0.10	0.04	0.25	0.35	0.50	1.34	0.17	0
AZ	0.72	0.33	3.00	0.02	0.28	0.26	0.10	0.04	0.25	0.35	0.50	2.42	0.17	0
CA	0.61	0.34	3.00	0.03	0.32	0.26	0.10	0.04	0.25	0.35	0.50	1.85	0.17	0
FL	0.39	0.35	3.00	0.03	0.35	0.26	0.10	0.04	0.25	0.35	0.50	1.61	0.17	0
GA	0.45	0.35	3.00	0.03	0.35	0.26	0.10	0.04	0.25	0.35	0.50	1.46	0.17	0
LA	0.42	0.36	3.00	0.03	0.36	0.26	0.10	0.04	0.25	0.35	0.50	1.77	0.17	0
TX	0.57	0.35	3.00	0.03	0.34	0.26	0.10	0.04	0.25	0.35	0.50	1.38	0.17	0

Table 29. LCI normalized per kg of biomass for DI/CFP/NGD pathways

State	Freshwater (m^3)	Wastewater Treatment (m^3)	CO2 Injected (kg)	PVC (kg)	Paddlewheels (MJ)	Urea (kg)	SSP (kg)	KCL (kg)	Flocculation (kg)	DI (MJ)	Pumping (MJ)	CF (MJ)	NGD (m^3 NG)
AL	0.41	0.36	3.00	0.03	0.37	0.26	0.10	0.04	0.25	0.24	1.34	0.17	0.32
AZ	0.72	0.33	3.00	0.02	0.28	0.26	0.10	0.04	0.25	0.24	2.42	0.17	0.32
CA	0.61	0.34	3.00	0.03	0.32	0.26	0.10	0.04	0.25	0.24	1.85	0.17	0.32
FL	0.39	0.35	3.00	0.03	0.35	0.26	0.10	0.04	0.25	0.24	1.61	0.17	0.32
GA	0.45	0.35	3.00	0.03	0.35	0.26	0.10	0.04	0.25	0.24	1.46	0.17	0.32
LA	0.42	0.36	3.00	0.03	0.36	0.26	0.10	0.04	0.25	0.24	1.77	0.17	0.32
TX	0.57	0.35	3.00	0.03	0.34	0.26	0.10	0.04	0.25	0.24	1.38	0.17	0.32

Table 30. LCI normalized per kg of biomass for DI/CFP/WHD pathways

State	Freshwater (m^3)	Wastewater Treatment (m^3)	CO2 Injected (kg)	PVC (kg)	Paddlewheels (MJ)	Urea (kg)	SSP (kg)	KCL (kg)	Flocculation (kg)	DI (MJ)	Pumping (MJ)	CF (MJ)	WHD (m^3 NG)
AL	0.41	0.36	3.00	0.03	0.37	0.26	0.10	0.04	0.25	0.24	1.34	0.17	0
AZ	0.72	0.33	3.00	0.02	0.28	0.26	0.10	0.04	0.25	0.24	2.42	0.17	0
CA	0.61	0.34	3.00	0.03	0.32	0.26	0.10	0.04	0.25	0.24	1.85	0.17	0
FL	0.39	0.35	3.00	0.03	0.35	0.26	0.10	0.04	0.25	0.24	1.61	0.17	0
GA	0.45	0.35	3.00	0.03	0.35	0.26	0.10	0.04	0.25	0.24	1.46	0.17	0
LA	0.42	0.36	3.00	0.03	0.36	0.26	0.10	0.04	0.25	0.24	1.77	0.17	0
TX	0.57	0.35	3.00	0.03	0.34	0.26	0.10	0.04	0.25	0.24	1.38	0.17	0

A.12 WATER DEMANDS

The direct WDs for biomass production were calculated as the difference between the amount of make-up water required due to evaporation (W*evap*), pond cleaning (W*cleaning*), pond leaking (W*leaking*), blowdown (W*blowdown*), photosynthesis (W*photosyn*), harvesting (W*harvest*), algal drying (W*drying*), water stored in the biomass that is transported offsite (W*biomass*), and annual precipitation (W*precip*), shown in equation 25.

$$Direct\ WD = W_{evap} + W_{cleaning} + W_{leaking} + W_{blowdown} + W_{photosyn} + W_{harvest} + W_{drying} + W_{biomass} - W_{precip} \quad (25)$$

A comparative breakdown of the direct water demands for Chamber filter press-based pathways for Phoenix, Arizona are provided below.

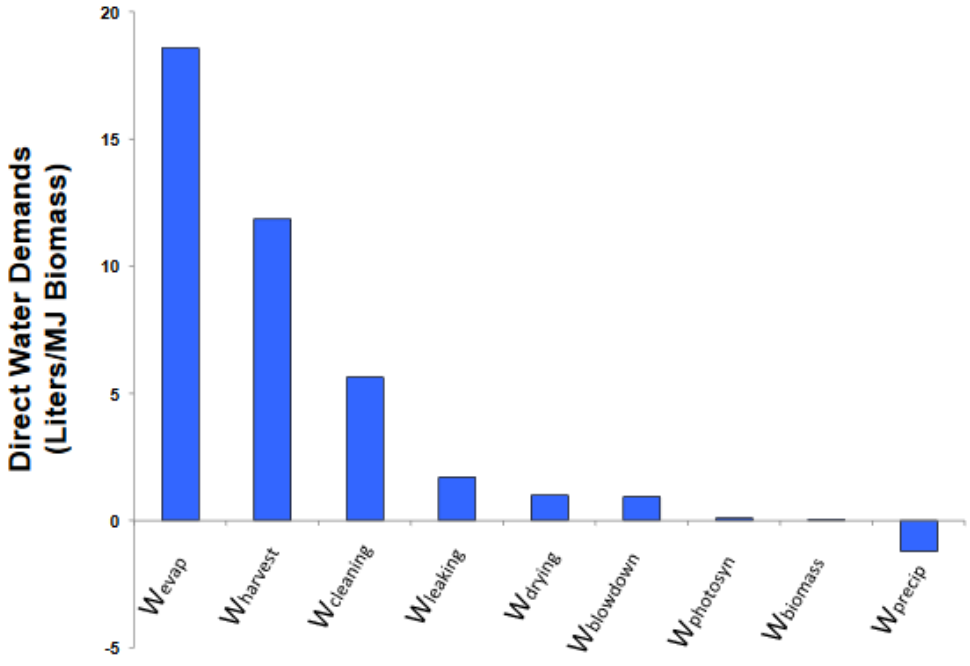

Figure 30. Direct Water Demands for CFP pathways for Phoenix, Arizona

A.13 ALLOCATION

In this study the energetic and environmental impacts of obtaining pure CO_2 via MEA scrubbing are allocated between the algae cultivation facility and Natural Gas (NG) fired power plants on an energy basis. The allocation scheme is as follows: for every X MJ of electricity produced at a NG fired power plant, Y kg of CO_2 are emitted which in turn produces Z MJ of algal biomass. The percentage of environmental and energetic impacts that are allocated to algal cultivation is equal to $\frac{Z}{(Z+X)}$. To estimate the amount of CO_2 produced per MJ of electricity at a Natural Gas power plant, emissions data for over 450 NG fired power plants were acquired from the eGRID database. Analysis of this data indicates that on average NG fired power plant produce approximately 470 kg of CO_2 per MWh of electricity. Under this assumption, 44.8% of the environmental impacts due to MEA are allocated to algae cultivation. Additionally, unallocated values for $EROI_{fossil}$ and life cycle GHG emissions are provided in the following summary tables.

A.14 SUMMARY TABLES

The following tables provide the direct WDs, $EROI_{fossil}$, and life cycle GHG emissions for biomass production with and without allocation under different combinations of cultivation and harvesting strategies.

Table 31. Allocated $EROI_{Fossil}$, net life cycle GHG emissions, and direct WDs for examined production pathways

Parameters		Cultivation and Harvesting Scenarios (Allocated)								WD[1]	
State	City	MEA/CF/NGD	MEA/CFP/NGD	DI/CF/ NGD	DI/CFP/NGD	MEA/CF/WHD	MEA/CFP/WHD	DI/CF/WHD	DI/CFP/WHD	CFP	CF
AL	Mobile	0.40 (44.2)	0.46 (22.5)	0.49 (18.9)	0.59 (-2.8)	0.60 (-0.4)	0.68 (-15.1)	0.86 (-25.7)	1.04 (-40.4)	22.1	22.3
AZ	Phoenix	0.38 (48.9)	0.43 (28.4)	0.47 (23.5)	0.56 (3.0)	0.57 (4.2)	0.64 (-9.2)	0.79 (-21.2)	0.94 (-34.6)	38.6	38.8
CA	San Diego	0.41 (32.0)	0.46 (16.0)	0.51 (6.3)	0.60 (-9.6)	0.63 (-12.6)	0.69 (-21.5)	0.91 (-38.3)	1.06 (-47.2)	32.8	33.0
FL	Daytona Beach	0.38 (43.0)	0.44 (22.7)	0.47 (17.5)	0.57 (-2.7)	0.58 (-1.6)	0.66 (-14.8)	0.81 (-27.1)	0.97 (-40.2)	24.1	24.3
FL	Jacksonville	0.38 (43.1)	0.44 (22.8)	0.47 (17.7)	0.57 (-2.6)	0.58 (-1.5)	0.66 (-14.7)	0.81 (-27.0)	0.97 (-40.1)	22.6	22.9
FL	Key West	0.38 (43.6)	0.44 (23.4)	0.47 (18.2)	0.57 (-2.1)	0.57 (-1.0)	0.65 (-14.2)	0.80 (-26.4)	0.97 (-39.6)	28.4	28.6
FL	Miami	0.38 (42.7)	0.44 (22.5)	0.48 (17.3)	0.57 (-3.0)	0.58 (-1.9)	0.66 (-15.1)	0.81 (-27.3)	0.98 (-40.5)	22.1	22.4
FL	Tallahassee	0.39 (42.4)	0.44 (22.2)	0.48 (17.0)	0.57 (-3.2)	0.58 (-2.2)	0.66 (-15.4)	0.82 (-27.6)	0.98 (-40.8)	20.8	21.1
FL	Tampa	0.38 (43.2)	0.44 (23.0)	0.47 (17.8)	0.57 (-2.5)	0.58 (-1.4)	0.65 (-14.6)	0.81 (-26.8)	0.97 (-40.0)	25.1	25.4
FL	West Palm Beach	0.38 (43.0)	0.44 (22.7)	0.47 (17.6)	0.57 (-2.7)	0.58 (-1.6)	0.66 (-14.8)	0.81 (-27.0)	0.97 (-40.2)	22.9	23.1
GA	Savannah	0.39 (45.0)	0.45 (23.2)	0.49 (19.7)	0.59 (-2.1)	0.60 (0.4)	0.68 (-14.3)	0.86 (-24.9)	1.03 (-39.6)	24.1	24.4
LA	Baton Rouge	0.39 (39.2)	0.45 (20.8)	0.49 (13.6)	0.58 (-4.7)	0.60 (-5.4)	0.67 (-16.8)	0.86 (-31.0)	1.01 (-42.3)	22.6	22.8
LA	Lake Charles	0.39 (39.0)	0.45 (20.6)	0.49 (13.5)	0.58 (-4.9)	0.60 (-5.6)	0.67 (-16.9)	0.86 (-31.1)	1.02 (-42.4)	23.0	23.2
LA	New Orleans	0.40 (38.9)	0.45 (20.5)	0.49 (13.4)	0.58 (-5.0)	0.60 (-5.7)	0.67 (-17.0)	0.86 (-31.2)	1.02 (-42.5)	22.1	22.3
TX	Austin	0.39 (41.5)	0.45 (20.6)	0.49 (16.1)	0.59 (-4.8)	0.59 (-3.1)	0.68 (-16.9)	0.85 (-28.5)	1.03 (-42.3)	29.8	30.0
TX	Brownsville	0.39 (41.8)	0.45 (20.9)	0.49 (16.4)	0.58 (-4.5)	0.59 (-2.8)	0.68 (-16.6)	0.84 (-28.2)	1.02 (-42.0)	30.6	30.8
TX	Corpus Christi	0.39 (42.1)	0.45 (21.3)	0.48 (16.8)	0.58 (-4.1)	0.59 (-2.5)	0.67 (-16.3)	0.84 (-27.8)	1.02 (-41.7)	29.7	29.9
TX	Houston	0.39 (42.0)	0.45 (21.1)	0.49 (16.7)	0.58 (-4.2)	0.59 (-2.6)	0.67 (-16.4)	0.84 (-27.9)	1.02 (-41.8)	25.6	25.8
TX	Lufkin	0.39 (41.5)	0.45 (20.6)	0.49 (16.1)	0.59 (-4.8)	0.59 (-3.1)	0.68 (-16.9)	0.85 (-28.5)	1.03 (-42.3)	26.1	26.3
TX	Port Arthur	0.40 (35.2)	0.46 (16.9)	0.51 (9.7)	0.60 (-8.6)	0.62 (-9.4)	0.70 (-20.6)	0.91 (-34.9)	1.08 (-46.2)	22.8	23.0
TX	San Antonio	0.39 (41.3)	0.45 (20.4)	0.49 (16.0)	0.59 (-4.9)	0.60 (-3.3)	0.68 (-17.1)	0.85 (-28.6)	1.03 (-42.5)	29.9	30.1
TX	Victoria	0.39 (41.9)	0.45 (21.0)	0.49 (16.5)	0.58 (-4.4)	0.59 (-2.7)	0.68 (-16.5)	0.84 (-28.1)	1.02 (-41.9)	27.4	27.7

Table 32. Allocated $EROI_{Fossil}$, net life cycle GHG emissions, and direct WDs for examined production pathways

Parameters		Cultivation and Harvesting Scenarios (Unallocated)								WD[1]	
State	City	MEA/CF/NGD	MEA/CFP/NGD	MEA/CF/WHD	MEA/CFP/WHD	DI/CF/ NGD	DI/CFP/NGD	DI/CF/WHD	DI/CFP/WHD	CFP	CF
AL	Mobile	0.31 (78.6)	0.35 (56.8)	0.43 (33.9)	0.47 (19.2)	0.49 (18.9)	0.59 (-2.8)	0.86 (-25.7)	1.04 (-40.4)	22.1	22.3
AZ	Phoenix	0.30 (83.0)	0.34 (62.5)	0.41 (38.4)	0.45 (25.0)	0.47 (23.5)	0.56 (3.0)	0.79 (-21.2)	0.94 (-34.6)	38.6	38.8
CA	San Diego	0.32 (65.5)	0.35 (49.5)	0.44 (20.9)	0.48 (12.0)	0.51 (6.3)	0.60 (-9.6)	0.91 (-38.3)	1.06 (-47.2)	32.8	33.0
FL	Daytona Beach	0.31 (77.1)	0.34 (56.8)	0.42 (32.4)	0.46 (19.3)	0.47 (17.5)	0.57 (-2.7)	0.81 (-27.1)	0.97 (-40.2)	24.1	24.3
FL	Jacksonville	0.31 (77.2)	0.34 (56.9)	0.42 (32.6)	0.46 (19.4)	0.47 (17.7)	0.57 (-2.6)	0.81 (-27.0)	0.97 (-40.1)	22.6	22.9
FL	Key West	0.31 (77.7)	0.34 (57.5)	0.42 (33.1)	0.46 (19.9)	0.47 (18.2)	0.57 (-2.1)	0.80 (-26.4)	0.97 (-39.6)	28.4	28.6
FL	Miami	0.31 (76.8)	0.34 (56.6)	0.42 (32.2)	0.46 (19.0)	0.48 (17.3)	0.57 (-3.0)	0.81 (-27.3)	0.98 (-40.5)	22.1	22.4
FL	Tallahassee	0.31 (76.5)	0.34 (56.3)	0.42 (31.9)	0.46 (18.7)	0.48 (17.0)	0.57 (-3.2)	0.82 (-27.6)	0.98 (-40.8)	20.8	21.1
FL	Tampa	0.31 (77.3)	0.34 (57.1)	0.42 (32.7)	0.46 (19.5)	0.47 (17.8)	0.57 (-2.5)	0.81 (-26.8)	0.97 (-40.0)	25.1	25.4
FL	West Palm Beach	0.31 (77.1)	0.34 (56.8)	0.42 (32.5)	0.46 (19.3)	0.47 (17.6)	0.57 (-2.7)	0.81 (-27.0)	0.97 (-40.2)	22.9	23.1
GA	Savannah	0.31 (79.3)	0.35 (57.5)	0.43 (34.7)	0.47 (20.0)	0.49 (19.7)	0.59 (-2.1)	0.86 (-24.9)	1.03 (-39.6)	24.1	24.4
LA	Baton Rouge	0.31 (73.0)	0.35 (54.6)	0.43 (28.4)	0.47 (17.1)	0.49 (13.6)	0.58 (-4.7)	0.86 (-31.0)	1.01 (-42.3)	22.6	22.8
LA	Lake Charles	0.31 (72.8)	0.35 (54.5)	0.43 (28.2)	0.47 (16.9)	0.49 (13.5)	0.58 (-4.9)	0.86 (-31.1)	1.02 (-42.4)	23.0	23.2
LA	New Orleans	0.31 (72.7)	0.35 (54.4)	0.43 (28.1)	0.47 (16.8)	0.49 (13.4)	0.58 (-5.0)	0.86 (-31.2)	1.02 (-42.5)	22.1	22.3
TX	Austin	0.31 (75.7)	0.35 (54.8)	0.43 (31.1)	0.47 (17.3)	0.49 (16.1)	0.59 (-4.8)	0.85 (-28.5)	1.03 (-42.3)	29.8	30.0
TX	Brownsville	0.31 (76.0)	0.35 (55.1)	0.43 (31.4)	0.47 (17.6)	0.49 (16.4)	0.58 (-4.5)	0.84 (-28.2)	1.02 (-42.0)	30.6	30.8
TX	Corpus Christi	0.31 (76.3)	0.35 (55.5)	0.43 (31.7)	0.47 (17.9)	0.48 (16.8)	0.58 (-4.1)	0.84 (-27.8)	1.02 (-41.7)	29.7	29.9
TX	Houston	0.31 (76.2)	0.35 (55.3)	0.43 (31.6)	0.47 (17.8)	0.49 (16.7)	0.58 (-4.2)	0.84 (-27.9)	1.02 (-41.8)	25.6	25.8
TX	Lufkin	0.31 (75.7)	0.35 (54.8)	0.43 (31.1)	0.47 (17.3)	0.49 (16.1)	0.59 (-4.8)	0.85 (-28.5)	1.03 (-42.3)	26.1	26.3
TX	Port Arthur	0.32 (69.1)	0.36 (50.7)	0.44 (24.5)	0.48 (13.2)	0.51 (9.7)	0.60 (-8.6)	0.91 (-34.9)	1.08 (-46.2)	22.8	23.0
TX	San Antonio	0.31 (75.7)	0.35 (54.6)	0.43 (30.9)	0.47 (17.1)	0.49 (16.0)	0.59 (-4.9)	0.85 (-28.6)	1.03 (-42.5)	29.9	30.1
TX	Victoria	0.31 (76.1)	0.35 (55.2)	0.43 (31.5)	0.47 (17.6)	0.49 (16.5)	0.58 (-4.4)	0.84 (-28.1)	1.02 (-41.9)	27.4	27.7

* The results are presented in the following format: $EROI_{fossil}$ (Net Life Cycle GHG Emissions) where Net life cycle GHG emissions are in units of (g CO_2 eq/MJ-Biomass)

[1] The results for the WD are presented in units of (liters/MJ-biomass)

A.15 LOW NITROGEN SCENARIO

Previous studies have suggested that cultivating algae in low-nitrogen conditions can substantially increase the lipid content of the biomass [373-375]. However, nitrogen deprivation may have adverse effects on the algae culture, and additional experimental data is required to validate the feasibility of this approach. A low-nitrogen scenario was considered in this analysis, the fractionalized composition of algae under nitrogen deprivation, taken from Lardon et al. 2009, was evaluated at 38.5% lipids, 52.9% carbohydrates, and 6.7% proteins [376]. The following tables provide the $EROI_{fossil}$, and life cycle GHG emissions for biomass production for the low-nitrogen scenario (with and without allocation).

Table 33. Low Nitrogen Scenario: Allocated $EROI_{Fossil}$, net life cycle GHG emissions, and direct WDs for examined production pathways

Parameters		Cultivation and Harvesting Scenarios (Allocated)							
State	City	MEA/CF/NGD	MEA/CFP/NGD	DI/CF/ NGD	DI/CFP/NGD	MEA/CF/WHD	MEA/CFP/WHD	DI/CF/WHD	DI/CFP/WHD
AL	Mobile	0.54 (22.8)	0.63 (4.8)	0.72 (-1.6)	0.90 (-19.5)	0.87 (-14.0)	1.02 (-26.1)	1.50 (-38.3)	1.97 (-50.4)
AZ	Phoenix	0.51 (27.3)	0.59 (10.5)	0.68 (3.0)	0.83 (-13.9)	0.81 (-9.4)	0.92 (-20.4)	1.31 (-33.8)	1.65 (-44.8)
CA	San Diego	0.55 (12.4)	0.64 (-0.7)	0.75 (-12.1)	0.92 (-25.2)	0.91 (-24.3)	1.03 (-31.6)	1.62 (-48.8)	2.04 (-56.1)
FL	Daytona Beach	0.52 (21.8)	0.61 (5.1)	0.69 (-2.6)	0.86 (-19.3)	0.83 (-15.0)	0.96 (-25.8)	1.36 (-39.3)	1.78 (-50.2)
FL	Jacksonville	0.52 (21.9)	0.61 (5.2)	0.69 (-2.5)	0.86 (-19.2)	0.82 (-14.9)	0.96 (-25.7)	1.36 (-39.2)	1.77 (-50.1)
FL	Key West	0.52 (22.4)	0.60 (5.7)	0.68 (-2.0)	0.85 (-18.6)	0.82 (-14.3)	0.95 (-25.2)	1.34 (-38.7)	1.75 (-49.6)
FL	Miami	0.52 (21.5)	0.61 (4.8)	0.69 (-2.9)	0.86 (-19.5)	0.83 (-15.2)	0.97 (-26.1)	1.37 (-39.6)	1.79 (-50.4)
FL	Tallahassee	0.52 (21.2)	0.61 (4.6)	0.69 (-3.1)	0.86 (-19.8)	0.83 (-15.5)	0.97 (-26.4)	1.38 (-39.9)	1.81 (-50.7)
FL	Tampa	0.52 (22.0)	0.61 (5.3)	0.69 (-2.4)	0.86 (-19.0)	0.82 (-14.7)	0.96 (-25.6)	1.35 (-39.1)	1.77 (-50.0)
FL	West Palm Beach	0.52 (21.8)	0.61 (5.1)	0.69 (-2.6)	0.86 (-19.3)	0.82 (-14.9)	0.96 (-25.8)	1.36 (-39.3)	1.78 (-50.2)
GA	Savannah	0.53 (23.4)	0.63 (5.5)	0.72 (-0.9)	0.89 (-18.8)	0.87 (-13.3)	1.01 (-25.4)	1.48 (-37.6)	1.94 (-49.7)
LA	Baton Rouge	0.53 (18.6)	0.62 (3.5)	0.72 (-5.8)	0.88 (-21.0)	0.87 (-18.1)	0.99 (-27.5)	1.48 (-42.6)	1.89 (-51.9)
LA	Lake Charles	0.54 (18.4)	0.62 (3.3)	0.72 (-6.0)	0.88 (-21.1)	0.87 (-18.3)	0.99 (-27.6)	1.49 (-42.7)	1.90 (-52.1)
LA	New Orleans	0.54 (18.3)	0.62 (3.2)	0.72 (-6.1)	0.89 (-21.3)	0.87 (-18.4)	1.00 (-27.7)	1.49 (-42.8)	1.90 (-52.2)
TX	Austin	0.53 (20.4)	0.63 (3.2)	0.71 (-4.0)	0.89 (-21.2)	0.86 (-16.3)	1.01 (-27.7)	1.46 (-40.7)	1.94 (-52.1)
TX	Brownsville	0.53 (20.7)	0.62 (3.5)	0.71 (-3.7)	0.89 (-20.9)	0.86 (-16.1)	1.00 (-27.4)	1.45 (-40.4)	1.92 (-51.8)
TX	Corpus Christi	0.53 (21.0)	0.62 (3.8)	0.71 (-3.3)	0.89 (-20.5)	0.85 (-15.7)	1.00 (-27.1)	1.44 (-40.1)	1.90 (-51.4)
TX	Houston	0.53 (20.9)	0.62 (3.7)	0.71 (-3.4)	0.89 (-20.6)	0.85 (-15.8)	1.00 (-27.2)	1.44 (-40.2)	1.91 (-51.6)
TX	Lufkin	0.53 (20.4)	0.63 (3.2)	0.71 (-4.0)	0.89 (-21.2)	0.86 (-16.4)	1.01 (-27.8)	1.46 (-40.7)	1.94 (-52.1)
TX	Port Arthur	0.55 (15.0)	0.64 (-0.1)	0.75 (-9.4)	0.93 (-24.5)	0.91 (-21.7)	1.05 (-31.0)	1.62 (-46.1)	2.11 (-55.4)
TX	San Antonio	0.53 (20.2)	0.63 (3.0)	0.71 (-4.1)	0.90 (-21.3)	0.86 (-16.5)	1.01 (-27.9)	1.46 (-40.9)	1.95 (-52.3)
TX	Victoria	0.53 (20.7)	0.62 (3.5)	0.71 (-3.6)	0.89 (-20.8)	0.85 (-16.0)	1.00 (-27.4)	1.44 (-40.3)	1.92 (-51.7)

Table 34. Low Nitrogen Scenario: Unallocated $EROI_{Fossil}$, net life cycle GHG emissions, and direct WDs for examined production pathways

Parameters		Cultivation and Harvesting Scenarios (Unallocated)							
State	City	MEA/CF/NGD	MEA/CFP/NGD	MEA/CF/WHD	MEA/CFP/WHD	DI/CF/ NGD	DI/CFP/NGD	DI/CF/WHD	DI/CFP/WHD
AL	Mobile	0.42 (49.6)	0.48 (31.7)	0.60 (12.9)	0.67 (0.8)	0.72 (-1.6)	0.90 (-19.5)	1.50 (-38.3)	1.97 (-50.4)
AZ	Phoenix	0.40 (54.0)	0.45 (37.2)	0.57 (17.3)	0.63 (6.3)	0.68 (2.9)	0.83 (-13.9)	1.31 (-33.8)	1.65 (-44.8)
CA	San Diego	0.43 (38.6)	0.48 (25.5)	0.62 (1.9)	0.68 (-5.4)	0.75 (-12.1)	0.92 (-25.2)	1.62 (-48.8)	2.04 (-56.1)
FL	Daytona Beach	0.41 (48.4)	0.46 (31.8)	0.58 (11.7)	0.64 (0.9)	0.69 (-2.7)	0.86 (-19.3)	1.36 (-39.3)	1.78 (-50.2)
FL	Jacksonville	0.41 (48.5)	0.46 (31.9)	0.58 (11.8)	0.64 (1.0)	0.69 (-2.5)	0.86 (-19.2)	1.36 (-39.2)	1.77 (-50.1)
FL	Key West	0.41 (49.1)	0.46 (32.4)	0.58 (12.4)	0.64 (1.5)	0.68 (-2.0)	0.85 (-18.6)	1.34 (-38.7)	1.75 (-49.6)
FL	Miami	0.41 (48.2)	0.46 (31.5)	0.58 (11.5)	0.64 (0.6)	0.69 (-2.9)	0.86 (-19.5)	1.37 (-39.6)	1.79 (-50.4)
FL	Tallahassee	0.41 (47.9)	0.46 (31.2)	0.58 (11.2)	0.65 (0.3)	0.69 (-3.2)	0.86 (-19.8)	1.38 (-39.9)	1.81 (-50.7)
FL	Tampa	0.41 (48.7)	0.46 (32.0)	0.58 (12.0)	0.64 (1.1)	0.69 (-2.4)	0.86 (-19.0)	1.35 (-39.1)	1.77 (-50.0)
FL	West Palm Beach	0.41 (48.4)	0.46 (31.8)	0.58 (11.7)	0.64 (0.9)	0.69 (-2.6)	0.86 (-19.3)	1.36 (-39.3)	1.78 (-50.2)
GA	Savannah	0.42 (50.2)	0.47 (32.3)	0.60 (13.5)	0.66 (1.4)	0.72 (-0.9)	0.89 (-18.8)	1.48 (-37.6)	1.94(-49.7)
LA	Baton Rouge	0.42 (45.0)	0.47 (29.9)	0.60 (8.4)	0.66 (-1.0)	0.72 (-5.9)	0.88 (-21.0)	1.48 (-42.6)	1.89 (-51.9)
LA	Lake Charles	0.42 (44.9)	0.47 (29.8)	0.60 (8.2)	0.66 (-1.1)	0.72 (-6.0)	0.88 (-21.1)	1.49 (-42.7)	1.90 (-52.1)
LA	New Orleans	0.42 (44.8)	0.47 (29.7)	0.60 (8.1)	0.66 (-1.2)	0.72 (-6.1)	0.89 (-21.3)	1.49 (-42.8)	1.90 (-52.2)
TX	Austin	0.42 (47.1)	0.47 (29.9)	0.60 (10.4)	0.66 (-1.0)	0.71 (-4.0)	0.89 (-21.2)	1.46 (-40.7)	1.94 (-52.1)
TX	Brownsville	0.42 (47.4)	0.47 (30.2)	0.59 (10.7)	0.66 (-0.7)	0.71 (-3.7)	0.89 (-20.9)	1.45 (-40.4)	1.92 (-51.8)
TX	Corpus Christi	0.42 (47.7)	0.47 (30.6)	0.59 (11.1)	0.66 (-0.3)	0.71 (-3.4)	0.89 (-20.5)	1.44 (-40.1)	1.90 (-51.4)
TX	Houston	0.42 (47.6)	0.47 (30.5)	0.59 (10.9)	0.66 (-0.4)	0.71 (-3.5)	0.89 (-20.6)	1.44 (-40.2)	1.91 (-51.6)
TX	Lufkin	0.42 (47.1)	0.47 (29.9)	0.60 (10.4)	0.66 (-1.0)	0.71 (-4.0)	0.89 (-21.2)	1.46 (-40.7)	1.94 (-52.1)
TX	Port Arthur	0.43 (41.5)	0.48 (26.4)	0.62 (4.8)	0.68 (-4.5)	0.75 (-9.5)	0.93 (-24.5)	1.62 (-46.1)	2.11 (-55.4)
TX	San Antonio	0.42 (46.9)	0.47 (29.8)	0.60 (10.2)	0.66 (-1.1)	0.71 (-4.2)	0.90 (-21.3)	1.46 (-40.9)	1.95 (-52.3)
TX	Victoria	0.42 (47.5)	0.47 (30.3)	0.59 (10.8)	0.66 (-0.6)	0.71 (-3.6)	0.89 (-20.8)	1.44 (-40.3)	1.92 (-51.7)

* The results are presented in the following format: $EROI_{fossil}$ (Net Life Cycle GHG Emissions) where Net life cycle GHG emissions are in units of (g CO_2 eq/MJ-Biomass)

A.16 ALTERNATIVE PRODUCTION SCENARIO

An alternate technological route was considered in this work. This production pathway assumes that microalgae undergo auto-flocculation (AF) to concentrate the biomass to .25% (w/w) [125]. Recent studies have suggested that cross flow filtration (CFF) is a low-energy intensive technology that can be used to dewater the algae culture, and has many advantages over conventional centrifugation, pressure filtration, and dissolved air and/or froth flotation [126]. Therefore, post auto-flocculation biomass is then sent to a cross-flow filtration unit for further dewatering to 16% (w/w); the electrical consumption for cross flow filtration was evaluated at .5 kWh/m^3 [126]. A chamber filter press (CFP) is then used to further concentrate the algae to 25% (w/w), and both natural gas (NG) and waste heat (WHD) are evaluated as processing options for drying the biomass to 90% (w/w). This technological route may be favorable, as it does not rely on a coagulant for biomass production and uses low-energy dewatering strategies.

Table 35. Alternate Production Scenario: Allocated $EROI_{Fossil}$, net life cycle GHG emissions, and direct WDs for examined production pathways

Parameters		Cultivation and Harvesting Scenarios (Allocated)							
Growth Conditions		Normal Growth Conditions				Low Nitrogen Scenario			
State	City	MEA/AF/CFF/ CFP/NG	DI/AF/CFF/ CFP/NG	MEA/AF/CFF/ CFP/WHD	DI/AF/CFF/ CFP/ WHD	MEA/AF/CFF/ CFP/NG	DI/AF/CFF/ CFP/NG	MEA/AF/CFF/ CFP/WHD	DI/AF/CFF/ CFP/ WHD
AL	Mobile	0.45 (14.6)	0.59 (-10.7)	0.68 (-22.9)	1.04 (-48.2)	0.63 (-1.6)	0.90 (-25.9)	1.01 (-32.5)	1.96 (-56.8)
AZ	Phoenix	0.43 (20.7)	0.56 (-4.7)	0.64 (-16.8)	0.94 (-42.2)	0.59 (4.2)	0.83 (-20.2)	0.92 (-26.7)	1.65 (-51.1)
CA	San Diego	0.46 (9.0)	0.60 (-16.7)	0.70 (-28.6)	1.08 (-54.2)	0.64 (-6.5)	0.93 (-31.1)	1.05 (-37.4)	2.10 (-61.9)
FL	Daytona Beach	0.44 (15.1)	0.57 (-10.3)	0.65 (-22.5)	0.97 (-47.9)	0.61 (-1.2)	0.85 (-25.6)	0.95 (-32.1)	1.76 (-56.5)
FL	Jacksonville	0.44 (15.2)	0.57 (-10.2)	0.65 (-22.3)	0.96 (-47.8)	0.61 (-1.1)	0.85 (-25.5)	0.95 (-32.0)	1.75 (-56.4)
FL	Key West	0.44 (15.7)	0.56 (-9.7)	0.65 (-21.8)	0.96 (-47.2)	0.60 (-0.6)	0.85 (-24.9)	0.95 (-31.5)	1.72 (-55.8)
FL	Miami	0.44 (14.8)	0.57 (-10.6)	0.65 (-22.7)	0.97 (-48.1)	0.61 (-1.5)	0.86 (-25.8)	0.96 (-32.3)	1.77 (-56.7)
FL	Tallahassee	0.44 (14.5)	0.57 (-10.9)	0.66 (-23.0)	0.97 (-48.4)	0.61 (-1.7)	0.86 (-26.1)	0.96 (-32.6)	1.78 (-57.0)
FL	Tampa	0.44 (15.3)	0.56 (-10.1)	0.65 (-22.2)	0.96 (-47.6)	0.60 (-1.0)	0.85 (-25.3)	0.95 (-31.9)	1.74 (-56.2)
FL	West Palm Beach	0.44 (15.1)	0.57 (-10.3)	0.65 (-22.4)	0.97 (-47.8)	0.61 (-1.2)	0.85 (-25.6)	0.95 (-32.1)	1.75 (-56.5)
GA	Savannah	0.45 (15.4)	0.59 (-9.9)	0.68 (-22.1)	1.03 (-47.5)	0.63 (-1.0)	0.89 (-25.3)	1.00 (-31.9)	1.93 (-56.2)
LA	Baton Rouge	0.45 (13.4)	0.58 (-12.1)	0.67 (-24.1)	1.02 (-49.6)	0.62 (-2.6)	0.89 (-27.1)	1.00 (-33.5)	1.91 (-58.0)
LA	Lake Charles	0.45 (13.2)	0.58 (-12.3)	0.68 (-24.3)	1.02 (-49.8)	0.62 (-2.8)	0.89 (-27.2)	1.00 (-33.7)	1.92 (-58.1)
LA	New Orleans	0.45 (13.1)	0.58 (-12.4)	0.68 (-24.4)	1.02 (-49.9)	0.62 (-2.9)	0.89 (-27.3)	1.00 (-33.8)	1.92 (-58.2)
TX	Austin	0.45 (12.9)	0.58 (-12.5)	0.67 (-24.6)	1.02 (-50.0)	0.62 (-3.2)	0.89 (-27.5)	1.00 (-34.1)	1.91 (-58.4)
TX	Brownsville	0.45 (13.2)	0.58(-12.2)	0.67 (-24.3)	1.01 (-49.7)	0.62 (-2.9)	0.88 (-27.2)	0.99 (-33.8)	1.89 (-58.1)
TX	Corpus Christi	0.45 (13.5)	0.58 (-11.9)	0.67 (-24.0)	1.01 (-49.4)	0.62 (-2.6)	0.88 (-26.9)	0.99 (-33.4)	1.88 (-57.8)
TX	Houston	0.45 (13.4)	0.58 (-12.0)	0.67 (-24.1)	1.01 (-49.5)	0.62 (-2.7)	0.88 (-27.0)	0.99 (-33.6)	1.88 (-57.9)
TX	Lufkin	0.45 (12.9)	0.58 (-12.5)	0.67 (-24.6)	1.02 (-50.0)	0.62 (-3.2)	0.89 (-27.6)	1.00 (-34.1)	1.91 (-58.4)
TX	Port Arthur	0.46 (9.5)	0.60 (-16.0)	0.70 (-28.0)	1.09 (-53.5)	0.64 (-6.2)	0.93 (-30.6)	1.05 (-37.0)	2.13 (-61.5)
TX	San Antonio	0.45 (12.7)	0.58 (-12.7)	0.68 (-24.8)	1.02 (-50.2)	0.62 (-3.4)	0.89 (-27.7)	1.00 (-34.3)	1.92 (-58.6)
TX	Victoria	0.45 (13.3)	0.58 (-12.1)	0.67 (-24.3)	1.01 (-49.6)	0.62 (-2.8)	0.88 (-27.2)	0.99 (-33.7)	1.89 (-58.1)

*The results are presented in the following format: $EROI_{fossil}$ (Net Life Cycle GHG Emissions) where Net life cycle GHG emissions are in units of (g CO_2 eq/MJ Biomass)

Table 36. Alternate Production Scenario: Unallocated $EROI_{Fossil}$, net life cycle GHG emissions, and direct WDs for examined production pathways

Parameters		Cultivation and Harvesting Scenarios (Unallocated)							
Growth Conditions		Normal Growth Conditions				Low Nitrogen Scenario			
State	City	MEA/AF/CFF/CFP /NG	MEA/AF/CFF/CFP/ WHD	DI/AF/CFF/CFP/ NG	DI/AF/CFF/ CFP/ WHD	MEA/AF/CFF/ CFP/NG	MEA/AF/CFF/ CFP/WHD	DI/AF/CFF/ CFP/NG	DI/AF/CFF/ CFP/ WHD
AL	Mobile	0.35 (48.9)	0.47 (11.4)	0.59 (-10.7)	1.04 (-48.2)	0.48 (25.2)	0.67 (-5.7)	0.90 (-25.9)	1.96 (-56.8)
AZ	Phoenix	0.34 (54.9)	0.45 (17.3)	0.56 (-4.7)	0.94 (-42.2)	0.45 (30.9)	0.63 (0.0)	0.83 (-20.2)	1.65 (-51.1)
CA	San Diego	0.36 (42.5)	0.48 (4.9)	0.60 (-16.7)	1.08 (-54.2)	0.48 (19.7)	0.68 (-11.2)	0.93 (-31.1)	2.10 (-61.9)
FL	Daytona Beach	0.34 (49.2)	0.46 (11.6)	0.57 (-10.3)	0.97 (-47.9)	0.46 (25.5)	0.64 (-5.4)	0.85 (-25.6)	1.76 (-56.5)
FL	Jacksonville	0.34 (49.3)	0.46 (11.7)	0.57 (-10.2)	0.96 (-47.8)	0.46 (25.6)	0.64 (-5.3)	0.85 (-25.5)	1.75 (-56.4)
FL	Key West	0.34 (49.8)	0.45 (12.3)	0.56 (-9.7)	0.96 (-47.2)	0.46 (26.1)	0.64 (-4.8)	0.85 (-24.9)	1.72 (-55.8)
FL	Miami	0.34 (48.9)	0.46 (11.4)	0.57 (-10.6)	0.97 (-48.1)	0.46 (25.2)	0.64 (-5.7)	0.86 (-25.8)	1.77 (-56.7)
FL	Tallahassee	0.34 (48.6)	0.46 (11.1)	0.57 (-10.9)	0.97 (-48.4)	0.46 (25.0)	0.64 (-5.9)	0.86 (-26.1)	1.78 (-57.0)
FL	Tampa	0.34 (49.4)	0.46 (11.9)	0.56 (-10.1)	0.96 (-47.6)	0.46 (25.7)	0.64 (-5.2)	0.85 (-25.3)	1.74 (-56.2)
FL	West Palm Beach	0.34 (49.2)	0.46 (11.7)	0.57 (-10.3)	0.97 (-47.8)	0.46 (25.5)	0.64 (-5.4)	0.85 (-25.6)	1.75 (-56.5)
GA	Savannah	0.35 (49.7)	0.47 (12.2)	0.59 (-9.9)	1.03 (-47.5)	0.47 (25.9)	0.66 (-5.0)	0.89 (-25.3)	1.93 (-56.2)
LA	Baton Rouge	0.35 (47.2)	0.47 (9.7)	0.58 (-12.1)	1.02 (-49.6)	0.47 (23.9)	0.66 (-7.0)	0.89 (-27.1)	1.91 (-58.0)
LA	Lake Charles	0.35 (47.1)	0.47 (9.5)	0.58 (-12.3)	1.02 (-49.8)	0.47 (23.7)	0.66 (-7.2)	0.89 (-27.2)	1.92 (-58.1)
LA	New Orleans	0.35 (47.0)	0.47 (9.4)	0.58 (-12.4)	1.02 (-49.9)	0.47 (23.6)	0.66 (-7.3)	0.89 (-27.3)	1.92 (-58.2)
TX	Austin	0.35 (47.1)	0.47 (9.6)	0.58 (-12.5)	1.02 (-50.0)	0.47 (23.6)	0.66 (-7.3)	0.89 (-27.5)	1.91 (-58.4)
TX	Brownsville	0.35 (47.4)	0.47 (9.9)	0.58(-12.2)	1.01 (-49.7)	0.47 (23.9)	0.66 (-7.0)	0.88 (-27.2)	1.89 (-58.1)
TX	Corpus Christi	0.35 (47.7)	0.46 (10.2)	0.58 (-11.9)	1.01 (-49.4)	0.47 (24.2)	0.65 (-6.7)	0.88 (-26.9)	1.88 (-57.8)
TX	Houston	0.35 (47.6)	0.47 (10.1)	0.58 (-12.0)	1.01 (-49.5)	0.47 (24.1)	0.66 (-6.8)	0.88 (-27.0)	1.88 (-57.9)
TX	Lufkin	0.35 (47.1)	0.47 (9.5)	0.58 (-12.5)	1.02 (-50.0)	0.47 (23.6)	0.66 (-7.3)	0.89 (-27.6)	1.91 (-58.4)
TX	Port Arthur	0.36 (43.4)	0.48 (5.8)	0.60 (-16.0)	1.09 (-53.5)	0.48 (20.3)	0.68 (-10.6)	0.93 (-30.6)	2.13 (-61.5)
TX	San Antonio	0.35 (46.9)	0.47 (9.4)	0.58 (-12.7)	1.02 (-50.2)	0.47 (23.4)	0.66 (-7.5)	0.89 (-27.7)	1.92 (-58.6)
TX	Victoria	0.35 (47.4)	0.47 (9.9)	0.58 (-12.1)	1.01 (-49.6)	0.47 (23.9)	0.66 (-6.9)	0.88 (-27.2)	1.89 (-58.1)

* The results are presented in the following format: $EROI_{fossil}$ (Net Life Cycle GHG Emissions) where Net life cycle GHG emissions are in units of (g CO_2 eq/MJ-Biomass)

APPENDIX B

SUPPORTING INFORMATION FOR ASSESSING THE CRITICAL ROLE OF ECOLOGICAL GOODS AND SERVICES IN MICROALGAL BIOFUEL LIFE CYCLES

B.1 MICROALGAL BIOFUEL PRODUCTION PATHWAYS

Two technological sets: *baseline* and *improved* biofuel production pathways are evaluated in this work. Baseline scenarios utilize current commercially proven technologies and process options for microalgae-to-fuel conversion, while improved scenarios consider technologies and process options that have yet to be proven commercially feasible. The examined biofuel production scenarios are tabulated in Table 37**.**

Table 37. Baseline and Improved Biofuel Production Pathways

Production Pathways	CO_2	Dewatering	Drying	Extraction	Residual Biomass
Baseline Scenarios	MEA	CF	NGD	Dry	AF
	MEA	CF	NGD	Dry	AD
	MEA	CF	NGD	Dry	CHP
Improved Scenarios	Flue Gas	CFP	WHD	Wet	AF
	Flue Gas	CFP	WHD	Wet	AD
	Flue Gas	CFP	WHD	Wet	CHP

Waste heat from a co-located power plant is utilized to dry the residual deoiled biomass (RDB) prior to combustion via CHP as well as algal derived biofertilizer, and animal feed prior to transportation.

B.2 HYBRID ECOLOGICALLY-BASED LIFE CYCLE ASSESSMENT

EcoLCA is a recent environmentally extended input-output life cycle oriented approach capable of accounting for the role of natural capital such as ecosystem goods and services in a life cycle framework. Eco-LCA considers a wide array of goods and services derived from nature and a hierarchical, thermodynamic-based resource aggregation scheme to permit meaningful interpretation [377]. EcoLCA was developed by researchers at the Ohio State University, and is available free of charge at http://resilience.eng.ohio-state.edu/eco-lca/

The hybrid Eco-LCA model developed in this study combines the 2002 Eco-LCA model of the US economy with detailed process level data [173]. This hybrid approach overcomes several of the shortcomings of traditional process LCA and Economic Input-Output (EIOLCA) [378].

B.3 METHODOLOGY

Steps in developing hybrid Eco-LCA

1.) Develop process scale inventory for fuel production pathways

2.) Determine the 2002 producer prices for economic inputs used in fuel production

3.) Quantify the 2002 economic activity for different industrial sectors via multiplying the mass and resources flows as developed in step (1) with their corresponding 2002 producer price as constructed in step (2)

4.) Input the economic activity for specific industrial sectors as developed in step (3) into EcoLCA to determine the energy, exergy, and emergy based resource consumption from these economic activities.

5.) Quantify direct ecological goods and services as well as fuel and energy products used in fuel production in regards to their energy, exergy and emergy.

6.) Combine the results from EcoLCA (step 4) with process level data (step 5) to calculate total ecological resource consumption on a life cycle basis

B.4 PROCESS LEVEL INVENTORY FOR MICROALGAL BIOFUEL PRODUCTION

Process inventory for an integrated microalgal ORP biorefinery operating in Phoenix, AZ was constructed based on prior research. A detailed description of the modeling assumptions, equations, and parameters can be found in ref [144, 147]. Mass, energy, and resources flows entering and leaving the product system for the renewable diesel production pathways evaluated in this analysis are provided in Table 38.

Table 38. Process inventory for microalgal renewable diesel production

Parameters		**Microalgal RD - Baseline Scenarios**			**Microalgal RD - Improved Scenarios**		
Inputs	Units	Animal Feed	Anaerobic Digestion	Combined Heat & Power	Animal Feed	Anaerobic Digestion	Combined Heat & Power
Electricity	MJ	1.34E+08	1.41E+08	1.34E+08	8.99E+07	9.65E+07	8.99E+07
Natural Gas	m^3	2.59E+07	2.68E+07	2.59E+07	3.59E+05	1.32E+06	3.59E+05
Aluminum Sulfate	kg	6.40E+06	6.40E+06	6.40E+06	6.40E+06	6.40E+06	6.40E+06
Urea	kg	6.28E+06	3.77E+06	6.28E+06	6.28E+06	3.77E+06	6.28E+06
SSP	kg	2.39E+06	1.72E+06	2.39E+06	2.39E+06	1.72E+06	2.39E+06
KCL	kg	1.00E+06	1.00E+06	1.00E+06	1.00E+06	1.00E+06	1.00E+06
PVC	m^2	5.00E+05	5.00E+05	5.00E+05	5.00E+05	5.00E+05	5.00E+05
Wastewater	m^3	8.75E+06	8.75E+06	8.75E+06	8.75E+06	8.75E+06	8.75E+06
Hexane	kg	5.20E+04	5.20E+04	5.20E+04	3.38E+04	3.38E+04	3.38E+04
Hydrogen	kg	1.72E+05	1.72E+05	1.72E+05	1.68E+05	1.68E+05	1.68E+05
Petrolem Diesel	gal	2.64E+04	4.94E+03	4.23E+03	2.63E+04	4.84E+03	4.14E+03
Pipeline Transport	gal	2.64E+04	4.94E+03	4.23E+03	2.63E+04	4.84E+03	4.14E+03
Outputs	Units	Animal Feed	Anaerobic Digestion	Combined Heat & Power	Animal Feed	Anaerobic Digestion	Combined Heat & Power
Animal Feed (soybean meal eq.)	kg	2.82E+07	0.00E+00	0.00E+00	2.82E+07	0.00E+00	0.00E+00
Electricity	MJ	0.00E+00	8.39E+07	7.86E+07	0.00E+00	8.39E+07	7.86E+07
Biofertilizer (Urea eq.)	kg	0.00E+00	8.28E+05	0.00E+00	0.00E+00	8.28E+05	0.00E+00
Biofertilizer (SSP eq.)	kg	0.00E+00	6.73E+04	0.00E+00	0.00E+00	6.73E+04	0.00E+00
Heat (NG eq.)	m^3	0.00E+00	0.00E+00	5.67E+06	0.00E+00	0.00E+00	5.67E+06
Propane (LPG eq.)	kg	3.17E+05	3.17E+05	3.17E+05	3.10E+05	3.10E+05	3.10E+05
Renewable Diesel	kg	5.38E+06	5.38E+06	5.38E+06	5.26E+06	5.26E+06	5.26E+06

B.5 PROCESS LEVEL INVENTORY FOR MICROALGAL BIOFUEL PRODUCTION

The Eco-LCA model is developed based on a 2002 input-output (IO) model of the US economy. In this model, the US economy is aggregated into over 488 different economic sectors. In Eco-LCA the final demand (economic activity) in each of the economic sectors is translated into ecological and natural resource consumption. As such, the 2002 producer price for economic inputs used in algal biofuel production must be obtained to properly account for the consumption

of ecological resources in algal-fuel production. Table 39 provides the price data for economic inputs used in microalgal RD production.

Table 39. Price data for economic inputs/outputs for microalgal renewable diesel production

Economic Inputs and Outputs in Microalgal Renewable Diesel Production						
Material or Energy Input/Output	*Sector Name*	*NAICS Code*	*Year*	*Unit*	*$/Unit*	*Source*
Inputs						
Electricity	Electricity Power Generation	221100	2002	MJ	1.36E-02	ref[379]
Natural Gas	Natural Gas Distribution	221200	2002	m^3	1.42E-01	ref[380]
Aluminum Sulfate	All other basic inorganic chemical manufacturing	325188	2000	kg	2.97E-01	ref[381]
Urea	Fertilizer Manufacturing	325310	2002	kg	2.11E-01	ref[382]
Superphosphate (SSP)	Fertilizer Manufacturing	325310	2002	kg	2.44E-01	ref[382]
Potassium Chloride (KCl)	Fertilizer Manufacturing	325310	2002	kg	1.81E-01	ref[382]
PVC	Plastics Material and Resin Manufacturing	325211	1999	m^2	2.58E+00	ref[383]
Wastewater	Water, Sewage and Other Systems	221300	2003	m^3	2.94E-02	ref[384]
Hexane	Other Basic Organic Chemical Manufacturing	325190	2003	kg	5.57E-01	ref[385]
Hydrogen	Industrial Gas Manufacturing	325120	2010	kg	1.50E+00	ref[386]
Diesel	Petroleum Refineries	324110	1997	gal	5.75E-01	ref[378]
Diesel	Pipeline Transportation	486000	2006	gal	2.30E-02	ref[387]
Coproducts						
Animal Feed (soybean meal eq.)	Other animal food manufacturing	311119	2002	kg	1.84E-01	Note*
Electricity	Electricity Power Generation	221100	2002	MJ	1.36E-02	ref[379]
Biofertilzier (Urea eq.)	Fertilizer Manufacturing	325310	2002	kg	2.11E-01	ref[382]
Biofertilzier (SSP eq.)	Fertilizer Manufacturing	325310	2002	kg	2.44E-01	ref[382]
Heat (NG eq.)	Natural Gas Distribution	221200	2002	m^3	1.42E-01	ref[380]
Propane (LGP eq.)	Petroleum Refineries	324110	2002	kg	2.46E-01	ref[388]

*Price of algal derived animal feed was based off of the market value of soybean meal estimated from http://www.indexmundi.com/commodities/?commodity=soybean-meal&months=12

An inflation calculator is used when 2002 price data cannot be obtained [174]. The inflation ratio is provided in Table 40. Furthermore, the inflation calculator can be accessed in the following link: http://www.bls.gov/data/inflation_calculator.htm

Table 40. Inflation Ratio

Year	**Inflation Ratio** (Relative to 2002)
1997	1.12
1998	1.10
1999	1.08
2000	1.04
2001	1.02
2002	1.00
2003	0.98
2004	0.95
2005	0.92
2006	0.89
2007	0.87
2008	0.84
2009	0.84
2010	0.83

To obtain 2002 price data for economic inputs and outputs in microalgal RD production the market value of economic inputs was multiplied by the corresponding inflation ratio, the results are provided in Table 41

Table 41. 2002 Price data for economic inputs/outputs for microalgal renewable diesel production

Material or Energy Product	Sector Name	NAICS Code	Unit	$2002 /Unit
Inputs				
Electricity	Electricity and Power Generation	221100	MJ	1.36E-02
Natural Gas	Natural Gas Distribution	221200	m^3	1.42E-01
Aluminum Sulfate	All other basic inorganic chemical manufacturing	325188	kg	3.10E-01
Urea	Fertilizer Manufacturing	325310	kg	2.11E-01
SSP	Fertilizer Manufacturing	325310	kg	2.44E-01
KCL	Fertilizer Manufacturing	325310	kg	1.81E-01
PVC	Plastics Material and Resin Manufacturing	325211	m^2	2.79E+00
Wastewater	Water, Sewage and Other Systems	221300	m^3	2.87E-02
Hexane	Other Basic Organic Chemical Manufacturing	325190	kg	5.45E-01
Hydrogen	Industrial Gas Manufacturing	325120	kg	1.24E+00
Diesel	Petroleum Refineries	324110	gal	6.44E-01
Diesel	Pipeline Transportation	486000	gal	2.05E-02
Coproducts				
Animal Feed (soybean meal eq.)	Other animal food manufacturing	311119	kg	1.84E-01
Electricity	Electricity Power Generation	221100	MJ	1.36E-02
Biofertilzier (Urea eq.)	Fertilizer Manufacturing	325310	kg	2.11E-01
Biofertilzier (SSP eq.)	Fertilizer Manufacturing	325310	kg	2.44E-01
Heat (NG eq.)	Natural Gas Distribution	221200	m^3	1.42E-01
Propane (LPG eq.)	Petroleum Refineries	324110	kg	2.46E-01

The economic input(s) and output(s) are aggregated into their corresponding industrial sector(s), the results of data aggregation are provided in Table 42**.**

Table 42. Economic Activity ($ 2002) for industrial sectors used in microalgal renewable diesel production

Parameters	Microalgae RD - Baseline Scenarios			Microalgal RD - Improved Scenarios		
Sector Name	AF	AD	CHP	AF	AD	CHP
Inputs						
Electricity and Power Generation	1.82E+06	1.91E+06	1.82E+06	1.22E+06	1.31E+06	1.22E+06
Natural Gas Distribution	3.67E+06	3.81E+06	3.67E+06	5.10E+04	1.87E+05	5.10E+04
All other basic inorganic chemical manuf.	1.98E+06	1.98E+06	1.98E+06	1.98E+06	1.98E+06	1.98E+06
Fertilizer Manufacturing	2.09E+06	1.39E+06	2.09E+06	2.09E+06	1.39E+06	2.09E+06
Plastics Material and Resin Manufacturing	1.39E+06	1.39E+06	1.39E+06	1.39E+06	1.39E+06	1.39E+06
Water, Sewage and Other Systems	2.51E+05	2.51E+05	2.51E+05	2.51E+05	2.51E+05	2.51E+05
Other Basic Organic Chemical Manufacturing	2.83E+04	2.83E+04	2.83E+04	1.84E+04	1.84E+04	1.84E+04
Industrial Gas Manufacturing	2.13E+05	2.13E+05	2.13E+05	2.08E+05	2.08E+05	2.08E+05
Petroleum Refineries	1.70E+04	3.18E+03	2.73E+03	1.70E+04	3.12E+03	2.66E+03
Pipeline Transportation	5.41E+02	1.01E+02	8.67E+01	5.39E+02	9.91E+01	8.47E+01
Coproducts						
Other animal food manufacturing	5.19E+06	0.00E+00	0.00E+00	5.19E+06	0.00E+00	0.00E+00
Electricity Power Generation	0.00E+00	1.14E+06	1.07E+06	0.00E+00	1.14E+06	1.07E+06
Fertilizer Manufacturing	0.00E+00	1.91E+05	0.00E+00	0.00E+00	1.91E+05	0.00E+00
Natural Gas Distribution	0.00E+00	0.00E+00	8.06E+05	0.00E+00	0.00E+00	8.06E+05
Petroleum Refineries	7.81E+04	7.81E+04	7.81E+04	7.64E+04	7.64E+04	7.64E+04

B.6 ECO-LCA RESULTS FOR MICROALGAL RENEWABLE DIESEL

The EcoLCA model translates the economic activity in industrial sectors into natural resource consumption. EcoLCA quantifies the Energy, ICEC, and ECEC consumption per unit throughput of economic activity for a specific industrial sector. The Energy, ICEC, and ECEC to money ratios for the industrial sectors utilized in microalgal renewable diesel production are presented in Table 43.

Table 43. Energy, ICEC, and ECEC to price ($2002) ratios for industrial sectors

Sector Name	NAICS Code	[1]Energy/ $	[2]ICEC/ $	[3]ECEC/ $
Electricity and Power Generation	221100	1.30E+08	1.41E+08	1.02E+13
Natural Gas Distribution	221200	7.56E+06	8.08E+06	1.08E+12
All other basic inorganic chemical manufacturing	325188	2.80E+07	5.01E+07	1.48E+13
Fertilizer Manufacturing	325310	8.01E+07	8.59E+07	1.25E+13
Plastics Material and Resin Manufacturing	325211	9.36E+07	1.01E+08	9.61E+12
Water, Sewage and Other Systems	221300	1.69E+06	1.93E+06	3.33E+12
Other Basic Organic Chemical Manufacturing	325190	6.58E+07	7.12E+07	7.24E+12
Industrial Gas Manufacturing	325120	2.54E+07	3.27E+07	5.40E+12
Petroleum Refineries	324110	1.88E+07	1.99E+07	7.36E+08
Pipeline Transportation	486000	7.15E+06	7.74E+06	9.17E+08
Other animal food manufacturing	311119	2.12E+07	2.30E+07	5.35E+12

[1] Units – Non-renewable energy (joules) per unit 2002 dollar
[2] Units – Non-renewable exergy (joules) per unit 2002 dollar
[3] Units - Solar equivalent joules (sej) per unit 2002 dollar

Energy, ICEC, and ECEC consumption obtained via EcoLCA was calculated by multiplying the results from Table 42 with their corresponding Energy, ICEC, and ECEC to price ratio(s) given in Table 43. The results are provided in Table 44.

Table 44. Energy, ICEC, and ECEC consumption obtained via EcoLCA

Parameters	Microaglal RD - Baseline Scenarios			Microalgal RD - Improved Scenarios		
Coproduct Scenarios	AF	AD	CHP	AF	AD	CHP
Inputs						
Non-Renewable Energy[1]	6.26E+14	5.83E+14	6.26E+14	5.20E+14	4.77E+14	5.19E+14
Non-Renewable ICEC [2]	7.15E+14	6.69E+14	7.15E+14	6.01E+14	5.55E+14	6.00E+14
ECEC[3]	9.37E+19	8.61E+19	9.36E+19	8.36E+19	7.59E+19	8.35E+19
Coproducts						
Non-Renewable Energy[1]	1.12E+14	1.65E+14	1.47E+14	1.12E+14	1.65E+14	1.47E+14
Non-Renewable ICEC [2]	1.21E+14	1.78E+14	1.58E+14	1.21E+14	1.78E+14	1.58E+14
ECEC[3]	2.79E+19	1.42E+19	1.20E+19	2.79E+19	1.42E+19	1.20E+19

[1] Units – Non-renewable energy (joules) per unit 2002 dollar
[2] Units – Non-renewable exergy (joules) per unit 2002 dollar
[3] Units - Solar equivalent joules (sej) per unit 2002 dollar

B.7 DIRECT ECOLOGICAL GOODS AND SERVICES AND USE PHASE OF ENERGY/FUEL PRODUCTS IN MICROALGAL RENEWABLE DIESEL PRODUCTION

EcoLCA does not consider the use phase of energy and fuel products or direct ecological good and services that are consumed at the process scale. Therefore, data from the process scale must be added to the results obtained via EcoLCA.

B.7.1 Direct Ecological Goods and Services

Direct ecological goods and services (EGS) considered in algal RD production include solar insolation (sunlight), freshwater, and photosynthetic CO_2. The energy and material flows for direct EGS are provided in Table 45**.** Furthermore, the energy, exergy, and transformity of direct EGS are provided in Table 46**.**

Table 45. Direct Ecological Goods and Services in Microalgal RD production

Direct EGS	Unit	Microalgal RD Baseline Scenarios	Microalgal RD Improved Scenarios
Solar Insolation[1]	Joule	3.01E+15	3.01E+15
Solar Insolation (Metabolized)	Joule	6.03E+13	6.03E+13
Atmospheric Carbon[2]	Grams	1.59E+10	1.59E+10
Freshwater[2]	Grams	1.11E+13	1.10E+13

[1]ref [105]
[2]Based on process calculations

Table 46. Energy, Exergy, and Transformity of Direct EGS

Direct EGS	Unit	Energy (j) /Unit	Exergy (j) /Unit	Transformity (sej/unit)
Solar Insolation	joule	1	1	1
Photosynthetic CO_2	grams carbon	N/A	N/A	103992000
Freshwater	grams	N/A	4.94	202540

The energy, exergy, and emergy of Direct EGS used in microalgal RD production were calculated via multiplying the resources flows as expressed in Table 45 with their corresponding energy, exergy, and transformity given in Table 46**.** The results are provided in Table 47.

Table 47. Energy, Exergy, and Emergy of direct EGS in microalgal RD production

Parameters	Microalgal RD - Baseline Scenarios			Microalgal RD - Improved Scenarios		
Direct EGS	Energy*	Exergy*	Emergy	Energy*	Exergy*	Emergy
Solar Insolation	6.03E+13	6.03E+13	3.01E+15	6.03E+13	6.03E+13	3.01E+15
Photosynthetic CO2	N/A	N/A	1.65E+18	N/A	N/A	1.65E+18
Freshwater	N/A	5.47E+13	2.24E+18	N/A	5.42E+13	2.22E+18

*Only metabolized sunlight was considered for energy and exergy analysis

B.7.2 Use Phase of Energy and Fuel Products

The specific energy, exergy, and transformity of fuel and energy products used in biofuel production are provided in Table 48. Futher, it is assumed that the transformity of diesel and LPG is equivalent to gasoline.

Table 48. Energy, Exergy, and Transformity of Fuel and Energy Products

Parameters	Unit	Density	Unit	Energy	Exergy	Unit	Transformity
Gasoline	kg/gal	2.78E+00	MJ/kg	[2]44.8	[2]48.3	sej/j	[6]111000
Diesel	kg/gal	3.18E+00	MJ/kg	[2]43.3	[2]44.4	sej/j	*111000
LPG	kg/gal	2.05E+00	MJ/kg	[2]47.3	[2]48.8	sej/j	*111000
Natural Gas	kg/scf	1.88E-02	MJ/kg	[3]55.1	[2]50.7	sej/j	[6]80600
Electricity[1]	-	-	MJ/MJ	2.4	2.8	sej/j	165542
Coal	-	-	MJ/kg	[3]20.6	[4]29	sej/j	[6]67200
Crude Oil	-	-	MJ/kg	[3]42.686	[5]46.2	sej/j	[6]90700
Nuclear	-	-	TJ/kg-U235	[7]79.5	[7]75.0	sej/g	[6]1880000000
Hydro	-	-	J/J	1	1	sej/j	[6]46643
Wind	-	-	J/J	1	1	sej/j	[6]2510
Geothermal	-	-	J/J	1	1	sej/j	[6]10200

[1]EcoLCA does not consider the feedstock energy consumed in electricity production (i.e. the combustion of coal, natural g, etc.). The energy, exergy, and transformity of electricity was developed based on the 2002 U.S. average electricity mix and electricity generation efficiency. (See below for specific details)
[2]ref[18]
[3]ref[269]
[4]ref[389]
[5]ref[158]
[6]ref [180]
[7]ref [390]
*The transformity of Diesel and LPG was assumed to be equivalent to gasoline **[378]**

To determine the energy, exergy, and emergy of natural resources consumed in the production of 1 MJ of electricity, it was first necessary to quantify the high and low estimates for electricity conversion by primary energy resource type and quantify the U.S. 2002 electricity generation mix. This data is provided in Table 49**.**

Table 49. 2002 U.S. Electricity generation mix and electricity generation conversion efficiencies

Primary Energy Resources	2002 U.S. Electricity Generation Mix (%)	Conversion Efficiency[1] % (Upper bound)	Conversion Efficiency[1] % (Lower bound)	Avg,
Coal	52.0	47	39	43
Crude Oil	2.5	44	38	41
Natural Gas	16.5	-	-	39
Nuclear	21.0	36	33	34.5
Hydroelectricity	7.3	95	90	92.5
Wind	0.3	-	-	35
Geothermal	0.4	-	-	15

[1] ref[253]

The amount of each primary resources (J) required to produce 1 J of electricity was calculated by multiplying by the inverse of the conversion efficiency, the results are shown in Table 50. The results should be interpreted as follows: on average it takes 2.3 J of coal to produce 1 J of coal-electricity. Additionally, it takes approximately 2.5 J of crude oil to produce 1 J of crude-oil derived electricity. The same interpretation applies to the other primary energy resources. The amount of each primary resource required to produce 1 J of the 2002 avg. electricity mix is given by the weighted average column shown in Table 50.

Table 50. Amount of each primary resource (J) required to produce 1 J of electricity based on the 2002 avg. electricity mix

Primary Energy Resource	Lower Bound	Upper Bound	Average	Weighted Average
Coal	2.6	2.1	2.3	1.22
Crude Oil	2.6	2.3	2.5	0.06
Natural Gas	-	2.6	2.6	0.42
Nuclear	3.0	2.8	2.9	0.61
Hydroelectricity	1.1	1.1	1.1	0.08
Wind	-	2.9	2.9	0.01
Geothermal	-	6.7	6.7	0.03

Direct primary energy resources consumed in the production of 1 J of electricity based on the 2002 U.S. electricity mix was calculated via multiplying the weighted average as obtained in Table 50 with the specific exergy and transformity values shown in Table 48**.** The results are provided in Table 51.

Table 51. Direct primary energy resources consumed in the production of 1 J of electricity based on the 2002 U.S. electricity mix. Consumption is reported in terms of energy, exergy, and emergy.

Parameters	Coal	Crude Oil	NG	Nuclear	Hydro	Wind	Geothermal	Total
Energy (J)	1.22E+00	6.13E-02	4.23E-01	6.10E-01	7.90E-02	8.57E-03	2.67E-02	2.43
Exergy (J)	1.56E+00	6.64E-02	4.53E-01	5.75E-01	7.90E-02	8.57E-03	2.67E-02	2.77
Emergy (sej)	1.05E+05	6.02E+03	3.65E+04	1.44E+04	3.68E+03	2.15E+01	2.72E+02	1.66E+05*

*Based on the analysis, the transformity of electricity is approximately 1.66 x 10^5 sej/J-electricity for the 2002 U.S.

The use phase of energy & fuel products in microalgal RD production were accounted for via multiplying the resources flows of electricity, natural gas, diesel, propane, etc. as developed in Table 38 with their corresponding specific energy, exergy, and transformity values given in in Table 48, the results are provided in Table 52.

Table 52. Use phase of energy/fuel products in miroalgal RD production

Parameters	**Microalgal RD - Baseline Scenarios**			**Microalgal RD - Improved Scenarios**		
Coproduct Scenarios	AF	AD	CHP	AF	AD	CHP
Inputs						
Non-Renewable Energy	1.32E+15	1.37E+15	1.32E+15	2.26E+14	2.75E+14	2.23E+14
Non-Renewable Exergy	1.30E+15	1.35E+15	1.30E+15	2.64E+14	3.13E+14	2.61E+14
Emergy	9.82E+19	1.02E+20	9.78E+19	1.68E+19	2.04E+19	1.65E+19
Coproducts						
Non-Renewable Energy	1.50E+13	2.10E+14	4.18E+14	1.47E+13	2.09E+14	4.18E+14
Non-Renewable Exergy	1.55E+13	2.38E+14	4.35E+14	1.51E+13	2.46E+14	4.35E+14
Emergy	3.52E+16	1.39E+19	2.99E+19	3.44E+16	1.44E+19	2.99E+19

B.7.3 Energy and Exergy of Microalgal Biofuels

Szargut 2005 [391] derived an empirical relationship between the specific exergy of a liquid technical fuel, its lower heating value, and its C,H,O, S composition provided in equation (26)

$$\beta = 1.041 + 0.1728\frac{Z_{H_2}}{Z_C} + 0.0432\frac{Z_{O_2}}{Z_C} + 0.2169\frac{Z_S}{Z_C}(1 - 2.0628\frac{Z_{H_2}}{Z_C}) \quad (26)$$

Where Z_X is the mass fraction of the X^{th} element in the liquid technical fuel. The exergy of the liquid technical fuel is given by equation (27)

$$\text{Exergy}_{\text{fuel}} = \text{LHV} * \beta \quad (27)$$

The lower heating value for renewable diesel II and biodiesel was taken from GREET [269] and is provided in Table 53.

Table 53. Fuel Properties of Renewable Diesel and Biodiesel

Transportation Fuel	% C	% H	% O	% S	LHV (MJ/kg-fuel)	β	Exergy (MJ/kg-fuel)
Renewable Diesel	87.1	12.9	0	0	43.97	1.066	46.90
Biodiesel	76.2	12.6	11.2	0	37.52	1.076	40.37

B.8 THERMODYNAMIC RETURN ON INVESTMENT FOR MICROALGAL RENEWABLE DIESEL

Total energy, ICEC, and ECEC consumption is obtained via combining the results from EcoLCA (Table 44) with process level data (Table 47 and Table 52). Equations for energy, exergy, and emergy return on investment are provided in Chapter 3. It is important to note that only processing and co-product flows are considered in the determination of return on investment, feedstock energy in not included (i.e. for microalgal biofuels direct sunlight is not included). The results of the analysis for microalgal renewable diesel are graphically represented via Figure 31.

Table 54. Thermodynamic return on investment for microalgal renewable diesel production based on energy, ICEC, and ECEC

Parameters	**Microalgal RD - Baseline Scenarios**			**Microalgal RD - Improved Scenarios**		
Coproduct Scenarios	AF	AD	CHP	AF	AD	CHP
Inputs = (EcoLCA + Use Phase + Direct EGS*)						
Non-Renewable Energy (J)	1.95E+15	1.96E+15	1.95E+15	7.45E+14	7.52E+14	7.42E+14
Non-Renewable ICEC (J)	2.02E+15	2.02E+15	2.01E+15	8.64E+14	8.68E+14	8.61E+14
ECEC (Sej)	1.96E+20	1.92E+20	1.95E+20	1.04E+20	1.00E+20	1.04E+20
Coproducts = (EcoLCA + Use Phase)						
Non-Renewable Energy (J)	1.27E+14	3.75E+14	5.65E+14	1.26E+14	3.74E+14	5.64E+14
Non-Renewable ICEC (J)	1.36E+14	4.24E+14	5.93E+14	1.36E+14	4.24E+14	5.93E+14
ECEC (Sej)	2.79E+19	2.86E+19	4.19E+19	2.79E+19	2.86E+19	4.19E+19
Difference = (Inputs-Coproducts)						
Non-Renewable Energy (J)	1.82E+15	1.58E+15	1.38E+15	6.19E+14	3.78E+14	1.78E+14
Non-Renewable ICEC (J)	1.88E+15	1.59E+15	1.42E+15	7.28E+14	4.44E+14	2.68E+14
ECEC (Sej)	1.68E+20	1.63E+20	1.54E+20	7.63E+19	7.16E+19	6.20E+19
Renewable Diesel						
Energy (J)	2.36E+14	2.36E+14	2.36E+14	2.31E+14	2.31E+14	2.31E+14
Exergy (J)	2.52E+14	2.52E+14	2.52E+14	2.47E+14	2.47E+14	2.47E+14
Exergy x τ_{max} (Sej)	2.80E+19	2.80E+19	2.80E+19	2.74E+19	2.74E+19	2.74E+19
Return on Investment = (Renewable Diesel / Difference)						
EROI	0.13	0.15	0.17	0.37	0.61	1.30
ExROI	0.13	0.16	0.18	0.34	0.55	0.92
EmROI[1]	0.17	0.17	0.18	0.36	0.38	0.44

[1]EmROI = $\frac{Exergy_{RD} \; x \; \tau_{max}}{Inputs \; ECEC - Coproduct \; ECEC}$, where $\boldsymbol{\tau_{max}}$ is the transformity of petroleum diesel ~ 1.11x10^5 sej/j.

[*]The feedstock energy (i.e. direct sunlight) is not considered in the analysis of ROI.

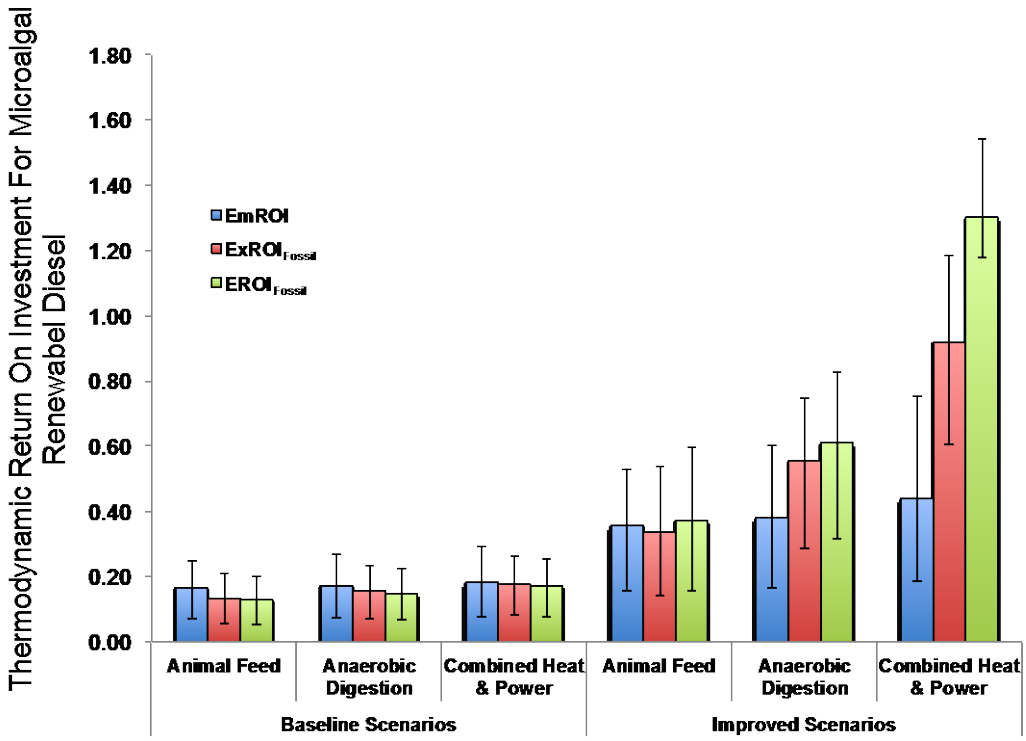

Figure 31. Thermodynamic Return on Investment (ROI) for the microalgal RD production under several coproduct scenarios for the de-oiled algal biomass

B.9 ECEC SUSTAINABILITY PERFORMANCE METRICS FOR MICROALGAL RENEWABLE DIESEL

Several ECEC-based metrics including yield ratio, Environmental Loading Ratio, Yield-to-Load Ratio, and Renewability (%) were used for quantifying the sustainability and performance of microalgae biofuel production. Detailed descriptions and definitions of these metrics are provided in Chapter 3. Traditional emergy analysis forbids allocation amongst coproducts [378]. Thus, for ECEC based performance and sustainability metrics, allocation/co-product credits were

not considered. A summary table of the ECEC sustainability/performance metrics for microaglal RD are provided in Table 55. Ecological resource intensity plots for baseline and improved microaglal RD fuel pathways are provided in Figure 32.

Table 55. ECEC sustainability and Performance Metrics for Microalgal Renewable Diesel

Parameters	**Microalgal RD - Baseline Scenarios**			**Microalgal RD - Improved Scenarios**		
Coproduct Scenarios	AF	AD	CHP	AF	AD	CHP
Total ECEC = (EcoLCA + Use Phase + Direct EGS)	1.96E+20	1.92E+20	1.95E+20	1.04E+20	1.00E+20	1.04E+20
Direct EGS ECEC = (ECEC solar insolation + ECEC Water +ECEC photosynthetic CO_2)	3.90E+18	3.90E+18	3.90E+18	3.88E+18	3.88E+18	3.88E+18
Non-Renewable ECEC	1.89E+20	1.85E+20	1.88E+20	9.77E+19	9.40E+19	9.73E+19
Renewable ECEC	7.09E+18	6.72E+18	7.09E+18	6.61E+18	6.24E+18	6.61E+18
ECEC Performance Metrics						
Yield Ratio[1]	1.02	1.02	1.02	1.04	1.04	1.04
Environmental Loading Ratio[2]	26.62	27.53	26.57	14.78	15.06	14.72
Yield-to-Load Ratio[3]	0.04	0.04	0.04	0.07	0.07	0.07
Renewability (%)[4]	3.62	3.51	3.63	6.34	6.23	6.36

[1]ECEC Yield Ratio is calculated as EYR = (Total ECEC / Indirect ECEC).
[2]Environmental Loading Ratio is calculated as ELR = (Non Ren ECEC / (Ren ECEC))
[3]Yield to Loading Ratio is calculated as YLR = (EYR / ELR)
[4]Renewablity Index % = (Ren ECEC / (Total ECEC)) x 100

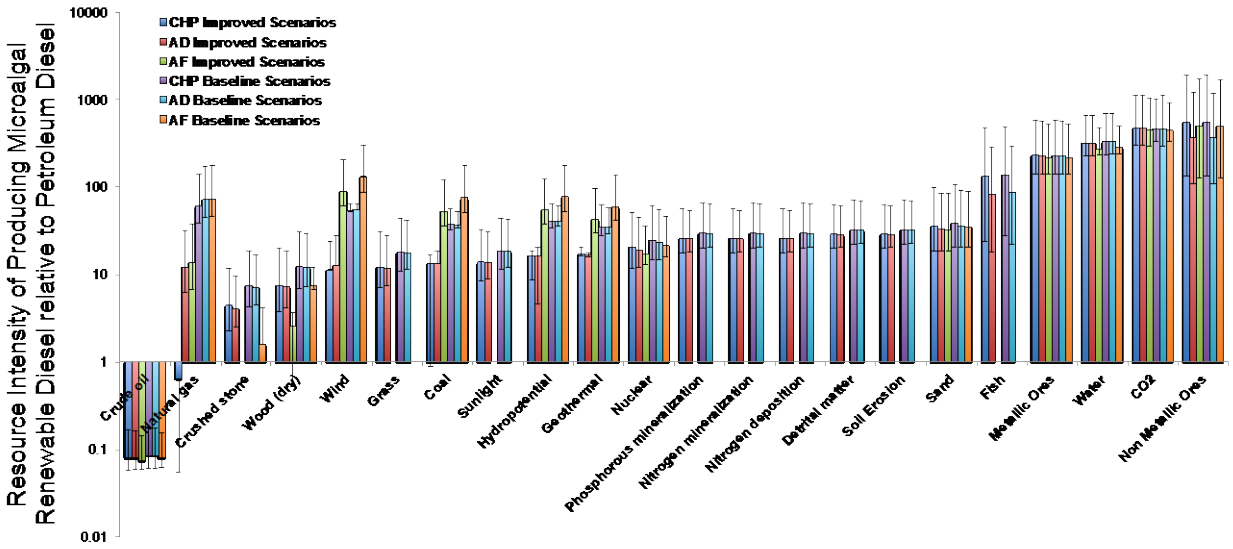

Figure 32. Ecological resource intensity of producing microalgal RD relative to petroleum diesel. Resource intensity ratios were developed via taking the ratio of ECEC of resources required to produce one mega-joule (MJ) of RD to the ECEC required to produce one MJ of PD. Coproduct(s) were accounted for via system boundary expansion, i.e. ECEC from coproduct(s) were subtracted from total resource use. Some columns are not shown on the logarithmic graph due to negative value(s) that occur as a result of displacement.

B.10 PROCESS INVENTORIES FOR PETROLEUM DIESEL

Process inventory for petroleum diesel was taken from Baral et al 2009 [378] and is provided in Table 56.

Table 56. Process Inventory for Petroleum Diesel

Inputs from the economy	**Units**	**Value**	**1997 $**	**Inflation Ratio**	**2002 $**
Crude Oil Transport	gal	2.08E+07	2.33E+05	1.12	2.61E+05
Diesel Production	***Units***	***Value***	***1997 $***	***Inflation Ratio***	***2002 $***
Crude Oil	gal	2.08E+07	1.02E+07	1.12	1.14E+07
LPG	gal	1.56E+04	5.78E+03	1.12	6.47E+03
Natural Gas	SCF	6.09E+07	2.18E+05	1.12	2.44E+05
Residual Fuel Oil	gal	8.26E+03	3.30E+03	1.12	3.70E+03
Still Gas	gal	8.92E+05	2.43E+05	1.12	2.72E+05
Petroleum Coke	gal	3.36E+05	4.19E+04	1.12	4.69E+04
Diesel	gal	2.83E+03	1.61E+03	1.12	1.80E+03
Coal	kg	2.70E+05	5.83E+03	1.12	6.53E+03
Electricity	kWh	3.26E+06	1.48E+05	1.12	1.66E+05
Steel in Refinery	kg	1.04E+04	7.40E+03	1.12	8.29E+03
Electricity (wastewater treatment)	kWh	1.92E+05	8.71E+03	1.12	9.76E+03
Rail Transportation for coal	kg	2.70E+05	2.97E+03	1.12	3.33E+03
Pipeline transportation of diesel	gal	4.00E+06	7.36E+04	1.12	8.24E+04
Outputs	***Units***	***Value***	***1997 $***	***Inflation Ratio***	***2002 $***
Diesel	gal	4.00E+06	N/A	N/A	N/A

B.11 ECONOMIC INPUTS FOR PETROLEUM DIESEL PRODUCTION

Aggregating the results from Table 56, the total economic activity (i.e. economic throughput) for industrial sectors used in the production of petroleum diesel is provided in Table 57.

Table 57. Economic activity ($2002) for industrial sectors used in petroleum diesel production

Sector Name	Sector Code	Economic Activity ($2002)
Pipeline Transportation	486000	3.43E+05
Oil and Gas Extraction	211000	1.14E+07
Petroleum Refineries	324110	3.31E+05
Natural gas distribution	221200	2.51E+05
Electric Power and Generation	221100	1.76E+05
Iron and Steel Mill	331110	8.29E+03
Rail Transportation	482000	3.33E+03

B.12 ECO-LCA, USE-PHASE, AND DIRECT EGS FOR PETROLEUM DIESEL PRODUCTION

Table 58. Direct Ecological Goods and Services as well as process fuel/energy consumption in petroleum diesel production

Direct Ecological Goods and Services	Units	Value	Energy (J)	Exergy (J)	Emergy (sej)
Crude Oil	gal	2.08E+07	2.84E+15	3.08E+15	2.79E+20
Inputs from the economy	***Units***	***Value***	***Energy (J)***	***Exergy (J)***	***Emergy (sej)***
LPG	gal	1.56E+04	1.51E+12	1.56E+12	1.73E+17
Natural Gas	SCF	6.09E+07	6.31E+13	5.80E+13	4.68E+18
Residual Fuel Oil	gal	8.26E+03	1.22E+12	1.31E+12	1.45E+17
Still Gas	gal	8.92E+05	1.21E+14	1.34E+14	1.49E+19
Petroleum Coke	gal	3.36E+05	4.84E+13	5.08E+13	5.64E+18
Diesel	gal	2.83E+03	3.90E+11	4.00E+11	4.44E+16
Coal	kg	2.70E+05	5.56E+12	7.83E+12	5.26E+17
Electricity	kWh	3.26E+06	2.85E+13	3.25E+13	1.94E+18
Electricity (wastewater treatment)	kWh	1.92E+05	1.68E+12	1.91E+12	1.14E+17
Outputs	***Units***	***Value***	***Energy (J)***	***Exergy (J)***	***Emergy (sej)***
Diesel	gal	4.00E+06	5.51E+08	5.65E+08	6.27E+19

Table 59. Results from EcoLCA and process analysis for the production of 4.0 x 10^6 gallons of petroleum diesel

Parameters	Use Phase + Direct EGS*	EcoLCA Results
Non-renewable Energy	2.70E+14	1.98E+14
Non-renewable Exergy	2.87E+14	2.10E+14
Emergy	2.82E+19	2.40E+19

*Does not consider feedstock energy, (i.e. the energy, exergy, or emergy of crude oil).

B.13 THERMODYNAMIC RETURN ON INVESTMENT AND ECEC BASED PERFORMANCE METRICS FOR PETROLEUM DIESEL

Table 60. Thermodynamic Return on Investment and ECEC based performance metrics for Petroleum Diesel production

Thermodynamics Return On Investment Metrics for Petroleum Diesel			
Parameters	***NR Energy***	***NR Exergy***	***Emergy***
EcoLCA	1.98E+14	2.10E+14	2.40E+19
Use Phase	2.70E+14	2.87E+14	2.82E+19
Total = EcoLCA+Use Phase+Direct EGS[1]	4.68E+14	4.98E+14	5.22E+19
Market Allocation[2]	9.93E+13	1.06E+14	1.11E+19
Mass Allocation[3]	8.94E+13	9.51E+13	9.97E+18
Output - Petroleum Diesel	5.51E+14	5.65E+14	6.27E+19
Thermodynamic Return On Investment (mass)	6.16	5.94	6.29
Thermodynamic Return On Investment (market)	5.55	5.35	5.66
Thermodynamic Return On Investment (avg.)	5.86	5.65	5.98
ECEC performance and sustainability metrics for Petroleum Diesel			
Total ECEC = (EcoLCA+Use Phase+Direct EGS)[2]	3.31E+20		
Direct EGS = ECEC crude oil	2.79E+20		
Non-Renewable ECEC	3.31E+20		
Renewable ECEC	4.35E+17		
ECEC Yield Ratio (EYR)	6.34		
Environmental Loading Ratio (ELR)	760.19		
Yield to Load Ratio (YLR)	0.01		
Renewability Index (%)	0.13		

[1]The feedstock energy (i.e. crude oil) is not considered in the analysis of ROI.
[2]The feedstock energy (crude oil) is considered in evaluation of ECEC performance indicators.
[2]In market allocation 21.1% of total environmental impacts are allocated to petroleum diesel
[3]In mass allocation 19.1% of total environmental impacts are allocated to petroleum diesel

B.14 THERMODYNAMIC RETURN ON INVESTMENT, ECEC BASED PERFORMANCE METRICS, AND ECOLOGICAL RESOURCE INTENSITY FOR MICROALGAL BIODIESEL PRODUCTION

Analysis was conducted to determine the thermynamic ROI and ECEC performance metrics for microalgal derived biodiesel (BD). The results of the analysis are provided in Table 61. Additional results showing the ecological resource intensity of microalgal biodiesel production (relative to petroleum diesel) is provided in Table 61.

Table 61. Thermodynamic Return on Investment and ECEC based performance metrics for Microalgal Biodiesel

	Microalgal BD - Baseline Scenarios			**Microalgal BD - Improved Scenarios**		
Coproduct Scenarios	AF	AD	CHP	AF	AD	CHP
$EROI_{fossil}$	0.13	0.17	0.17	0.37	0.61	1.28
$ExROI_{fossil}$	0.14	0.16	0.18	0.34	0.56	0.93
EmROI	0.18	0.15	0.18	0.37	0.40	0.46
Renewability (%)	3.86	3.45	3.57	6.29	6.18	6.31
EYR	1.02	1.02	1.02	1.04	1.04	1.04
ELR	26.18	27.96	26.99	14.90	15.19	14.84
YLR	0.04	0.04	0.04	0.07	0.07	0.07

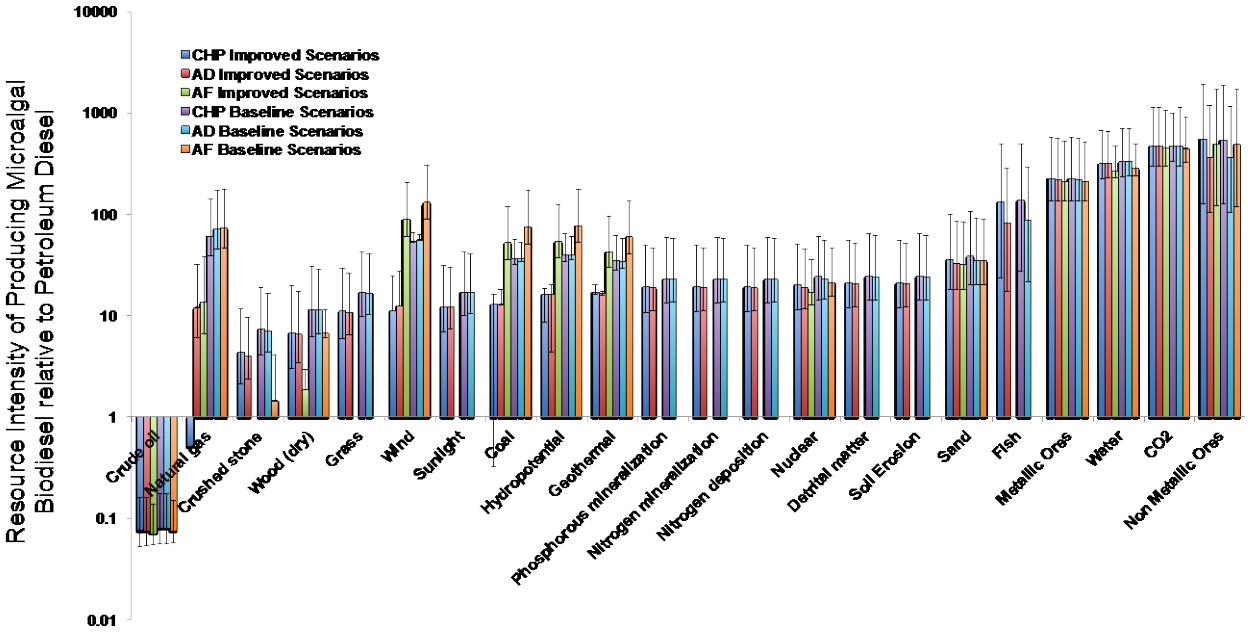

Figure 33. Ecological resource intensity of producing microalgal BD relative to petroleum diesel. Resource intensity ratios were developed via taking the ratio of ECEC of resources required to produce one mega-joule (MJ) of BD to the ECEC required to produce one MJ of PD. Coproduct(s) were accounted for via system boundary expansion, i.e. ECEC from coproduct(s) were subtracted from total resource use. Some columns are not shown on the logarithmic graph due to negative value(s) that occur as a result of displacement.

APPENDIX C

SUPPORTING INFROMATION FOR BIOFUELS VIA FAST PYROLYSIS OF PERENNIAL GRASSES: A LIFE CYCLE EVALUATION OF ENERGY CONSUMPTION AND GREENHOUSE GAS EMISSIONS

C.1 MODEL DEVELOPMENT

A hybrid life cycle model was developed to determine the environmental sustainability of fast pyrolysis biofuel production via coupling a detailed agricultural model with Aspen simulation and life cycle assessment. The hybrid model provides detailed process level material, energy, and emissions flows for fast pyrolysis and upgrading of bio-oil from switchgrass and/or miscanthus feedstock. Life cycle impact assessment (LCIA) is performed on the life cycle inventory (LCI) data obtained from the hybrid model. Uncertainty in the analysis is propagated via monte-carlo simulation, and used to determine bounds for sustainability criteria such as Energy Return On Investment (EROI) and life cycle GHG emissions. Aspen Plus version V8.6 was used to simulate the thermochemical conversion of lignocellulosic biomass to renewable transportation fuel. The biofeedstocks (Switchgrass and Miscanthus), biochar, and ash were defined in the simulation as non-conventional components, based on their Ultimate, Proximate, and Sulfanal analysis. The Peng-Robinson property method was used in the simulation. Information for some of the bio-oil

components produced via fast pyrolysis is not available in commercial Aspen Plus database(s); thermochemical properties for these components are estimated via the built-in Aspen property estimator based on their chemical structure (i.e. imported MOL File) and any available thermochemical and physical property data. It is important to note that combustion of biochar/ash as well as light hydrocarbons via CHP is not modeled in the Aspen simulation environment, but instead based on side calculations using reported estimates for commercial CHP electricity and heating conversion efficiencies. Additionally, loss of bio-oil due to catalyst coking is manually adjusted outside of the simulation environment.

C.2 SUSTAINABILITY METRICS

The carbon footprint was calculated via multiplying the material and energy consumption, as well as emissions flows for each unit process in the production chain by their corresponding impact factors to convert to a common unit of CO_2 equivalence (CO_2e) evaluated over a 100-year timeframe. The carbon footprint for biofuel production was evaluated as the sum of direct and indirect CO_2e emissions that occur throughout the supply chain. Negative carbon credits are given to CO_2 deposition from the atmosphere (Biogenic CO_2), and may also be attributed to coproducts generated in the system (i.e. electricity, etc). Combustion of biofuel and bioenergy products was based on stoichiometry and assumes that all carbon in said products is converted to CO_2. Definitions for EROI and carbon footprint under the differing allocation schemes and co-product scenarios are provided below.

Table 62. Key Parameters in the calculation of EROI and Life Cycle GHG Emissions

Parameter	Symbol	Units	Notes
Biofuel Energy	$E_{biofuel}$	MJ	$(LHV_{biofuel})*(Mass_{biofuel})$
Coproduct Electricity	C_{Elec}	MJ	Based on CHP Electrical conversion efficiency. $C_{Elec} = C_{Elec,Exp} + C_{Elec,Recycle}$
Electricity Export	$C_{Elec,Exp}$	MJ	If Coproduct Electricity (C_{Elec}) exceeds Process Electricity Requirements (P_{Elec}), surplus electricity is exported offsite and displaces the U.S. average electricity mix. Electricity Export $(C_{elec,Exp}) = (C_{Elec}-P_{Elec})$.
Electricity Recycle	$C_{Elec,Recycle}$	MJ	Coproduct electricity that is used onsite to meet process electricity utility, $C_{Elec,Recycle} \leq P_{Elec}$
Coproduct Heat	C_{Heat}	MJ	Based on CHP Heat conversion efficiency. Only usable heat is considered (i.e. $C_{Heat,Recycle} \leq P_{Heat}$).
Process Electricity	P_{Elec}	MJ	Based on Elec. Utility from Hybrid model
Process Heat	P_{Heat}	MJ	Based on Heat Duty from ASPEN simulation
Primary Energy Impact Factor - Electricity	$IF_{PE,Elec}$	MJ Primary Fossil Energy/MJ-Electricity	Based on data obtained from life cycle databases
Primary Energy Impact Factor - Heat	$IF_{PE,Heat}$	MJ Primary Fossil Energy/MJ-Heat	Based on data obtained from life cycle databases
Global Warming Potential Impact Factor - Electricity	$IF_{GHG,Elec}$	gCO_2e./MJ-Electricity	Based on data obtained from life cycle databases
Global Warming Potential Impact Factor - Heat	$IF_{GHG,Heat}$	gCO_2e./MJ-Heat	Based on data obtained from life cycle databases
Primary fossil energy for all other material, energy, and emissions flows	PE_{Misc}	MJ Primary Fossil Energy	Primary Fossil Energy consumption for all material and energy flows (excluding process heating and electrical utility)
Life Cycle GHG emissions for all other material, energy, and emissions flows	GHG_{Misc}	gCO_2e	Life cycle GHG emissions for all material, energy, and emissions flows (excluding process heating, electrical utility)
GHG sequestration from Biochar	GHG_{Char}	gCO_2e	Based on carbon content (C%) of biochar, as well as fraction of carbon remitted to atm. as CO_2

$$EROI_{Disp} = \frac{E_{biofuel}}{[(PE_{Misc})+IF_{PE,Heat}*(P_{Heat}-C_{Heat})+IF_{PE,Elec}*(P_{Elec}-C_{Elec,Recycle})]-[IF_{PE,Elec}*(C_{Elec,Exp})]} \quad (28)$$

$$EROI_{Alloc} = \frac{E_{biofuel}}{[(PE_{Misc})+IF_{PE,Heat}*(P_{Heat}-C_{Heat})+IF_{PE,Elec}*(P_{Elec}-C_{Elec,Recycle})]*[\frac{E_{biofuel}}{E_{biofuel}+C_{Elec,Exp}}]} \quad (29)$$

$$GHG_{Disp,SA} = \frac{[(GHG_{Misc})+IF_{GHG,Heat}*(P_{Heat}-C_{Heat})+IF_{GHG,Elec}*(P_{Elec}-C_{Elec,Recycle})-GHG_{Char}]-[IF_{GHG,Elec}*(C_{Elec,Exp})]}{E_{biofuel}} \quad (30)$$

$$GHG_{Disp,BE} = \frac{[(GHG_{Misc})+IF_{GHG,Heat}*(P_{Heat}-C_{Heat})+IF_{GHG,Elec}*(P_{Elec}-C_{Elec,Recycle})]-[IF_{GHG,Elec}*(C_{Elec,Exp})]}{E_{biofuel}} \quad (31)$$

$$GHG_{Alloc,SA} = \frac{\left[(GHG_{Misc}) + IF_{GHG,Heat} * (P_{Heat} - C_{Heat}) + IF_{GHG,Elec} * (P_{Elec} - C_{Elec,Recycle}) - GHG_{Char}\right] * \left[\frac{E_{biofuel}}{E_{biofuel} + C_{Elec,Exp}}\right]}{E_{biofuel}} \quad (32)$$

$$GHG_{Alloc,BE} = \frac{\left[(GHG_{Misc}) + IF_{GHG,Heat} * (P_{Heat} - C_{Heat}) + IF_{GHG,Elec} * (P_{Elec} - C_{Elec,Recycle})\right] * \left[\frac{E_{biofuel}}{E_{biofuel} + C_{Elec,Exp}}\right]}{E_{biofuel}} \quad (33)$$

C.3 CULTIVATION AND HARVESTING: MISCANTHUS AND SWITCHGRASS BIOFEEDSTOCK

Distributions for miscanthus yields were estimated based on values of dry yield reported in nine peer-reviewed studies and field trials spanning 20 different cultivation locations, see Table 63.

Table 63. Reported Growth Rates for Miscanthus Feedstock

Location	Year	Age of Stand (yrs)	Yield (dry Mg/ha)	Source
Dekalb, IL (north)	2004–2011	3–5	16.3	[a,*]Heaton et al. [207]
Urbana, IL (central)	2004–2011	3–5	31.1	[a,*]Heaton et al. [207]
Dixon Springs, IL (south)	2004–2011	3–5	30	[a,*]Heaton et al. [207]
Booneville, AK	2005	2	5.9	[*]Adapted from Burner et al. [244]
Troy, KS	2007	2	13.7	[b,*]Propheter et al. [245]
Manhattan, KS	2007	2	11.8	[b,*]Propheter et al. [245]
Gainesville, FL	2009	2	6.2	[*]Sollenberger et al.
Ona, FL	2009	2	4.5	[*]Sollenberger et al.
Belle Glade, FL	2009	2	10.8	[*]Sollenberger et al.
Urbana, IL	2009–2011	2–4	13.1	[c,*]Maughan et al. [221]
Lexington, KY	2009–2011	2–4	18.4	[c,*]Maughan et al. [221]
Mead, NE	2009–2011	2–4	24.7	[c,*]Maughan et al. [221]
Adelphia, NJ	2009–2011	2–4	15.1	[c,*]Maughan et al. [221]
Gretna, VA	2011	2	9.4	[c,*]Maughan et al. [221]
Valle Crucis, NC	2014	2	16.95	Teat et al. [246]
Mills River, NC	2014	2	15.57	Teat et al. [246]
Urbana, IL	2012	2	15.9	[+]Behnke et al. [219]
Mills River, NC	2014	3-4	17.7-19.0 (avg 18.35)	[+]Palmer et al. [222]
Wallace, NC	2014	3-4	20.3-21.3 (avg 20.8)	[+]Palmer et al. [222]
Burneyville, OK	2012	3	6.0	[+]Kering et al. [220]

[*]Adopted from ref [217]

[+]Adopted from ref [246]

[a]Yields are the average of four replicates at each site. Miscanthus giganteus was not fertilized. Yield averages include unpublished 2007–2011 production

[b]Variably fertilized in both 2007 and 2008

[c]Yields are the average of plots treated with three nitrogen levels (0, 60, 120 kg N $ha^{-1}year^{-1}$) at each site. Yield averages include unpublished 2011 production

Table 64. Fertilizer Application Rates for Miscanthus

	Units	DEFRA (2001)[392]	Christian et al. (2008)[215]	Styles et al. (2008)[393]	Smeets et al. (2009)[394]	Fazio et al. (2011)[395]
N	g dry-ton^{-1}	3,857	3,322	4,093	2,630	3,681
P	g dry-ton^{-1}	482	276	815	526	581
K	g dry-ton^{-1}	4,163	3,883	4,093	5,697	2,939

Probability distribution functions for switchgrass yields were developed based on the Global Switchgrass database [227], which contains over 1190 observations from 39 field trials conducted across the United States [[228-243].

Table 65. Fertilizer Application Rates for Switchgrass

	Units	Guretzky et al. (2011)[347]	Bai et al. (2010)[396]	Parrish and Fike (2005)[397]
N	g dry-ton^{-1}	8,000	7,700	6,300
P	g dry-ton^{-1}	50	150	0
K	g dry-ton^{-1}	200	300	0

Table 66. Norms for diesel use in crop production (Dn) compared to values found in the referenced literature or monitored on private farms; data is representative of common farming practices

Operation	Unit	*Dn* norm	Literature
			Low-High
Tilling and sowing			
Ploughing (21 cm), spring	L ha^{-1}	20.0	8.4-32.7
Ploughing (21 cm), autumn	L ha^{-1}	23.0	8.4-32.7
Soil Compactification	L ha^{-1}	2.0	1.8
Seedbed harrowing, light	L ha^{-1}	4.0	2.2-4.7
Seedbend harrowing, heavy	L ha^{-1}	6.0	4.9-16.8
Rolling	L ha^{-1}	2.0	1.8
Sowing	L ha^{-1}	3.0	0.9-21.6
Stubble cultivation	L ha^{-1}	7.0	2.8-30.9
Fertilizing and liming			
Spreading and loading manure	L $tonne^{-1}$	0.6	0.4-1.8
Spreading slurry	L $tonne^{-1}$	0.3	0.2-1.1
Spreading fertilizer	L ha^{-1}	2.0	0.9-4.7
Liming	L $ha^{-1}year^{-1}$	1.5	
Plant protection			
Pesticide spraying	L ha^{-1}	1.5	0.8-1.7
Weed Harrowing	L ha^{-1}	2.0	1.5-2.4
Row Listing	L ha^{-1}	3.0	3.0-4.9
Harvesting and Baling			
Combine harvesting	L ha^{-1}	14.0	7.0-19.0
Sugar beet harvesting	L ha^{-1}	17.0	8.4-22.0
Cutting, sugar beet top	L ha^{-1}	10.0	7.8-21.0
Mowing	L ha^{-1}	5.0	5.3-10.4
Baling (high pressure) + handling	L $tonne^{-1}$	1.5+0.5	1.3-1.7
Mowing	L $tonne^{-1}$	0.5	0.3-0.9
Stalk breaking	L $tonne^{-1}$	+0.2	0.7-2.1
Chopping	L $tonne^{-1}$	1.0	
Transport			
Machine transport	L km^{-1}	0.04	0.3-0.4
Manure and fodder transport	L $tonne^{-1}$ km^{-1}	0.2	0.1-0.5
Loading and Handling			
Loading	L $tonne^{-1}$	0.3	0.1-0.5
Loading and handling	L $tonne^{-1}$	0.5	0.3-1.1
Feeding	L $tonne^{-1}$	0.3	0.1-0.4
Other handling	L $tonne^{-1}$	0.5	
Handling (total average)	L $tonne^{-1}$	1.3	0.3-3.8

Data used to generate this table was obtained from values reported in Dalgaard et al (2000) [248].

Table 67. Machinery used during cultivation of perennial grasses and resulting diesel fuel consumption

Parameter	Unit	Frequency/year	Miscanthus (Years)	Switchgrass (Years)	Diesel Use (min, max)	Most Likely	Ref
Ploughing	L diesel/ha	1	1	1	(8.4, 32.7)	23.0	ref[248]
Harrowing (Heavy)	L diesel/ha	2	1	1	(4.9, 16.8)	6	ref[248]
Soil Compactification	L diesel/ha	1	1	1	(1.8, 2)	-	ref[248]
Stubble Conversion	L diesel/ha	1	3-15	3-10	(2.8, 30.9)	7	ref[248]
Rhizome/Seedling planting	L diesel/ha	1	1	1	-	22	ref[394]
Rolling	L diesel/ha	1	1	1	(1.8, 2)	-	ref[248]
Herbicide Application	L diesel/ha	1	1, 2	1, 2	(0.8, 1.7)	1.5	ref[248]
Spreading Fertilizer	L diesel/ha	1	3-15	3-10	(0.9, 4.7)	2	ref[248]
Weed Harrowing	L diesel/ha	1	1, 2	1, 2	(1.5, 2.4)	2	ref[248]
Residue removal	L diesel/ha	2	15	10	-	35.2	ref[394]

Table 68. Diesel consumption for harvesting equipment

Equipment	Units	Diesel Consumption (Min, Max); Avg	References
Windrow w/ disc header	L diesel/dry- tonne	1.1	ref[223]
Tractor and Baler	L diesel/dry- tonne	2.1	ref[223]
Stacker	L diesel/dry- tonne	0.5	ref[248]
Handling (total average)	L diesel/dry- tonne	(0.3-3.8); 1.3	ref[248]

Table 69. Field Efficiency (%)

Parameters	(Min, Max); Avg	Reference
Field Efficiency: Windrower (%)	(75, 90); 80	ref[223]
Field Efficiency: Baler (%)	(70, 90); 80	ref[223]

PDFs for direct volatilization of N fertilizer (i.e. N_2O conversion rates) were estimated based on 59 trials conducted on various agricultural lands [398-424], and provided in Table 70.

Table 70. Direct Nitrogen Volatilization Rates (%)

N_2O Conversion Rate (%)	Measurement Year(s)	Reference
0.52	2005 and 2006	Halvorson et al. 2008
0.45	2005 and 2006	Halvorson et al. 2008
0.75	2005 and 2006	Halvorson et al. 2008
0.90	Prior to 2001	Bouwman et al. 2002
6.60	2004-2006	Chantigny et al. 2010
0.40	2004-2006	Chantigny et al. 2010
0.83	2007-2008	Halvorson et al. 2010
0.85	2007-2008	Halvorson et al. 2010
0.14	2007-2008	Halvorson et al. 2010
0.33	2007-2008	Halvorson et al. 2010
0.06	2007	Halvorson et al. 2010
0.09	2008	Halvorson et al. 2010
0.21	2007	Halvorson et al. 2010
0.26	2008	Halvorson et al. 2010
0.32	2007	Halvorson et al. 2010
0.09	2008	Halvorson et al. 2010
0.41	2007	Halvorson et al. 2010
0.26	2008	Halvorson et al. 2010
1.02	2000-2001	Wagner-Riddle et al. 2007
0.73	2003-2004	Wagner-Riddle et al. 2007
0.14	2008	Venterea et al. 2011
0.17	2009	Venterea et al. 2011
0.42	2010	Venterea et al. 2011
0.69	2002-2006	Del Grosso et al. 2008
0.63	2002-2006	Del Grosso et al. 2008
0.34	2009	Halvorson et al. 2011
0.51	2010	Halvorson et al. 2011
0.20	2007	Halvorson et al. 2010
0.16	2008	Halvorson et al. 2010
0.69	2009-2010	Halvorson and Del Grosso 2012
0.21	2009-2010	Halvorson and Del Grosso 2012
0.26	2009-2010	Halvorson and Del Grosso 2012
0.38	2009-2010	Halvorson and Del Grosso 2012
0.91	2009	Sistani et al. 2011
1.60	2009	Sistani et al. 2011
2.60	2009	Sistani et al. 2011
1.20	2009	Sistani et al. 2011
2.80	2009	Sistani et al. 2011

Table 70 (continued).

3.20	2009	Sistani et al. 2011
0.48	2010	Sistani et al. 2011
0.36	2010	Sistani et al. 2011
1.40	2010	Sistani et al. 2011
0.40	2010	Sistani et al. 2011
0.60	2010	Sistani et al. 2011
0.058	2010	Sistani et al. 2011
0.50	2005-2006	Haile-Mariam et al. 2008
0.30	2005-2006	Haile-Mariam et al. 2008
1.29	1979-1987	Eichner 1990
0.77	Unspecified	Skiba et al. 1996
2.1	Unspecified	Benckiser et al. 1996
0.39	Unspecified	Hutchinson et al. 1992
6.8	Unspecified	Williams et al. 1992
1.25	Unspecified	Mosier and Hutchinson. 1981
1.0	Unspecified	Qian et al. 1997
0.95	Unspecified	Vermoesen et al. 1996
5	Unspecified	Shepherd et al. 1991
1.25	Unspecified	Bounman et al. 1995
0.36	Unspecified	Mosier et al. 1986
1.20	Unspecified	Anderson et al. 1987

Indirect N volatilization was developed based on estimates of soil nitrogen leaching and run-off rates as well as conversion rates of soil N to N_2O as reported by the Intergovernmental Panel for Climate Change (IPCC) [247] and are provided in Table 71.

Table 71. Indirect Nitrogen Volatilization Rates (%)

Parameters	**Min**	**Max**	**Most Likely**
Soil Nitrogen Volatilization Rate (%)	3%	30%	10%
Leaching and runoff rate of soil nitrogen (%)	10%	80%	30%
The conversion rate of leached and runoff nitrogen to N in N2O (%)	0.05%	2.5%	0.75%

C.4 MISCANTHUS AND SWITCHGRASS BIOFEEDSTOCK AND BIOCHAR COMPOSITION

Table 72. Switchgrass and Miscanthus Composition

Biofeedstock	Hemicellulose (wt %)	Cellulose (wt %)	Lignin (wt %)	Acid Detergent Lignin (wt %)	Crude Protein (wt %)	Ash (wt %)	Total	Ref
Switchgrass	28.45	37.25	19.05	6.35	3.05	5.85	100	ref[425]
Miscanthus	25.76	52.13	12.58	-	-	2.74	93.21	ref[198]

Table 73. Proximate and Ultimate Analysis of Switchgrass and Miscanthus biofeedstocks

	Proximate Analysis (% Dry Basis)					Ultimate Analysis (% DAF)						
Biofeedstock	VM	FC	Ash	MC	Total	C	H	O	N	S	Total	Ref
Switchgrass	80.4	14.5	5.1	0	100	49.70	6.10	43.40	0.70	0.10	100.00	ref*
Miscanthus	81.2	15.8	3	0	100	49.20	6.00	44.20	0.45	0.15	100.00	ref*

*Data Obtained from the Phyllis2 database[426]

Table 74. Composition of Switchgrass and Miscanthus Biochars produced via fast pyrolysis at 500°C

Biochar	C (%)	H (%)	O (%)	N (%)	S (%)	Ash (%)	Total	References
Switchgrass[1]	63	3.7	6.6	0.8	0	25.9	100	ref[42]
Switchgrass[2]	85.0	5.0	8.9	1.1	0.0	0	100	Calculation
Miscanthus[2]	86.4	2.7	10.41	0.4	0.09	0	100	ref[427]

[1]Values are reported on As Received (AS) basis
[2]Values are reported on a Dry, Ash Free (DAF) basis

C.5 PRETREATMENT: CHOPPING AND GRINDING

The specific energy requirement for grinding/chopping [251] of switchgrass or miscanthus at 15% moisture content is represented via equation 34, and it is assumed that the electricity would be utilized to operate the machinery.

$$E = aX^{-b} \quad (34)$$

Where E = specific energy requirement (kJ/kg-dry biomass), X = aperture size (mm). A screen size of 3mm was chosen for the analysis, and it was assumed that the grinding/chopping energy is provided via electricity. Regression coefficient were taken from Miao et al. [251] and are provided in Table 75.

Table 75. Key Parameters for Grinding and Chopping of Switchgrass and Miscanthus Feedstock

Feedstock	Regression Coefficient (a)	Regression Coefficient (b)	Specific Energy Consumption (kJ/kg-dry biomass)
Miscanthus at 15% MC	1447	-1.191	391
Switchgrass at 15% MC	1364	-1.103	406

C.6 PRODUCT DISTRIBUTION: FAST PYROLYSIS

Table 76. Primary pyrolysis product distribution resulting from hemicellulose pyrolysis at 500°C

Compound	Average* (%w/w)	Standard Deviation*
Carbon Monoxide	2.8	0.1
Carbon Dioxide	18.8	0.2
Acetaldehyde	0.7	0.1
Formic Acid	11.0	0.3
2-methyl furan	1.5	0.1
Acetic acid	1.1	0.1
Acetol	3.0	0.1
2-furaldehyde	2.2	0.1
DAXP 1	1.6	0.1
DAXP 2	7.0	0.1
Other DAXP	0.6	0.1
AXP	2.0	0.1
Other AXP	1.4	0.2
Char	10.7	0.5
Xylose	4.9	1.1
Water	15.1	-
Total	84.3	-

*Four pyrolysis runs.
Adapted from ref[38, 39]

Table 77. Primary pyrolysis product distribution resulting from cellulose pyrolysis at 500°C

Compound	Average* (%w/w)	Standard Deviation*
Formic Acid	6.6	0.23
Furan/Acetone	0.7	0.01
Glycolaldehyde	6.7	0.72
Acetic acid	0.0	0.00
2-Methyl furan	0.4	0.01
Acetol	0.3	0.02
2-Furaldehyde	1.3	0.05
2-Furan methanol	0.5	0.03
3-Furan methanol	0.3	0.00
5-Methyl furfural	0.2	0.02
2-Hydroxy-3-methyl cyclopenten-1-one	0.2	0.01
Levoglucosenone	0.4	0.03
5-Hydroxymethyl furfural	2.8	0.18
Anhydro xylopyranose	3.0	0.66
Levoglucosan – pyranose	58.8	0.27
Levoglucosan – furanose	4.1	0.09
Other Anhydro Sugars	1.4	0.04
Char	5.4	1.21
Total	92.9	2.75

*Four pyrolysis runs.
Adapted from ref[38, 39]

Table 78. Primary pyrolysis product distribution resulting from lignin pyrolysis at 500°C

Compound	Average* (%w/w)	Standard Deviation*
Carbon Monoxide	1.8	0.10
Carbon Dioxide	15.2	0.37
Acetaldehyde	0.9	0.00
Formic acid/Acetone[1]	0.7	0.03
2-methyl furan	0.1	0.03
Acetic acid	11.5	0.87
2-furaldehyde	0.2	0.01
Phenol	1.9	0.08
2-methoxy phenol	0.9	0.02
2-methyl phenol	0.1	0.00
4-methyl phenol	0.6	0.04
2-methoxy-4-methyl phenol	0.7	0.02
3,5-dimethyl phenol	0.1	0.00
3-ethyl phenol	0.6	0.03
4-ethyl-2-methoxy phenol	0.4	0.02
4-vinyl phenol	3.5	0.15
2-methoxy-4-vinyl phenol	1.8	0.03
Unidentified (Mol. Wt. 114)	1.4	0.32
2,6-dimethoxy phenol	1.0	0.05
2-methoxy-4-(1-propenyl)-phenol (Euginol)	0.2	0.00
4-methyl-2,6-dimethoxyphenol	0.8	0.03
3,5-dimethoxy-4-hydroxy benzaldehyde	0.4	0.02
3‘,4‘-dimethoxy acetophenone	0.8	0.03
4-allyl-2,6-dimethoxyphenol	0.2	0.00
4-allyl-2,5-dimethoxyphenol	0.3	0.00
3‘,5‘-dimethoxy-4‘-hydroxy acetophenone	0.3	0.01
Sinapyl alcohol	0.7	0.03
Unidentified (Mol. Wt. 280)	0.4	0.00
Char	37.0	0.22
Total	84.5	1.36

*Four pyrolysis runs.
[1]Assumed to be Formic Acid
Adapted from ref[38, 39]

Table 79. Product distribution resulting from fast pyrolysis at 500°C in increasing carbon number

Component	**Model Compounds**	**Fast Pyrolysis Yield (wt. %)**		
	Compounds	Hemicellulose	Cellulose	Lignin
Biochar (Dry, Ash-free)	N/A[1]	10.7	5.4	37
Water	H_2O	15.1	0	0
Formic acid	CH_2O_2	11	6.6	0.7
Carbon Monoxide	CO	2.8	0	1.8
Carbon Dioxide	CO_2	18.8	0	15.2
Glycolaldehyde	$C_2H_4O_2$	0	6.7	0
Acetic acid	$C_2H_4O_2$	1.1	0	11.5
Acetaldehyde	C_2H_4O	0.7	0	0.9
Acetol	$C_3H_6O_2$	3	0.3	0
Furan	C_4H_4O	0	0.7	0
Xylose	$C_5H_{10}O_5$	4.9	0	0
Anhydro xylopyranose	$C_5H_8O_4$	0	3	0
AXP	$C_5H_8O_4$	2	0	0
Other AXP	$C_5H_8O_4$	1.4	0	0
Other Anhydro Sugars	$C_5H_8O_4$	0	1.4	0
2-Furan methanol	$C_5H_6O_2$	0	0.5	0
3-Furan methanol	$C_5H_6O_2$	0	0.3	0
2-Furaldehyde	$C_5H_4O_2$	2.2	1.3	0.2
2-methyl furan	C_5H_6O	1.5	0.4	0.1
Levoglucosan – pyranose	$C_6H_{10}O_5$	0	58.8	0
Levoglucosan – furanose	$C_6H_{10}O_5$	0	4.1	0
DAXP 1	$C_6H_8O_4$	1.6	0	0
DAXP 2	$C_6H_8O_4$	7	0	0
Other DAXP	$C_6H_8O_4$	0.6	0	0
5-Hydroxymethyl furfural	$C_6H_6O_3$	0	2.8	0
Levoglucosenone	$C_6H_6O_3$	0	0.4	0
2-Hydroxy-3-methyl cyclopenten-1-one	$C_6H_8O_2$	0	0.2	0
5-Methyl furfural	$C_6H_6O_2$	0	0.2	0
Phenol	C_6H_6O	0	0	1.9
2-methyl phenol	C_7H_8O	0	0	0.1
4-methyl phenol	C_7H_8O	0	0	0.6
2-methoxy phenol	$C_7H_8O_2$	0	0	0.9
2,6-dimethoxy phenol	$C_8H_{10}O_3$	0	0	1
2-methoxy-4-(1-propenyl)-phenol	$C_8H_{10}O_2$	0	0	0.2
2-methoxy-4-methyl phenol	$C_8H_{10}O_2$	0	0	0.7
3-ethyl phenol	$C_8H_{10}O$	0	0	0.6
3,5-dimethyl phenol	$C_8H_{10}O$	0	0	0.1
4-vinyl phenol	C_8H_8O	0	0	3.5
3,5-dimethoxy-4-hydroxy benzaldehyde	$C_9H_{10}O_4$	0	0	0.4

Table 79 (continued).

2-methoxy-4-vinyl phenol	$C_9H_{10}O_2$	0	0	1.8
4-ethyl-2-methoxy phenol	$C_9H_{12}O_2$	0	0	0.4
4-methyl-2,6-dimethoxyphenol	$C_9H_{12}O_3$	0	0	0.8
3‘,4‘-dimethoxy acetophenone	$C_{10}H_{12}O_3$	0	0	0.8
3‘,5‘-dimethoxy-4‘-hydroxy acetophenone	$C_{10}H_{12}O_4$	0	0	0.3
4-allyl-2,6-dimethoxyphenol	$C_{11}H_{14}O_3$	0	0	0.2
4-allyl-2,5-dimethoxyphenol[2]	$C_{11}H_{14}O_3$	0	0	0.3
Sinapyl alcohol	$C_{11}H_{14}O_4$	0	0	0.7

Unidentified compounds were removed from the analysis

C.7 PRODUCT DISTRIBUTION: FAST PYROLYSIS

This work models hydrodeoxygenation (HDO) of bio-oil formed via fast pyrolysis. In HDO, hydrogen is used to remove oxygen from model bio-oil compounds to form renewable fuel compounds as well as water. The analytic framework used in this study assumes that renewable fuel compounds formed via HDO retain the same carbon number as it’s preceding bio-oil compound, and ignores any complex C-C coupling interactions between compounds. Table 80 shows the mapping between bio-oil compounds and their hydroprocessed product. For example, in catalytic HDO formic acid (CH2O2) is converted to methane (CH4). Loss of biofuel due to coking was considered in the analysis, and was based on experimental results provided in ref [428], see Table 81.

Table 80. Hydrodeoxygenation of Bio-Oil

Bio-Oil Compound	Molecular Formula	Hydroprocessed Product	Molecular Formula
Formic acid	CH2O2	Methane	CH4
Glycolaldehyde	C2H4O2	Ethane	C2H6
Acetic acid	C2H4O2	Ethane	C2H6
Acetaldehyde	C2H4O	Ethane	C2H6
Acetol	C3H6O2	Propane	C3H8
Furan	C4H4O	Butane	C4H10
Xylose	C5H10O5	Cyclopentane	C5H10
Anhydro xylopyranose	C5H8O4	Cyclopentane	C5H10
AXP	C5H8O4	Cyclopentane	C5H10
Other AXP	C5H8O4	Cyclopentane	C5H10
Other Anhydro Sugars	C5H8O4	Cyclopentane	C5H10
2-Furan methanol	C5H6O2	Cyclopentane	C5H10
3-Furan methanol	C5H6O2	Cyclopentane	C5H10
2-Furaldehyde	C5H4O2	Cyclopentane	C5H10
2-methyl furan	C5H6O	Cyclopentane	C5H10
Levoglucosan – pyranose	C6H10O5	Cyclohexane	C6H12
Levoglucosan – furanose	C6H10O5	Cyclohexane	C6H12
DAXP 1	C6H8O4	Cyclohexane	C6H12
DAXP 2	C6H8O4	Cyclohexane	C6H12
Other DAXP	C6H8O4	Cyclohexane	C6H12
5-Hydroxymethyl furfural	C6H6O3	Benzene	C6H6
Levoglucosenone	C6H6O3	Benzene	C6H6
2-Hydroxy-3-methyl cyclopenten-1-one	C6H8O2	Cyclohexane	C6H12
5-Methyl furfural	C6H6O2	Benzene	C6H6
Phenol	C6H6O	Benzene	C6H6
2-methyl phenol	C7H8O	Toluene	C7H8
4-methyl phenol	C7H8O	Toluene	C7H8
2-methoxy phenol	C7H8O2	Toluene	C7H8
2,6-dimethoxy phenol	C8H10O3	Xylene	C8H10
2-methoxy-4-(1-propenyl)-phenol	C8H10O2	Xylene	C8H10
2-methoxy-4-methyl phenol	C8H10O2	Xylene	C8H10
3-ethyl phenol	C8H10O	Xylene	C8H10
3,5-dimethyl phenol	C8H10O	Xylene	C8H10
4-vinyl phenol	C8H8O	Xylene	C8H10
3,5-dimethoxy-4-hydroxy benzaldehyde	C9H10O4	Indane	C9H10
2-methoxy-4-vinyl phenol	C9H10O2	Indane	C9H10
4-ethyl-2-methoxy phenol	C9H12O2	Cumene	C9H12
4-methyl-2,6-dimethoxyphenol	C9H12O3	Cumene	C9H12
3‘,4‘-dimethoxy acetophenone	C10H12O3	Cymene	C10H12

Table 80 (continued).

3‘,5‘-dimethoxy-4‘-hydroxy acetophenone	C10H12O4	Cymene	C10H12
4-allyl-2,6-dimethoxyphenol	C11H14O3	N-Pentylbenzene	C11H16
4-allyl-2,5-dimethoxyphenol2	C11H14O3	N-Pentylbenzene	C11H16
Sinapyl alcohol	C11H14O4	N-Pentylbenzene	C11H16

Table 81. Coke formation in hydro-upgrading of bio-oil products

Run Number	Char/Coke Formation (% w/w)
Ru1	9.1
Ru2	8.4
Ru3	9.6
Ru4	9.1
Ru5	10.4
Ru6	7.9
Ru7	13.0
Ru8	14.0
Ru9	9.0
Pt1	10.3
Pt2	14.9
Pt3	12.8
Pt4	7.2
Pt5	6.2
Pt6	11.5
Pt7	8.7
Pt8	6.1
Pt9	7.7

A high hydrogen pressure is considered in catalytic HDO for, “ensuring a higher solubility of hydrogen in the oil and thereby a higher availability of hydrogen in the vicinity of the catalyst. This increases the reaction rate and further decreases coking in the reactor”, see reference [429]. An overview of HDO catalysts and operating conditions from prior bio-oil and/or model compound studies are provided in Table 82. Literature review reveals that the hydrogen pressure commonly used in catalytic HDO ranges from 80 to 300 bar (~1160 to 4351 psig). Prior studies from PNNL report that a pressure of 2000 psig is required for hydroprocessing of bio-oil compounds [268], which is within the range of prior reported values and thus was used as the basis for this study.

Table 82. Overview of HDO catalysts and operating conditions

Catalyst	Feed	Pressure (Bar)	Pressure (Psig)	T (ºC)	Ref #
Co-MoS_2/Al_2O_3	Bio-Oil	200	2901	350	Ref[430]
Co-MoS_2/Al_2O_3	Bio-Oil	300	4351	370	Ref[431]
Ni-MoS_2/Al_2O_3	Bio-Oil	200	2901	350	Ref[430]
Ni-MoS_2/Al_2O_3	Bio-Oil	85	1233	400	Ref[432]
Pd/C	Bio-Oil	200	2901	350	Ref[430]
Pd/C	Bio-Oil	140	2031	340	Ref[40]
Pd/ZrO_2	Guaiacol	80	1160	300	Ref[433]
$Pd/Al_2O_3/SiO_2$	Bio-Oil	85	1233	400	Ref[432]
Pt/ZrO_2	Guaiacol	80	1160	300	Ref[433]
Rh/ZrO_2	Guaiacol	80	1160	300	Ref[433]
Ru/Al_2O_3	Bio-Oil	200	2901	350	Ref[430]
Ru/C	Bio-Oil	230	3336	350-400	Ref[434]
Ru/C	Bio-Oil	200	2901	350	Ref[430]
Ru/TiO_2	Bio-Oil	200	2901	350	Ref[430]
Pd/Re	Bio-Oil	105	1523	350	Ref[435]
Ru/Pd	Bio-Oil	121	1755	370	Ref[435]
Rd/Pd	Bio-Oil	121	1755	370	Ref[435]
CoMo	Bio-Oil	104	1508	400	Ref[435]
CoMo	Bio-Oil	125	1813	400	Ref[435]
FeW/Si-Al	Bio-Oil	103	1500	300-375	Ref[436]
CoMo/γ-Al_2O_3	Bio-Oil	103	1500	300-375	Ref[436]
Fe-Cr mixed oxide	Bio-Oil	103	1500	300-375	Ref[436]
Ru/Al_2O_3 & B: Ni/Si-Al	Bio-Oil	103	1500	300-375	Ref[436]

Data used to generate this table was obtained from values reported in Mortensen et al. 2011[429], Elliot et al. 2015[435], and Parapati et al. 2014[436].

C.8 ESTIMATION OF BIOMASS AND BIOCHAR/ASH HIGHER HEATING VALUE

The higher heating values (HHV) for switchgrass and miscanthus biochar/ash are estimated to be 23.81 and 24.22 MJ/kg, respectively; see Table 83. The HHVs are constructed based on correlations provided in Channiwala and Parikh [252], see equation 35.

$$\boldsymbol{HHV}\ (\tfrac{\boldsymbol{MJ}}{\boldsymbol{kg}}) = \mathbf{0.3491} * [\boldsymbol{C}\%] + \mathbf{1.1783} * [\boldsymbol{H}\%] + \mathbf{0.105} * [\boldsymbol{S}\%] - \mathbf{0.1034} * [\boldsymbol{O}\%] - \mathbf{0.0151} * [\boldsymbol{N}\%] - \mathbf{0.0211} * [\boldsymbol{A}\%] \quad (35)$$

Where C%, H%, O%, N%, S%, A% represent the carbon, hydrogen, oxygen, nitrogen, sulfur, and ash content respectively, expressed in mass percentages on a dry basis.

Table 83. Estimation of Biomass and Biochar/Ash Higher Heating Value

Parameter	C	H	O	N	S	Ash	HHV (MJ/kg)
SWG Feedstock Dry Basis (kg/hr)	39304.42	4824.08	34322.17	553.58	79.08	4250.00	-
SWG Elemental Fraction (%)	47.17	5.79	41.19	0.66	0.09	5.10	18.58
MSC Feedstock Dry Basis (kg/hr)	39770.00	4850.00	35728.33	363.75	121.25	2500.00	-
MSC Elemental Fraction (%)	47.724	5.82	42.874	0.4365	0.1455	3	18.69
SWG Biochar/Ash Dry Basis (kg/hr)	9718.18	570.75	1018.09	123.41	0.00	4250.00	-
SWG Elemental Fraction (%)	61.98	3.64	6.49	0.79	0.00	27.10	24.22
MSC Biochar/Ash Dry Basis (kg/hr)	7141.8	223.2	860.5	33.1	7.4	2500.0	-
MSC Elemental Fraction (%)	66.3	2.1	8.0	0.3	0.1	23.2	23.8

SWG: Switchgrass; **MSC**: Miscanthus

C.9 FAST PYROLYSIS OF SWITCHGRASS AND CATALYTIC UPGRADING OF BIO-OIL TO FUEL

Table 84. Switchgrass: Fast Pyrolysis Production Distribution

Parameter	Mass Flow (kg/hr)	Mass Fraction (%)	Carbon Flow (kg/hr)	Carbon Fraction (%)
Bio-Oil (wet basis)	49594.65	55.35	18249.82	46.43
Bio-Oil (dry)	39924.86	44.56	18249.82	46.43
Water	9669.78	10.79	0.00	0.00
Biochar & Ash	15680.43	17.50	9718.18	24.73
Gases	24330.66	27.15	11336.33	28.84
Total	89605.73	100.00	39304.33	100.00

Table 85. Switchgrass: HDO derived Renewable Fuels

Component	Model Compound	Mass Flow (kg/hr)	LHV (MJ/kg)	Energy Flow (MJ/hr)
Methane	CH_4	1589.34	50.01	79481.54
Ethane	C_2H_6	2499.77	47.79	119473.90
Propane	C_3H_8	454.39	46.36	21064.11
Butane	C_4H_8	176.06	45.75	8055.28
Cyclopentane	C_5H_{10}	2853.91	44.64	127387.07
Cyclohexane	C_6H_{12}	10870.66	43.45	472330.29
Benzene	C_6H_6	942.45	40.17	37858.40
Toluene	C_7H_8	253.99	40.59	10309.20
Xylene	C_8H_{10}	1020.67	40.80	41641.16
Indane	C_9H_{10}	336.65	41.00	13802.61
Cumene	C_9H_{12}	178.29	41.22	7348.67
Cymene	$C_{10}H_{14}$	160.92	41.45	6670.23
N-Pentylbenzene	$C_{11}H_{16}$	175.81	41.66	7323.67
Total	N/A	21512.92	N/A	952746.13

Not adjusted for loss of biofuel due to coking

Table 86. Switchgrass: HDO Renewable Fuel Product Distribution

Parameter	Mass Flow (kg/hr)	Mass Fraction (%)	Carbon Flow (kg/hr)	Carbon Fraction (%)	Energy Flow (MJ/hr)	Energy Fraction (%)
C1	1589.34	7.39	1189.91	6.52	79481.54	8.34
C2	2499.77	11.62	1997.00	10.94	119473.90	12.54
C3	454.39	2.11	371.30	2.03	21064.11	2.21
C4	176.06	0.82	145.53	0.80	8055.28	0.85
C5	2853.91	13.27	2443.75	13.39	127387.07	13.37
C6	11813.12	54.91	10177.83	55.77	510188.69	53.55
C7	253.99	1.18	231.76	1.27	10309.20	1.08
C8	1020.67	4.74	923.76	5.06	41641.16	4.37
C9	514.94	2.39	468.29	2.57	21151.28	2.22
C10	160.92	0.75	144.00	0.79	6670.23	0.70
C11	175.81	0.82	156.69	0.86	7323.67	0.77
Total	21512.92	100.00	18249.82	100.00	952746.13	100.00

Not adjusted for loss of biofuel due to coking

Table 87. Switchgrass: Fast Pyrolysis System Flows

Inputs	Model Compound	Unit	Value	C	H	O	N	S
Switchgrass (DAF)	N/A	kg/hr	79083.33	39304.42	4824.08	34322.17	553.58	79.08
Ash	N/A	kg/hr	4250.00	0.00	0.00	0.00	0.00	0.00
Water (Moisture)	H_2O	kg/hr	20833.33	0.00	2331.22	18502.12	0.00	0.00
Hydrogen	H_2	kg/hr	3260.81	0.00	3260.81	0.00	0.00	0.00
Total	N/A	kg/hr	107427.48	39304.42	10416.11	52824.28	553.58	79.08
Outputs	**Model Compound**	**Unit**	**Value**	**C**	**H**	**O**	**N**	**S**
Water (1st Stage Drying)	H_2O	kg/hr	6127.45	0.00	685.65	5441.80	0.00	0.00
Water (2nd Stage Drying)	H_2O	kg/hr	8433.48	0.00	943.69	7489.79	0.00	0.00
Water (Decanter)	H_2O	kg/hr	31342.54	0.00	3507.18	27835.36	0.00	0.00
NCGs	N/A	kg/hr	24330.66	11336.33	1445.77	11039.29	430.18	79.08
Ash	N/A	kg/hr	4250.00	0.00	0.00	0.00	0.00	0.00
Biochar	N/A	kg/hr	11430.43	9718.18	570.75	1018.09	123.41	0.00
Renewable Fuel (C1 to C4)	N/A	kg/hr	4719.57	3703.74	1015.82	0.00	0.00	0.00
Renewable Fuel (C5+)	N/A	kg/hr	16793.35	14546.08	2247.27	0.00	0.00	0.00
Total	N/A	kg/hr	107427.48	39304.33	10416.14	52824.34	553.58	79.08
Overall Mass and Elemental Balance								
Component	Model Compound	Unit	Value	C	H	O	N	S
Difference (Outputs – Inputs)	N/A	kg/hr	0.00	-0.08	0.03	0.06	0.00	0.00
Difference (Output/Input)	N/A	Unitless	1.00	1.00	1.00	1.00	1.00	1.00

Not adjusted for loss of biofuel due to coking

Table 88. Switchgrass: Overview Product Distribution

Parameter	Mass Flow (kg/hr)	Mass Fraction (%)	Carbon Flow (kg/hr)	Carbon Fraction (%)
Renewable Fuel (C5+)	16793.35	27.30	14546.08	37.01
Renewable Fuel (C1 to C4)	4719.57	7.67	3703.74	9.42
Biochar & Ash	15680.43	25.49	9718.18	24.73
Non Condensable Gases	24330.66	39.55	11336.33	28.84
Total	61524.00	100.00	39304.33	100.00

Not adjusted for loss of biofuel due to coking

Table 89. Switchgrass: Energy Products

Parameter	Mass Flow (kg/hr)	HHV (MJ/kg)	Energy Flow (MJ/hr)	Energy Flow (%)
Renewable Fuel (C5+)	16793.35	43.15	724671.31	54.38
Renewable Fuel (C1 to C4)	4719.57	48.33	228074.83	17.12
Biochar & Ash	15680.43	24.22	379835.04	28.50
Total	37193.35	N/A	1332581.18	100.00

Not adjusted for loss of biofuel due to coking

Table 90. Switchgrass: Pretreatment, Conversion, and Upgrading Utilities

Parameter	Unit	Value
Pretreatment (Grinding and Chopping)	Electricity (MJ/hr)	33835.17
Compressors	Electricity (MJ/hr)	17986.42
Pumps	Electricity (MJ/hr)	925.51
Net Heat Req. After Optimal Heat Exchange Network	Heat (MJ/hr)	104231.81

C.10 FAST PYROLYSIS OF MISCANTHUS AND CATALYTIC UPGRADING OF BIO-OIL TO FUEL

Table 91. Miscanthus: Fast Pyrolysis Production Distribution

Parameter	Mass Flow (kg/hr)	Mass Fraction (%)	Carbon Flow (kg/hr)	Carbon Fraction (%)
Bio-Oil (wet basis)	56994.86	63.61	21253.63	53.44
Bio-Oil (dry)	47578.23	53.10	21253.63	53.44
Water	9416.62	10.51	0.00	0.00
Biochar & Ash	10765.97	12.01	7141.80	17.96
Gases	21844.91	24.38	11374.51	28.60
Total	89605.73	100.00	39769.93	100.00

Table 92. Miscanthus: HDO derived Renewable Fuels

Component	Model Compound	Mass Flow (kg/hr)	LHV (MJ/kg)	Energy Flow (MJ/hr)
Methane	CH_4	1792.56	50.01	89644.22
Ethane	C_2H_6	2275.86	47.79	108772.27
Propane	C_3H_8	447.09	46.36	20725.90
Butane	C_4H_8	251.85	45.75	11522.52
Cyclopentane	C_5H_{10}	3246.25	44.64	144899.56
Cyclohexane	C_6H_{12}	14939.41	43.45	649117.21
Benzene	C_6H_6	1055.36	40.17	42393.67
Toluene	C_7H_8	128.58	40.59	5218.88
Xylene	C_8H_{10}	516.70	40.80	21080.23
Indane	C_9H_{10}	170.42	41.00	6987.37
Cumene	C_9H_{12}	90.26	41.22	3720.16
Cymene	$C_{10}H_{14}$	81.46	41.45	3376.71
N-Pentylbenzene	$C_{11}H_{16}$	89.00	41.66	3707.50
Total	N/A	25084.79	N/A	1111166.19

Not adjusted for loss of biofuel due to coking

Table 93. Miscanthus: HDO Renewable Fuel Product Distribution

Parameter	Mass Flow (kg/hr)	Mass Fraction (%)	Carbon Flow (kg/hr)	Carbon Fraction (%)	Energy Flow (MJ/hr)	Energy Fraction (%)
C1	1792.56	7.15	1342.06	6.31	89644.22	8.07
C2	2275.86	9.07	1818.12	8.55	108772.27	9.79
C3	447.09	1.78	365.34	1.72	20725.90	1.87
C4	251.85	1.00	208.17	0.98	11522.52	1.04
C5	3246.25	12.94	2779.70	13.08	144899.56	13.04
C6	15994.76	63.76	13765.98	64.77	691510.88	62.23
C7	128.58	0.51	117.33	0.55	5218.88	0.47
C8	516.70	2.06	467.64	2.20	21080.23	1.90
C9	260.68	1.04	237.06	1.12	10707.52	0.96
C10	81.46	0.32	72.90	0.34	3376.71	0.30
C11	89.00	0.35	79.32	0.37	3707.50	0.33
Total	25084.79	100.00	21253.63	100.00	1111166.19	100.00

Not adjusted for loss of biofuel due to coking

Table 94. Miscanthus: Fast Pyrolysis System Flows

Inputs	**Model Compound**	**Unit**	**Value**	**C**	**H**	**O**	**N**	**S**
Miscanthus (DAF)	N/A	kg/hr	80833.33	39770.00	4850.00	35728.33	363.75	121.25
Ash	N/A	kg/hr	2500.00	0.00	0.00	0.00	0.00	0.00
Water (Moisture)	H_2O	kg/hr	20833.33	0.00	2331.22	18502.12	0.00	0.00
Hydrogen	H_2	kg/hr	3915.84	0.00	3915.84	0.00	0.00	0.00
Total	N/A	kg/hr	108082.51	39770.00	11097.06	54230.45	363.75	121.25
Outputs	**Model Compound**	**Unit**	**Value**	**C**	**H**	**O**	**N**	**S**
Water (1st Stage Drying)	H_2O	kg/hr	6127.45	0.00	685.65	5441.80	0.00	0.00
Water (2nd Stage Drying)	H_2O	kg/hr	8433.48	0.00	943.69	7489.79	0.00	0.00
Water (Decanter)	H_2O	kg/hr	35825.91	0.00	4008.86	31817.05	0.00	0.00
NCGs	N/A	kg/hr	21844.91	11374.51	1404.54	8621.37	330.69	113.81
Ash	N/A	kg/hr	2500.00	0.00	0.00	0.00	0.00	0.00
Biochar	N/A	kg/hr	8265.97	7141.80	223.18	860.49	33.06	7.44
Renewable Fuel (C1 to C4)	N/A	kg/hr	4767.36	3733.69	1033.67	0.00	0.00	0.00
Renewable Fuel (C5+)	N/A	kg/hr	20317.43	17519.93	2797.50	0.00	0.00	0.00
Total	N/A	kg/hr	108082.51	39769.93	11097.09	54230.50	363.75	121.25
Overall Mass and Elemental Balance								
Component	Model Compound	Unit	Value	C	H	O	N	S
Difference (Outputs – Inputs)	N/A	kg/hr	0.00	-0.07	0.03	0.04	0.00	0.00
Difference (Output/Input)	N/A	Unitless	1.00	1.00	1.00	1.00	1.00	1.00

Not adjusted for loss of biofuel due to coking

Table 95. Miscanthus: Overview Product Distribution

Parameter	**Mass Flow (kg/hr)**	**Mass Fraction (%)**	**Carbon Flow (kg/hr)**	**Carbon Fraction (%)**
Renewable Fuel (C5+)	20317.43	35.21	17519.93	44.05
Renewable Fuel (C1 to C4)	4767.36	8.26	3733.69	9.39
Biochar & Ash	10765.97	18.66	7141.80	17.96
Non Condensable Gases	21844.91	37.86	11374.51	28.60
Total	57695.67	100.00	39769.93	100.00

Not adjusted for loss of biofuel due to coking

Table 96. Miscanthus: Energy Products

Parameter	Mass Flow (kg/hr)	HHV (MJ/kg)	Energy Flow (MJ/hr)	Energy Flow (%)
Renewable Fuel (C5+)	20317.43	43.34	880501.28	64.39
Renewable Fuel (C1 to C4)	4767.36	48.38	230664.90	16.87
Biochar & Ash	10765.97	23.81	256331.20	18.74
Total	35850.76	N/A	1367497.39	100.00

Not adjusted for loss of biofuel due to coking

Table 97. Miscanthus: Pretreatment, Conversion, and Upgrading Utilities

Parameter	Unit	Value
Pretreatment (Grinding and Chopping)	Electricity (MJ/hr)	32586.36
Compressors	Electricity (MJ/hr)	19382.38
Pumps	Electricity (MJ/hr)	892.99
Net Heat Req. After Optimal Heat Exchange Network	Heat (MJ/hr)	101505.51

The results of this work indicate that biofuel produced via fast pyrolysis and catalytic upgrading of perennial grasses has a product distribution ranging from C5 to C11 in carbon number, with the majority of the fuel comprised of C6 products. Petroleum gasoline typically contains compounds ranging from C5-C12 in carbon number, while petroleum diesel typically contains compounds ranging from C10 to C28 in carbon number. Based on carbon distribution, this work finds that renewable fuel derived via fast pyrolysis is primarily in the gasoline range. The ratio of C5+ biofuel energy produced to input bioenergy (i.e. $HHV_{biomass}$ x $Mass_{biomass}$) provides a useful measure of the energy efficiency of the system. After accounting for biofuel loss due to coking, the ratio of C5+ biofuel energy produced to bioenergy input is on average 51.0% for miscanthus and 41.3% for switchgrass.

C.11 LIFE CYCLE DATA ACQUISITION

Table 98 provides an overview of life cycle data sources and life cycle impact assessment (LCIA) methods used in this study. As catalyst production relies on propriety technologies, open source and/or commercial life cycle inventory data for catalyst production is scarce. Due to the lack of available life cycle data for commercial hydroprocessing catalysts, it is assumed that the life cycle impacts for hydroprocessing catalysts can be represented via a zeolite product from the Ecoinvent database. This assumption is consistent with several prior studies; see references [203, 268]. Future work should consider the impact of hydropocessing catalysts (i,e, CoMo, NiMo, etc.), as life cycle data for commercial catalysts becomes available.

Table 98. Life Cycle Data Sources

Material or Process Description	Unit	Database	Method	C.I.	N
Urea, as N, at regional storehouse/RER U	kg	Ecoinvent	IPCC 2007 GWP 100a V1.02	95%	10,000
Urea, as N, at regional storehouse/RER U	kg	Ecoinvent	Cumulative Energy Demand V 1.08	95%	10,000
Triple Superphospate, as P2O5, at regional storehouse/RER U	kg	Ecoinvent	IPCC 2007 GWP 100a V1.02	95%	10,000
Triple Superphospate, as P2O5, at regional storehouse/RER U	kg	Ecoinvent	Cumulative Energy Demand V 1.08	95%	10,000
Potassium Sulphate, as K2O, at regional storehouse/RER U	kg	Ecoinvent	IPCC 2007 GWP 100a V1.02	95%	10,000
Potassium Sulphate, as K2O, at regional storehouse/RER U	kg	Ecoinvent	Cumulative Energy Demand V 1.08	95%	10,000
Glyphosate, at regional storehouse/RER U	kg	Ecoinvent	IPCC 2007 GWP 100a V1.02	95%	10,000
Glyphosate, at regional storehouse/RER U	kg	Ecoinvent	Cumulative Energy Demand V 1.08	95%	10,000
Diesel, at regional storage/RER U	kg	Ecoinvent	IPCC 2007 GWP 100a V1.02	95%	10,000
Diesel, at regional storage/RER U	kg	Ecoinvent	Cumulative Energy Demand V 1.08	95%	10,000
Transport, Lorry 3.5-16t, fleet average/RER U	tkm	Ecoinvent	IPCC 2007 GWP 100a V1.02	95%	10,000
Transport, Lorry 3.5-16t, fleet average/RER U	tkm	Ecoinvent	Cumulative Energy Demand V 1.08	95%	10,000
Electricity Production Mix US/US U	MJ	Ecoinvent	IPCC 2007 GWP 100a V1.02	95%	10,000
Electricity Production Mix US/US U	MJ	Ecoinvent	Cumulative Energy Demand V 1.08	95%	10,000
Zeolite, powder, at plant/RER S	kg	Ecoinvent	IPCC 2007 GWP 100a V1.02	N/A	N/A
Zeolite, powder, at plant/RER S	kg	Ecoinvent	Cumulative Energy Demand V 1.08	N/A	N/A
Hydrogen (reformer) E	kg	Industry data 2.0	IPCC 2007 GWP 100a V1.02	N/A	N/A
Hydrogen (reformer) E	kg	Industry data 2.0	Cumulative Energy Demand V 1.08	N/A	N/A
Heat, natural gas, at industrial furnace >100 kW/RER U	MJ	Ecoinvent	IPCC 2007 GWP 100a V1.02	95%	10,000
Heat, natural gas, at industrial furnace >100 kW/RER U	MJ	Ecoinvent	Cumulative Energy Demand V 1.08	95%	10,000

C.12 OVERVIEW OF KEY PARAMETERS AND DISTRIBUTIONS

Anderson-Darling statistical tests were performed to determine the distribution type and parameters that best fit the sample data. All relevant and/or possible families of distributions are considered including: normal, triangular, lognormal, weibull, gamma, extreme value, exponential, and loglogistic.

Table 99. Overview of key parameters and probability distributions

Parameter	Unit	Distribution	Location	Shape	Scale	Threshold	Min	Max	Most Likely	Point Est.
Switchgrass - Cultivation										
Switchgrass Yield	Dry Tonne/ha	Weibull	-	2.05247	12.50196	-	-	-	-	-
N Fertilizer application	kg/dry tonne-biomass	Triangular	-	-	-	-	6.3	8	7.33	-
P Fertilizer application	kg/dry tonne-biomass	Triangular	-	-	-	-	0.05	0.15	0.1	-
K Fertilizer application	kg/dry tonne-biomass	Triangular	-	-	-	-	0.2	0.3	0.25	-
Herbicide application	kg/ha	Triangular	-	-	-	-	0.56	2.24	1.1	-
Miscanthus - Cultivation										
Miscanthus Yield	Dry Tonne/ha	Weibull	-	2.23841	17.23841	-	-	-	-	-
N Fertilizer application	kg/dry tonne-biomass	Triangular	-	-	-	-	2.63	4.09	3.52	-
P Fertilizer application	kg/dry tonne-biomass	Triangular	-	-	-	-	0.28	0.82	0.54	-
K Fertilizer application	kg/dry tonne-biomass	Triangular	-	-	-	-	2.94	5.70	4.16	-
Herbicide application	kg/ha	Triangular	-	-	-	-	0.56	2.24	1.1	-
Perennial Grass Cultivation/Harvesting										
Rhizome /Seedling Planting	L diesel/ha	Point Est.	-	-	-	-	-	-	-	22
Ploughing	L diesel/ha	Triangular	-	-	-	-	8.4	32.7	23	-
Soil Compactification	L diesel/ha	Uniform	-	-	-	-	1.8	2	-	-
Harrowing (heavy)	L diesel/ha	Triangular	-	-	-	-	4.9	16.8	6	-
Rolling	L diesel/ha	Uniform	-	-	-	-	1.8	2	-	-
Stubble Cultivation	L diesel/ha	Triangular	-	-	-	-	2.8	30.9	7	-
Spreading fertilizer	L diesel/ha	Triangular	-	-	-	-	0.9	4.7	2	-
Weed harrowing	L diesel/ha	Triangular	-	-	-	-	1.5	2.4	2	-
Residue Removal	L diesel/ha	Point Est.	-	-	-	-	-	-	-	35.2
Windrow w/ disc header	L diesel/dry tonne	Point Est.	-	-	-	-	-	-	-	1.1
Tractor and Baler	L diesel/dry tonne- biomass	Point Est.	-	-	-	-	-	-	-	2.1
Stacker	L diesel/dry tonne- biomass	Point Est.	-	-	-	-	-	-	-	0.5
Handling (total average)	L diesel/dry tonne- biomass	Triangular	-	-	-	-	0.3	3.8	1.3	-
Transport Distance	km	Triangular	-	-	-	-	50	150	100	-
Field Efficiency - Windrower	(%)	Triangular	-	-	-	-	75	90	80	-
Field Efficiency Baler	(%)	Triangular	-	-	-	-	70	90	80	-
Biomass - Moisture Content	(%)	Point Est.	-	-	-	-	-	-	-	20
Direct N_2O Emissions	(% N volatilized)	Lognormal	0.58299	-	1.05755	-	-	-	-	-
Indirect N_2O	Soil N Vol. Rate (%)	Triangular	-	-	-	-	3%	30%	10%	-
Indirect N_2O	Leaching/Runoff rate (%)	Triangular	-	-	-	-	10%	80%	30%	-
Indirect N_2O	Conv. Rate (%)	Triangular	-	-	-	-	0.05%	2.5%	0.75%	-
Fuel Upgrading and Conversion										
Weight Hourly Space Velocity (WHSV)	$Hour^{-1}$	Uniform	-	-	-	-	0.5	1	-	-
Catalyst Lifetime	Days	Uniform	-	-	-	-	60	365	-	-
Biofuel Loss to Coking	(% Biofuel Mass)	Lognormal	2.24740	-	0.26056	-	-	-	-	-
CHP – Eff. Conv. Electricity	(%)	Triangular	-	-	-	-	20	35	25	-
CHP – Eff. Conv. Heat	(%)	Triangular	-	-	-	-	44	48	52	-
Biochar Carbon Loss	(% C emitted to atm.)	Uniform	-	-	-	-	0	20	-	-

C.13 HYPOTHESIS TESTING

Hypothesis tests were performed to determine if the median value for energy return on investment (EROI) and carbon footprint (CF) of pyrolysis derived fuels are statistically different from key sustainability performance thresholds. The results (*p-values*) for the hypothesis tests are provided in Table 100. 1-sample sign tests were used in favor of other common statistical tests, as the distributions for CF and EROI are highly skewed, non-normal, and non-symmetric. For testing the hypothesis that the median EROI is equal to 1 against the alternative hypothesis the median EROI is greater than 1, the *p-value* is *0.00* for all examined biofeedstocks, allocation schemes, and coproduct scenarios. This indicates that for a significance level of $\alpha = 0.05$ the null hypothesis should be rejected, and the median value of the EROI is greater than unity for *all examined scenarios*. Similarly, for testing the hypothesis that the median CF is equal to the RFS2 GHG threshold (~37 g CO_2/MJ-fuel) against the alternative hypothesis the median CF is less than the RFS2 GHG threshold, the *p-value* is *1.00* for all SA pathways and the *pvalue* is *0.00* for all BE pathways. If the *pvalue* is less than the significance value $\alpha = 0.05$, the null hypothesis should be rejected and the median value of the CF is less than the RFS2 GHG threshold.

Table 100. Hypothesis Testing: 1 Sample Sign Test is performed to determine if median value is statistically different from key sustainability performance thresholds.

Feedstock	**Switchgrass**				**Miscanthus**			
Allocation Scheme	*Disp.*		*Energy Alloc*		*Disp.*		*Energy Alloc.*	
Coproduct Scenario	SA	BE	SA	BE	SA	BE	SA	BE
H_o: EROI = 1 H_a: EROI > 1	0.00	0.00	0.00	0.00	0.00	0.00	0.00	0.00
H_o: CF = RSF2 Threshold H_a: CF < RFS2 Threshold	0.00	1.00	0.00	1.00	0.00	1.00	0.00	1.00

SA: Soil Amendment; **BE**: Bioenergy
Reject null hypothesis if *pvalue* < $\alpha = 0.05$

C.14 WELL TO WHEEL (WTW) COMPARISON: LIFE CYCLE GHG EMISSIONS AND EROI FOR FAST PYROLYSIS GASOLINE AND SELECT PETROLEUM, FIRST GENERATION, AND SECOND GENERATION BIOFUELS

The 10th, 50th, and 90th percentile for EROI and life cycle GHG emission for fast pyrolysis biofuels as well as reference petroleum fuels, 1st generation, 2nd generation biofuels (including and excluding LUC impacts) are provided in Table 101 and Table 102.

Table 101. EROI and life cycle GHG emission for fast pyrolysis gasoline derived from switchgrass and miscanthus

Biofuel	**Fast Pyrolysis Gasoline**							
Feedstock	SWG	SWG	SWG	SWG	MSC	MSC	MSC	MSC
Coproduct Scenario	SA	SA	BE	BE	SA	SA	BE	BE
Alloc./Disp.	Alloc.	Disp.	Alloc.	Disp.	Alloc.	Disp.	Alloc.	Disp.
EROI (MJ/MJ-Fossil Energy)	1.5 (1.3,1.7)	1.5 (1.3,1.7)	1.8 (1.6,2.0)	2.6 (2.0,6.1)	1.8 (1.6,1.9)	1.8 (1.6,2.0)	2.0 (1.8,2.1)	2.4 (2.0,4.4)
[1]Life Cycle GHG Emissions (gCO_2e/MJ-Biofuel)	23 (12,50)	23 (11,49)	61 (52,84)	39 (25,66)	28 (22,38)	27 (20,38)	52 (47,62)	38 (31,50)

Results for EROI and Life cycle GHG emissions are tabulated as X (Y,Z) where X=50th Percentile, Y=10th Percentile, Z=90th Percentile

[1]Excludes direct and indirect land use change impacts

SWG: Switchgrass; **MSC**: Miscanthus

Table 102. EROI and life cycle GHG emission for select 1st generation, 2nd generation, and petroleum fuels

Transportation Fuel	**Diesel**	**Ethanol**				
Feedstock	Crude Oil	Corn	Sugarcane	Corn Stover	SWG	MSC
EROI (MJ/MJ-Fossil Energy)	4.82	1.61	4.32	4.77	5.44	6.01
[1]Life Cycle GHG Emissions (gCO_2e/MJ-Biofuel)	92.8	52.6 (40.4,66.7)	30.1 (27.3,32.0)	5.6 (-1.9,10.3)	10.3 (1.9,19.7)	4.7 (-1.9,11.3)
[2]Life Cycle GHG Emissions (gCO_2e./MJ-Biofuel)	N/A	62.0 (48.9,76.1)	46.1 (35.7,56.4)	3.8 (-2.8,9.4)	11.3 (2.8,21.6)	-7.5 (-0.9,-14.1)

Results for EROI and Life cycle GHG emissions are tabulated as X (Y,Z) where X=50th Percentile, Y=10th Percentile, Z=90th Percentile. Some values are not present due to lack of available data.
Values for petroleum diesel were adapted based on data obtained from the 2014 GREET model[269]
Values for 1st & 2nd generation bioethanol were obtained from Wang et al. 2012[261]
[1]Excludes direct and indirect land use change impacts
[2]Includes direct and indirect land use change impacts
SWG: Switchgrass; **MSC**: Miscanthus

C.15 IMPORTANT MODELING ASSUMPTIONS AND STUDY LIMITATIONS

Key Modeling Assumptions and Limitations:

1. In this work it is assumed that the N and S content of the biofeedstock are converted to NH_3 and H_2S respectively, consistent with previous analysis[37]. Both NH_3 and H_2S streams are separated from the bio-oil stream prior to hydroprocessing to transportation fuel.
2. Fast Pyrolysis reactor operates at 1 atm and at a temperature of 500 ^{O}C
3. Coproduct NCGs are recycled in the pyrolysis reactor to act as a fluidizing agent and are flared onsite. Prior experimental research has shown that recycling of NCGs may provide some benefit in suppressing coke formation, reducing acidity, and increasing the yield of desirable bio-oil compounds[437].
4. The higher heating values (HHV) for switchgrass and miscanthus biochar/ash are estimated to be 23.81 and 24.22 MJ/kg, respectively; and are constructed based on correlations provided in Channiwala and Parikh[252].
5. Hydrogen must be pressurized from 25 atm to 2000 psig prior to hydrodeoxygenation (HDO)

6. Hydro-processing reactor operates at 2000 psig and a temperature of 400 ^{O}C[258, 259, 268]
7. Loss of biofuel due to coking is considered in catalytic HDO[428]
8. Hydrogen required for HDO is externally sourced and produced via steam methane reforming
9. Zeolite power is used as a proxy for the life cycle impacts of hydrotreating catalysts[203, 268]
10. Infrastructure as well as direct and indirect land-use change impacts are not considered in this work
11. For soil amendment pathways, up to 20% of the carbon content of the biochar is re-emitted to the atmosphere over a 100-year time horizon[257]
12. Environmental impacts for wastewater treatment (i.e. of blow-down and cooling water) is not considered in this work
13. The heat duty for flaring is assumed to be minimal and thus not considered in the analysis
14. The 2007 IPCC[262] GWP 100a V1.02 and the Cumulative Energy Demand[263] V1.08 methodology are used to calculate total life cycle GHG emissions and primary fossil energy use
15. The unit process "Hydrogen (reformer) E" is used to represent the upstream impacts of hydrogen produced via steam methane reforming
16. Coproduct bioelectricity is used internally within the biorefinery; surplus electricity is sent to the grid and assumed to displace the U.S. average electricity mix.
17. Only "useful heat", i.e. heat that can be used to meet process-heating requirements is considered in the calculation of coproduct credits for EROI and carbon footprint.
18. Hydrocracking is not modeled in biofuel production as the longest carbon-chain biofuel compound is C11
19. Differences in simulation results may occur between models and versions of Aspen Plus
20. Aspen Energy analyzer is used to determine the optimal heat exchange network that minimizes the heating and cooling duties of the system

C.16 FAST PYROLYSIS: SENSITIVITY ANALYSIS

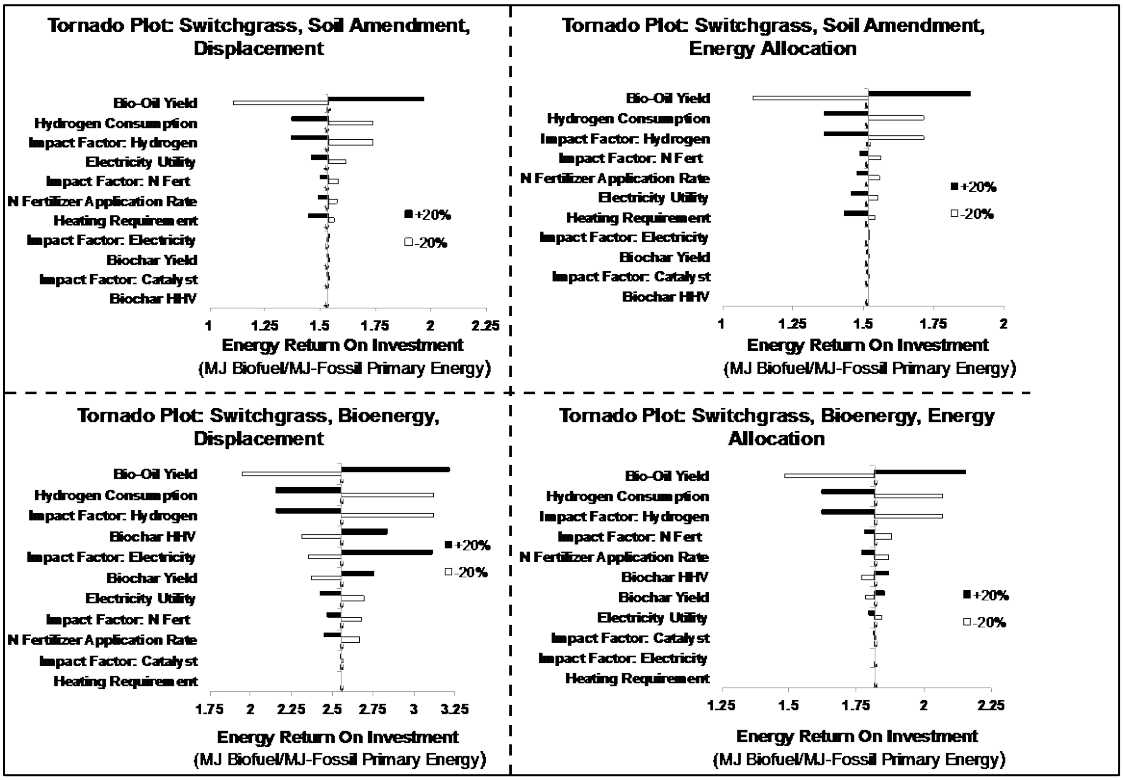

Figure 34. Tornado Plots: Median EROI, Switchgrass

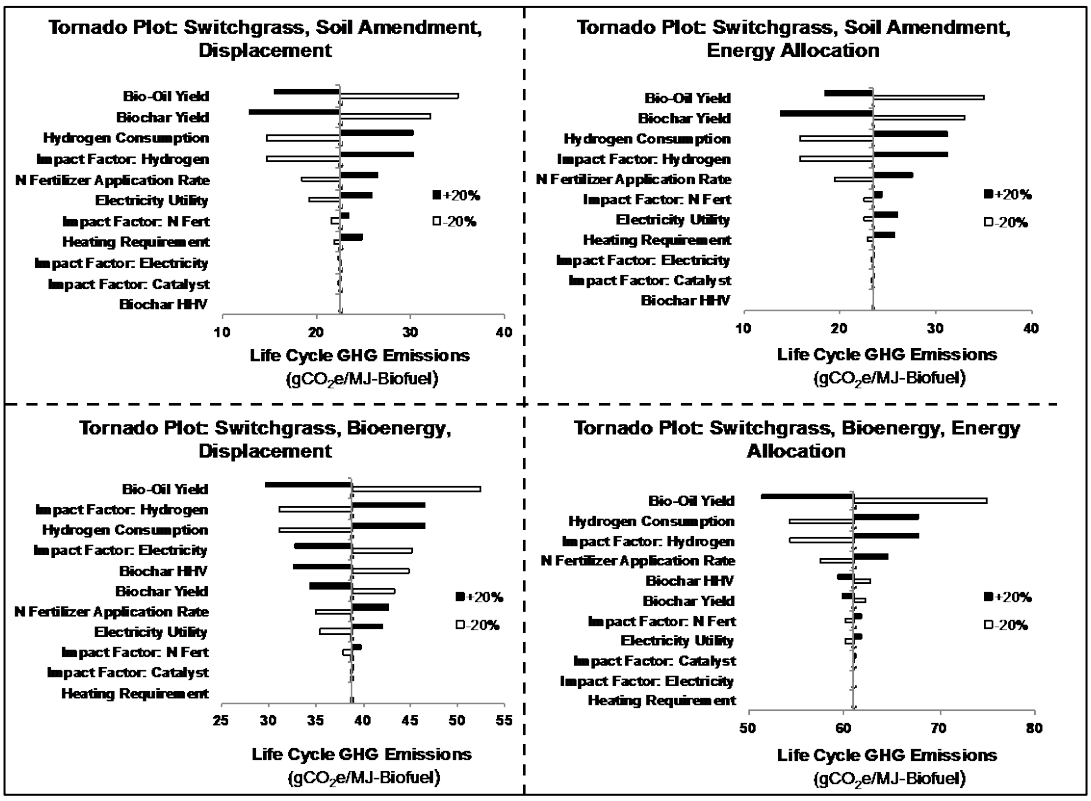

Figure 35. Tornado Plots: Median Life Cycle GHG Emissions, Switchgrass

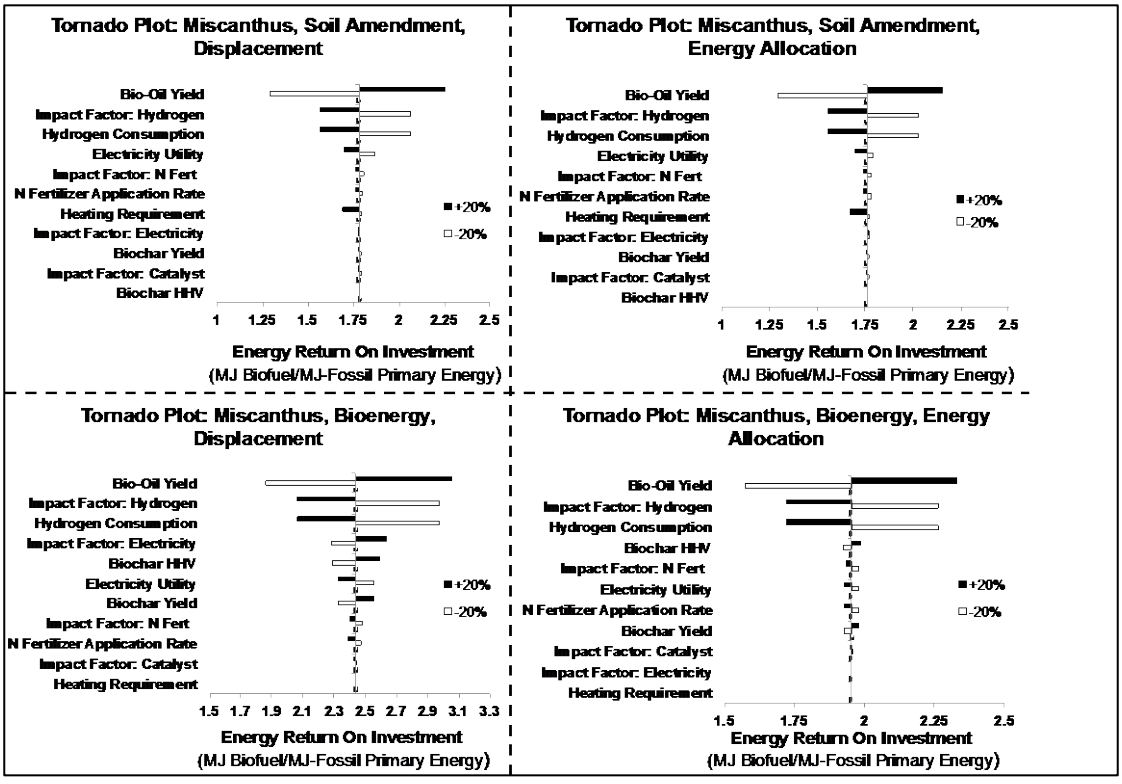

Figure 36. Tornado Plots: Median EROI, Miscanthus

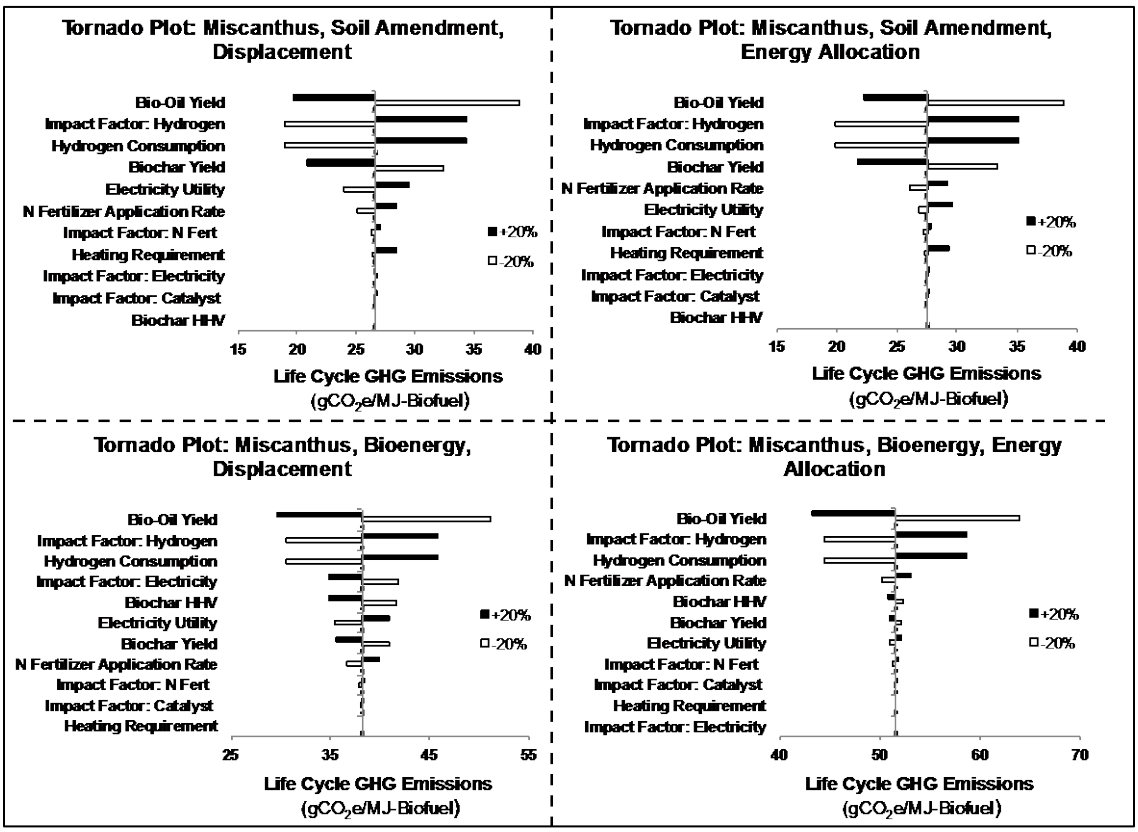

Figure 37. Tornado Plots: Median Life Cycle GHG Emissions, Miscanthus

APPENDIX D

SUPPORTING INFORMATION FOR MULTISTAGE TORREFACTION OF BIOMASS AND *IN-SITU* CATALYTIC UPGRADING TO HYDROCARBON BOIFUELS: ANALYSIS OF LIFE CYCLE ENERGY USE AND GREENHOUSE GAS EMISSIONS

D.1 DIRECT LAND USE CHANGE

Direct land-use change impacts are calculated using guidelines provided via the intergovernmental panel for climate change (IPCC). This work assumes that only grasslands-land coverage is converted to SRWC plantations, as grasslands are considered an ideal candidate for conversion to SRWC plantations relative to other land-types. For example, wetlands play multiple important ecological functions are often located on protected lands, established forestland provide free "waste" forestry resources and due to high biomass concentration represent a significant carbon-sink, conversion of cropland for biofuel production may lead to increased competition between the use of land for food or fuel production, and conversion of developed land i.e. ‘settlements’ is often cost prohibitive. Thus, it is likely that grasslands would be targeted for conversion to SRWC plantations.

Large-scale geospatial crop modeling and databases, such as the biofuel ecophysiological traits and yields database, predict the highest yields of SRWCs poplar and willow are concentrated in the northeastern region of the U.S., which is characteristically a temperate (cold, wet) climate zone, and whose soil characteristics are primarily represented by high activity clays (HAC), and thus representative

of nominal direct land-use change impacts. The soil organic carbon concentration for HACs in Temperate (cold, wet) climates regions is assumed to be 95 (Tonnes C ha^{-1} in 0-30 cm depth) based on data provided via the IPCC, further details are provided in Table 103.

Table 103. Soil Organic Carbon Stocks (SOC_{REF}) for Mineral Soils (Tonnes C ha^{-1} in 0-30 cm depth)

Climate Region	HAC Soils	LAC Soils	Sandy Soils	Spodic Soils	Volcanic Soils	Wetland Soils
Boreal – Dry & Wet	68	N/A	10	117	20	146
Cold Temperate – Dry	50	33	34	N/A	20	87
Cold Temperate – Wet	95	85	71	115	130	87
Warm Temperate – Dry	38	24	19	N/A	70	88
Warm Temperate – Wet	88	63	34	N/A	80	88
Tropical – Dry	38	35	31	N/A	50	86
Tropical – Moist	65	47	39	N/A	70	86
Tropical –Wet	44	60	66	N/A	130	86
Tropical – Montane	88	63	34	N/A	80	86

Obtained from IPCC - Table 2.3: Default reference (under native vegetation) soil organic C stocks (SOC_{REF}) for Mineral Soils (Tonnes C ha^{-1} in 0-30 cm depth)

In the IPCC methodology, the SOC concentrations of land-types (i.e. Grasslands, Croplands, Forestlands, etc.) are estimated via adjusting the reference SOC_{REF} for mineral soils, based on land-use (F_{LU}) and land management (F_{MG}) factors. Coefficients for F_{LU} and F_{MG} factors are provided in Table 104. A triangular distribution is utilized to randomly sample land management (F_{MG}) factors, with an upper bound of 1, most likely value of 0.95, and a minimum of 0.7.

Table 104. Carbon Stock Factors For Grassland Management

Factor	Level	Climate Regime	IPCC default	Error (%)
[1]Land Use (F_{LU})	All	All	1	N/A
[2]Management (F_{MG})	Nominally managed (non-degraded)	All	1	N/A
[3]Management (F_{MG})	Moderately Degraded grassland	Temperate	0.95	13
[4]Management (F_{MG})	Severely Degraded	All	0.7	40

Obtained from IPCC - Table 6.2: Relative Stock Change Factors for Grassland Management
[1]All permanent grassland is assigned a land-use factor of 1
[2]Represents non-degraded and sustainably managed grassland, but without significant management improvements.
[3]Represents overgrazed or moderately degraded grassland, with somewhat reduced productivity (relative to the native or nominally managed grassland) and receiving no management inputs
[4]Implies major long-term loss of productivity and vegetation cover, due to severe mechanical damage to the vegetation and/or severe soil erosion

The SOC for grasslands are estimated via the product of the SOC_{REF} (i.e. 95 Tonnes C ha^{-1}) and land-use and land-management factors, see equation 36.

$$SOC = SOC_{REF} \times F_{LU} \times F_{MG} \quad (36)$$

In this work it is assumed that the SOC carbon concentrations for SRWC plantations can be represented via IPCC defined *Forestlands.* Due to uncertainty regards the SOC concentrations for forestlands, IPCC methodology suggest that the SOC_{REF} be used as a proxy to estimate the SOC for forestlands. Using this methodological framework, changes in SOC resulting from conversion of grassland to SRWC plantations are estimated via equation 37.

$$\Delta SOC = SOC_{REF} \times (F_{Grasslands} \times F_{MG} - 1) \quad (37)$$

Estimates for the total above- and below- ground biomass (tonnes d.m. ha^{-1}) for grasslands are provided in Table 105.

Table 105. Above-ground and Below-ground Grassland Biomass Stocks

IPCC Climate Zone	Peak above-ground biomass (tonnes d.m. ha^{-1})	Total* above-ground and below-ground non-woody biomass (tonnes d.m. ha^{-1})	Error (%)[1]
Boreal – Dry & Wet	1.7	8.5	75
Cold Temperate – Dry	1.7	6.5	75
Cold Temperate – Wet	2.4	13.6	75
Warm Temperate – Dry	1.6	6.1	75
Warm Temperate – Wet	2.7	13.5	75
Tropical – Dry	2.3	8.7	75
Tropical – Moist & Wet	6.2	16.1	75

[1]Represents a nominal estimate of error, equivalent to two times standard deviation, as a percentage of the mean. Obtained from IPCC - Table 6.4: Default biomass stocks present on grassland, after conversion from other land use

Total GHG emissions and/or reductions (Tonnes CO_2 ha^{-1}) from direct LUC are calculated based on the mass of CO_2 emitted via removal of above-ground and below-ground

biomass due to conversion of grassland to SRWC plantations, and changes in the soil-organic carbon concentrations, and is provided in equation 38.

$$GHG\ Emissions = \ (Biomass_{Above+Below} \times \left(\frac{47\ kg\ C}{100\ kg\ d.m.}\right) + \Delta SOC) \times (\frac{44\ kg\ CO_2}{12\ kg\ C}) \quad (38)$$

Values for $Biomass_{Above+Below}$ are estimated via IPCC defined climate zone: Cold Temperate – Wet (tonnes d.m. ha^{-1}). A normal probability distribution is utilized to randomly sample from the total above-ground and below-ground biomass, based on reported standard deviation. Biomass is assumed to have an average carbon concentration of 0.47 kg C / kg Biomass-Dry Matter, consistent with IPCC guidelines. A conversion factor of 44/12 is utilized to convert from an elemental carbon to CO_2-basis. It is assumed that total dLUC impacts are normalized over the 20-year life-time of the biorefinery.

D.2 CULTIVATION AND HARVESTING: WOODY BIOMASS

Process inventories for woody biomass production are randomly sampled via statistical bootstrapping and are developed based on harmonized field trials reported in ref[302], see Table 107 through Table 121. Direct GHG emissions due to application of Urea (CH_4N_2O) as well as Lime ($CaCO_3$) are modeling assuming that all carbon is converted to carbon dioxide (CO_2).

Table 106. Reported Growth Rates for Woody Biomass*

Country	Location	Species	Age (yrs)	Yield (MT $ha^{-1}yr^{-1}$)
Spain	Granada	Poplar	3	13.7
Spain	Madrid	Poplar+Willow	2	13.5
Spain	Soria	Poplar	4	12
Spain	Zamora	Poplar	3	7.7
Italy	Bagni di Tivoli	Poplar	8	10
Spain	Girona	Poplar+Willow	2	15.5
Spain	Leon	Poplar	3	6.9
Spain	Navarra	Poplar	3	16
Italy	Pisa	Poplar	15	8
Italy	Pisa	Poplar	15	11.3
Italy	Cavallermaggiore	Poplar+Willow	9	5.5
Italy	Caramagna piemonte	Poplar/Willow	9	8.2
Italy	Lombriasco	Poplar/Willow	9	1.3
Italy	Casale Monferrato	Poplar/willow	9	9.5
Italy	Bigarello	Poplar	10	4.4
Italy	Ostiano	Poplar	10	16
Italy	Ostiano	Poplar	10	20
Slovakia	Malanta	Willow	13	14.3
Czech Rep.	Nová Olešná	Poplar/Willow	na	10.2
Czech Rep.	Bystřice	Poplar	16	3.2
Czech Rep.	Smilkov	Poplar	16	7.2
Czech Rep.	Rosice	Poplar	12	13.2
Germany	Arnsfeld	Poplar	14	5.6
Germany	Großschirma	Willow	3	10.1
Germany	Großschirma	Poplar	na	9.4
Germany	Krummenhennersdorf	Poplar/Willow	8	11.3
Belgium	Zwijnaarde	Poplar/Willow	4	3.5
Belgium	Boom	Poplar	16	5.2
Belgium	Lochristi	Poplar/Willow	2	4
Germany	Gersdorf	Willow	7	7.8
Germany	Zschadrass	Willow	5	14.7
Germany	Commichau	Poplar	6	9.1
Germany	Skäßchen	Poplar	15	2.9
Germany	Großthiemig	Poplar	na	7
Germany	Thammenhain	Poplar/Willow	15	7.1
Germany	Nochten	Poplar	15	2.8
Germany	Vetschau	Poplar	7	3.4
Germany	Methau I	Poplar/Willow	17	12.9
Germany	Methau II	Poplar	17	9.2
Germany	Köllitsch	Poplar/Willow	5	5.95
Netherlands	Lelystad	Willow	na	8
Germany	Kuhstorf	Poplar/Willow	na	7.7
Germany	Laage	Poplar	na	23.9
Ireland	Loughgall	Willow	21	11
Denmark	Vråvej	Willow	16	9.2
Estonia	Saare	Willow	12	9.1
Sweden	Hjulsta	Willow	15	9.5

*Adapted from ref [302]

Table 107. Process Inventory for SRWC System 1

SRWC System 1 (Stand life: 15 yrs)	Diesel Use (L ha^{-1})	Input Rate (unit ha^{-1})	Frequency (# times over stand life)
Plowing	25.77	-	1
Harrowing	7.21	-	1
Disking	-	-	-
Mechanical Weeding	-	-	-
Chemical Weeding	7.5	4 l gly	6
Fertilizing (lime)	-	-	-
Fertilizing (N/P/K)	4.32	107 kg (N)	4
Planting	45.25	11,500 cuttings	1
Pest Control	-	-	-
Irrigation	-	-	-
Coppicing	30	-	1
Harvesting/Chipping	75	-	4
Stump Removal	38.70	-	1

Based on site: Hjulsta

Table 108. Process Inventory for SRWC System 2

SRWC System 2 (Stand life: 21 yrs)	Diesel Use (L ha^{-1})	Input Rate (unit ha^{-1})	Frequency (# times over stand life)
Plowing	7	-	1
Harrowing	2.3	-	1
Disking	-	-	-
Mechanical Weeding	2.2	-	-
Chemical Weeding	1.2	2.25 kg gly	5
Fertilizing (lime)	2.3	3 MT	1
Fertilizing (N/P/K)	2.8	128/28/178 (kg)	5
Planting	2.8	15,000 cuttings	1
Pest Control	-	-	-
Irrigation	-	-	-
Coppicing	-	-	-
Harvesting/Chipping	74.85	-	7
Stump Removal	38.70	-	1

Based on site : Loughgall

Table 109. Process Inventory for SRWC System 3

SRWC System 3 (Stand life: 2 yrs)	Diesel Use (L ha^{-1})	Input Rate (unit ha^{-1})	Frequency (# times over stand life)
Plowing	40	-	2
Harrowing	32	-	1
Disking	20	-	1
Mechanical Weeding	14	-	2
Chemical Weeding	10	5 l oxy	2
Fertilizing (lime)	-	-	-
Fertilizing (N/P/K)	-	-	-
Planting	16.3	10,000 cuttings	1
Pest Control	10.5	0.18 kg cyp	2
Irrigation	165.5	3397 m3	3
Coppicing	-	-	-
Harvesting/Chipping	34.0	-	2
Stump Removal	38.70	-	1

Based on site: Girona

Table 110. Process Inventory for SRWC System 4

SRWC System 4 (Stand life: 4 yrs)	Diesel Use (L ha^{-1})	Input Rate (unit ha^{-1})	Frequency (# times over stand life)
Plowing	18	-	1
Harrowing	8	-	1
Disking	-	-	-
Mechanical Weeding	25	-	-
Chemical Weeding	4	4 l oxy, 4 l gly	4
Fertilizing (lime)	-	-	-
Fertilizing (N/P/K)	4	400 kg (12N/22P/22K) & 230 kg CAN (27%)	5
Planting	98	19,700 cuttings	1
Pest Control	-	-	-
Irrigation	-	1333 m3	4
Coppicing	48	-	1
Harvesting/Chipping	160	-	1
Stump Removal	38.70	-	1

Based on site: Soria

Table 111. Process Inventory for SRWC System 5

SRWC System 5 (Stand life: 15 yrs)	Diesel Use (L ha^{-1})	Input Rate (unit ha^{-1})	Frequency (# times over stand life)
Plowing	45	-	1
Harrowing	30	-	1
Disking	30	-	1
Mechanical Weeding	19	-	2
Chemical Weeding	-	-	-
Fertilizing (lime)	-	-	-
Fertilizing (N/P/K)	18	30 kg N	4
Planting	30	7,142 cuttings	1
Pest Control	-	-	-
Irrigation	45	300 m3	3
Coppicing	-	-	-
Harvesting/Chipping	132	-	5
Stump Removal	38.70	-	1

Based on site: Pisa

Table 112. Process Inventory for SRWC System 6

SRWC System 6 (Stand life: 8 yrs)	Diesel Use (L ha^{-1})	Input Rate (unit ha^{-1})	Frequency (# times over stand life)
Plowing	46.54	-	1
Harrowing	46.14	-	2
Disking	-	-	-
Mechanical Weeding	8.74	-	16
Chemical Weeding	2	2 l met & 1 l lu	12
Fertilizing (lime)	-	-	-
Fertilizing (N/P/K)	5.6	500 kg (8/24/24)	6
Planting	75.35	10,000 cuttings	1
Pest Control	-	-	-
Irrigation	-	-	-
Coppicing	-	-	-
Harvesting/Chipping	122.2	-	4
Stump Removal	38.70	-	1

Based on site: Bagni di Tivoli

Table 113. Process Inventory for SRWC System 7

SRWC System 7 (Stand life: 16 yrs)	Diesel Use (L ha^{-1})	Input Rate (unit ha^{-1})	Frequency (# times over stand life)
Plowing	33.2	-	1
Harrowing	11.8	-	1
Disking	-	-	-
Mechanical Weeding	2.7	-	7
Chemical Weeding	2.8	3 kg gly; 9 kg oxa	6
Fertilizing (lime)	-	-	-
Fertilizing (N/P/K)	-	-	-
Planting	-	10,000 cuttings	1
Pest Control	-	-	-
Irrigation	-	-	-
Coppicing	-	-	-
Harvesting/Chipping	74.9	-	4
Stump Removal	38.70	-	1

Based on site: Boom

Table 114. Process Inventory for SRWC System 8

SRWC System 8 (Stand life: 2 yrs)	Diesel Use (L ha^{-1})	Input Rate (unit ha^{-1})	Frequency (# times over stand life)
Plowing	16.66	-	1
Harrowing	13.51	-	1
Disking	11.4	-	1
Mechanical Weeding	8.36	-	5
Chemical Weeding	6.88	0.3 l Az, 2.5 l Ar, & 3.5 l gly	7
Fertilizing (lime)	-	-	-
Fertilizing (N/P/K)	-	-	-
Planting	21.04	8,000 cuttings	1
Pest Control	9.84	1 l tom & 1 l mat	1
Irrigation	-	-	-
Coppicing	-	-	-
Harvesting/Chipping	49.47	-	1
Stump Removal	38.70	-	1

Based on site: Lochristi

Table 115. Process Inventory for SRWC System 9

SRWC System 9 (Stand life: 16 yrs)	Diesel Use (L ha^{-1})	Input Rate (unit ha^{-1})	Frequency (# times over stand life)
Plowing	46.5	-	1
Harrowing	6	-	1
Disking	4	-	1
Mechanical Weeding	2	-	5
Chemical Weeding	1.2	4 l sto	3
Fertilizing (lime)	1.9	-	1
Fertilizing (N/P/K)	1.9	120 kg (21/3/10)	7
Planting	4.2	12,000 cuttings	1
Pest Control	-	-	-
Irrigation	1	-	3
Coppicing	-	-	-
Harvesting/Chipping	14.0	-	7
Stump Removal	38.7	-	1

Based on site: Vravej

Table 116. Process Inventory for SRWC System 10

SRWC System 10 (Stand life: 3 yrs)	Diesel Use (L ha^{-1})	Input Rate (unit ha^{-1})	Frequency (# times over stand life)
Plowing	21.7	-	1
Harrowing	17.6	-	1
Disking	10.2	-	1
Mechanical Weeding	5.1	-	2
Chemical Weeding	4.9	2 kg gly	4
Fertilizing (lime)	2.6	-	1
Fertilizing (N/P/K)	2.6	(90/8/60)	3
Planting	27.3	13,500 cuttings	1
Pest Control	1.2	0.42 kg del	3
Irrigation	1.2	300 m3	1
Coppicing	-	-	-
Harvesting/Chipping	27.4	-	4
Stump Removal	38.7	-	1

Based on site: Großschirma

Table 117. Process Inventory for SRWC System 11

SRWC System 11 (Stand life: 10 yrs)	Diesel Use (L ha^{-1})	Input Rate (unit ha^{-1})	Frequency (# times over stand life)
Plowing	22.9	-	1
Harrowing	26.3	-	1
Disking	-	-	-
Mechanical Weeding	28.3	-	5
Chemical Weeding	3.7	4 l gly	5
Fertilizing (lime)	5.5	1 MT	1
Fertilizing (N/P/K)	3.8	80 kg Urea	4
Planting	22.7	5,560 cuttings	1
Pest Control	3.7	2 kg del	5
Irrigation	6.5	400 m3	5
Coppicing	-	-	-
Harvesting/Chipping	80.6	-	5
Stump Removal	39	-	1

Based on site: Ostiano

Table 118. Process Inventory for SRWC System 12

SRWC System 12 (Stand life: 9 yrs)	Diesel Use (L ha^{-1})	Input Rate (unit ha^{-1})	Frequency (# times over stand life)
Plowing	27	-	2
Harrowing	24	-	1
Disking	22	-	1
Mechanical Weeding	13	-	6
Chemical Weeding	7	3 kg gly	6
Fertilizing (lime)	-	-	1
Fertilizing (N/P/K)	14	(30/44/83)	4
Planting	40	8,330 cuttings	1
Pest Control	-	-	-
Irrigation	-	1500 m3	4
Coppicing	-	-	-
Harvesting/Chipping	97	-	5
Stump Removal	39	-	1

Based on site: Casale Monferrato

Table 119. Process Inventory for SRWC System 13

SRWC System 13 (Stand life: 3 yrs)	Diesel Use (L ha^{-1})	Input Rate (unit ha^{-1})	Frequency (# times over stand life)
Plowing	30	-	1
Harrowing	16	-	1
Disking	-	-	-
Mechanical Weeding	12	-	3
Chemical Weeding	8	4 l oxy	1
Fertilizing (lime)	-	-	-
Fertilizing (N/P/K)	8	450 kg (8/15/15)	1
Planting	17	13,333 cuttings	1
Pest Control	20	0.5 kg del	1
Irrigation	210	1333 m3	3
Coppicing	-	-	-
Harvesting/Chipping	36	-	1
Stump Removal	39	-	1

Based on site: Leon

Table 120. Process Inventory for SRWC System 14

SRWC System 14 (Stand life: 3 yrs)	Diesel Use (L ha^{-1})	Input Rate (unit ha^{-1})	Frequency (# times over stand life)
Plowing	25.0	-	1
Harrowing	20	-	1
Disking	-	-	-
Mechanical Weeding	17	-	4
Chemical Weeding	6	3 l gly	3
Fertilizing (lime)	-	-	-
Fertilizing (N/P/K)	-	-	-
Planting	17	13,333 cuttings	1
Pest Control	-	-	-
Irrigation	-	1,667 m3	3
Coppicing	-	-	-
Harvesting/Chipping	37	-	1
Stump Removal	39	-	1

Based on site: Granada

Table 121. Process Inventory for SRWC System 15

SRWC System 15 (Stand life: 3 yrs)	Diesel Use (L ha^{-1})	Input Rate (unit ha^{-1})	Frequency (# times over stand life)
Plowing	30	-	2
Harrowing	14	-	3
Disking	-	-	-
Mechanical Weeding	17	-	8
Chemical Weeding	3.6	4 l (oxy + gly)	4
Fertilizing (lime)	-	-	-
Fertilizing (N/P/K)	4.4	235 kg (15/15/15)	6
Planting	17	13,333 cuttings	1
Pest Control	3.6	1.5 l Ch1	5
Irrigation	-	1,890 m3	3
Coppicing	-	-	-
Harvesting/Chipping	36	-	1
Stump Removal	39	-	1

Based on site: Zamora

Table 122. Process Inventory for Cuttings Production

Activities	Diesel Use ($L\ ha^{-1}$)	Input Rate ($unit\ ha^{-1}$)
Plowing	24	-
Flattening	18	-
Fertilizing	7	80 kg N
Fertilizing	7	100 kg P
Fertilizing	7	60 kg K
Fertilizing	11	1000 kg CaCo3
Chemical Weeding	7	1 l AZ 500
Chemical Weeding	7	1 l Kerb50
Chemical Weeding	7	1 l Basts
Mechanical Weeding	20	-
*Manual Weeding	-	65 h

Data is based on 1 ha land use, and an average production of 153,000 cuttings per ha. Adapted from ref[304]
*Impacts due to Labor are not considered in this work

Harvest efficiency, i.e. the fraction of dry matter yield that is harvested, is dependent on the harvesting technology. This work assumes a uniform distribution for harvesting efficiency with a lower bound of 77.4% and upper bound of 94.5%, see Table 123 for additional information.

Table 123. Harvest Efficiency

Harvesting Technology	Avg Efficiency (%)	Reference
Self propelled cut-and-chip harvester	77.4	Ref [303]
Tractor-pulled stem harvester	94.5	Ref [303]

Direct volatilization of N fertilizer to N_2O is randomly sampled via statistical bootstrapping, based on 59 trials conducted on various agricultural lands [398-424], and are provided in Table 124.

Table 124. Direct Nitrogen Volatilization Rates (%)

N_2O Conversion Rate (%)	Measurement Year(s)	Reference
0.52	2005 and 2006	Halvorson et al. 2008
0.45	2005 and 2006	Halvorson et al. 2008
0.75	2005 and 2006	Halvorson et al. 2008
0.90	Prior to 2001	Bouwman et al. 2002
6.60	2004-2006	Chantigny et al. 2010
0.40	2004-2006	Chantigny et al. 2010
0.83	2007-2008	Halvorson et al. 2010
0.85	2007-2008	Halvorson et al. 2010
0.14	2007-2008	Halvorson et al. 2010
0.33	2007-2008	Halvorson et al. 2010
0.06	2007	Halvorson et al. 2010
0.09	2008	Halvorson et al. 2010
0.21	2007	Halvorson et al. 2010
0.26	2008	Halvorson et al. 2010
0.32	2007	Halvorson et al. 2010
0.09	2008	Halvorson et al. 2010
0.41	2007	Halvorson et al. 2010
0.26	2008	Halvorson et al. 2010
1.02	2000-2001	Wagner-Riddle et al. 2007
0.73	2003-2004	Wagner-Riddle et al. 2007
0.14	2008	Venterea et al. 2011
0.17	2009	Venterea et al. 2011
0.42	2010	Venterea et al. 2011
0.69	2002-2006	Del Grosso et al. 2008
0.63	2002-2006	Del Grosso et al. 2008
0.34	2009	Halvorson et al. 2011
0.51	2010	Halvorson et al. 2011
0.20	2007	Halvorson et al. 2010
0.16	2008	Halvorson et al. 2010
0.69	2009-2010	Halvorson and Del Grosso 2012
0.21	2009-2010	Halvorson and Del Grosso 2012
0.26	2009-2010	Halvorson and Del Grosso 2012
0.38	2009-2010	Halvorson and Del Grosso 2012
0.91	2009	Sistani et al. 2011
1.60	2009	Sistani et al. 2011
2.60	2009	Sistani et al. 2011
1.20	2009	Sistani et al. 2011
2.80	2009	Sistani et al. 2011

Table 124 (continued).

3.20	2009	Sistani et al. 2011
0.48	2010	Sistani et al. 2011
0.36	2010	Sistani et al. 2011
1.40	2010	Sistani et al. 2011
0.40	2010	Sistani et al. 2011
0.60	2010	Sistani et al. 2011
0.058	2010	Sistani et al. 2011
0.50	2005-2006	Haile-Mariam et al. 2008
0.30	2005-2006	Haile-Mariam et al. 2008
1.29	1979-1987	Eichner 1990
0.77	Unspecified	Skiba et al. 1996
2.1	Unspecified	Benckiser et al. 1996
0.39	Unspecified	Hutchinson et al. 1992
6.8	Unspecified	Williams et al. 1992
1.25	Unspecified	Mosier and Hutchinson. 1981
1.0	Unspecified	Qian et al. 1997
0.95	Unspecified	Vermoesen et al. 1996
5	Unspecified	Shepherd et al. 1991
1.25	Unspecified	Bounman et al. 1995
0.36	Unspecified	Mosier et al. 1986
1.20	Unspecified	Anderson et al. 1987

Indirect N volatilization was developed based on estimates of soil nitrogen leaching and run-off rates as well as conversion rates of soil N to N_2O as reported by the Intergovernmental Panel for Climate Change (IPCC) [247] and are provided in Table 125. Triangular distributions are utilized to estimate key parameters for indirect nitrogen volatilization rates, based on minimum, maximum and most likely values.

Table 125. Indirect Nitrogen Volatilization Rates (%)

Parameters	**Min**	**Max**	**Most Likely**
Soil Nitrogen Volatilization Rate (%)	3%	30%	10%
Leaching and runoff rate of soil nitrogen (%)	10%	80%	30%
The conversion rate of leached and runoff nitrogen to N in N2O (%)	0.05%	2.5%	0.75%

D.3 SHORT-TERM STORAGE OF BIOMASS

Regression equations are utilized to estimate dry matter loss as a function of storage time, based on experimental data provided in ref [306], see Table 126.

Table 126. Dry Matter Loss (%) as a function of Storage Time

Storage Time (Days)	Dry Matter Loss (%)
2.1	0.5
3.4	0.8
7.7	1.9
35.7	6.3
51.7	8.3
63.2	9.6

Linear regression provides a good fit to experimental data (R^2=0.99), the regression equation is provided in equation 39.

$$Dry\ Matter\ Loss\ (\%) = 0.1498 \times Storage\ Time\ (days) + 0.4767 \quad (39)$$

The emissions factors for storage off-gases (kg-off-gases kg-biomass^{-1}) during biomass storage are estimated using equation 40.

$$EF_i = \frac{P \times Vg \times M_{wt} \times C_i \times Storage\ Time\ (days)}{R \times T \times M \times 10^9} \quad (40)$$

Where P is the pressure of the container (101,300 Pa), Vg is the volume of gas (0.00152 m^3), M_{wt} is the molecular weight (g mole^{-1}) of the off gases (CO: 28, CO_2: 44, and CH_4: 16), R is the ideal gas constant (8.31 J mol^{-1} K^{-1}), T is the temperature of the storage (293.15 K), M is the mass of the stored biomass on a dry basis (0.562 kg), and C_i is the volumetric concentration increase of the *ith* off-gas (ppmv 10^{-6} day^{-1}), based on experimental values reported in ref [307].

Table 127. Parameters used in calculating emissions factors for storage off-gases

Parameter	Type	Unit	Value	Definition
P	Constant	Pa	101,300	Pressure of Storage Gas
Vg	Constant	m^3	0.00152	Volume of Gas
M_{wt}	Constant	g $mole^{-1}$	CO:28, CO_2:44, CH_4:16	Molecular Weight of Off-gasses
R	Constant	J mol^{-1} K^{-1}	8.31	Ideal Gas Constant
T	Constant	Kelvin	293.15	Temperature
M	Constant	kg-dry biomass	0.562	Mass of stored Biomass
C_i	Constant	ppmv day^{-1}	CO:59.5, CO_2:190.1, CH_4:3.82	Off Gas Concentration Increase
Storage Time	Variable	Days	30 to 60	Storage Period

PPM concentrations for storage off-gases for the 11th day were reverse calculated via equation 40 and emissions factors reported in ref [307].It was assumed that the off-gas concentration of CO, CO_2, and CH_4 increase linearly with time when biomass is stored at 20 ^{O}C [307]. The increase in off-gas concentration (PPMV increase per day) is estimated via dividing the experimental concentration PPM at the 11th day by the storage time (days). For example, the rate of CO_2 PPM per day is assumed to be 654.2 PPM/11 Days = 190.1 PPM day^{-1}. The concentration rate is used to extrapolate total off-gas concentration for a nominal storage period.

Table 128. Storage Off-Gas Concentration and Concentration Rate

Storage Off-Gases	Concentration (PPM after 11 days)	Concentration Increase (C_i) (PPM increase per day)
CO	654.2	59.5
CO_2	2090.7	190.1
*CH_4	42	3.82

*Due to data limitations PPM for CH_4 could not be calculated direct, and was estimated via graphical interpretation. Results from ref [307], indicate that the 11-day PPM for CH_4 at a storage temperature of 20^{O}C lies between 40 and 45 PPM. In this work it is assumed that the 11-day CH_4 concentration is 42 PPM.

For example, the mass of CO_2 emitted over an 11-day storage on a dry basis is estimated to be:

$$Emissions\ Factor\ CO_2 = \frac{(101{,}300) \times (0.00152) \times (44) \times (190.1) \times (11)}{(8.31) \times (293.15) \times (0.562) \times 10^9} = 1.03 \times 10^{-5} \frac{kg\ CO_2}{kg\ Dry\ Matter}$$

The emissions factor on a wet basis is estimated to be 9.09×10^{-6} (i.e. 9.09 mg CO_2/kg-biomass) equivalent to the results reported in ref [307] as shown below.

$$CO_2 = \frac{(101{,}300) \times (0.00152) \times (44) \times (190.1) \times (11)}{(8.31) \times (293.15) \times (0.64) \times 10^9} = 9.09 \times 10^{-6} \frac{kg\ CO_2}{kg\ Biomass\ (wet)}$$

A uniform distribution was assumed for short-term storage, with a minimum of 30 days and a maximum of 60 days.

D.4 TRANSPORTATION OF STORED BIOMASS TO REFINERY GATE

Transportation distance from farm-to-refinery was modeled via a triangular distribution assuming one-way transport via lorries and is outlined in 129 and Table 130. A minimum one-way transportation distance of 50 km, most likely value of 100 km, and maximum of 150 km were selected, and capture a broad range of values reported via prior published literature [201, 250, 308].

Table 129. Literature Survey: Transportation of Biomass from Farm to Refinery

Transport Distance: Farm to Refinery	References
50 miles (~80 km)	Jones et al. 2013 [250]
100 km (to BTL) or 50 km (to CHP)	Roedl et al. 2010 [308]
60 miles (~96 km)	Zhang et al. 2013 [201]

BTL: Biomass to Liquid; CHP: Combined Heat and Power

Table 130. Triangular Distribution: Transportation of Biomass from Farm to Refinery

Parameters	Transport Distance: Farm to Refinery
Min	50 km
Max	150 km
Most Likely	100 km

D.5 PRETREATMENT: GRINDING AND CHOPPING

The specific energy requirement for grinding/chopping of woody biomass is represented via the following formula [251]:

$$E = aX^{-b} \quad (41)$$

Where E is the specific energy requirement (kJ/kg-dry biomass) and X is the aperture size in millimeters (mm). It assumed that woody biomass is chopped/ground to a particle size of 3mm [249], and all grinding/chopping energy is provided via electricity. Regression coefficients were taken from Miao et al. [251] and are provided in Table 131.

Table 131. Key Parameters for Grinding and Chopping of Woody Biomass

Feedstock	Regression Coefficient (a)	Regression Coefficient (b)	Specific Energy Consumption (kJ/kg-dry biomass)
Air-Dry Willow	2408	-1.103	716.8

D.6 EXPERIMENTAL SETUP, MODEL COMPOUND METHODOLOGY, AND LABORATORY SCALE RESULTS

Feedstock: Red oak sawdust was used as a starting material for single stage fast pyrolysis and stage 1 experiments. For stage 2, the solid product (solid residue) obtained from stage 1 was used as the feedstock, while for stage 3 (or fast pyrolysis), the solid residue produced from stage 2 was the starting material.

Apparatus: A CDS Analytical Pyroprobe 5250T apparatus (milligrams scale unit) was used to obtain the composition of organic compounds for each stage in the case of multi-stage scenario as well as

for the single stage fast pyrolysis case (see Figure 38). Samples were prepared by loading 0.60-0.80 mg of biomass into a fire polished quartz tube with a filler rod and quartz wool above the rod to prevent the biomass from falling out of the bottom (see Figure 39).

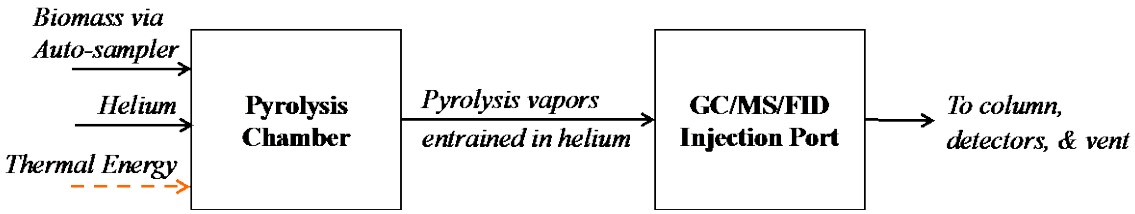

Figure 38. Pyroprobe Schematic

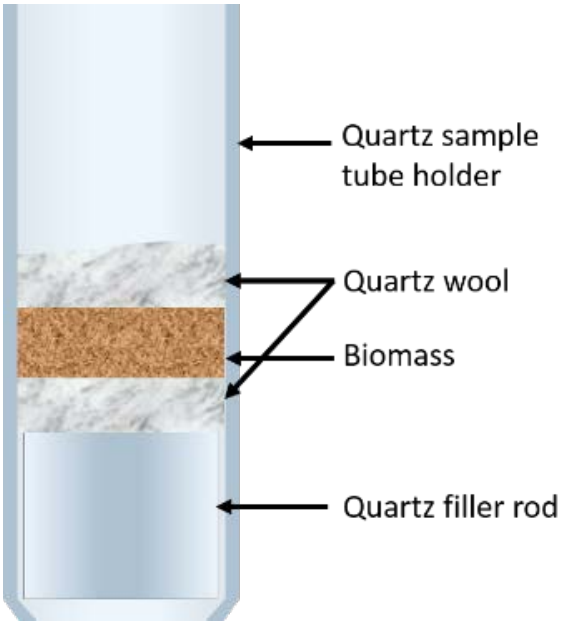

Figure 39. Quartz Sample Tube Diagram

All reactions were carried out in a helium carrier gas at one atmosphere and 94 ml/min total flow. All experiments utilized a 1000°C / second temperature ramp. Evolved vapors were transported via transfer lines heated to 300°C into a Shimadzu QP-2010+ GC/MS-FID system with a 60m long semi-polar RTX-1701 column (250µm diameter, 0.25µm film thickness) for the identification and

quantification of organic compounds. Over 100 individual compounds are identified and quantified. These compounds are listed in Table 132, and are aggregated into groups, which have common upgrading strategies. Each of the groups is assigned a model compound based on the most prevalent and/or chemically representative compound within the group. For example, large non-furanic anhydrosugar compounds are represented by levoglucosan; the group of methoxy phenols (phenols with at least one methoxy group attached to the ring) is represented by guaiacol, a major compound in that group.

Table 132. Model compound aggregation scheme based on identified compounds in the Pyroprobe chromatogram.

Compound Identified by GC	**Model compound**
Acetic acid	*Acetic Acid*
2-Propenal Acetaldehyde Propanal-2-one Butanal 1-Penten-3-one 2,3-Butanedione 3-Pentanone 2-Butanone Hydroxyacetaldehyde 2-Butenal (cis or trans) c2-Hydroxypropanal Hydroxypropanone 2-Propenoic acid methyl ester 1-Hydroxy-2-butanone 3-Hydroxypropanal 2-Hydroxy-3-oxobutanal 1-Acetyloxypropane-2-one 2-Hydroxy-butanedial Butanedial 2,3-Dihydroxyhex-1-ene-4-one	*Acetol*
Furan 2-Methylfuran 2,5-dimethylfuran 2-Acetylfuran 2,3-Dihydro Furan (2H)-Furan-3-one	*Furan*
2-Furaldehyde 2-Furfuryl alcohol 5-Methyl-2-furaldehyde (5H)-Furan-2-one Dihydro-methyl-furanone	*Furfural*

Table 132 (continued).

2-Hydroxy-1-methyl-1-cyclopentene-3-one	
Methyl-butyraldehyde derivative	
gamma-Lactone derivative	
gamma-Butyrolactone	
5-Hydroxymethyl-2-furaldehyde	
4-Cyclopentene-1,3-dione	
2-Furoic acid methyl ester	
OH-methyl-dihydropyranone	
4-Hydroxy-5,6-dihydro-(2H)-pyran-2-one	
3-Hydroxy-2-methyl-pyran-4-one	
Methyl-dihydro-(2H)-pyran-2-one	
2-Cyclopenten-1-one, 2-methyl-	
Cyclopentanone	
Levoglucosan	
1,4:3,6-Dianhydro-glucopyranose	
1,6-Anhydro-beta-D-mannopyranose	*Levoglucosan*
1,5-Anhydro-beta-D-xylofuranose	
Anhydrosugar: unknown	
Toluene	
Phenol	
Styrene	
Benzene, ethyl-	
Benzene, 1,2-dimethyl-	*Toluene*
Benzaldehyde	
Anisole	
1,2,4-Trimethoxybenzene	
Benzylalcohol	
o-Cresol	
m-cresol	
Catechol	
Acetophenone	
Phenol, 4-vinyl-	
Phenol, 2,6-dimethyl-	
Phenol, 2-ethyl-	*Cresol*
Benzaldehyde, 4-hydroxy-	
Catechol, 3-methyl-	
Phenol, 4-allyl-	
Phenol, 4-propenyl-	
Anisole, 2,4-/2,5-dimethyl-	
Phenol, 2-propyl-	

Table 132 (continued).

Guaiacol	*Guaiacol*
Guaiacol, 3-methyl-	
Guaiacol, 4-vinyl-	
Guaiacol, 3-ethyl	
Vanillin	
Syringol	
Eugenol	
Isoeugenol	
Guaiacol, 4-propyl-	
Homovanillin	
Acetoguaiacone	
Syringol, 4-methyl-	
Vanillic acid	
Guaiacol, 4-(oxy-allyl)-	
Coniferaldehyde	
Syringol, 4-vinyl-	
Guaiacyl acetone	
Propioguaiacone	
Coniferyl alcohol	
Syringol, 3-ethyl-	
Dihydroconiferyl alcohol	
Syringaldehyde	
Syringol, 4-allyl-	
Propioguaiacone, alpha-oxy-	
Syringol, 4-propenyl-	
Syringol, 4-propyl-	
Homosyringaldehyde	
Acetosyringone	
Syringol, 4-(oxy-allyl)-	
Sinapaldehyde	
Syringyl acetone	
Propiosyringone	
Sinapyl alcohol	
Propiosyringone, alpha-oxy-	

The total area of the identified compounds accounts for typically ~85% of the total chromatogram area. The remainder of the chromatogram area is in numerous very small peaks distributed throughout the chromatogram, isomeric or chemically similar compounds to those positively identified. The remaining chromatogram area is attributed proportionally to the compound groups. The resulting volatile organic product yields (reported as the mass fraction of the original dry oak biomass) are reported in Table S31, as well as the final biochar resulting from the third stage (pyrolytic) treatment in the Pyroprobe based on tube weight following the third stage thermal treatment.

Table 133. Model compound characterization of bio-oil produced via three-stage torrefaction and Pyrolysis system, and base-case single stage pyrolysis system. Results are presented as the mass fraction of total input ash-free dry biomass, and are based on volatile organic product yields obtained from the Pyroprobe.

	Multistage Torrefaction and Pyrolysis (Mass Fraction %)				**Single Stage Pyrolysis** (Mass Fraction %)
Product	1st Stage	2nd Stage	Pyrolysis (3rd stage)	Total	Total
H_2O	9.20	6.80	0.00	16.00	13.20
Acetic Acid	5.21	1.79	0.39	7.38	8.47
Acetol	2.34	1.80	1.29	5.43	9.24
Furan	0.01	0.14	0.09	0.23	0.28
Furfural	3.99	3.81	0.54	8.33	5.01
Levoglucosan	0.00	6.89	3.48	10.37	18.44
Toluene	0.00	0.64	0.23	0.87	0.37
Guaiacol	2.51	2.26	1.25	6.01	5.86
Cresol	0.03	0.80	0.28	1.12	1.17
Biochar	-	-	10.50	10.50	9.01

In order to accurately measure non-condensable gases and water in the volatilized product, a larger-scale micropyrolysis unit was used. The micropyrolyzer consists of a gram scale reactor and utilizes a twin-screw loss-in-weight feeding auger to load the biomass into the reactor. The unit is divided into three sections, viz., feeding section, reaction section and collection section. The entire feeding unit (comprising hopper, twin-screw auger and motor) rests on a 120 kg capacity scale which continuously measures mass of the feeding unit and an automated controls system maintains a constant mass flow-rate. In the reaction section, a stainless steel reactor was placed inside an electrical furnace, which acts as a heat source and heats the reactor to the desired temperature. The reactor was heated to the desired temperature before the biomass was introduced into it. A thermocouple was inserted inside the reactor from the bottom to directly measure the biomass temperature. Two streams of nitrogen gas, one to the bottom of the reactor and another one to the end of the feeding tube (but above the furnace), were used as fluidizing and sweep gas (or carrier gas). The nitrogen gas with a flow rate of 550 ml/min was pre-heated by flowing through stainless steel tubing coiled around the reactor before flowing into the reactor from the bottom. This pre-heated gas sweeps (or carries) the vapors produced inside the reactor to the sequential ice water and liquid nitrogen condensers (or traps) where the vapors were condensed and the

liquid was collected for further analyses. The nitrogen flow at the end of feeding tube prevents any vapors produced inside the reactor from entering and subsequently condensing in the feeding channel. A cyclone separator was positioned in series between the reactor and the condensers to ensure the solid residue was not carried into the condensers along with the effluent gas. The effluent gas (carrier gas + non-condensable gases) exiting the liquid nitrogen condenser flows through the wet test meter before it is vented in order to measure the volume of non-condensable gases. Total liquid product includes the liquid collected in both the condensers.

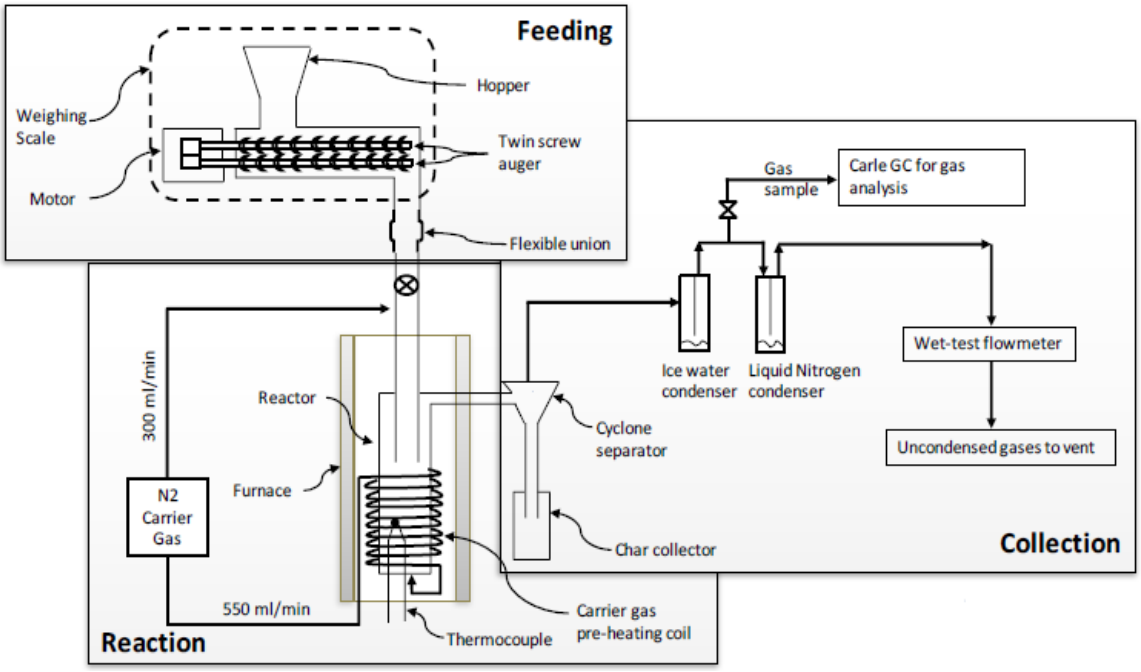

Figure 40. Bench Scale Reactor System

Water content analysis (reported as liquid weight percent) was carried out using a METTLER-TOLEDO V20 Volumetric Karl Fischer Titration Unit. Typically, 0.01-0.1mg (depending on the water content in the liquid sample; larger amount in the case of lower water content) of liquid sample was injected into the titration cell using a syringe and the result was displayed as weight percent (wt. %) of the injected amount. It is assumed that the yield of water (grams of water/g of raw oak) obtained from micro-pyrolyzer for each stage is similar to that obtained from the pyroprobe.

During the pyrolysis and torrefaction experiments carried out in the micropyrolysis system, the non-condensable gases were quantitatively analyzed using a CARLE® Series 400 Analytical Gas Chromatograph (AGC) equipped with a dual thermal conductivity detector. The gas was sampled after the ice water condenser using a 20 ml syringe at different reaction times and injected into the AGC. Effluent gas flowrate was measured using the wet test meter. PeakSimple Chromatography Software from SRI Instruments was used to integrate the chromatogram peaks. After obtaining the peak area, the calibration curves were used to estimate the concentration (mole %) of non-condensable gases in the injected samples. Finally, the mass of non-condensable gases was calculated by using the effluent gas flowrate and assuming STP conditions (one mole of an ideal gas at STP occupies 22.4 liters). Based on GC measurements of volatile products from the Pyroprobe coupled with micropyrolysis unit values for H_2O and non-condensable gases content, the product distributions for each stage are shown in Table 134. The oligomers content was calculated by difference and is defined in equation 41.

Table 134. Model compound characterization of bio-oil produced via three-stage torrefaction and Pyrolysis system, and base-case single stage pyrolysis system. Results are presented as the mass fraction of total input ash-free dry biomass, and are constructed based on coupling the volatile composition obtained from the Pyroprobe with analysis of NCG and water formation obtained from the micropyrolysis unit.

	Multistage Torrefaction and Pyrolysis (Mass Fraction %)				**Single Stage Pyrolysis** (Mass Fraction %)
Product	1st Stage	2nd Stage	Pyrolysis	Total	Total
H_2O	9.20	6.80	0.00	16.00	13.20
Acetic Acid	5.21	1.79	0.39	7.38	8.47
Acetol	2.34	1.80	1.29	5.43	9.24
Furan	0.01	0.14	0.09	0.23	0.28
Furfural	3.99	3.81	0.54	8.33	5.01
Levoglucosan	0.00	6.89	3.48	10.37	18.44
Toluene	0.00	0.64	0.23	0.87	0.37
Guaiacol	2.51	2.26	1.25	6.01	5.86
Cresol	0.03	0.80	0.28	1.12	1.17
Oligomers	-	-	-	6.56	4.66
Bio-Oil (Wet Basis)	23.29	24.92	7.53	55.74	62.04
Gases	7.20	8.50	11.50	27.20	24.30
Biochar			10.50	10.50	9.01
Total	30.49	33.42	29.53	100.00	100.00

$$\begin{pmatrix} Mass\ fraction \\ oligomers \end{pmatrix} = 1 - \begin{pmatrix} mass\ fraction \\ biochar \end{pmatrix} - \begin{pmatrix} mass\ fraction \\ noncondensable\ gases \end{pmatrix} - \begin{pmatrix} mass\ fraction \\ water \end{pmatrix} - \begin{pmatrix} mass\ fraction \\ GC-quantified\ volatiles \end{pmatrix} \quad (41)$$

In this study, the oligomeric content was assumed to be upgradable and was distributed evenly among all the organic compounds, resulting in the product distribution given below in Table 135. The data provided in Table 135 provides the analytical basis and underlying framework for the ASPEN model.

Table 135. Model compound characterization of bio-oil derived via a three-stage torrefaction and pyrolysis design, and comparison with single-stage fast pyrolysis (500 ^{O}C). Results are presented as the mass fraction (%) of total input ash-free dry biomass**.**

	Multistage Torrefaction and Pyrolysis (Mass Fraction %)				**Single Stage Pyrolysis (Mass Fraction %)**
Product	1st Stage	2nd Stage	Pyrolysis	Total	Total
H_2O	9.20	6.80	0.00	16.00	13.20
Acetic Acid	6.06	2.09	0.45	8.60	9.28
Acetol	2.73	2.10	1.50	6.33	10.12
Furan	0.01	0.16	0.10	0.27	0.31
Furfural	4.65	4.43	0.63	9.71	5.49
Levoglucosan	0.00	8.02	4.05	12.08	20.20
Toluene	0.00	0.75	0.26	1.01	0.40
Guaiacol	2.93	2.63	1.45	7.01	6.42
Cresol	0.04	0.93	0.33	1.30	1.29
Bio-Oil (Wet Basis)	25.61	27.91	8.78	62.30	66.69
Gases	7.20	8.50	11.50	27.20	24.30
Biochar	0.00	0.00	10.50	10.50	9.01
Total	32.81	36.41	30.78	100.00	100.00

D.7 WOODY BIOMASS, TORREFIED BIOMASS, AND BIOCHAR COMPOSITION

Composition of woody and torrefied biomass, was based on experimental data for oak feedstock, obtained via the University of Oklahoma, see Table 136. The carbon and hydrogen content in the solid products as well as the raw oak was measured using a CE-440 Elemental Analyzer, purchased from Exeter

Analytical, Inc. Oxygen content was obtained by difference based on the assumption that the amount of other elements (S, Mg, Ca, K, N, etc.) in the raw biomass as well as the solid products is negligible. Biochar produced via multistage and base-case single stage pyrolysis system is assumed to have the same elemental composition. Further, it is assumed that the elemental composition of solid product obtained from micro-pyrolyzer for each stage is similar to that obtained from pyroprobe.

Table 136. Biomass and Biochar Composition

	Elemental Composition (%)				**Proximate Analysis**			
Parameters (Ash Free Dry Basis)	C	H	O	Total	Moisture Content	Ash Content	Volatile Matter	Fixed Carbon
Oak[1,2]	46.9	6.0	47.1	100	0	0	83.9	16.1
1st Stage Torrefied Oak[1,*]	53.9	5.4	40.7	100	0	0	83.9	16.1
2nd Stage Torrefied Oak[1,*]	62.9	4.8	32.3	100	0	0	83.9	16.1
Biochar[3]	86.1	3.4	10.4	100	0	0	32	68

[1]Element composition of Oak and torrefied biomass was based on experimental trials conducted at the University of Oklahoma (Personal Communication).
[2]The Volatile Mater and Fixed Carbon for woody-biomass were obtained via the Phyllis2 Database
*Due to data limitations the Volatile Matter and Fixed Carbon for torrefied biomass was assumed to be equivalent to oak biomass.
[3]Biochar elemental composition and proximate analysis is based on values reported from ref[325]. Elemental composition of biochar was adjusted from their original value(s) to conserve total elemental balance (i.e. so that C, H, and O % sum to 100%). Biochar produced via multistage and base-case single stage pyrolysis system is assumed to have the same elemental composition.

D.8 ESTIMATION OF WOODY BIOMASS AND BIOCHAR/ASH HIGHER HEATING VALUE

The higher heating values (HHV) for oak biochar/ash for multistage and fast pyrolysis systems are estimated to be 30.8 and 30.2 MJ/kg, respectively, see Table 137. The HHVs are constructed based on correlations provided in Channiwala and Parikh [252], see equation 42.

$$\boldsymbol{HHV}\ (\tfrac{\boldsymbol{MJ}}{\boldsymbol{kg}}) = \mathbf{0.3491} * [\boldsymbol{C}\%] + \mathbf{1.1783} * [\boldsymbol{H}\%] + \mathbf{0.105} * [\boldsymbol{S}\%] - \mathbf{0.1034} * [\boldsymbol{O}\%] - \mathbf{0.0151} * [\boldsymbol{N}\%] - \mathbf{0.0211} * [\boldsymbol{A}\%] \quad (42)$$

Where C%, H%, O%, N%, S%, A% represent the carbon, hydrogen, oxygen, nitrogen, sulfur, and ash content respectively, expressed in mass percentages on a dry basis.

Table 137. Estimation of Biochar/Ash Higher Heating Value for Woody Biomass

Parameter	C	H	O	Ash	HHV (MJ/kg)
Fast Pyrolysis - Biochar/Ash Dry Basis (kg/hr)	6376.4	254.2	772.4	1141.7	-
Elemental Fraction (%)	74.6	3.0	9.0	13.4	30.2
Multistage Torrefaction/Pyrolysis - Biochar/Ash Dry Basis (kg/hr)	7434.4	296.3	900.5	1141.7	-
Elemental Fraction (%)	76.1	3.0	9.2	11.7	30.8

D.9 CATALYTIC UPGRADING STRATEGIES

Process yields for catalytic upgrading strategies (ketonization, alkylation, hydrogenation, hydrodeoxygenation) were modeled using equilibrium design blocks in AspenPlus. Specific reaction stoichiometry considered for each of the strategies is described below.

D.9.1 Ketonization

In ketonization two carboxylic acids react to form a ketone, producing carbon dioxide and water as by-products in the reaction, see equation 43.

$$R_1COOH + R_2COOH \rightarrow R_1COR_2 + CO_2 + H_2O \quad (43)$$

Using equation 43, all possible ketones that can be produced via ketonization of carboxylic acids in bio-oil, are provided in Table 138.

Table 138. Ketonization Products

KET#	Carboxylic Acid	Carboxylic Acid	Ketone	Product 1	Product 2
KET1	CH_2O_2	CH_2O_2	CH_2O	H_2O	CO_2
KET2	CH_2O_2	$C_2H_4O_2$	C_2H_4O	H_2O	CO_2
KET3	CH_2O_2	$C_3H_4O_3$	$C_3H_4O_2$	H_2O	CO_2
KET4	CH_2O_2	$C_4H_4O_4$	$C_4H_4O_3$	H_2O	CO_2
KET5	CH_2O_2	$C_4H_6O_4$	$C_4H_6O_3$	H_2O	CO_2
KET6	CH_2O_2	$C_6H_{12}O_7$	$C_6H_{12}O_6$	H_2O	CO_2
KET7	$C_2H_4O_2$	$C_2H_4O_2$	C_3H_6O	H_2O	CO_2
KET8	$C_2H_4O_2$	$C_3H_4O_3$	$C_4H_6O_2$	H_2O	CO_2
KET9	$C_2H_4O_2$	$C_4H_4O_4$	$C_5H_6O_3$	H_2O	CO_2
KET10	$C_2H_4O_2$	$C_4H_6O_4$	$C_5H_8O_3$	H_2O	CO_2
KET11	$C_2H_4O_2$	$C_6H_{12}O_7$	$C_7H_{14}O_6$	H_2O	CO_2
KET12	$C_3H_4O_3$	$C_3H_4O_3$	$C_5H_6O_3$	H_2O	CO_2
KET13	$C_3H_4O_3$	$C_4H_4O_4$	$C_6H_6O_4$	H_2O	CO_2
KET14	$C_3H_4O_3$	$C_4H_6O_4$	$C_6H_8O_4$	H_2O	CO_2
KET15	$C_3H_4O_3$	$C_6H_{12}O_7$	$C_8H_{14}O_7$	H_2O	CO_2
KET16	$C_4H_4O_4$	$C_4H_4O_4$	$C_7H_6O_5$	H_2O	CO_2
KET17	$C_4H_4O_4$	$C_4H_6O_4$	$C_7H_8O_5$	H_2O	CO_2
KET18	$C_4H_4O_4$	$C_6H_{12}O_7$	$C_9H_{14}O_8$	H_2O	CO_2
KET19	$C_4H_6O_4$	$C_4H_6O_4$	$C_7H_{10}O_5$	H_2O	CO_2
KET20	$C_4H_6O_4$	$C_6H_{12}O_7$	$C_9H_{16}O_8$	H_2O	CO_2
KET21	$C_6H_{12}O_7$	$C_6H_{12}O_7$	$C_{11}H_{22}O_{11}$	H_2O	CO_2

D.9.2 Alkylation

During alkylation, an alkylating agent is utilized to upgrade furanic and phenolic compounds, producing a higher carbon chain alkylate as well as H_2O, see equation 44. Alkylates formed via alkylation of different reagents and alkylating agents is provided in Table 139.

$$C_aH_bO_c + C_dH_eO_f \rightarrow C_{a+d}H_{b+e-2}O_{c+f-1} + H_2O \quad (44)$$

Table 139. Alkylation Products

	Reagent	Alkylating Agent	Alkylate	Reagent			Alkylating Agent			Alkylate		
				C	H	O	C	H	O	C	H	O
Alkylation #1	Furan	Ethylene Glycol	ALK1 (C6H8O2)	4	4	1	2	6	2	6	8	2
	Furan	Propylene Glycol	ALK2 (C7H10O2)	4	4	1	3	8	2	7	10	2
	Furan	Isopropanol	ALK3 (C7H10O1)	4	4	1	3	8	1	7	10	1
	Furan	Butylene Glycol	ALK4 (C8H12O2)	4	4	1	4	10	2	8	12	2
	Methylfuran	Ethylene Glycol	ALK5 (C7H10O2)	5	6	1	2	6	2	7	10	2
	Methylfuran	Propylene Glycol	ALK6 (C8H12O2)	5	6	1	3	8	2	8	12	2
	Methylfuran	Isopropanol	ALK7 (C8H12O1)	5	6	1	3	8	1	8	12	1
	Methylfuran	Butylene Glycol	ALK8 (C9H14O2)	5	6	1	4	10	2	9	14	2
	Guaiacol	Ethylene Glycol	ALK9 (C9H12O3)	7	8	2	2	6	2	9	12	3
	Guaiacol	Propylene Glycol	ALK10 (C10H14O3)	7	8	2	3	8	2	10	14	3
	Guaiacol	Isopropanol	ALK11 (C10H14O2)	7	8	2	3	8	1	10	14	2
	Guaiacol	Butylene Glycol	ALK12 (C11H16O3)	7	8	2	4	10	2	11	16	3
	Cresol	Ethylene Glycol	ALK13 (C9H12O2)	7	8	1	2	6	2	9	12	2
	Cresol	Propylene Glycol	ALK14 (C10H14O2)	7	8	1	3	8	2	10	14	2
	Cresol	Isopropanol	ALK15 (C10H14O1)	7	8	1	3	8	1	10	14	1
	Cresol	Butylene Glycol	ALK16 (C11H16O2)	7	8	1	4	10	2	11	16	2
	Toluene	Ethylene Glycol	ALK17 (C9H12O1)	7	8	0	2	6	2	9	12	1
	Toluene	Propylene Glycol	ALK18 (C10H14O1)	7	8	0	3	8	2	10	14	1
	Toluene	Isopropanol	ALK19 (C10H14)	7	8	0	3	8	1	10	14	0
	Toluene	Butylene Glycol	ALK20 (C11H16O1)	7	8	0	4	10	2	11	16	1

Table 139 (continued).

Alkylation #2	ALK1 (C6H8O2)	Ethylene Glycol	2ALK1 (C8H12O3)	6	8	2	2	6	2	8	12	3
	ALK1 (C6H8O2)	Propylene Glycol	2ALK2 (C9H14O3)	6	8	2	3	8	2	9	14	3
	ALK1 (C6H8O2)	Isopropanol	2ALK3 (C9H14O2)	6	8	2	3	8	1	9	14	2
	ALK1 (C6H8O2)	Butylene Glycol	2ALK4 (C10H16O3)	6	8	2	4	10	2	10	16	3
	ALK2 (C7H10O2)	Ethylene Glycol	2ALK5 (C9H14O3)	7	10	2	2	6	2	9	14	3
	ALK2 (C7H10O2)	Propylene Glycol	2ALK6 (C10H16O3)	7	10	2	3	8	2	10	16	3
	ALK2 (C7H10O2)	Isopropanol	2ALK7 (C10H16O2)	7	10	2	3	8	1	10	16	2
	ALK2 (C7H10O2)	Butylene Glycol	2ALK8 (C11H18O3)	7	10	2	4	10	2	11	18	3
	ALK3 (C7H10O1)	Ethylene Glycol	2ALK9 (C9H14O2)	7	10	1	2	6	2	9	14	2
	ALK3 (C7H10O1)	Propylene Glycol	2ALK10 (C10H16O2)	7	10	1	3	8	2	10	16	2
	ALK3 (C7H10O1)	Isopropanol	2ALK11 (C10H16O1)	7	10	1	3	8	1	10	16	1
	ALK3 (C7H10O1)	Butylene Glycol	2ALK12 (C11H18O2)	7	10	1	4	10	2	11	18	2
	ALK4 (C8H12O2)	Ethylene Glycol	2ALK13 (C10H16O3)	8	12	2	2	6	2	10	16	3
	ALK4 (C8H12O2)	Propylene Glycol	2ALK14 (C11H18O3)	8	12	2	3	8	2	11	18	3
	ALK4 (C8H12O2)	Isopropanol	2ALK15 (C11H18O2)	8	12	2	3	8	1	11	18	2
	ALK4 (C8H12O2)	Butylene Glycol	2ALK16 (C12H20O3)	8	12	2	4	10	2	12	20	3
	ALK5 (C7H10O2)	Ethylene Glycol	2ALK17 (C9H14O3)	7	10	2	2	6	2	9	14	3
	ALK5 (C7H10O2)	Propylene Glycol	2ALK18 (C10H16O3)	7	10	2	3	8	2	10	16	3
	ALK5 (C7H10O2)	Isopropanol	2ALK19 (C10H16O2)	7	10	2	3	8	1	10	16	2
	ALK5 (C7H10O2)	Butylene Glycol	2ALK20 (C11H18O3)	7	10	2	4	10	2	11	18	3
	ALK6 (C8H12O2)	Ethylene Glycol	2ALK21 (C10H16O3)	8	12	2	2	6	2	10	16	3
	ALK6 (C8H12O2)	Propylene Glycol	2ALK22 (C11H18O3)	8	12	2	3	8	2	11	18	3
	ALK6 (C8H12O2)	Isopropanol	2ALK23 (C11H18O2)	8	12	2	3	8	1	11	18	2
	ALK6 (C8H12O2)	Butylene Glycol	2ALK24 (C12H20O3)	8	12	2	4	10	2	12	20	3
	ALK7 (C8H12O1)	Ethylene Glycol	2ALK25 (C10H16O2)	8	12	1	2	6	2	10	16	2
	ALK7 (C8H12O1)	Propylene Glycol	2ALK26 (C11H18O2)	8	12	1	3	8	2	11	18	2

Table 139 (continued).

Alkylation #2	ALK7 (C8H12O1)	Isopropanol	2ALK27 (C11H18O1)	8	12	1	3	8	1	11	18	1
	ALK7 (C8H12O1)	Butylene Glycol	2ALK28 (C12H20O2)	8	12	1	4	10	2	12	20	2
	ALK8 (C9H14O2)	Ethylene Glycol	2ALK29 (C11H18O3)	9	14	2	2	6	2	11	18	3
	ALK8 (C9H14O2)	Propylene Glycol	2ALK30 (C12H20O3)	9	14	2	3	8	2	12	20	3
	ALK8 (C9H14O2)	Isopropanol	2ALK31 (C12H20O2)	9	14	2	3	8	1	12	20	2
	ALK8 (C9H14O2)	Butylene Glycol	2ALK32 (C13H22O3)	9	14	2	4	10	2	13	22	3
	ALK9 (C9H12O3)	Ethylene Glycol	2ALK33 (C11H16O4)	9	12	3	2	6	2	11	16	4
	ALK9 (C9H12O3)	Propylene Glycol	2ALK34 (C12H18O4)	9	12	3	3	8	2	12	18	4
	ALK9 (C9H12O3)	Isopropanol	2ALK35 (C12H18O3)	9	12	3	3	8	1	12	18	3
	ALK9 (C9H12O3)	Butylene Glycol	2ALK36 (C13H20O4)	9	12	3	4	10	2	13	20	4
	ALK0 (C10H14O3)	Ethylene Glycol	2ALK37 (C12H18O4)	10	14	3	2	6	2	12	18	4
	ALK10 (C10H14O3)	Propylene Glycol	2ALK38 (C13H20O4)	10	14	3	3	8	2	13	20	4
	ALK10 (C10H14O3)	Isopropanol	2ALK39 (C13H20O3)	10	14	3	3	8	1	13	20	3
	ALK10 (C10H14O3)	Butylene Glycol	2ALK40 (C14H22O4)	10	14	3	4	10	2	14	22	4
	ALK11 (C10H14O2)	Ethylene Glycol	2ALK41 (C12H18O3)	10	14	2	2	6	2	12	18	3
	ALK11 (C10H14O2)	Propylene Glycol	2ALK42 (C13H20O3)	10	14	2	3	8	2	13	20	3
	ALK11 (C10H14O2)	Isopropanol	2ALK43 (C13H20O2)	10	14	2	3	8	1	13	20	2
	ALK11 (C10H14O2)	Butylene Glycol	2ALK44 (C14H22O3)	10	14	2	4	10	2	14	22	3
	ALK12 (C11H16O3)	Ethylene Glycol	2ALK45 (C13H20O4)	11	16	3	2	6	2	13	20	4
	ALK12 (C11H16O3)	Propylene Glycol	2ALK46 (C14H22O4)	11	16	3	3	8	2	14	22	4
	ALK12 (C11H16O3)	Isopropanol	2ALK47 (C14H22O3)	11	16	3	3	8	1	14	22	3
	ALK12 (C11H16O3)	Butylene Glycol	2ALK48 (C15H24O4)	11	16	3	4	10	2	15	24	4
	ALK13 (C9H12O2)	Ethylene Glycol	2ALK49 (C11H16O3)	9	12	2	2	6	2	11	16	3
	ALK13 (C9H12O2)	Propylene Glycol	2ALK50 (C12H18O3)	9	12	2	3	8	2	12	18	3
	AlLK13 (C9H12O2)	Isopropanol	2ALK51 (C12H18O2)	9	12	2	3	8	1	12	18	2
	ALK13 (C9H12O2)	Butylene Glycol	2ALK52 (C13H20O3)	9	12	2	4	10	2	13	20	3
	ALK14 (C10H14O2)	Ethylene Glycol	2ALK53 (C12H18O3)	10	14	2	2	6	2	12	18	3

Table 139 (continued).

Alkylation #2	ALK14 (C10H14O2)	Propylene Glycol	2ALK54 (C13H20O3)	10	14	2	3	8	2	13	20	3
	ALK14 (C10H14O2)	Isopropanol	2ALK55 (C13H20O2)	10	14	2	3	8	1	13	20	2
	ALK14 (C10H14O2)	Butylene Glycol	2ALK56 (C14H22O3)	10	14	2	4	10	2	14	22	3
	ALK15 (C10H14O1)	Ethylene Glycol	2ALK57 (C12H18O2)	10	14	1	2	6	2	12	18	2
	ALK15 (C10H14O1)	Propylene Glycol	2ALK58 (C13H20O2)	10	14	1	3	8	2	13	20	2
	ALK15 (C10H14O1)	Isopropanol	2ALK59 (C13H20O1)	10	14	1	3	8	1	13	20	1
	ALK15 (C10H14O1)	Butylene Glycol	2ALK60 (C14H22O2)	10	14	1	4	10	2	14	22	2
	ALK16 (C11H16O2)	Ethylene Glycol	2ALK61 (C13H20O3)	11	16	2	2	6	2	13	20	3
	ALK16 (C11H16O2)	Propylene Glycol	2ALK62 (C14H22O3)	11	16	2	3	8	2	14	22	3
	ALK16 (C11H16O2)	Isopropanol	2ALK63 (C14H22O2)	11	16	2	3	8	1	14	22	2
	ALK16 (C11H16O2)	Butylene Glycol	2ALK64 (C15H24O3)	11	16	2	4	10	2	15	24	3
	ALK17 (C9H12O1)	Ethylene Glycol	2ALK65 (C11H16O2)	9	12	1	2	6	2	11	16	2
	ALK17 (C9H12O1)	Propylene Glycol	2ALK66 (C12H18O2)	9	12	1	3	8	2	12	18	2
	ALK17 (C9H12O1)	Isopropanol	2ALK67 (C12H18O1)	9	12	1	3	8	1	12	18	1
	ALK17 (C9H12O1)	Butylene Glycol	2ALK68 (C13H20O2)	9	12	1	4	10	2	13	20	2
	ALK18 (C10H14O1)	Ethylene Glycol	2ALK69 (C12H18O2)	10	14	1	2	6	2	12	18	2
	ALK18 (C10H14O1)	Propylene Glycol	2ALK70 (C13H20O2)	10	14	1	3	8	2	13	20	2
	ALK18 (C10H14O1)	Isopropanol	2ALK71 (C13H20O1)	10	14	1	3	8	1	13	20	1
	ALK18 (C10H14O1)	Butylene Glycol	2ALK72 (C14H22O2)	10	14	1	4	10	2	14	22	2
	ALK19 (C10H14)	Ethylene Glycol	2ALK73 (C12H18O1)	10	14	0	2	6	2	12	18	1
	ALK19 (C10H14)	Propylene Glycol	2ALK74 (C13H20O1)	10	14	0	3	8	2	13	20	1
	ALK19 (C10H14)	Isopropanol	2ALK75 (C13H20)	10	14	0	3	8	1	13	20	0
	ALK19 (C10H14)	Butylene Glycol	2ALK76 (C14H22O1)	10	14	0	4	10	2	14	22	1
	ALK20 (C11H16O1)	Ethylene Glycol	2ALK77 (C13H20O2)	11	16	1	2	6	2	13	20	2
	ALK20 (C11H16O1)	Propylene Glycol	2ALK78 (C14H22O2)	11	16	1	3	8	2	14	22	2
	ALK20 (C11H16O1)	Isopropanol	2ALK79 (C14H22O1)	11	16	1	3	8	1	14	22	1
	ALK20 (C11H16O1)	Butylene Glycol	2ALK80 (C15H24O2)	11	16	1	4	10	2	15	24	2

D.9.3 Hydrolysis and Oxidation

During hydrolysis and oxidation bio-oil compounds are converted to carboxylic acids via the use of an oxidizing agent, see equations 45 to 48.

$$C_3H_6O_2 + 2H_2O_2 \rightarrow C_3H_4O_3 + 3H_2O \quad (45)$$

$$C_4H_4O + 3H_2O_2 \rightarrow C_4H_4O_4 + 3H_2O \quad (46)$$

$$C_5H_4O_2 + 2H_2O_2 \rightarrow C_4H_6O_4 + CH_2O_2 \quad (47)$$

$$C_6H_{10}O_5 + H_2O_2 \rightarrow C_6H_{12}O_7 \quad (48)$$

D.9.4 Hydrogenation

Hydrogenation utilizes mild hydro-processing conditions to convert bio-oils compounds to stable intermediates, see equations 49 to 53.

$$C_2H_4O_2 + 3H_2 \rightarrow C_2H_6 + 2H_2O \quad (49)$$

$$C_3H_6O_2 + H_2 \rightarrow C_3H_8O_2 \quad (50)$$

$$C_3H_6O + H_2 \rightarrow C_3H_8O \quad (51)$$

$$C_5H_4O_2 + 2H_2 \rightarrow C_5H_6O_1 + H_2O \quad (52)$$

$$2C_6H_{10}O_5 + 8H_2 \rightarrow C_2H_6O_2 + 2C_3H_8O_2 + C_4H_{10}O_2 + 2H_2O \quad (53)$$

D.9.5 Hydrodeoxygenation

Hydrodeoxygenation utilizes severe hydroprocessing conditions to completely remove oxygen from bio-oil compounds, producing water as a byproduct. A generalized form of the reaction is defined in equation 54. The set of all possible reactions considered in HDO are provided in Table 140.

$$C_aH_bO_c + (\frac{d-b+2c}{2})H_2 \rightarrow C_aH_d + cH_2O \quad (54)$$

Table 140. Hydrodeoygenation - Products

HDO Reactions	Reaction Stoichiometry
Acetic Acid + Hydrogen = Ethane + Water	C2H4O2 + 3H2 = C2H6 + 2H2O
Formic Acid + Hydrogen = Methane + H2O	CH2O2+3H2 = CH4+2H2O
Pyruvic Acid + Hydrogen = Propane + H2O	C3H4O3 + 5H2 = C3H8+3H2O
Maleic Acid + Hydrogen = Butane + H2O	C4H4O4 + 7H2 = C4H10 + 4H2O
Succinic Acid + Hydrogen = Butane + H2O	C4H6O4 + 6H2 = C4H10 + 4H2O
Glucionic Acid + Hydrogen = Hexane + H2O	C6H12O7 + 8H2 = C6H14 + 7H2O
Acetone + Hydrogen = Propane + Water	C3H6O + 2H2 = C3H8 + H2O
Isopropanol + Hydrogen = Propane + Water	C3H8O+H2=C3H8+H2O
Ethylene Glycol + Hydrogen = Ethane + Water	C2H6O2 + 2H2 = C2H6 + 2H2O
Propylene Glycol + Hydrogen = Ethane + Water	C3H8O2+ 2H2 = C3H8 + 2H2O
Butylene Glycol + Hydrogen = Ethane + Water	C4H10O2 + 2H2 = C4H10 + 2H2O
Acetol + Hydrogen = Propane + Water	C3H6O2 + 3H2 = C3H8 + 2H2O
Furan + Hydrogen = Butane + Water	C4H4O + 4H2 = C4H10 + H2O
Furfural + Hydrogen = Pentane + Water	C5H4O2 + 6H2 = C5H12 + 2H2O
Methylfuran + Hydrogen = Pentane + Water	C5H6O + 4H2 = C5H12 + H2O
Levoglucosan + Hydrogen = Ethane + Propane + Butane + Water	2C6H10O5 + 10H2 = C2H6 + 2C3H8 + C4H10 + 10H2O
Guaiacol + Hydrogen = Cresol + Water	C7H8O2 +H2 = C7H8O + H2O
Cresol + Hydrogen = Toluene + Water	C7H8O +H2 = C7H8 + H2O
Ket1 + Hydrogen = Methane + Water	C1H2O1 + 2H2 = CH4 + H2O
Ket2 + Hydrogen = Ethane + Water	C2H4O1 + 2H2 = C2H6 + H2O
Ket3 + Hydrogen = Propane + Water	C3H4O2+ 4H2 = C3H8 + 2H2O
Ket4 + Hydrogen = Butane + Water	C4H4O3+ 6H2 = C4H10 +3 H2O
Ket5 + Hydrogen = Butane + Water	C4H6O3+ 5H2 = C4H10 + 3H2O
Ket6 + Hydrogen = Hexane + Water	C6H12O6+ 7H2 = C6H14 + 6H2O
Ket8 + Hydrogen = Butane + Water	C4H6O2+ 4H2 = C4H10 + 2H2O
Ket9 + Hydrogen = Pentane + Water	C5H6O3+ 6H2 = C5H12 + 3H2O
Ket10 + Hydrogen = Pentane + Water	C5H8O3+ 5H2 = C5H12 + 3H2O
Ket11 + Hydrogen = Heptane + Water	C7H14O6+ 7H2 = C7H16 + 6H2O
Ket12 + Hydrogen = Pentane + Water	C5H6O3+ 6H2 = C5H12 + 3H2O
Ket13 + Hydrogen = Hexane + Water	C6H6O4+ 8H2 = C6H14 + 4H2O
Ket14 + Hydrogen = Hexane + Water	C6H8O4+ 7H2 = C6H14 + 4H2O
Ket15 + Hydrogen = Octane + Water	C8H14O7+ 9H2 = C8H18 + 7H2O
Ket16 + Hydrogen = Heptane + Water	C7H6O5+ 10H2 = C7H16 + 5H2O
Ket17 + Hydrogen = Heptane + Water	C7H8O5+ 9H2 = C7H16 + 5H2O
Ket18 + Hydrogen = Nonane + Water	C9H14O8+ 11H2 = C9H20 + 8H2O
Ket19 + Hydrogen = Heptane + Water	C7H10O5+ 8H2 = C7H16 + 5H2O
Ket20 + Hydrogen = Nonane + Water	C9H16O8+ 10H2 = C9H20 + 8H2O
Ket21 + Hydrogen = Undecane + Water	C11H22O11+ 12H2 = C11H24 + 11H2O
1ALK1 + Hydrogen = Hexane + Water	C6H8O2 + 5H2 = C6H14 + 2H2O
1ALK2 + Hydrogen = Heptane + Water	C7H10O2+ 5H2 = C7H16 + 2H2O
1ALK3 + Hydrogen = Heptane + Water	C7H10O1+ 4H2 =C7H16 + H2O
1ALK4 + Hydrogen = Octane + Water	C8H12O2+ 5H2 = C8H18 + 2H2O
1ALK5 + Hydrogen = Heptane + Water	C7H10O2+ 5H2 = C7H16 + 2H2O
1ALK6 + Hydrogen = Octane + Water	C8H12O2+ 5H2 = C8H18 + 2H2O
1ALK7 + Hydrogen = Octane + Water	C8H12O1+ 4H2 = C8H18 + H2O
1ALK8 + Hydrogen = Nonane + Water	C9H14O2+ 5H2 = C9H20 + 2H2O
1ALK9 + Hydrogen = HDO1 + Water	C9H12O3+ 2H2 = C9H12O + 2H2O
1ALK10 + Hydrogen = HDO2 + Water	C10H14O3+ 2H2 = C10H14O + 2H2O
1ALK11 + Hydrogen = HDO3 + Water	C10H14O2+ H2 = C10H14O + H2O
1ALK12 + Hydrogen = HDO4 + Water	C11H16O3+ 2H2 = C11H16O + 2H2O
1ALK13 + Hydrogen = HDO5 + Water	C9H12O2+ 2H2 = C9H12 + 2H2O
1ALK14 + Hydrogen = HDO6 + Water	C10H14O2+ 2H2 = C10H14 + 2H2O
1ALK15 + Hydrogen = HDO7 + Water	C10H14O1+ H2 = C10H14 + H2O
1ALK16 + Hydrogen = HDO8 + Water	C11H16O2+ 2H2 = C11H16 + 2H2O
1ALK17 + Hydrogen = HDO9 + Water	C9H12O1+ H2 = C9H12 + H2O
1ALK18 + Hydrogen = HDO10 + Water	C10H14O1+ H2 = C10H14 + H2O
1ALK19 + Hydrogen = HDO11 + Water	C10H14 + H2 = C10H14 + H2O
1ALK20 + Hydrogen = HDO12 + Water	C11H16O1+ H2 = C11H16 + H2O

Table 140 (continued).

2ALK1 + Hydrogen = Octane + Water	C8H12O3 + 6H2 = C8H18 + 3H2O
2ALK2 + Hydrogen = Nonane + Water	C9H14O3 + 6 H2 = C9H20 + 3H2O
2ALK3 + Hydrogen = Nonane + Water	C9H14O2 + 5H2 = C9H20 + 2H2O
2ALK4 + Hydrogen = Decane + Water	C10H16O3 + 6H2 = C10H22 + 3H2O
2ALK5 + Hydrogen = Decane + Water	C10H16O3 + 6H2 = C10H22 + 3H2O
2ALK6 + Hydrogen = Decane + Water	C10H16O2 + 5H2 = C10H22 + 2H2O
2ALK7 + Hydrogen = Undecane + Water	C11H18O3 + 6H2 = C11H24 + 3H2O
2ALK8 + Hydrogen = Decane + Water	C10H16O1 + 4H2 = C10H22 + H2O
2ALK9 + Hydrogen = Undecane + Water	C11H18O2 + 5H2 = C11H24 + 2H2O
2ALK10 + Hydrogen = Dodecane + Water	C12H20O3 + 6H2 = C12H26 + 3H2O
2ALK11 + Hydrogen = Nonane + Water	C9H14O3 + 6H2 = C9H20 + 3H2O
2ALK12 + Hydrogen = Decane + Water	C10H16O3 + 6H2 = C10H22 + 3H2O
2ALK13 + Hydrogen = Decane + Water	C10H16O2 + 5H2 = C10H22 + 2H2O
2ALK14 + Hydrogen = Undecane + Water	C11H18O3 + 6H2 = C11H24 + 3H2O
2ALK15 + Hydrogen = Undecane + Water	C11H18O3 + 6H2 = C11H24 + 3H2O
2ALK16 + Hydrogen = Undecane + Water	C11H18O2 + 5H2 = C11H24 + 2H2O
2ALK17 + Hydrogen = Dodecane + Water	C12H20O3 + 6H2 = C12H26 + 3H2O
2ALK18 + Hydrogen = Undecane + Water	C11H18O1 + 4H2 = C11H24 + H2O
2ALK19 + Hydrogen = Dodecane + Water	C12H20O2 + 5H2 = C12H26 + 2H2O
2ALK20 + Hydrogen = Tridecane + Water	C13H22O3 + 6H2 = C13H28 + 3H2O
2ALK21 + Hydrogen = HDO13 + Water	C11H16O4 + 3H2 = C11H16O + 3H2O
2ALK22 + Hydrogen = HDO14 + Water	C12H18O4 + 3H2 = C12H18O + 3H2O
2ALK23 + Hydrogen = HDO15 + Water	C12H18O3 + 2H2 = C12H18O + 2H2O
2ALK24 + Hydrogen = HDO16 + Water	C13H20O4 + 3H2 = C13H20O + 3H2O
2ALK25 + Hydrogen = HDO17 + Water	C13H20O4 + 3H2 = C13H20O + 3H2O
2ALK26 + Hydrogen = HDO18 + Water	C13H20O3 + 2H2 = C13H20O + 2H2O
2ALK27 + Hydrogen = HDO19 + Water	C14H22O4 + 3H2 =C14H22O + 3H2O
2ALK28 + Hydrogen = HDO20 + Water	C13H20O2 + H2 = C13H20O + H2O
2ALK29 + Hydrogen = HDO21 + Water	C14H22O3 + 2H2 = C14H22O + 2H2O
2ALK30 + Hydrogen = HDO22 + Water	C15H24O4 + 3H2 = C15H24O + 3H2O
2ALK31 + Hydrogen = HDO23 + Water	C11H16O3 + 3H2 = C11H16 + 3H2O
2ALK32 + Hydrogen = HDO24 + Water	C12H18O3 + 3H2 = C12H18 + 3H2O
2ALK33 + Hydrogen = HDO25 + Water	C12H18O2 + 2H2 = C12H18 + 2H2O
2ALK34 + Hydrogen = HDO26 + Water	C13H20O3 + 3H2 = C13H20 + 3H2O
2ALK35 + Hydrogen = HDO27 + Water	C13H20O3 + 3H2 = C13H20 + 3H2O
2ALK36 + Hydrogen = HDO28 + Water	C13H20O2 + 2H2 = C13H20 + 2H2O
2ALK37 + Hydrogen = HDO29 + Water	C14H22O3 + 3H2 = C14H22 + 3H2O
2ALK38 + Hydrogen = HDO30 + Water	C13H20O1 + H2 = C13H20 + H2O
2ALK39 + Hydrogen = HDO31 + Water	C14H22O2 + 2H2 = C14H22 + 2H2O
2ALK40 + Hydrogen = HDO32 + Water	C15H24O3 + 3H2 = C15H24 + 3H2O
2ALK41 + Hydrogen = HDO33 + Water	C11H16O2 + 2H2 = C11H16 + 2H2O
2ALK42 + Hydrogen = HDO34 + Water	C12H18O2 + 2H2 = C12H18 + 2H2O
2ALK43 + Hydrogen = HDO35 + Water	C12H18O1 + H2 = C12H18 + H2O
2ALK44 + Hydrogen = HDO36 + Water	C13H20O2 + 2H2 = C13H20 + 2H2O
2ALK45 + Hydrogen = HDO37 + Water	C13H20O2 + 2H2 = C13H20 + 2H2O
2ALK46 + Hydrogen = HDO38 + Water	C13H20O1 + H2 = C13H20 + H2O
2ALK47 + Hydrogen = HDO39 + Water	C14H22O2 + 2H2 = C14H22 + 2H2O
2ALK48 + Hydrogen = HDO40 + Water	C13H20O0 + 0H2 = C13H20 + 0H2O
2ALK49 + Hydrogen = HDO41 + Water	C14H22O1 + H2 = C14H22 + H2O
2ALK50 + Hydrogen = HDO42 + Water	C15H24O2 + 2H2 = C15H24 + 2H2O

*1ALK19 and 2ALK48 are unaffected by HDO as the oxygen content of these compounds is null.

Several multistage design cases, consisting of different catalytic strategies for upgrading fractionated bio-oil are considered. A detailed summary of the multistage systems is provided below.

Multistage System 1 upgrades bio-oil fractions independently, targeting promising conversion pathways based on the composition of each stream. In this configuration, stage 1 bio-oil undergoes ketonization (180 ^{O}C, 27 atm) to convert carboxylic acids (acetic acid) to ketones (acetone) and byproducts (CO_2, H_2O). Mild hydrogenation (100 ^{O}C, 27 atm) is performed to convert acetol to propylene glycol, acetone to isopropanol, and furfural to 2-methylfuran, producing water as a secondary product in the reaction. Post hydrogenation, stage 1 bio-oil is sent to an alkylation reactor (125 ^{O}C, 27 atm) in which alcohols act as alkylating agents to upgrade furanics (furan and 2-methylfuran) and aromatics (guaiacol, cresol, toluene) producing alkylates as well as water as a secondary product in the reaction. Stage 2 bio-oil undergoes an initial hydrolysis and oxidation (80 ^{O}C, 1 atm) step, using hydrogen-peroxide as an oxidizing agent to convert levoglucosan to glucionic acid, furfural to succinic and formic acid, furan to maleic acid, and acetol to pyruvic acid. Stage 2 bio-oil is sent to a ketonization reactor (360 ^{0}C, 27 atm), which converts carboxylic acids into ketones ranging from C1-C11 in carbon chain length, producing H_2O and CO_2 as byproducts. Stage 3 bio-oil is hydrogenated (100 ^{0}C, 27 atm), decomposing levoglucosan into alcohols (Ethylene Glycol, Propylene Glycol, Butylene Glycol), and converting acetic acid to ethane, acetol to propylene glycol, furfural to 2-methylfuran, producing water as a byproduct in the reaction. Stage 3 bio-oil is subsequently sent to an alkylation reactor (125 ^{0}C, 27 atm) in which alcohols act as alkylating agents to upgrade furanics (furan and 2-methylfuran) and aromatics (guaiaicol, cresol, toluene) producing alkylates as well

as byproduct H_2O. All streams are hydrodeoxygenated (400 ^{0}C, 55 atm) for removal of oxygen from bio-oil compounds, forming H_2O in the reaction.

Multistage System 2 employs an integrated strategy, upgrading stage 1 & 2 bio-oil concurrently. In this design, hydrolysis and oxidation (80 ^{0}C, 1 atm) using H_2O_2 as an oxidizing agent, is utilized to convert light oxygenates, furanics, and anhydrosugars present in stage 1 & 2 bio-oil, into a host of carboxylic acids including formic acid, acetic acid, pyruvic acid, maleic acid, succinic acid, and glucionic acid, yielding water and carbon dioxide as byproducts. Integrated stage 1 & 2 bio-oil is sent to a ketonization reactor (360 ^{0}C, 27 atm) to produce ketones ranging from C1-C11 in carbon number, forming byproduct CO_2 and H_2O. Aromatics (guaiacol, cresol, toluene) and light ketones are separated from the integrated stage 1 & 2 bio-oil stream, and coupled with stage 3 bio-oil. Partial hydrogenation (100 ^{0}C, 27 atm) of coupled stage 3 bio-oil is utilized to convert levoglucosan into alcohols, acetone to isopropanol, acetic acid to ethane, acetol to propylene glycol, and furfural to 2-methylfuran, producing H_2O during the reaction. Coupled stage 3 bio-oil is subsequently sent to an alkylation reactor (125 ^{0}C, 27 atm) in which alcohols (Ethylene Glycol, Propylene Glycol, Isopropanol, and Butylene Glycol) act as alkylating agents to upgrade furanics (furan and 2-methylfuran) and aromatics (guaiaicol, cresol, toluene) producing alkylates as well as byproduct H_2O. All streams are hydrodeoxygenated (400 ^{0}C, 55 atm) for removal of oxygen from bio-oil compounds, forming H_2O in the reaction.

Multistage System 3 adopts an integrated minimalist approach, utilizing a minimal number of design blocks to upgrade bio-oil. In this design, integrated stage 1 & 2 bio-oil streams undergo ketonization (180 ^{0}C, 27 atm) to convert acetic acid into acetone, producing CO_2 and H_2O as byproducts in the reaction. Post-ketonization, integrated stage 1 & 2 bio-oil are coupled with stage 3 bio-oil and subsequently hydrogenated (100 ^{0}C, 27 atm). Hydroprocessing converts

levoglucosan into alcohols, acetone to isopropanol, acetic acid to ethane, acetol to propylene glycol, and furfural to 2-methylfuran, producing H_2O during the reaction. Bio-oil is subsequently sent to an alkylation reactor (125 ^{0}C, 27 atm) in which alcohols (Ethylene Glycol, Propylene Glycol, Isopropanol, and Butylene Glycol) act as alkylating agents to upgrade furanics (furan and 2-methylfuran) and aromatics (guaiacol, cresol, toluene) producing alkylates as well as byproduct H_2O. All streams are hydrodeoxygenated (400 ^{0}C, 55 atm) to remove oxygen from bio-oil compounds, forming H_2O in the reaction.

D.10 BIOREFINERY UTILITIES

Net heating and cooling duties for the evaluated design cases were constructed based on pinch analysis, assuming a dTmin of 10 ^{O}C. The hot and cold composite curves for each of the examined design cases are provided in the following figures.

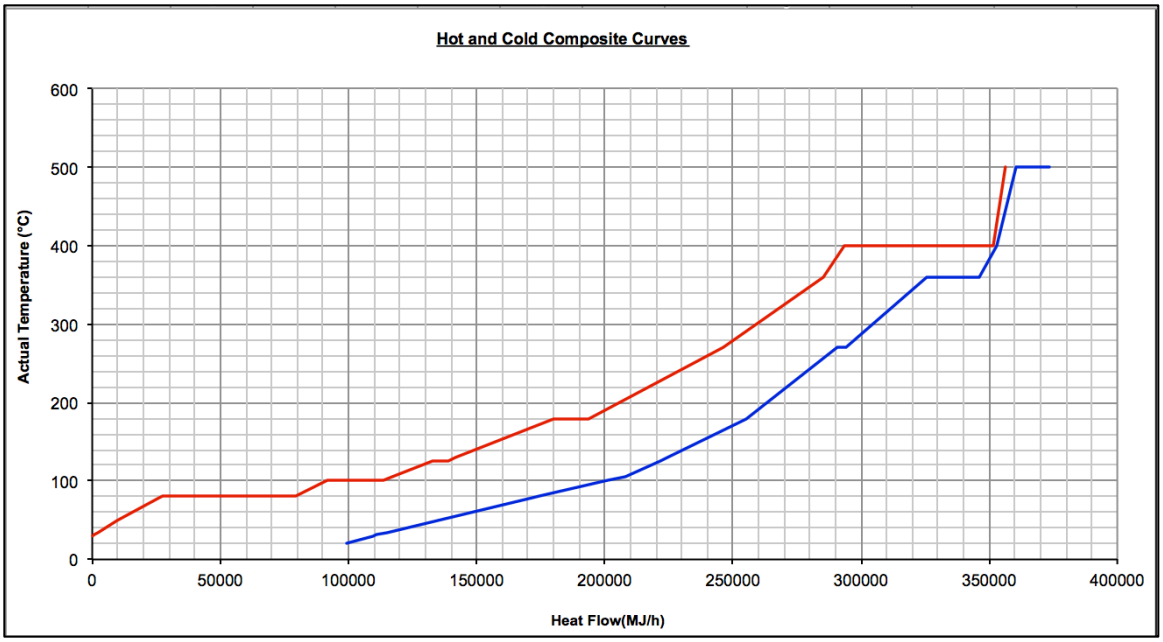

Figure 41. Multistage System 1: Hot and Cold Composite Curves

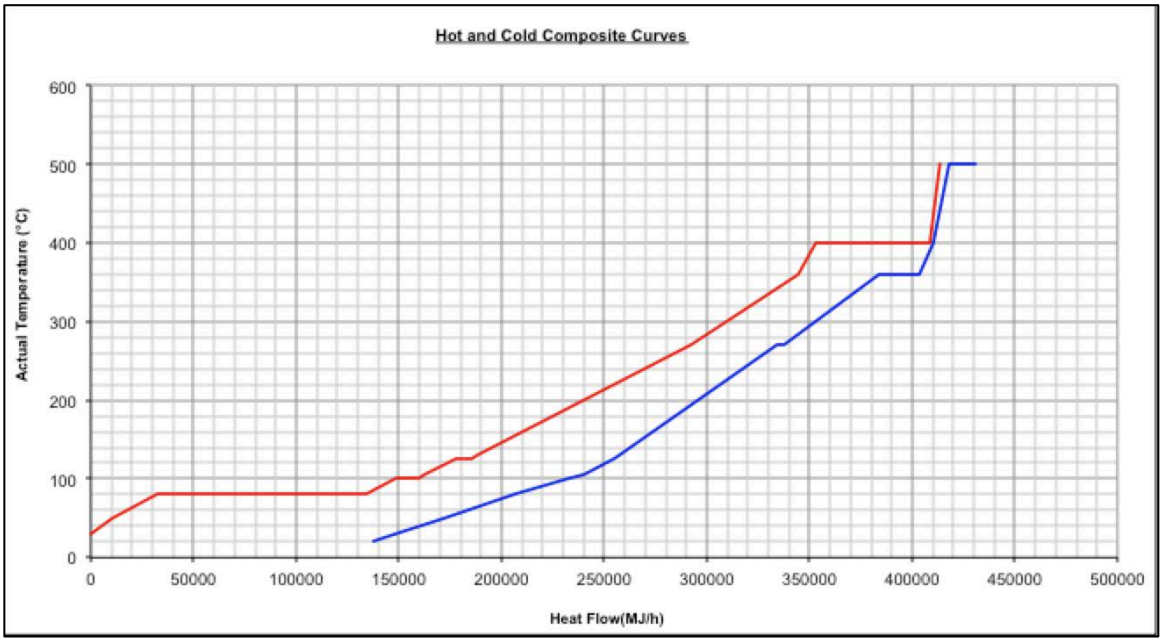

Figure 42. Multistage System 2: Hot and Cold Composite Curves

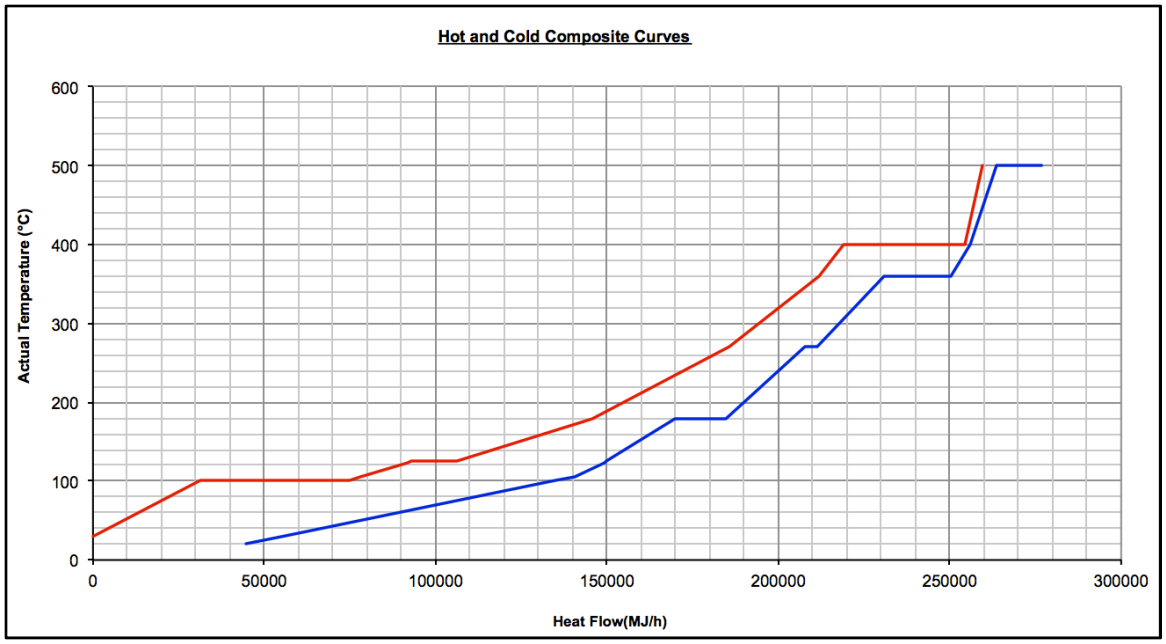

Figure 43. Multistage System 3: Hot and Cold Composite Curves

Figure 44. Single Stage Fast Pyrolysis and HDO: Hot and Cold Composite Curves

Electricity consumption for net cooling duty was estimated via the work required for pumping cooling water. The mass flow of cooling water (m) was estimated based on the specific heat capacity (C_p) of water (4180 J/kg-water), nominal temperature differential (10 ^{O}C), and net cooling duty (MJ/hr), defined in equation 55.

$$mC_p\Delta T = Net\ Cooling\ Duty \quad (55)$$

The total pressure drop across the cooling water loop is estimated to be 38.7 psi (266.7 kPa), constructed based on 15 psi (pipe head losses) + 5 psi (exchanger losses) + 10 psi (control valve loss) + 8.7 psi of static head assuming water must be pumped to the top of the cooling tower an average height of 20 ft, Power required for cooling water pumps with a volumetric flow rate V, and an overall efficiency of 75% is provided in equation 56. Process utilities for all examined design cases are provided in Table 141.

$$Pump\ Power\ (\frac{MJ}{Hr}) = \frac{1}{\varepsilon}V\Delta P = \frac{1}{0.75} * \left(\frac{V}{10^6}\right)(266.7) \quad (56)$$

Table 141. Biorefinery Utilities

Parameter	**Unit**	**Fast Pyrolysis HDO**	**Multistage Torrefaction & Pyrolysis**		
			System 1	*System 2*	*System 3*
Pretreatment	Electricity (MJ/hr)	59733	59733	59733	59733
Compressors	Electricity (MJ/hr)	6095	2792	2980	1856
Pumps	Electricity (MJ/hr)	339	488	415	391
Cooling Utility	Electricity (MJ/hr)	1019	843	1173	381
***Heating Duty**	Heat Input (MJ/hr)	48170	17372	17319	17198
***Cooling Duty**	Heat Removed (MJ/hr)	119829	99068	137895	44830

*Based on Optimal Heat Exchange Network

D.11 TRANSPORTATION OF BIOFUEL FROM REFINERY GATE TO PUMP

Transportation of biomass-based diesel from the refinery-to-pump is based on the 2016 GREET model[269]. It is assumed that biomass-based diesel is transported from refinery to bulk terminal assuming a transportation mix of 8% by barge, 29% by rail, 63% by heavy duty truck (on a mass basis) and a corresponding average transportation distance of 520 miles, 800 miles, and 50 miles respectively. Biomass-based diesel is subsequently transported from bulk terminal to refueling station via heavy-duty trucks assuming a one-way transportation distance of 30 miles.

Table 142. Transportation of Biofuel Diesel from Refinery to Bulk Terminal

	Transportation Mix (% Mass Basis)	**Transport Distance: Refinery to Bulk Terminal (Miles)**
Heavy Truck	8 %	50 Miles
Rail	29 %	800 Miles
Barge	63 %	520 Miles

*Constructed based on data for pyrolysis diesel fuel pathways in the GREET 2016 Model [269].

Table 143. Transportation of Biofuel from Bulk Terminal to Refueling Station

	Transportation Mix (% Mass Basis)	**Transport Distance: Bulk Terminal to Refueling Station (Miles)**
Heavy Truck	100 %	30 Miles
Rail	-	-
Barge	-	-

*Constructed based on data for pyrolysis diesel fuel pathways in the GREET 2016 Model [269].

D.12 LIFE CYCLE DATA AQUISITION

Table 144 provides an overview of life cycle data sources and life cycle impact assessment (LCIA) methods used in this study.

Table 144. Life cycle data sources

Material or Process Description	Unit	Database	Method	C.I.	N
Urea, as N (RER) | production | Alloc Def U	kg	Ecoinvent	IPCC 2013 GWP 100a V1.01	95%	10,000
Urea, as N (RER) | production | Alloc Def U	kg	Ecoinvent	Cumulative Energy Demand V 1.09	95%	10,000
Nitrogen fertilizer, as N (RER) | calcium ammonium nitrate production | Alloc, Def U	kg	Ecoinvent	IPCC 2013 GWP 100a V1.01	95%	10,000
Nitrogen fertilizer, as N (RER) | calcium ammonium nitrate production | Alloc, Def U	kg	Ecoinvent	Cumulative Energy Demand V 1.09	95%	10,000
Phosphate fertilizer, as P2O5 (RER) | triple superphosphate production | Alloc Def U	kg	Ecoinvent	IPCC 2013 GWP 100a V1.01	95%	10,000
Phosphate fertilizer, as P2O5 (RER) | triple superphosphate production | Alloc Def U	kg	Ecoinvent	Cumulative Energy Demand V 1.09	95%	10,000
Potassium Sulfate, as K2O (RER) | potassium sulfate production | Alloc Def, U	kg	Ecoinvent	IPCC 2013 GWP 100a V1.01	95%	10,000
Potassium Sulfate, as K2O (RER) | potassium sulfate production | Alloc Def, U	kg	Ecoinvent	Cumulative Energy Demand V 1.09	95%	10,000
Lime Fertilizer, at regional storehouse/RER Mass	kg	Agri-footprint	IPCC 2013 GWP 100a V1.01	N/A	N/A
Lime Fertilizer, at regional storehouse/RER Mass	kg	Agri-footprint	Cumulative Energy Demand V 1.09	N/A	N/A
Ground Calcium Carbonate (GCC) – Dry, uncoated, at plant, RER S	kg	Ecoinvent	IPCC 2013 GWP 100a V1.01	N/A	N/A
Ground Calcium Carbonate (GCC) – Dry, uncoated, at plant, RER S	kg	Ecoinvent	Cumulative Energy Demand V 1.09	N/A	N/A
Irrigation (US) | Processing | Alloc Def, U	kg	Ecoinvent	IPCC 2013 GWP 100a V1.01	N/A	N/A
Irrigation (US) | Processing | Alloc Def, U	kg	Ecoinvent	Cumulative Energy Demand V 1.09	N/A	N/A
Glyphosate (RER) | production | Alloc Def U	kg	Ecoinvent	IPCC 2013 GWP 100a V1.01	95%	10,000
Glyphosate (RER) | production | Alloc Def U	kg	Ecoinvent	Cumulative Energy Demand V 1.09	95%	10,000

Table 144 (continued).

Pesticide, unspecified (RER) | production | Alloc Def, U	kg	Ecoinvent	IPCC 2013 GWP 100a V1.01	95%	10,000
Pesticide, unspecified (RER) | production | Alloc Def, U	kg	Ecoinvent	Cumulative Energy Demand V 1.09	95%	10,000
Diesel (RoW) market for | Alloc Def U	Kg	Ecoinvent	IPCC 2013 GWP 100a V1.01	95%	10,000
Diesel (RoW) market for | Alloc Def U	kg	Ecoinvent	Cumulative Energy Demand V 1.09	95%	10,000
Transport, freight, lorry > 32 metric tons, EURO5 (ROW) | Alloc Def U	tkm	Ecoinvent	IPCC 2013 GWP 100a V1.01	95%	10,000
Transport, freight, lorry > 32 metric tons, EURO5 (ROW) | Alloc Def U	tkm	Ecoinvent	Cumulative Energy Demand V 1.09	95%	10,000
Electricity, High Voltage U.S. | Production Mix | Alloc, Def U	MJ	Ecoinvent	IPCC 2013 GWP 100a V1.01	95%	10,000
Electricity, High Voltage U.S. | Production Mix | Alloc, Def U	MJ	Ecoinvent	Cumulative Energy Demand V 1.09	95%	10,000
Zeolite, powder (RER) | Production | Alloc Def U	kg	Ecoinvent	IPCC 2013 GWP 100a V1.01	N/A	N/A
Zeolite, powder (RER) | Production | Alloc Def U	kg	Ecoinvent	Cumulative Energy Demand V 1.09	N/A	N/A
Hydrogen (reformer) E	kg	Industry data 2.0	IPCC 2013 GWP 100a V1.01	N/A	N/A
Hydrogen (reformer) E	kg	Industry data 2.0	Cumulative Energy Demand V 1.09	N/A	N/A
Heat, natural gas, at industrial furnace >100 kW/RER U	MJ	Ecoinvent	IPCC 2013 GWP 100a V1.01	95%	10,000
Heat, natural gas, at industrial furnace >100 kW/RER U	MJ	Ecoinvent	Cumulative Energy Demand V 1.09	95%	10,000
Hydrogen peroxide, without water, in 50% solution state (RER) | hydrogen peroxide production, product in 50% solution state | Alloc Def, U	kg	Ecoinvent	IPCC 2013 GWP 100a V1.01	95%	10,000
Hydrogen peroxide, without water, in 50% solution state (RER) | hydrogen peroxide production, product in 50% solution state | Alloc Def, U	kg	Ecoinvent	Cumulative Energy Demand V 1.09	95%	10,000
Transport, freight, inland waterways, barge (RER) |processing| Alloc Def, U	tkm	Ecoinvent	IPCC 2013 GWP 100a V1.01	95%	10,000
Transport, freight, inland waterways, barge (RER) |processing| Alloc Def, U	tkm	Ecoinvent	Cumulative Energy Demand V 1.09	95%	10,000
Transport, freight train (US)| diesel| Alloc Def, U	tkm	Ecoinvent	IPCC 2013 GWP 100a V1.01	95%	10,000
Transport, freight train (US)| diesel| Alloc Def, U	tkm	Ecoinvent	Cumulative Energy Demand V 1.09	95%	10,000

D.13 OVERVIEW OF KEY PARAMETERS AND DISTRIBUTIONS

Table 145. Overview of key parameters and probability distributions

Parameter	Unit	Distribution	Mean	St. Dev.	Min	Max	Most Likely	Point Est.
Direct Land Use Change								
SOCREF	Tonnes C ha-1	Point Est.	-	-	-	-	-	95
FLU	Unitless	Point Est.	-	-	-	-	-	1
FMG	Unitless	Triangular	-	-	0.7	1	0.95	-
Above and Below Ground Biomass	Tonnes d.m ha-1	Normal	13.6	5.1	-	-	-	-
Biomass Carbon Content	% C	Point Est.						47%
Cuttings Production								
N-Fertilizer application	kg N Cutting-1	Point Est.	-	-	-	-	-	5.2E-04
P-Fertilizer application	kg P Cutting-1	Point Est.	-	-	-	-	-	6.5E-04
K-Fertilizer application	kg K Cutting-1	Point Est.	-	-	-	-	-	3.9E-04
CaCO3 application	kg CaCO3 Cutting-1	Point Est.	-	-	-	-	-	6.5E-03
Herbicide Application	L Herbicide Cutting-1	Point Est.	-	-	-	-	-	2.0E-05
Diesel Use	L Diesel Cutting-1	Point Est.	-	-	-	-	-	7.5E-04
Woody Biomass Production								
Woody Biomass Growth Rates	Tonnes d.m ha-1	Bootstrapping	-	-	-	-	-	-
SRWC Stand Life	Years	Bootstrapping	-	-	-	-	-	-
Cuttings	Cuttings ha-1	Bootstrapping	-	-	-	-	-	-
N Fertilizer application	kg ha-1	Bootstrapping	-	-	-	-	-	-
P Fertilizer application	kg ha-1	Bootstrapping	-	-	-	-	-	-
K Fertilizer application	kg ha-1	Bootstrapping	-	-	-	-	-	-
Lime Fertilizer application	kg ha-1	Bootstrapping	-	-	-	-	-	-
Herbicide application	kg ha-1	Bootstrapping	-	-	-	-	-	-
Irrigation application	m3 ha-1	Bootstrapping	-	-	-	-	-	-
Frequency - Plowing	Unitless	Bootstrapping	-	-	-	-	-	-
Frequency - Harrowing	Unitless	Bootstrapping	-	-	-	-	-	-
Frequency - Disking	Unitless	Bootstrapping	-	-	-	-	-	-
Frequency – Mechanical Weeding	Unitless	Bootstrapping	-	-	-	-	-	-
Frequency – Chemical Weeding	Unitless	Bootstrapping	-	-	-	-	-	-
Frequency – Fertilizing (Lime)	Unitless	Bootstrapping	-	-	-	-	-	-
Frequency – Fertilizing (N/P/K)	Unitless	Bootstrapping	-	-	-	-	-	-
Frequency – Planting	Unitless	Bootstrapping	-	-	-	-	-	-
Frequency – Pest Control	Unitless	Bootstrapping	-	-	-	-	-	-
Frequency – Irrigation	Unitless	Bootstrapping	-	-	-	-	-	-
Frequency – Coppicing	Unitless	Bootstrapping	-	-	-	-	-	-
Frequency – Harvesting/Chipping	Unitless	Bootstrapping	-	-	-	-	-	-
Frequency – Stump Removal	Unitless	Bootstrapping	-	-	-	-	-	-
Diesel Use - Plowing	L-Diesel ha-1	Bootstrapping	-	-	-	-	-	-
Diesel Use - Harrowing	L-Diesel ha-1	Bootstrapping	-	-	-	-	-	-
Diesel Use - Disking	L-Diesel ha-1	Bootstrapping	-	-	-	-	-	-
Diesel Use – Mechanical Weeding	L-Diesel ha-1	Bootstrapping	-	-	-	-	-	-
Diesel Use – Chemical Weeding	L-Diesel ha-1	Bootstrapping	-	-	-	-	-	-
Diesel Use – Fertilizer (Lime)	L-Diesel ha-1	Bootstrapping	-	-	-	-	-	-

Table 145 (continued).

Diesel Use – Fertilizer (N/P/K)	L-Diesel ha-1	Bootstrapping	-	-	-	-	-	-
Diesel Use – Planting	L-Diesel ha-1	Bootstrapping	-	-	-	-	-	-
Diesel Use – Pest Control	L-Diesel ha-1	Bootstrapping	-	-	-	-	-	-
Diesel Use – Irrigation	L-Diesel ha-1	Bootstrapping	-	-	-	-	-	-
Diesel Use – Coppicing	L-Diesel ha-1	Bootstrapping	-	-	-	-	-	-
Diesel Use – Harvesting/Chipping	L-Diesel ha-1	Bootstrapping	-	-	-	-	-	-
Diesel Use – Stump Removal	L-Diesel ha-1	Bootstrapping	-	-	-	-	-	-
Direct N2O Emissions	(% N volatilized)	Bootstrapping	-	-	-	-	-	-
Indirect N2O	Soil N Vol. Rate (%)	Triangular	-	-	3%	30%	10%	-
Indirect N2O	Runoff rate (%)	Triangular	-	-	10%	80%	30%	-
Indirect N2O	Conv. Rate (%)	Triangular	-	-	0.05%	2.5%	0.75%	-
Harvest Efficiency	(%)	Uniform	-	-	77.4%	94.5%	-	-
Moisture Content Biomass (Pre-Storage)	(%)	Point Est.	-	-	-	-	-	50
Storage Period	Days	Uniform	-	-	30	60	-	-
Moisture Content Biomass (Post-Storage)	(%)	Point Est.	-	-	-	-	-	25
Local Transport								
Transport Biomass (Farm-to-Refinery)	Km	Triangular	-	-	50	150	100	-
Fuel Conversion & Upgrading								
Weight Hourly Space Velocity	Hr-1	Point Est.	-	-	-	-	-	0.2
Catalyst Lifetime	Days	Uniform	-	-	60	365	-	-
Fuel Transport and Distribution								
Transport Biofuel (Refinery-to-Bulk Terminal) via Barge	Miles	Point Est.	-	-	-	-	-	520
Transport Biofuel (Refinery-to-Bulk Terminal) via Rail	Miles	Point Est.	-	-	-	-	-	800
Transport Biofuel (Refinery-to-Bulk Terminal) via Heavy Duty Truck	Miles	Point Est.	-	-	-	-	-	50
Transportation Mix (Barge)	%	Point Est.	-	-	-	-	-	8%
Transportation Mix (Rail)	%	Point Est.	-	-	-	-	-	29%
Transportation Mix (Heavy Duty Truck)	%	Point Est.	-	-	-	-	-	63%
Transport Biofuel (Bulk Terminal-to-Refueling station)	Miles	Point Est.	-	-	-	-	-	30
Coproduct and Scenario Analyiss								
CHP – Heat Conv. Efficiency	(%)	Triangular	-	-	44%	48%	52%	-
CHP – Electrical Conv. Efficiency	(%)	Triangular			20%	35%	25%	
Biochar Carbon Loss	(% C emitted to atm.)	Uniform	-	-	0%	20%	-	-
Transport Biochar (Refinery-to-Farm) via Heavy Duty Truck	Km	Triangular	-	-	50	150	100	-
Diesel Use - Biochar land application	L Diesel ha-1	Triangular	-	-	0.9	4.7	2	-

Table 146. Key parameters in the calculation of EROI and Life Cycle GHG Emissions

Parameter	Symbol	Units	Notes
Biofuel Energy	$E_{biofuel}$	MJ	$(LHV_{biofuel})*(Mass_{biofuel})$
Coproduct Electricity	C_{Elec}	MJ	Based on CHP Electrical conversion efficiency. $C_{Elec} = C_{Elec,Exp} + C_{Elec,Recycle}$
Electricity Export	$C_{Elec,Exp}$	MJ	If Coproduct Electricity (C_{Elec}) exceeds Process Electricity Requirements (P_{Elec}), surplus electricity is exported offsite and displaces the U.S. average electricity mix. Electricity Export ($C_{elec,Exp}$) = (C_{Elec}-P_{Elec}).
Electricity Recycle	$C_{Elec,Recycle}$	MJ	Coproduct electricity that is used onsite to meet process electricity utility, $C_{Elec,Recycle} \leq P_{Elec}$
Coproduct Heat	C_{Heat}	MJ	Based on CHP Heat conversion efficiency. Only usable heat is considered (i.e. $C_{Heat,Recycle} \leq P_{Heat}$).
Process Electricity	P_{Elec}	MJ	Based on Elec. Utility from Hybrid model
Process Heat	P_{Heat}	MJ	Based on Heat Duty from ASPEN simulation
Primary Energy Impact Factor - Electricity	$IF_{PE,Elec}$	MJ Primary Fossil Energy/MJ-Electricity	Based on data obtained from life cycle databases
Primary Energy Impact Factor - Heat	$IF_{PE,Heat}$	MJ Primary Fossil Energy/MJ-Heat	Based on data obtained from life cycle databases
Global Warming Potential Impact Factor - Electricity	$IF_{GHG,Elec}$	kg CO_2e./MJ-Electricity	Based on data obtained from life cycle databases
Global Warming Potential Impact Factor - Heat	$IF_{GHG,Heat}$	kg CO_2e./MJ-Heat	Based on data obtained from life cycle databases
Primary fossil energy for all other material, energy, and emissions flows	PE_{Misc}	MJ Primary Fossil Energy	Primary Fossil Energy consumption for all material and energy flows (excluding process heating, electrical utility, and biofuel transport)
Life Cycle GHG emissions for all other material, energy, and emissions flows	GHG_{Misc}	kg CO_2e	Life cycle GHG emissions for all material, energy, and emissions flows (excluding process heating, electrical utility, and biofuel transport)
GHG sequestration from Biochar	GHG_{Char}	kg CO_2e	Based on carbon content (C%) of biochar, as well as fraction of carbon remitted to atm. as CO2
Life Cycle GHG emissions from Biofuel Transport	$GHG_{Fuel\ Transport}$	kg CO_2e	Life cycle GHG emissions for transporting biofuel to regional fuel facility
Primary Energy Consumption from Biofuel Transport	$PE_{Fuel\ Transport}$	MJ Primary Fossil Energy	Primary Energy Consumption for transporting biofuel to regional fuel facility

$$EROI_{Disp} = \frac{E_{biofuel}}{[(PE_{Misc})+IF_{PE,Heat}*(P_{Heat}-C_{Heat})+IF_{PE,Elec}*(P_{Elec}-C_{Elec,Recycle})]-[IF_{PE,Elec}*(C_{Elec,Exp})]+PE_{Fuel\ Transport}} \quad (57)$$

$$EROI_{Energy\ Alloc} = \frac{E_{biofuel}}{[(PE_{Misc})+IF_{PE,Heat}*(P_{Heat}-C_{Heat})+IF_{PE,Elec}*(P_{Elec}-C_{Elec,Recycle})]*\left[\frac{E_{biofuel}}{E_{biofuel}+C_{Elec,Exp}}\right]+PE_{Fuel\ Transport}} \quad (58)$$

$$GHG_{Disp,SA} = \frac{[(GHG_{Misc})+IF_{GHG,Heat}*(P_{Heat}-C_{Heat})+IF_{GHG,Elec}*(P_{Elec}-C_{Elec,Recycle})-GHG_{Char}]-[IF_{GHG,Elec}*(C_{Elec,Exp})]+GHG_{Fuel\ Trasport}}{E_{biofuel}} \quad (59)$$

$$GHG_{Disp,CHP} = \frac{[(GHG_{Misc})+IF_{GHG,Heat}*(P_{Heat}-C_{Heat})+IF_{GHG,Elec}*(P_{Elec}-C_{Elec,Recycle})]-[IF_{GHG,Elec}*(C_{Elec,Exp})]+GHG_{Fuel\ Trasport}}{E_{biofuel}} \quad (60)$$

$$GHG_{Energy\ Alloc,SA} = \frac{[(GHG_{Misc})+IF_{GHG,Heat}*(P_{Heat}-C_{Heat})+IF_{GHG,Elec}*(P_{Elec}-C_{Elec,Recycle})-GHG_{Char}]*\left[\frac{E_{biofuel}}{E_{biofuel}+C_{Elec,Exp}}\right]+GHG_{Fuel\ Trasport}}{E_{biofuel}} \quad (61)$$

$$GHG_{Energy\ Alloc,CHP} = \frac{\left[(GHG_{Misc}) + IF_{GHG,Heat} * (P_{Heat} - C_{Heat}) + IF_{GHG,Elec} * (P_{Elec} - C_{Elec,Recycle})\right] * \left[\frac{E_{biofuel}}{E_{biofuel} + C_{Elec,Exp}}\right] + GHG_{Fuel\ Trasport}}{E_{biofuel}} \quad (62)$$

The 10th, 50th, and 90th percentiles for EROI and life cycle GHG emission for renewable fuels produced via Fast Pyrolysis HDO and Multistage Systems are provided in Table 147 and Table 148 respectively.

Table 147. Median EROI (MJ-Fuel/MJ-Primary Fossil Energy) for base-case Fast Pyrolysis HDO and Multistage Systems

LCA Scheme	Biochar Coproduct Scenario	Fast Pyrolysis HDO	Multistage System 1	Multistage System 2	Multistage System 3
Displacement	Soil Amendment	-	1.66 (1.20,2.10)	1.32 (0.98,1.64)	2.07 (1.48,2.65)
Energy Allocation	Soil Amendment	0.96 (0.67,1.25)	1.66 (1.20,2.10)	1.32 (0.98,1.64)	2.07 (1.48,2.65)
Displacement	Combined Heat & Power	-	2.90 (1.73,4.95)	2.14 (1.36,3.38)	3.76 (2.17,6.51)
Energy Allocation	Combined Heat & Power	1.11 (0.78,1.45)	1.95 (1.38,2.53)	1.50 (1.11,1.88)	2.89 (1.89,4.07)

Results for EROI are tabulated as X (Y,Z) where X=50th Percentile, Y=10th Percentile, Z=90th Percentile

Table 148. Median Life cycle GHG emissions (gCO_2e/MJ-Fuel) for base-case Fast Pyrolysis HDO and Multistage Systems

LCA Scheme	Biochar Coproduct Scenario	Fast Pyrolysis HDO	Multistage System 1	Multistage System 2	Multistage System 3
Displacement	Soil Amendment	-	20 (11,40)	27 (16,49)	17 (10,35)
Energy Allocation	Soil Amendment	52 (35,89)	20 (11,40)	27 (16,49)	17 (10,35)
Displacement	Combined Heat & Power	-	30 (20,50)	38 (26,60)	38 (26,60)
Energy Allocation	Combined Heat & Power	87 (71,120)	42 (35,61)	53 (44,73)	53 (44,73)

Results for EROI are tabulated as X (Y,Z) where X=50th Percentile, Y=10th Percentile, Z=90th Percentile

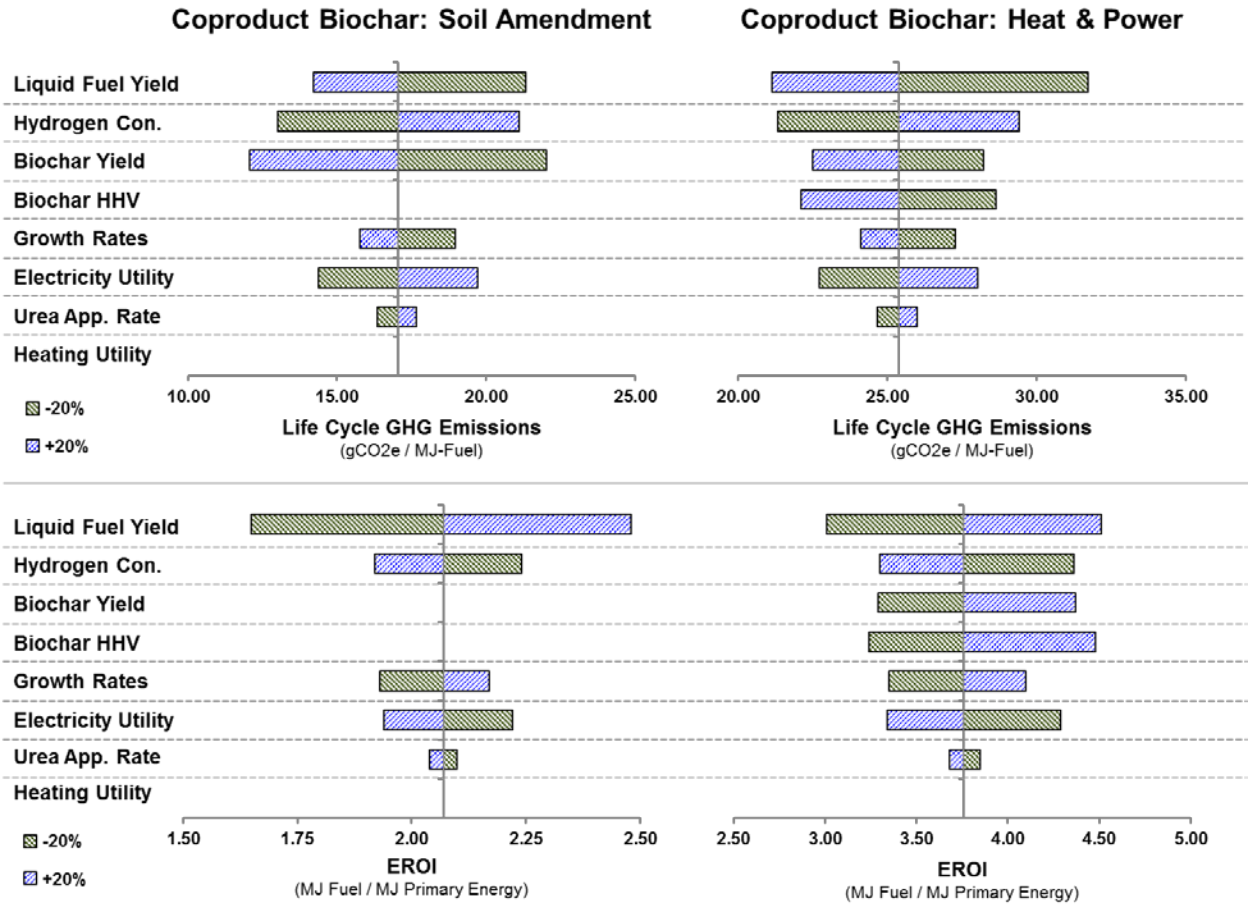

Figure 45. Sensitivity Analysis: Multistage Design Case #3. Tornado Plots for median EROI and Life Cycle GHG emissions using displacement method**.**

BIBLIOGRAPHY

[1] J. Sarukhan, A. Whyte, R. Hassan, R. Scholes, N. Ash, S. Carpenter, *et al.*, "Millenium Ecosystem Assessment: Ecosystems and human well-being," 2005.

[2] S. Q. Solomon, D.; Manning, M.; Chen, Z.; Marquis, M.; and K. T. Averyt, M.; Miller, H., "IPCC, 2007: Climate Change 2007: The Physical Science Basis," ed. New York: Cambridge University Press, 2007.

[3] O. Edenhofer, R. Pichs-Madruga, Y. Sokona, E. Farahani, S. Kadner, K. Seyboth, *et al.*, "Climate change 2014: mitigation of climate change," *Contribution of Working Group III to the Fifth Assessment Report of the Intergovernmental Panel on Climate Change*, pp. 511-597, 2014.

[4] R. K. Pachauri, M. R. Allen, V. R. Barros, J. Broome, W. Cramer, R. Christ, *et al.*, "Climate Change 2014: Synthesis Report. Contribution of Working Groups I, II and III to the Fifth Assessment Report of the Intergovernmental Panel on Climate Change," 2014.

[5] C. D. Thomas, A. Cameron, R. E. Green, M. Bakkenes, L. J. Beaumont, Y. C. Collingham, *et al.*, "Extinction risk from climate change," *Nature*, vol. 427, pp. 145-148, 01/08/print 2004.

[6] J. Rockstrom, W. Steffen, K. Noone, A. Persson, F. S. Chapin, E. F. Lambin, *et al.*, "A safe operating space for humanity," *Nature*, vol. 461, pp. 472-475, 09/24/print 2009.

[7] D. M. Alonso, J. Q. Bond, and J. A. Dumesic, "Catalytic conversion of biomass to biofuels," *Green Chemistry*, vol. 12, pp. 1493-1513, 2010.

[8] M. J. Climent, A. Corma, and S. Iborra, "Conversion of biomass platform molecules into fuel additives and liquid hydrocarbon fuels," *Green Chemistry*, vol. 16, pp. 516-547, 2014.

[9] P. Fairley, "Introduction: Next generation biofuels," *Nature*, vol. 474, pp. S2-S5, 2011.

[10] F. Sissine, "Energy Independence and Security Act of 2007: A summary of major provisions," Library of Congress, Congressional Research Service., Washington DC CRS Order Code RL34294, 2007.

[11] F. Sissine, "Energy Independence and Security Act of 2007: A Summary of Major Provisions," Congressional Research Service Report for Congress, Order Code RL34294, Washington, DC2007.

[12] E. Commission, "Directive 2009/28/EC of the European Parliament and of the Council of 23 April 2009 on the promotion of the use of energy from renewable sources and amending and subsequently repealing Directives 2001/77/EC and 2003/30," *Official Journal of the European Union,* vol. 5, p. 2009, 2009.

[13] D. Pimentel, T. Patzek, and G. Cecil, "Ethanol production: Energy, economic, and environmental losses," in *Reviews of Environmental Contamination and Toxicology*. vol. 189, D. Whitacre, G. Ware, H. Nigg, D. Doerge, L. Albert, P. Voogt, *et al.*, Eds., ed: Springer New York, 2007, pp. 25-41.

[14] R. Sims, M. Taylor, J. Saddler, and W. Mabee, "From 1st-to 2nd-Generation Biofuel Technologies: An overview of current industry and RD&D activities," *International Energy Agency and Organization for Economic Cooperation and Development,* 2008.

[15] R. E. H. Sims, W. Mabee, J. N. Saddler, and M. Taylor, "An overview of second generation biofuel technologies," *Bioresource Technology,* vol. 101, pp. 1570-1580, Mar 2010.

[16] J. Fargione, J. Hill, D. Tilman, S. Polasky, and P. Hawthorne, "Land clearing and the biofuel carbon debt," *Science,* vol. 319, pp. 1235-8, Feb 29 2008.

[17] T. Searchinger, R. Heimlich, R. A. Houghton, F. X. Dong, A. Elobeid, J. Fabiosa, *et al.*, "Use of US croplands for biofuels increases greenhouse gases through emissions from land-use change," *Science,* vol. 319, pp. 1238-1240, Feb 29 2008.

[18] T. W. Patzek, "Thermodynamics of the corn-ethanol biofuel cycle," *Critical Reviews in Plant Sciences,* vol. 23, pp. 519-567, 2004/11/01 2004.

[19] R. Hammerschlag, "Ethanol's energy return on investment: A survey of the literature 1990−present," *Environmental science & technology,* vol. 40, pp. 1744-1750, 2006/03/01 2006.

[20] G. R. Timilsina, J. C. Beghin, D. van der Mensbrugghe, and S. Mevel, "The impacts of biofuels targets on land-use change and food supply: A global CGE assessment," *Agricultural Economics,* vol. 43, pp. 315-332, May 2012.

[21] S. Nonhebel, "Global food supply and the impacts of increased use of biofuels," *Energy,* vol. 37, pp. 115-121, Jan 2012.

[22] R. D. Perlack and B. J. Stokes, *US billion-ton update: biomass supply for a bioenergy and bioproducts industry*: Oak Ridge National Laboratory, 2011.

[23] P. S. Nigam and A. Singh, "Production of liquid biofuels from renewable resources," *Progress in Energy and Combustion Science,* vol. 37, pp. 52-68, 2// 2011.

[24] G. W. Huber and J. A. Dumesic, "An overview of aqueous-phase catalytic processes for production of hydrogen and alkanes in a biorefinery," *Catalysis Today,* vol. 111, pp. 119-132, 1/15/ 2006.

[25] G. W. Huber, S. Iborra, and A. Corma, "Synthesis of Transportation Fuels from Biomass: Chemistry, Catalysts, and Engineering," *Chemical Reviews,* vol. 106, pp. 4044-4098, 2006/09/01 2006.

[26] S. K. Lee, H. Chou, T. S. Ham, T. S. Lee, and J. D. Keasling, "Metabolic engineering of microorganisms for biofuels production: from bugs to synthetic biology to fuels," *Current Opinion in Biotechnology,* vol. 19, pp. 556-563, 12// 2008.

[27] J. N. Chheda and J. A. Dumesic, "An overview of dehydration, aldol-condensation and hydrogenation processes for production of liquid alkanes from biomass-derived carbohydrates," *Catalysis Today,* vol. 123, pp. 59-70, 5/30/ 2007.

[28] J. N. Chheda, G. W. Huber, and J. A. Dumesic, "Liquid-Phase Catalytic Processing of Biomass-Derived Oxygenated Hydrocarbons to Fuels and Chemicals," *Angewandte Chemie International Edition,* vol. 46, pp. 7164-7183, 2007.

[29] J. N. Chheda, Y. Roman-Leshkov, and J. A. Dumesic, "Production of 5-hydroxymethylfurfural and furfural by dehydration of biomass-derived mono- and poly-saccharides," *Green Chemistry,* vol. 9, pp. 342-350, 2007.

[30] G. W. Huber, J. N. Chheda, C. J. Barrett, and J. A. Dumesic, "Production of Liquid Alkanes by Aqueous-Phase Processing of Biomass-Derived Carbohydrates," *Science,* vol. 308, pp. 1446-1450, 2005.

[31] G. W. Huber, J. W. Shabaker, and J. A. Dumesic, "Raney Ni-Sn Catalyst for H2 Production from Biomass-Derived Hydrocarbons," *Science,* vol. 300, pp. 2075-2077, 2003.

[32] H. Olcay, A. V. Subrahmanyam, R. Xing, J. Lajoie, J. A. Dumesic, and G. W. Huber, "Production of renewable petroleum refinery diesel and jet fuel feedstocks from hemicellulose sugar streams," *Energy & Environmental Science,* vol. 6, pp. 205-216, 2013.

[33] J. Q. Bond, A. A. Upadhye, H. Olcay, G. A. Tompsett, J. Jae, R. Xing, *et al.*, "Production of renewable jet fuel range alkanes and commodity chemicals from integrated catalytic processing of biomass," *Energy & Environmental Science,* vol. 7, pp. 1500-1523, 2014.

[34] J. Q. Bond, D. M. Alonso, D. Wang, R. M. West, and J. A. Dumesic, "Integrated Catalytic Conversion of γ-Valerolactone to Liquid Alkenes for Transportation Fuels," *Science,* vol. 327, pp. 1110-1114, 2010.

[35] A. V. Bridgwater, "Review of fast pyrolysis of biomass and product upgrading," *Biomass and Bioenergy,* vol. 38, pp. 68-94, 3// 2012.

[36] R. French and S. Czernik, "Catalytic pyrolysis of biomass for biofuels production," *Fuel Processing Technology,* vol. 91, pp. 25-32, 1// 2010.

[37] M. M. Wright, D. E. Daugaard, J. A. Satrio, and R. C. Brown, "Techno-economic analysis of biomass fast pyrolysis to transportation fuels," *Fuel,* vol. 89, Supplement 1, pp. S2-S10, 11/1/ 2010.

[38] P. R. Patwardhan, R. C. Brown, and B. H. Shanks, "Understanding the Fast Pyrolysis of Lignin," *ChemSusChem,* vol. 4, pp. 1629-1636, 2011.

[39] P. R. Patwardhan, R. C. Brown, and B. H. Shanks, "Product Distribution from the Fast Pyrolysis of Hemicellulose," *ChemSusChem,* vol. 4, pp. 636-643, 2011.

[40] D. C. Elliott, T. R. Hart, G. G. Neuenschwander, L. J. Rotness, and A. H. Zacher, "Catalytic hydroprocessing of biomass fast pyrolysis bio-oil to produce hydrocarbon products," *Environmental Progress & Sustainable Energy,* vol. 28, pp. 441-449, 2009.

[41] K. Wang and R. C. Brown, "Catalytic Pyrolysis of Corn Dried Distillers Grains with Solubles to Produce Hydrocarbons," *ACS Sustainable Chemistry & Engineering,* vol. 2, pp. 2142-2148, 2014/09/02 2014.

[42] C. E. Brewer, K. Schmidt-Rohr, J. A. Satrio, and R. C. Brown, "Characterization of biochar from fast pyrolysis and gasification systems," *Environmental Progress & Sustainable Energy,* vol. 28, pp. 386-396, 2009.

[43] E. Graber, Y. Meller Harel, M. Kolton, E. Cytryn, A. Silber, D. Rav David, *et al.*, "Biochar impact on development and productivity of pepper and tomato grown in fertigated soilless media," *Plant and Soil,* vol. 337, pp. 481-496, 2010/12/01 2010.

[44] D. A. Laird, P. Fleming, D. D. Davis, R. Horton, B. Wang, and D. L. Karlen, "Impact of biochar amendments on the quality of a typical Midwestern agricultural soil," *Geoderma,* vol. 158, pp. 443-449, 9/15/ 2010.

[45] J. Major, J. Lehmann, M. Rondon, and C. Goodale, "Fate of soil-applied black carbon: downward migration, leaching and soil respiration," *Global Change Biology,* vol. 16, pp. 1366-1379, 2010.

[46] F. P. Vaccari, S. Baronti, E. Lugato, L. Genesio, S. Castaldi, F. Fornasier, *et al.*, "Biochar as a strategy to sequester carbon and increase yield in durum wheat," *European Journal of Agronomy,* vol. 34, pp. 231-238, 5// 2011.

[47] F. G. A. Verheijen, E. R. Graber, N. Ameloot, A. C. Bastos, S. Sohi, and H. Knicker, "Biochars in soils: new insights and emerging research needs," *European Journal of Soil Science,* vol. 65, pp. 22-27, 2014.

[48] D. Woolf, J. E. Amonette, F. A. Street-Perrott, J. Lehmann, and S. Joseph, "Sustainable biochar to mitigate global climate change," *Nature communications,* vol. 1, p. 56, 2010.

[49] R. Agrawal and N. R. Singh, "Synergistic routes to liquid fuel for a petroleum-deprived future," *AIChE Journal,* vol. 55, pp. 1898-1905, 2009.

[50] P. J. Dauenhauer, B. J. Dreyer, N. J. Degenstein, and L. D. Schmidt, "Millisecond Reforming of Solid Biomass for Sustainable Fuels," *Angewandte Chemie International Edition,* vol. 46, pp. 5864-5867, 2007.

[51] D. E. Brune, T. J. Lundquist, and J. R. Benemann, *Microalgal Biomass for Greenhouse Gas Reductions: Potential for Replacement of Fossil Fuels and Animal Feeds* vol. 135: ASCE, 2009.

[52] K. M. Weyer, D. R. Bush, A. Darzins, and B. D. Willson, "Theoretical Maximum Algal Oil Production," *Bioenergy Research,* vol. 3, pp. 204-213, Jun 2010.

[53] Y. Chisti, "Biodiesel from Microalgae," *Biotechnology Advances,* vol. 25, p. 13, Feb 13, 2007 2007.

[54] J. Yang, M. Xu, X. Zhang, Q. Hu, M. Sommerfeld, and Y. Chen, "Life-cycle analysis on biodiesel production from microalgae: water footprint and nutrients balance," *Bioresource technology,* vol. 102, pp. 159-65, Jan 2011.

[55] L. Brennan and P. Owende, "Biofuels from microalgae—A review of technologies for production, processing, and extractions of biofuels and co-products," *Renewable and Sustainable Energy Reviews,* vol. 14, pp. 557-577, 2// 2010.

[56] V. Vasudevan, R. W. Stratton, M. N. Pearlson, G. R. Jersey, A. G. Beyene, J. C. Weissman, *et al.*, "Environmental Performance of Algal Biofuel Technology Options," *Environmental Science & Technology,* vol. 46, pp. 2451-2459, 2012/02/21 2012.

[57] W. Steffen, K. Richardson, J. Rockström, S. E. Cornell, I. Fetzer, E. M. Bennett, *et al.*, "Planetary boundaries: Guiding human development on a changing planet," *Science,* vol. 347, 2015.

[58] T. P. Hughes, S. Carpenter, J. Rockström, M. Scheffer, and B. Walker, "Multiscale regime shifts and planetary boundaries," *Trends in Ecology & Evolution,* vol. 28, pp. 389-395, 7// 2013.

[59] W. Steffen, Å. Persson, L. Deutsch, J. Zalasiewicz, M. Williams, K. Richardson, *et al.*, "The Anthropocene: From Global Change to Planetary Stewardship," *AMBIO,* vol. 40, pp. 739-761, 2011/11/01 2011.

[60] B. S. Ballew, "Elsevier's Scopus® Database," *Journal of Electronic Resources in Medical Libraries,* vol. 6, pp. 245-252, 2009/09/09 2009.

[61] C. E. Ridley, C. M. Clark, S. D. LeDuc, B. G. Bierwagen, B. B. Lin, A. Mehl, *et al.*, "Biofuels: Network Analysis of the Literature Reveals Key Environmental and Economic Unknowns," *Environmental Science & Technology,* vol. 46, pp. 1309-1315, 2012/02/07 2012.

[62] N. J. Van Eck and L. Waltman, "Software survey: VOSviewer, a computer program for bibliometric mapping," *Scientometrics,* vol. 84, pp. 523-538, 2010.

[63] K. M. Carley and M. DeReno, "ORA: Organization Risk Analyzer, ORA User's Guide," Technical Report, School of Computer Science, Institute for Software Research, Carnegie Mellon University2006.

[64] M. E. Dias De Oliveira, B. E. Vaughan, and E. J. Rykiel, "Ethanol as Fuel: Energy, Carbon Dioxide Balances, and Ecological Footprint," *BioScience*, vol. 55, pp. 593-602, 2005.

[65] H. Greenwell, L. Laurens, R. Shields, R. Lovitt, and K. Flynn, "Placing microalgae on the biofuels priority list: a review of the technological challenges," *Journal of the Royal Society Interface*, vol. 7, pp. 703-726, 2010.

[66] R. H. Wijffels and M. J. Barbosa, "An Outlook on Microalgal Biofuels," *Science*, vol. 329, pp. 796-799, August 13, 2010 2010.

[67] Y. Chisti, "Response to Reijnders: Do biofuels from microalgae beat biofuels from terrestrial plants?," *Trends in Biotechnology*, vol. 26, pp. 351-352, 2008.

[68] G. C. Dismukes, D. Carrieri, N. Bennette, G. M. Ananyev, and M. C. Posewitz, "Aquatic phototrophs: efficient alternatives to land-based crops for biofuels," *Current Opinion in Biotechnology*, vol. 19, pp. 235-240, Jun 2008.

[69] F. X. Malcata, "Microalgae and biofuels: A promising partnership?," *Trends in Biotechnology*, vol. 29, pp. 542-549, Nov 2011.

[70] P. J. l. B. Williams and L. M. L. Laurens, "Microalgae as biodiesel & biomass feedstocks: Review & analysis of the biochemistry, energetics & economics," *Energy & Environmental Science*, vol. 3, pp. 554-590, 2010.

[71] Y. Chisti, "Biodiesel from microalgae beats bioethanol," *Trends in Biotechnology*, vol. 26, pp. 126-131, Mar 2008.

[72] *A look back at the U.S. Department of Energy's Aquatic Species Program [electronic resource] : biodiesel from algae / by John Sheehan ... [et al.] ; prepared by the National Renewable Energy Laboratory*. Golden, Colo. :: National Renewable Energy Laboratory, 1998.

[73] M. Huntley and D. Redalje, "CO2 Mitigation and Renewable Oil from Photosynthetic Microbes: A New Appraisal," *Mitigation and Adaptation Strategies for Global Change*, vol. 12, pp. 573-608, 2007/05/01 2007.

[74] L. B. Brentner, M. J. Eckelman, and J. B. Zimmerman, "Combinatorial life cycle assessment to inform process design of industrial production of algal biodiesel," *Environmental science & technology*, vol. 45, pp. 7060-7, Aug 15 2011.

[75] A. F. Clarens, H. Nassau, E. P. Resurreccion, M. A. White, and L. M. Colosi, "Environmental impacts of algae-derived biodiesel and bioelectricity for transportation," *Environmental Science & Technology*, vol. 45, pp. 7554-7560, 2011/09/01 2011.

[76] A. F. Clarens, E. P. Resurreccion, M. A. White, and L. M. Colosi, "Environmental life cycle comparison of algae to other bioenergy feedstocks," *Environmental Science & Technology,* vol. 44, pp. 1813-1819, Mar 1 2010.

[77] P. Collet, A. Hélias, L. Lardon, M. Ras, R.-A. Goy, and J.-P. Steyer, "Life-cycle assessment of microalgae culture coupled to biogas production," *Bioresource Technology,* vol. 102, pp. 207-214, 2011.

[78] O. Jorquera, A. Kiperstok, E. A. Sales, M. Embiruçu, and M. L. Ghirardi, "Comparative energy life-cycle analyses of microalgal biomass production in open ponds and photobioreactors," *Bioresource Technology,* vol. 101, pp. 1406-1413, 2010.

[79] K. L. Kadam, "Microalgae production from power plant flue gas: Environmental implications on life cycle basis," National Renewable Energy Laboratory NREL/TP-510-29417, 2001.

[80] C. F. Murphy and D. T. Allen, "Energy-water nexus for mass cultivation of algae," *Environmental science & technology,* vol. 45, pp. 5861-8, Jul 1 2011.

[81] T. Shirvani, X. Yan, O. R. Inderwildi, P. P. Edwards, and D. A. King, "Life cycle energy and greenhouse gas analysis for algae-derived biodiesel," *Energy & Environmental Science,* vol. 4, pp. 3773-3778, 2011.

[82] K. Soratana and A. E. Landis, "Evaluating industrial symbiosis and algae cultivation from a life cycle perspective," *Bioresource Technology,* vol. 102, pp. 6892-6901, Jul 2011.

[83] A. L. Stephenson, E. Kazamia, J. S. Dennis, C. J. Howe, S. A. Scott, and A. G. Smith, "Life-Cycle Assessment of Potential Algal Biodiesel Production in the United Kingdom: A Comparison of Raceways and Air-Lift Tubular Bioreactors," *Energy & Fuels,* vol. 24, pp. 4062-4077, 2010.

[84] P. K. Campbell, T. Beer, and D. Batten, "Life cycle assessment of biodiesel production from microalgae in ponds," *Bioresource technology,* vol. 102, pp. 50-6, Jan 2011.

[85] L. Xu, D. W. F. Brilman, J. A. M. Withag, G. Brem, and S. Kersten, "Assessment of a dry and a wet route for the production of biofuels from microalgae: Energy balance analysis," *Bioresource Technology,* vol. 102, pp. 5113-5122, 2011.

[86] J. Yang, M. Xu, X. Z. Zhang, Q. A. Hu, M. Sommerfeld, and Y. S. Chen, "Life-cycle analysis on biodiesel production from microalgae: Water footprint and nutrients balance," *Bioresource Technology,* vol. 102, pp. 159-165, Jan 2011.

[87] Y. Li, M. Horsman, N. Wu, C. Q. Lan, and N. Dubois-Calero, "Biofuels from microalgae," *Biotechnology Progress,* vol. 24, pp. 815-820, Jul-Aug 2008.

[88] D. X. Luo, Z. S. Hu, D. G. Choi, V. M. Thomas, M. J. Realff, and R. R. Chance, "Life Cycle Energy and Greenhouse Gas Emissions for an Ethanol Production Process Based

on Blue-Green Algae," *Environmental Science & Technology,* vol. 44, pp. 8670-8677, Nov 2010.

[89] L. Batan, J. Quinn, B. Willson, and T. Bradley, "Net Energy and Greenhouse Gas Emission Evaluation of Biodiesel Derived from Microalgae," *Environmental Science & Technology,* vol. 44, pp. 7975-7980, Oct 2010.

[90] H. H. Khoo, P. N. Sharratt, P. Das, R. K. Balasubramanian, P. K. Naraharisetti, and S. Shaik, "Life cycle energy and CO(2) analysis of microalgae-to-biodiesel: Preliminary results and comparisons," *Bioresource Technology,* vol. 102, pp. 5800-5807, May 2011.

[91] D. B. Agusdinata, F. Zhao, K. Ileleji, and D. DeLaurentis, "Life cycle assessment of potential biojet fuel production in the United States," *Environmental Science & Technology,* vol. 45, pp. 9133-9143, Nov 2011.

[92] R. Chowdhury, S. Viamajala, and R. Gerlach, "Reduction of environmental and energy footprint of microalgal biodiesel production through material and energy integration," *Bioresource Technology,* vol. 108, pp. 102-111, 2012.

[93] K. Sander and G. Murthy, "Life cycle analysis of algae biodiesel," *The International Journal of Life Cycle Assessment,* vol. 15, pp. 704-714, 2010.

[94] L. Lardon, A. Hélias, B. Sialve, J.-P. Steyer, and O. Bernard, "Life-cycle assessment of biodiesel production from microalgae," *Environmental Science & Technology,* vol. 43, pp. 6475-6481, 2009.

[95] P. Schenk, S. Thomas-Hall, E. Stephens, U. Marx, J. Mussgnug, C. Posten, *et al.*, "Second Generation Biofuels: High-Efficiency Microalgae for Biodiesel Production," *Bioenergy Research,* vol. 1, pp. 20-43, 2008.

[96] A. F. Ferreira, A. C. Marques, A. P. Batista, P. A. S. S. Marques, L. Gouveia, and C. M. Silva, "Biological hydrogen production by Anabaena sp. – Yield, energy and CO2 analysis including fermentative biomass recovery," *International Journal of Hydrogen Energy,* vol. 37, pp. 179-190, 2012.

[97] A. F. Ferreira, J. Ortigueira, L. Alves, L. Gouveia, P. Moura, and C. M. Silva, "Energy requirement and CO2 emissions of bioH2 production from microalgal biomass," *Biomass and Bioenergy,* vol. 49, pp. 249-259, 2013.

[98] A. F. Ferreira, L. A. Ribeiro, A. P. Batista, P. A. S. S. Marques, B. P. Nobre, A. M. F. Palavra, *et al.*, "A biorefinery from Nannochloropsis sp. microalga – Energy and CO2 emission and economic analyses," *Bioresource Technology,* vol. 138, pp. 235-244, 2013.

[99] L. Xu, P. J. Weathers, X. R. Xiong, and C. Z. Liu, "Microalgal bioreactors: Challenges and opportunities," *Engineering in Life Sciences,* vol. 9, pp. 178-189, Jun 2009.

[100] B. J. Oswald, "Systems and Economic Analysis of Microalgae Ponds for Conversion of CO2 to Biomass - Final Report," Pittsburgh1996.

[101] NREL, "National Solar Radiation Database (1961-1990)," National Renewable Energy Laboratory, Ed., ed. Golden, CO, 1994.

[102] T. Harmelen and H. Oonk, "Microalge biofixation process: applicatinos and potential contributions to greenhouse gas mitigation options," TNO Built Environment and Geosciences2006.

[103] N. Uduman, Y. Qi, M. K. Danquah, G. M. Forde, and A. Hoadley, "Dewatering of microalgal cultures: A major bottleneck to algae-based fuels," *Journal of Renewable and Sustainable Energy,* vol. 2, Jan 2010.

[104] C. T. Matos, M. Santos, B. P. Nobre, and L. Gouveia, "Nannochloropsis sp. biomass recovery by Electro-Coagulation for biodiesel and pigment production," *Bioresource Technology,* vol. 134, pp. 219-226, 2013.

[105] NREL, "National Solar Radiation Database (1961-1990)," National Renewable Energy Laboratory, Ed., ed. Golden, CO, 1994.

[106] J. C. Goldman, "OUTDOOR ALGAL MASS-CULTURES .2. PHOTOSYNTHETIC YIELD LIMITATIONS," *Water Research,* vol. 13, pp. 119-136, 1979.

[107] B. E.W, "Micro-algae as a source of protein," *Biotechnology Advances,* vol. 25, pp. 207-210.

[108] US Environmental Protection Agency. *Power Profiler*. Available: http://www.epa.gov/cleanenergy/energy-and-you/how-clean.html

[109] K. L. Kadam, "Environmental implications of power generation via coal-microalgae cofiring," *Energy,* vol. 27, pp. 905-922, Oct 2002.

[110] M. FH, *Experiences and Strategies in the recovery of biomass from mass cultures of microalgae*. Amsterdam: Elsevier, 1980.

[111] Ecoinvent Centre, "Ecoinvent data v2.0," Swiss Centre for Life Cycle Inventories, Ed., ed. Dubendorf, 2007.

[112] M. P. Deru and NREL, *U.S. Life Cycle Inventory Database Roadmap*: National Renewable Energy Laboratory, U.S. Dept. of Energy, 2009.

[113] C. W. King and M. E. Webber, "Water Intensity of Transportation," *Environmental Science & Technology,* vol. 42, pp. 7866-7872, 2008/11/01 2008.

[114] P. W. Gerbens-Leenes, A. Y. Hoekstra, and T. van der Meer, "The water footprint of energy from biomass: A quantitative assessment and consequences of an increasing share of bio-energy in energy supply," *Ecological Economics,* vol. 68, pp. 1052-1060, 2009.

[115] R. Dominguez-Faus, S. E. Powers, J. G. Burken, and P. J. Alvarez, "The Water Footprint of Biofuels: A Drink or Drive Issue?," *Environmental Science & Technology,* vol. 43, pp. 3005-3010, 2009/05/01 2009.

[116] Y.-W. Chiu, B. Walseth, and S. Suh, "Water Embodied in Bioethanol in the United States," *Environmental Science & Technology,* vol. 43, pp. 2688-2692, 2009/04/15 2009.

[117] W. Gerbens-Leenes, A. Y. Hoekstra, and T. H. van der Meer, "The water footprint of bioenergy," *Proceedings of the National Academy of Sciences,* vol. 106, pp. 10219-10223, June 23, 2009 2009.

[118] W. J. Shuttleworth, "Putting the "vap" into evaporation," *Hydrol. EarthSyst. Sci.,* 2007.

[119] NOAA. Monthly Average Precipitation by State [Online]. Available: http://www.wrcc.dri.edu/htmlfiles/A-L_compare.html

[120] J. C. Weissman and R. P. Goebel, "Design and analysis of microalgal open pond systems for the purpose of producing fuels: A subcontract report," SERI/STR-231-2840; Other: ON: DE87001164, 1987.

[121] J. R. Benemann, "CO_2 mitigation with microalgae systems," *Energy Conversion and Management,* vol. 38, pp. S475-S479, 1997.

[122] S. H. Ho, C. Y. Chen, D. J. Lee, and J. S. Chang, "Perspectives on microalgal CO(2)-emission mitigation systems - A review," *Biotechnology Advances,* vol. 29, pp. 189-198, Mar-Apr 2011.

[123] S. Cho, D. Lee, T. T. Luong, S. Park, Y. K. Oh, and T. Lee, "Effects of Carbon and Nitrogen Sources on Fatty Acid Contents and Composition in the Green Microalga, Chlorella sp 227," *Journal of Microbiology and Biotechnology,* vol. 21, pp. 1073-1080, Oct 2011.

[124] J. M. Lv, L. H. Cheng, X. H. Xu, L. Zhang, and H. L. Chen, "Enhanced lipid production of Chlorella vulgaris by adjustment of cultivation conditions," *Bioresource Technology,* vol. 101, pp. 6797-6804, Sep 2010.

[125] A. Sukenik and G. Shelef, "Algal autoflocculation—verification and proposed mechanism," *Biotechnology and bioengineering,* vol. 26, pp. 142-147, 1984.

[126] R. Bhave, T. Kuritz, L. Powell, and D. Adcock, "Membrane-Based Energy Efficient Dewatering of Microalgae in Biofuels Production and Recovery of Value Added Co-Products," *Environmental Science & Technology,* vol. 46, pp. 5599-5606, 2012/05/15 2012.

[127] J. Hanotu, H. C. H. Bandulasena, and W. B. Zimmerman, "Microflotation performance for algal separation," *Biotechnology and bioengineering,* vol. 109, pp. 1663-1673, 2012.

[128] K. R. Jensen, R. P. Allen, and D. Keys, "Water remediation and biosolids collection system and associated methods," ed: US Patent 8,075,783, 2011.

[129] S. Mukhtar, K. Wagner, and L. Gregory, "Field Demonstration of the Performance of a Geotube® Dewatering System to Reduce Phosphorus and Other Substances from Dairy Lagoon Effluent," *Texas Water Resources Institute. Available electronically from* *http://repository.tamu.edu/bitstream/handle/1969.1/86145/TR-345%20GTFinalReport_2006-08-04.pdf?sequence=1*, vol. 1, p. 86145, 2009.

[130] A. Bhatnagar, S. Chinnasamy, M. Singh, and K. C. Das, "Renewable biomass production by mixotrophic algae in the presence of various carbon sources and wastewaters," *Applied Energy*, vol. 88, pp. 3425-3431, Oct 2011.

[131] I. Rawat, R. R. Kumar, T. Mutanda, and F. Bux, "Dual role of microalgae: Phycoremediation of domestic wastewater and biomass production for sustainable biofuels production," *Applied Energy*, vol. 88, pp. 3411-3424, Oct 2011.

[132] M.-O. P. Fortier and B. S. Sturm, "Geographic Analysis of the Feasibility of Collocating Algal Biomass Production with Wastewater Treatment Plants," *Environmental Science & Technology*, vol. 46, pp. 11426-11434, 2012.

[133] B. Sialve, N. Bernet, and O. Bernard, "Anaerobic digestion of microalgae as a necessary step to make microalgal biodiesel sustainable," *Biotechnology Advances*, vol. 27, pp. 409-416, Jul-Aug 2009.

[134] A. Hughes, M. Kelly, K. Black, and M. Stanley, "Biogas from Macroalgae: is it time to revisit the idea?," *Biotechnology for Biofuels*, vol. 5, p. 86, 2012.

[135] D. Tilman, R. Socolow, J. A. Foley, J. Hill, E. Larson, L. Lynd, *et al.*, "Beneficial Biofuels—The Food, Energy, and Environment Trilemma," *Science*, vol. 325, pp. 270-271, July 17, 2009 2009.

[136] J. M. Melillo, J. M. Reilly, D. W. Kicklighter, A. C. Gurgel, T. W. Cronin, S. Paltsev, *et al.*, "Indirect emissions from biofuels: How important?," *Science*, vol. 326, pp. 1397-1399, Dec 4 2009.

[137] T. E. McKone, W. W. Nazaroff, P. Berck, M. Auffhammer, T. Lipman, M. S. Torn, *et al.*, "Grand challenges for life-cycle assessment of biofuels," *Environmental science & technology*, vol. 45, pp. 1751-1756, 2011/03/01 2011.

[138] U. S. DOE, "National Algal Biofuels Technology Roadmap," U.S. Department of Energy, Office of Energy Efficiency and Renewable Energy, BIomass Program2010.

[139] D. Brune, T. Lundquist, and J. Benemann, "Microalgal Biomass for Greenhouse Gas Reductions: Potential for Replacement of Fossil Fuels and Animal Feeds," *Journal of Environmental Engineering*, vol. 135, pp. 1136-1144, 2009.

[140] R. M. Handler, D. R. Shonnard, T. N. Kalnes, and F. S. Lupton, "Life cycle assessment of algal biofuels: Influence of feedstock cultivation systems and conversion platforms," *Algal Research,* vol. 4, pp. 105-115, 4// 2014.

[141] K. Cox, M. Renouf, A. Dargan, C. Turner, and D. Klein-Marcuschamer, "Environmental life cycle assessment (LCA) of aviation biofuel from microalgae, Pongamia pinnata, and sugarcane molasses," *Biofuels, Bioproducts and Biorefining,* pp. n/a-n/a, 2014.

[142] L. Yanfen, H. Zehao, and M. Xiaoqian, "Energy analysis and environmental impacts of microalgal biodiesel in China," *Energy Policy,* vol. 45, pp. 142-151, 2012.

[143] D. L. Sills, V. Paramita, M. J. Franke, M. C. Johnson, T. M. Akabas, C. H. Greene, *et al.*, "Quantitative Uncertainty Analysis of Life Cycle Assessment for Algal Biofuel Production," *Environmental Science & Technology,* vol. 47, pp. 687-694, 2013/01/15 2012.

[144] G. G. Zaimes and V. Khanna, "Environmental sustainability of emerging algal biofuels: A comparative life cycle evaluation of algal biodiesel and renewable diesel," *Environmental Progress & Sustainable Energy,* vol. 32, pp. 926-936, 2013.

[145] L. F. Razon and R. R. Tan, "Net energy analysis of the production of biodiesel and biogas from the microalgae: Haematococcus pluvialis and Nannochloropsis," *Applied Energy,* vol. 88, pp. 3507-3514, 2011.

[146] L. Batan, J. C. Quinn, and T. H. Bradley, "Analysis of water footprint of a photobioreactor microalgae biofuel production system from blue, green and lifecycle perspectives," *Algal Research,* vol. 2, pp. 196-203, 2013.

[147] G. Zaimes and V. Khanna, "Microalgal biomass production pathways: evaluation of life cycle environmental impacts," *Biotechnology for Biofuels,* vol. 6, p. 88, 2013.

[148] R. E. Davis, D. B. Fishman, E. D. Frank, M. C. Johnson, S. B. Jones, C. M. Kinchin, *et al.*, "Integrated Evaluation of Cost, Emissions, and Resource Potential for Algal Biofuels at the National Scale," *Environmental Science & Technology*, vol. 48, pp. 6035-6042, 2014/05/20 2014.

[149] E. R. Venteris, R. L. Skaggs, A. M. Coleman, and M. S. Wigmosta, "An assessment of land availability and price in the coterminous United States for conversion to algal biofuel production," *Biomass and Bioenergy,* vol. 47, pp. 483-497, 2012.

[150] A. Baral and B. R. Bakshi, "Thermodynamic Metrics for Aggregation of Natural Resources in Life Cycle Analysis: Insight via Application to Some Transportation Fuels," *Environmental Science & Technology,* vol. 44, pp. 800-807, 2010/01/15 2010.

[151] J. L. Hau and B. R. Bakshi, "Expanding Exergy Analysis to Account for Ecosystem Products and Services," *Environmental Science & Technology,* vol. 38, pp. 3768-3777, 2004/07/01 2004.

[152] J. Dewulf, H. Van Langenhove, B. Muys, S. Bruers, B. R. Bakshi, G. F. Grubb, *et al.*, "Exergy: Its Potential and Limitations in Environmental Science and Technology," *Environmental Science & Technology,* vol. 42, pp. 2221-2232, 2008/04/01 2008.

[153] A. Baral, B. R. Bakshi, and R. L. Smith, "Assessing Resource Intensity and Renewability of Cellulosic Ethanol Technologies Using Eco-LCA," *Environmental Science & Technology,* vol. 46, pp. 2436-2444, 2012/02/21 2012.

[154] J. Dewulf, H. Van Langenhove, and B. Van De Velde, "Exergy-Based Efficiency and Renewability Assessment of Biofuel Production," *Environmental Science & Technology,* vol. 39, pp. 3878-3882, 2005/05/01 2005.

[155] Y. Zhang, A. Baral, and B. R. Bakshi, "Accounting for Ecosystem Services in Life Cycle Assessment, Part II: Toward an Ecologically Based LCA," *Environmental Science & Technology,* vol. 44, pp. 2624-2631, 2010/04/01 2010.

[156] Y. Zhang, S. Singh, and B. R. Bakshi, "Accounting for Ecosystem Services in Life Cycle Assessment, Part I: A Critical Review," *Environmental Science & Technology,* vol. 44, pp. 2232-2242, 2010/04/01 2010.

[157] B. De Meester, J. Dewulf, A. Janssens, and H. Van Langenhove, "An Improved Calculation of the Exergy of Natural Resources for Exergetic Life Cycle Assessment (ELCA)," *Environmental Science & Technology,* vol. 40, pp. 6844-6851, 2006/11/01 2006.

[158] J. Dewulf, M. E. Bösch, B. D. Meester, G. V. d. Vorst, H. V. Langenhove, S. Hellweg, *et al.*, "Cumulative exergy extraction from the natural environment (CEENE): a comprehensive life cycle impact assessment method for resource accounting," *Environmental Science & Technology,* vol. 41, pp. 8477-8483, 2007.

[159] S. R. Carpenter, H. A. Mooney, J. Agard, D. Capistrano, R. S. DeFries, S. Diaz, *et al.*, "Science for managing ecosystem services: Beyond the Millennium Ecosystem Assessment," *Proceedings of the National Academy of Sciences,* vol. 106, pp. 1305-1312, 2009.

[160] S. Pimm, C. Jenkins, R. Abell, T. Brooks, J. Gittleman, L. Joppa, *et al.*, "The biodiversity of species and their rates of extinction, distribution, and protection," *Science,* vol. 344, p. 1246752, 2014.

[161] Ecologically-Based Life Cycle Assessment. (2012). *The Ohio State University, The Center For Resilience*. Available: http://resilience.eng.ohio-state.edu/eco-lca/

[162] T. Kalnes, T. Marker, and D. R. Shonnard, "Green diesel: A second generation biofuel," *International Journal of Chemical Reactor Engineering,* vol. 5, 2007.

[163] NOAA, "Monthly Average Precipitation," ed: National Climatic Data Center, National Oceanic and Atmospheric Administration, 2006.

[164] H. Matsumoto, N. Shioji, A. Hamasaki, Y. Ikuta, Y. Fukuda, M. Sato, *et al.*, "Carbon dioxide fixation by microalgae photosynthesis using actual flue gas discharged from a boiler," *Applied Biochemistry and Biotechnology*, vol. 51, pp. 681-692, 1995.

[165] M. Negoro, N. Shioji, K. Miyamoto, and Y. Micira, "Growth of Microalgae in High CO2 Gas and Effects of SOX and NOX," *Applied Biochemistry and Biotechnology*, vol. 28-29, pp. 877-886, 1991/03/01 1991.

[166] U. NASS, "Farm and ranch irrigation survey.," *US Department of Agriculture, National Agricultural Statistics Service*, 2008.

[167] F. H. Mohn, *Experiences and Strategies in the recovery of biomass from mass cultures of microalgae*. Amsterdam: Elsevier, 1980.

[168] C. G. Golueke and W. J. Oswald, "Harvesting and processing sewage-grown planktonic algae," *Journal (Water Pollution Control Federation)*, pp. 471-498, 1965.

[169] G. Shelef, A. Sukenik, and M. Green, "Microalgae Harvesting and Processing: A Literature Review," Solar Energy Research Institute, Golden, Colorado SERI/STR-231-2396, 1984.

[170] E. Frank, J. Han, I. Palou-Rivera, A. Elgowainy, and M. Wang, "Life-cycle analysis of algal lipid fuels with the greet model," *Center for Transportation Research, Energy Systems Division, Argonne National Laboratory, Oak Ridge,* 2011.

[171] A. Prabhu, C. Pham, A. Glabe, and J. Duffy, "Detailed California-Modified GREET Pathway for Biodiesel (Esterified Soyoil) from Midwest Soybeans," ed: Draft.

[172] H. H. R. Rauch, K. Bosch, I. Siefert, C. Aichernig, H. Tremmel, K. Voigtlaender, R. Koch, R. Lehner, , "2004 Steam Gasification of Biomass at CHP Plant in Guessing-Status of the Demonstration Plant," presented at the World Conference and Technology Exhibition on Biomass for Energy, Italy.

[173] N. U. Ukidwe and B. R. Bakshi, "Thermodynamic Accounting of Ecosystem Contribution to Economic Sectors with Application to 1992 U.S. Economy," *Environmental Science & Technology,* vol. 38, pp. 4810-4827, 2004/09/01 2004.

[174] CPI Inflation Calculator, "US Department of Labor, Bureau of Labor Statistics," ed, 2013.

[175] C. J. Cleveland. (2010, July 4, 2011). *Net energy analysis*. Available: www.eoearth.org/article/Net_energy_analysis

[176] K. Mulder and N. J. Hagens, "Energy Return on Investment: Toward a Consistent Framework," *AMBIO: A Journal of the Human Environment,* vol. 37, pp. 74-79, 2008/03/01 2008.

[177] D. J. Murphy and C. A. S. Hall, "Year in review—EROI or energy return on (energy) invested," *Annals of the New York Academy of Sciences,* vol. 1185, pp. 102-118, 2010.

[178] C. A. Hall, S. Balogh, and D. J. Murphy, "What is the minimum EROI that a sustainable society must have?," *Energies,* vol. 2, pp. 25-47, 2009.

[179] B. E. Dale, "Thinking clearly about biofuels: ending the irrelevant 'net energy' debate and developing better performance metrics for alternative fuels," *Biofuels, Bioproducts and Biorefining,* vol. 1, pp. 14-17, 2007.

[180] H. T. Odum, *Environmental Accounting: Emergy and Environmental Decision Making*: Wiley, 1996.

[181] H. T. Odum, "Energy, ecology, and economics," *Ambio,* pp. 220-227, 1973.

[182] M. T. Brown and R. A. Herendeen, "Embodied energy analysis and EMERGY analysis: a comparative view," *Ecological Economics,* vol. 19, pp. 219-235, 1996.

[183] J. L. Hau and B. R. Bakshi, "Promise and problems of emergy analysis," *Ecological Modelling,* vol. 178, pp. 215-225, 2004.

[184] N. Uduman, Y. Qi, M. K. Danquah, G. M. Forde, and A. Hoadley, "Dewatering of microalgal cultures: A major bottleneck to algae-based fuels," *Journal of Renewable and Sustainable Energy,* vol. 2, pp. 012701-15, 2010.

[185] J. G. Lambert, C. A. S. Hall, S. Balogh, A. Gupta, and M. Arnold, "Energy, EROI and quality of life," *Energy Policy*.

[186] A. J. Guswa, K. A. Brauman, C. Brown, P. Hamel, B. L. Keeler, and S. S. Sayre, "Ecosystem services: Challenges and opportunities for hydrologic modeling to support decision making," *Water resources research,* pp. n/a-n/a, 2014.

[187] C. J. Cleveland, R. K. Kaufmann, and D. I. Stern, "Aggregation and the role of energy in the economy," *Ecological Economics,* vol. 32, pp. 301-317, 2000.

[188] R. Radakovits, R. E. Jinkerson, A. Darzins, and M. C. Posewitz, "Genetic engineering of algae for enhanced biofuel production," *Eukaryotic Cell,* vol. 9, pp. 486-501, 2010.

[189] P. E. Savage, "Algae Under Pressure and in Hot Water," *Science,* vol. 338, pp. 1039-1040, 2012.

[190] M.-O. P. Fortier, G. W. Roberts, S. M. Stagg-Williams, and B. S. M. Sturm, "Life cycle assessment of bio-jet fuel from hydrothermal liquefaction of microalgae," *Applied Energy,* vol. 122, pp. 73-82, 6/1/ 2014.

[191] J. B. K. Park, R. J. Craggs, and A. N. Shilton, "Wastewater treatment high rate algal ponds for biofuel production," *Bioresource Technology,* vol. 102, pp. 35-42, 2011.

[192] E. Menger-Krug, J. Niederste-Hollenberg, T. Hillenbrand, and H. Hiessl, "Integration of Microalgae Systems at Municipal Wastewater Treatment Plants: Implications for Energy

and Emission Balances," *Environmental Science & Technology,* vol. 46, pp. 11505-11514, 2012/11/06 2012.

[193] C. M. Beal, R. E. Hebner, and M. E. Webber, "Thermodynamic analysis of algal biocrude production," *Energy,* vol. 44, pp. 925-943, 2012.

[194] V. R. Wiggers, A. Wisniewski Jr, L. A. S. Madureira, A. A. C. Barros, and H. F. Meier, "Biofuels from waste fish oil pyrolysis: Continuous production in a pilot plant," *Fuel,* vol. 88, pp. 2135-2141, 2009.

[195] S. N. Naik, V. V. Goud, P. K. Rout, and A. K. Dalai, "Production of first and second generation biofuels: A comprehensive review," *Renewable and Sustainable Energy Reviews,* vol. 14, pp. 578-597, 2010.

[196] G. G. Zaimes and V. Khanna, "The role of allocation and coproducts in environmental evaluation of microalgal biofuels: How important?," *Sustainable Energy Technologies and Assessments,* vol. 7, pp. 247-256, 9// 2014.

[197] G. G. Zaimes and V. Khanna, "Assessing the critical role of ecological goods and services in microalgal biofuel life cycles," *RSC Advances,* vol. 4, pp. 44980-44990, 2014.

[198] N. Brosse, A. Dufour, X. Meng, Q. Sun, and A. Ragauskas, "Miscanthus: a fast-growing crop for biofuels and chemicals production," *Biofuels, Bioproducts and Biorefining,* vol. 6, pp. 580-598, 2012.

[199] S. B. McLaughlin and L. Adams Kszos, "Development of switchgrass (Panicum virgatum) as a bioenergy feedstock in the United States," *Biomass and Bioenergy,* vol. 28, pp. 515-535, 6// 2005.

[200] G. W. Huber, *Breaking the chemical and engineering barriers to lignocellulosic biofuels: next generation hydrocarbon biorefineries*. Washington, DC: National Science Foundation, Chemical, Biogengineering, Environmental and Transport Systems Division, 2008.

[201] Y. Zhang, G. Hu, and R. C. Brown, "Life cycle assessment of the production of hydrogen and transportation fuels from corn stover via fast pyrolysis," *Environmental Research Letters,* vol. 8, p. 025001, 2013.

[202] M. Ringer, V. Putsche, and J. Scahil, "Large-scale pyrolysis oil production: a technology assessment and economic analysis. Golden (CO): National Renewable Energy Laboratory; 2006 Nov. Report No.: NREL/TP-510e37779," *Contract No.: DE-AC36-99-GO10337,* 2006.

[203] D. D. Hsu, "Life cycle assessment of gasoline and diesel produced via fast pyrolysis and hydroprocessing," *Biomass and Bioenergy,* vol. 45, pp. 41-47, 2012.

[204] F.-X. Collard and J. Blin, "A review on pyrolysis of biomass constituents: Mechanisms and composition of the products obtained from the conversion of cellulose,

hemicelluloses and lignin," *Renewable and Sustainable Energy Reviews,* vol. 38, pp. 594-608, 10// 2014.

[205] A. V. Bridgwater, D. Meier, and D. Radlein, "An overview of fast pyrolysis of biomass," *Organic Geochemistry,* vol. 30, pp. 1479-1493, 12// 1999.

[206] D. C. Elliott, H. Wang, R. French, S. Deutch, and K. Iisa, "Hydrocarbon Liquid Production from Biomass via Hot-Vapor-Filtered Fast Pyrolysis and Catalytic Hydroprocessing of the Bio-oil," *Energy & Fuels,* vol. 28, pp. 5909-5917, 2014/09/18 2014.

[207] E. A. Heaton, F. G. Dohleman, and S. P. Long, "Meeting US biofuel goals with less land: the potential of Miscanthus," *Global Change Biology,* vol. 14, pp. 2000-2014, 2008.

[208] G. Pourhashem, S. Spatari, A. A. Boateng, A. J. McAloon, and C. A. Mullen, "Life Cycle Environmental and Economic Tradeoffs of Using Fast Pyrolysis Products for Power Generation," *Energy & Fuels,* vol. 27, pp. 2578-2587, 2013/05/16 2013.

[209] J. C. Clifton-brown, P. F. Stampfl, and M. B. Jones, "Miscanthus biomass production for energy in Europe and its potential contribution to decreasing fossil fuel carbon emissions," *Global Change Biology,* vol. 10, pp. 509-518, 2004.

[210] S. Grierson, V. Strezov, and J. Bengtsson, "Life cycle assessment of a microalgae biomass cultivation, bio-oil extraction and pyrolysis processing regime," *Algal Research,* vol. 2, pp. 299-311, 7// 2013.

[211] Q. Dang, C. Yu, and Z. Luo, "Environmental life cycle assessment of bio-fuel production via fast pyrolysis of corn stover and hydroprocessing," *Fuel,* vol. 131, pp. 36-42, 9/1/ 2014.

[212] J. F. Peters, D. Iribarren, and J. Dufour, "Simulation and life cycle assessment of biofuel production via fast pyrolysis and hydroupgrading," *Fuel,* vol. 139, pp. 441-456, 1/1/ 2015.

[213] D. Iribarren, J. F. Peters, and J. Dufour, "Life cycle assessment of transportation fuels from biomass pyrolysis," *Fuel,* vol. 97, pp. 812-821, 7// 2012.

[214] J. Fan, T. N. Kalnes, M. Alward, J. Klinger, A. Sadehvandi, and D. R. Shonnard, "Life cycle assessment of electricity generation using fast pyrolysis bio-oil," *Renewable Energy,* vol. 36, pp. 632-641, 2// 2011.

[215] D. G. Christian, A. B. Riche, and N. E. Yates, "Growth, yield and mineral content of Miscanthus giganteus grown as a biofuel for 14 successive harvests," *Industrial Crops and Products,* vol. 28, pp. 320-327, 11// 2008.

[216] R. Pyter, E. Heaton, F. Dohleman, T. Voigt, and S. Long, "Agronomic Experiences with Miscanthus x giganteus in Illinois, USA," in *Biofuels*. vol. 581, J. R. Mielenz, Ed., ed: Humana Press, 2009, pp. 41-52.

[217] D. K. Lee, A. S. Parrish, and T. B. Voigt, "Switchgrass and Giant Miscanthus Agronomy," in *Engineering and Science of Biomass Feedstock Production and Provision*, Y. Shastri, A. Hansen, L. Rodríguez, and K. C. Ting, Eds., ed: Springer New York, 2014, pp. 37-59.

[218] DEFRA, "Planting and growing Miscanthus, Best Practice guide-lines, for Applications to DEFRA's Energy Crops Scheme," 2007.

[219] G. Behnke, M. David, and T. Voigt, "Greenhouse Gas Emissions, Nitrate Leaching, and Biomass Yields from Production of Miscanthus × giganteus in Illinois, USA," *BioEnergy Research*, vol. 5, pp. 801-813, 2012/12/01 2012.

[220] M. K. Kering, T. J. Butler, J. T. Biermacher, and J. A. Guretzky, "Biomass Yield and Nutrient Removal Rates of Perennial Grasses under Nitrogen Fertilization," *BioEnergy Research*, vol. 5, pp. 61-70, 2012/03/01 2012.

[221] M. Maughan, G. Bollero, D. K. Lee, R. Darmody, S. Bonos, L. Cortese, *et al.*, "Miscanthus × giganteus productivity: the effects of management in different environments," *GCB Bioenergy*, vol. 4, pp. 253-265, 2012.

[222] I. E. Palmer, R. J. Gehl, T. G. Ranney, D. Touchell, and N. George, "Biomass yield, nitrogen response, and nutrient uptake of perennial bioenergy grasses in North Carolina," *Biomass and Bioenergy*, vol. 63, pp. 218-228, 4// 2014.

[223] J. Hess, K. Kenney, L. Ovard, E. Searcy, and C. Wright, "Commodity-scale production of an infrastructure-compatible bulk solid from herbaceous lignocellulosic biomass," *Idaho National Laboratory, Idaho Falls, ID*, 2009.

[224] P. R. Adler, M. A. Sanderson, A. A. Boateng, P. J. Weimer, and H.-J. G. Jung, "Biomass Yield and Biofuel Quality of Switchgrass Harvested in Fall or Spring " *Agron. J.*, vol. 98, pp. 1518-1525, 2006/11 2006.

[225] I. Lewandowski and A. Heinz, "Delayed harvest of miscanthus—influences on biomass quantity and quality and environmental impacts of energy production," *European Journal of Agronomy*, vol. 19, pp. 45-63, 2003.

[226] J. Han, A. Elgowainy, J. B. Dunn, and M. Q. Wang, "Life cycle analysis of fuel production from fast pyrolysis of biomass," *Bioresource Technology*, vol. 133, pp. 421-428, 4// 2013.

[227] S. D. Wullschleger, E. B. Davis, M. E. Borsuk, C. A. Gunderson, and L. R. Lynd, "Biomass Production in Switchgrass across the United States: Database Description and Determinants of Yield " *Agron. J.*, vol. 102, pp. 1158-1168, 2010/7 2010.

[228] J. D. Berdahl, A. B. Frank, J. M. Krupinsky, P. M. Carr, J. D. Hanson, and H. A. Johnson, "Biomass yield, phenology, and survival of diverse switchgrass cultivars and experimental strains in western North Dakota," *Agronomy Journal*, vol. 97, pp. 549-555, 2005.

[229] J. Bouton, "Bioenergy Crop Breeding and Production Research in the Southeast. Final report for 1996 to 2001," ORNL/SUB-02-19XSV810C/012002.

[230] M. Casler and A. Boe, "Cultivar× environment interactions in switchgrass," *Crop Science,* vol. 43, pp. 2226-2233, 2003.

[231] M. D. Casler, K. P. Vogel, C. M. Taliaferro, and R. L. Wynia, "Latitudinal Adaptation of Switchgrass Populations " *Crop Sci.,* vol. 44, pp. 293-303, 2004/1 2004.

[232] K. A. Cassida, J. P. Muir, M. A. Hussey, J. C. Read, B. C. Venuto, and W. R. Ocumpaugh, "Biomass Yield and Stand Characteristics of Switchgrass in South Central U.S. Environments " *Crop Sci.,* vol. 45, pp. 673-681, 2005/3 2005.

[233] J. H. Fike, D. J. Parrish, D. D. Wolf, J. A. Balasko, J. T. Green Jr, M. Rasnake, *et al.*, "Long-term yield potential of switchgrass-for-biofuel systems," *Biomass and Bioenergy,* vol. 30, pp. 198-206, 3// 2006.

[234] J. R. Kiniry, M. A. Sanderson, J. R. Williams, C. R. Tischler, M. A. Hussey, W. R. Ocumpaugh, *et al.*, "Simulating Alamo Switchgrass with the ALMANAC Model," *Agron. J.,* vol. 88, pp. 602-606, 1996 1996.

[235] J. R. Kiniry, K. A. Cassida, M. A. Hussey, J. P. Muir, W. R. Ocumpaugh, J. C. Read, *et al.*, "Switchgrass simulation by the ALMANAC model at diverse sites in the southern US," *Biomass and Bioenergy,* vol. 29, pp. 419-425, 12// 2005.

[236] R. Lemus, E. C. Brummer, K. J. Moore, N. E. Molstad, C. L. Burras, and M. F. Barker, "Biomass yield and quality of 20 switchgrass populations in southern Iowa, USA," *Biomass and Bioenergy,* vol. 23, pp. 433-442, 12// 2002.

[237] J. P. Muir, M. A. Sanderson, W. R. Ocumpaugh, R. M. Jones, and R. L. Reed, "Biomass Production of 'Alamo' Switchgrass in Response to Nitrogen, Phosphorus, and Row Spacing " *Agron. J.,* vol. 93, pp. 896-901, 2001/7 2001.

[238] M. A. Sanderson, R. L. Reed, S. B. McLaughlin, S. D. Wullschleger, B. V. Conger, D. J. Parrish, *et al.*, "Switchgrass as a sustainable bioenergy crop," *Bioresource Technology,* vol. 56, pp. 83-93, 4// 1996.

[239] M. A. Sanderson, J. C. Read, and R. L. Reed, "Harvest Management of Switchgrass for Biomass Feedstock and Forage Production," *Agron. J.,* vol. 91, pp. 5-10, 1999 1999.

[240] M. A. Sanderson, R. L. Reed, W. R. Ocumpaugh, M. A. Hussey, G. Van Esbroeck, J. C. Read, *et al.*, "Switchgrass cultivars and germplasm for biomass feedstock production in Texas," *Bioresource Technology,* vol. 67, pp. 209-219, 3// 1999.

[241] M. A. Sanderson, R. R. Schnabel, W. S. Curran, W. L. Stout, D. Genito, and B. F. Tracy, "Switchgrass and Big Bluestem Hay, Biomass, and Seed Yield Response to Fire and Glyphosate Treatment," *Agron. J.,* vol. 96, pp. 1688-1692, 2004/11 2004.

[242] S. E. Sladden, D. I. Bransby, and G. E. Aiken, "Biomass yield, composition and production costs for eight switchgrass varieties in Alabama," *Biomass and Bioenergy*, vol. 1, pp. 119-122, // 1991.

[243] W. E. Thomason, W. R. Raun, G. V. Johnson, C. M. Taliaferro, K. W. Freeman, K. J. Wynn, *et al.*, "Switchgrass Response to Harvest Frequency and Time and Rate of Applied Nitrogen," *Journal of Plant Nutrition*, vol. 27, pp. 1199-1226, 2005/01/02 2005.

[244] D. M. Burner, T. L. Tew, J. J. Harvey, and D. P. Belesky, "Dry matter partitioning and quality of Miscanthus, Panicum, and Saccharum genotypes in Arkansas, USA," *Biomass and Bioenergy*, vol. 33, pp. 610-619, 4// 2009.

[245] J. L. Propheter and S. Staggenborg, "Performance of Annual and Perennial Biofuel Crops: Nutrient Removal during the First Two Years All rights reserved. No part of this periodical may be reproduced or transmitted in any form or by any means, electronic or mechanical, including photocopying, recording, or any information storage and retrieval system, without permission in writing from the publisher," *Agron. J.*, pp. 798-805, 2010.

[246] A. L. Teat, "Growth, Yield and Physiological Responses of the Bioenergy Crop Miscanthus × Giganteus To Fertilizer, Biochar and Drought.," 2014.

[247] Cecile De Klein, Rafael S.A. Novoa, Stephen Ogle, Keith A. Smith, Philippe Rochette, Thomas C. Wirth, *et al.*, "N2O emissions from managed soils and CO2 emissions from lime and urea application," in *IPCC Guidelines for National Greenhouse Gas Inventories*. vol. 4, Ch 11, ed: Intergovernmental Panel on Climate Change 2006.

[248] T. Dalgaard, N. Halberg, and J. R. Porter, "A model for fossil energy use in Danish agriculture used to compare organic and conventional farming," *Agriculture, Ecosystems & Environment*, vol. 87, pp. 51-65, 10// 2001.

[249] S. B. Jones, C. Valkenburg, C. W. Walton, D. C. Elliott, J. E. Holladay, D. J. Stevens, *et al.*, "Production of gasoline and diesel from biomass via fast pyrolysis, hydrotreating and hydrocracking: a design case," Pacific Northwest National Laboratory Richland, WA2009. http://www.pnl.gov/main/publications/external/technical_reports/pnnl-18284.pdf.

[250] S. Jones, P. Meyer, L. Snowden-Swan, A. Padmaperuma, E. Tan, A. Dutta, *et al.*, "Process Design and Economics for the Conversion of Lignocellulosic Biomass to Hydrocarbon Fuels: Fast Pyrolysis and Hydrotreating Bio-oil Pathway," National Renewable Energy Laboratory (NREL), Golden, CO.2013. http://www.pnnl.gov/main/publications/external/technical_reports/PNNL-23053.pdf.

[251] Z. Miao, T. E. Grift, A. C. Hansen, and K. C. Ting, "Energy requirement for comminution of biomass in relation to particle physical properties," *Industrial Crops and Products*, vol. 33, pp. 504-513, 3// 2011.

[252] S. A. Channiwala and P. P. Parikh, "A unified correlation for estimating HHV of solid, liquid and gaseous fuels," *Fuel*, vol. 81, pp. 1051-1063, 5// 2002.

[253] EURELECTRIC. (2003). *Efficiency in Electricity Generation*. Available: http://www.eurelectric.org/Download/Download.aspx?DocumentID=13549

[254] J. F. Peters, D. Iribarren, and J. Dufour, "Biomass Pyrolysis for Biochar or Energy Applications? A Life Cycle Assessment," *Environmental Science & Technology*, 2015/04/01 2015.

[255] D. A. Laird, "The Charcoal Vision: A Win–Win–Win Scenario for Simultaneously Producing Bioenergy, Permanently Sequestering Carbon, while Improving Soil and Water Quality " *Agron. J.*, vol. 100, pp. 178-181, 2008/1 2008.

[256] M. J. Bell and F. Worrall, "Charcoal addition to soils in NE England: A carbon sink with environmental co-benefits?," *Science of The Total Environment*, vol. 409, pp. 1704-1714, 4/1/ 2011.

[257] K. G. Roberts, B. A. Gloy, S. Joseph, N. R. Scott, and J. Lehmann, "Life Cycle Assessment of Biochar Systems: Estimating the Energetic, Economic, and Climate Change Potential," *Environmental Science & Technology*, vol. 44, pp. 827-833, 2010/01/15 2009.

[258] D. C. Elliott, T. R. Hart, G. G. Neuenschwander, L. J. Rotness, M. V. Olarte, A. H. Zacher, *et al.*, "Catalytic Hydroprocessing of Fast Pyrolysis Bio-oil from Pine Sawdust," *Energy & Fuels*, vol. 26, pp. 3891-3896, 2012/06/21 2012.

[259] R. J. French, J. Hrdlicka, and R. Baldwin, "Mild hydrotreating of biomass pyrolysis oils to produce a suitable refinery feedstock," *Environmental Progress & Sustainable Energy*, vol. 29, pp. 142-150, 2010.

[260] T. V. Choudhary and C. B. Phillips, "Renewable fuels via catalytic hydrodeoxygenation," *Applied Catalysis A: General*, vol. 397, pp. 1-12, 4/30/ 2011.

[261] M. Wang, J. Han, J. B. Dunn, H. Cai, and A. Elgowainy, "Well-to-wheels energy use and greenhouse gas emissions of ethanol from corn, sugarcane and cellulosic biomass for US use," *Environmental Research Letters*, vol. 7, p. 045905, 2012.

[262] S. Solomon, D. Qin, M. Manning, Z. Chen, M. Marquis, K. B. Averyt, *et al.*, "IPCC, 2007: Climate change 2007: The physical science basis," *Contribution of Working Group I to the fourth assessment report of the Intergovernmental Panel on Climate Change*, 2007.

[263] N. Jungbluth and R. Frischknecht, "Cumulative energy demand," *LCIA Implementation. Final report ecoinvent*, 2000.

[264] R. J. Plevin, J. Beckman, A. A. Golub, J. Witcover, and M. O'Hare, "Carbon Accounting and Economic Model Uncertainty of Emissions from Biofuels-Induced Land Use Change," *Environmental Science & Technology*, vol. 49, pp. 2656-2664, 2015/03/03 2015.

[265] H. Huo, M. Wang, C. Bloyd, and V. Putsche, "Life-cycle assessment of energy use and greenhouse gas emissions of soybean-derived biodiesel and renewable fuels," *Environmental science & technology,* vol. 43, pp. 750-756, 2009/02/01 2008.

[266] C. A. S. Hall, J. G. Lambert, and S. B. Balogh, "EROI of different fuels and the implications for society," *Energy Policy,* vol. 64, pp. 141-152, 1// 2014.

[267] J. G. Lambert, C. A. S. Hall, S. Balogh, A. Gupta, and M. Arnold, "Energy, EROI and quality of life," *Energy Policy,* vol. 64, pp. 153-167, 1// 2014.

[268] S. B. Jones, L. J. Snowden-Swan, P. A. Meyer, A. H. Zacher, M. V. Olarte, and C. Drennan, "Fast Pyrolysis and Hydrotreating: 2013 State of Technology R&D and Projections to 2017," Pacific Northwest National Laboratory (PNNL), Richland, WA (US)2014.

[269] ANL. The Greenhouse Gases, Regulated Emissions, and Energy Use in Transportation Model [Online]. Available: greet.es.anl.gov

[270] S. Mueller, J. Dunn, and M. Wang, "Carbon Calculator for Land-use Change from Biofuels Production (CCLUB)," *Contract No: ANL/ESD/12-5. Argonne National Laboratory (ANL), Chicago, IL,* 2012.

[271] J. Dunn, S. Mueller, H.-y. Kwon, and M. Wang, "Land-use change and greenhouse gas emissions from corn and cellulosic ethanol," *Biotechnology for Biofuels,* vol. 6, p. 51, 2013.

[272] B. Niblick, J. D. Monnell, X. Zhao, and A. E. Landis, "Using geographic information systems to assess potential biofuel crop production on urban marginal lands," *Applied Energy,* vol. 103, pp. 234-242, 3// 2013.

[273] T. N. Pham, T. Sooknoi, S. P. Crossley, and D. E. Resasco, "Ketonization of Carboxylic Acids: Mechanisms, Catalysts, and Implications for Biomass Conversion," *ACS Catalysis,* vol. 3, pp. 2456-2473, 2013/11/01 2013.

[274] S. A. Miller, A. E. Landis, and T. L. Theis, "Feature: Environmental trade-offs of biobased production," *Environmental science & technology,* vol. 41, pp. 5176-5182, 2007.

[275] K. Soratana, V. Khanna, and A. E. Landis, "Re-envisioning the renewable fuel standard to minimize unintended consequences: A comparison of microalgal diesel with other biodiesels," *Applied Energy,* vol. 112, pp. 194-204, 12// 2013.

[276] EPA, "Inventory of U.S. Greenhouse Gas Emissions and Sinks: 1990-2013," United States Environmental Protection Agency, Washington, DC2015.

[277] L. Tomlinson, "Introduction," in *Procedural Justice in the United Nations Framework Convention on Climate Change: Negotiating Fairness*, L. Tomlinson, Ed., ed Cham: Springer International Publishing, 2015, pp. 1-27.

[278] European Parliament & Council, "EC (2009) Directive 2009/28/EC of the European Parliament and of the Council of 23 April 2009 on the promotion of the use of energy from renewable sources and amending and subsequently repealing Directives 2001/77/EC and 2003/30/EC.," 2009.

[279] T. Damartzis and A. Zabaniotou, "Thermochemical conversion of biomass to second generation biofuels through integrated process design—A review," *Renewable and Sustainable Energy Reviews,* vol. 15, pp. 366-378, 1// 2011.

[280] D. C. Elliott, "Transportation fuels from biomass via fast pyrolysis and hydroprocessing," *Wiley Interdisciplinary Reviews: Energy and Environment,* vol. 2, pp. 525-533, 2013.

[281] S. De, B. Saha, and R. Luque, "Hydrodeoxygenation processes: Advances on catalytic transformations of biomass-derived platform chemicals into hydrocarbon fuels," *Bioresource Technology,* vol. 178, pp. 108-118, 2// 2015.

[282] D. A. Laird, R. C. Brown, J. E. Amonette, and J. Lehmann, "Review of the pyrolysis platform for coproducing bio-oil and biochar," *Biofuels, Bioproducts and Biorefining,* vol. 3, pp. 547-562, 2009.

[283] C. Somerville, H. Youngs, C. Taylor, S. C. Davis, and S. P. Long, "Feedstocks for Lignocellulosic Biofuels," *Science,* vol. 329, pp. 790-792, 2010.

[284] J. R. Regalbuto, "Cellulosic biofuels-got gasoline," *Science,* vol. 325, pp. 822-824, 2009.

[285] M. Peplow, "Cellulosic ethanol fights for life," *Nature,* vol. 507, pp. 152-153, 2014.

[286] R. A. Sheldon, "Green and sustainable manufacture of chemicals from biomass: state of the art," *Green Chemistry,* vol. 16, pp. 950-963, 2014.

[287] T. R. Brown, R. Thilakaratne, R. C. Brown, and G. Hu, "Techno-economic analysis of biomass to transportation fuels and electricity via fast pyrolysis and hydroprocessing," *Fuel,* vol. 106, pp. 463-469, 4// 2013.

[288] F. K. Kazi, J. A. Fortman, R. P. Anex, D. D. Hsu, A. Aden, A. Dutta, *et al.*, "Techno-economic comparison of process technologies for biochemical ethanol production from corn stover," *Fuel,* vol. 89, Supplement 1, pp. S20-S28, 11/1/ 2010.

[289] R. M. Swanson, A. Platon, J. A. Satrio, and R. C. Brown, "Techno-economic analysis of biomass-to-liquids production based on gasification," *Fuel,* vol. 89, Supplement 1, pp. S11-S19, 11/1/ 2010.

[290] Z. Yanan, H. Guiping, and C. B. Robert, "Life cycle assessment of the production of hydrogen and transportation fuels from corn stover via fast pyrolysis," *Environmental Research Letters,* vol. 8, p. 025001, 2013.

[291] G. G. Zaimes, K. Soratana, C. L. Harden, A. E. Landis, and V. Khanna, "Biofuels via Fast Pyrolysis of Perennial Grasses: A Life Cycle Evaluation of Energy Consumption and

Greenhouse Gas Emissions," *Environmental Science & Technology*, vol. 49, pp. 10007-10018, 2015/08/18 2015.

[292] J. F. Peters, D. Iribarren, and J. Dufour, "Biomass Pyrolysis for Biochar or Energy Applications? A Life Cycle Assessment," *Environmental Science & Technology*, vol. 49, pp. 5195-5202, 2015/04/21 2015.

[293] M. J. C. Van der Stelt, H. Gerhauser, J. H. A. Kiel, and K. J. Ptasinski, "Biomass upgrading by torrefaction for the production of biofuels: A review," *Biomass and bioenergy*, vol. 35, pp. 3748-3762, 2011.

[294] J. Meng, J. Park, D. Tilotta, and S. Park, "The effect of torrefaction on the chemistry of fast-pyrolysis bio-oil," *Bioresource Technology*, vol. 111, pp. 439-446, 5// 2012.

[295] D. E. Resasco and S. P. Crossley, "Implementation of concepts derived from model compound studies in the separation and conversion of bio-oil to fuel," *Catalysis Today*, vol. 257, Part 2, pp. 185-199, 11/15/ 2015.

[296] J. A. Herron, T. Vann, N. Duong, D. E. Resasco, S. Crossley, L. L. Lobban, *et al.*, "A Systems-Level Roadmap for Biomass Thermal Fractionation and Catalytic Upgrading Strategies," *Energy Technology*, pp. n/a-n/a, 2016.

[297] B. A. Wender, R. W. Foley, V. Prado-Lopez, D. Ravikumar, D. A. Eisenberg, T. A. Hottle, *et al.*, "Illustrating Anticipatory Life Cycle Assessment for Emerging Photovoltaic Technologies," *Environmental Science & Technology*, vol. 48, pp. 10531-10538, 2014/09/16 2014.

[298] B. Subramaniam, R. K. Helling, and C. J. Bode, "Quantitative sustainability analysis: A powerful tool to develop resource-efficient catalytic technologies," *ACS Sustainable Chemistry & Engineering*, 2016/09/05 2016.

[299] D. Carpenter, T. L. Westover, S. Czernik, and W. Jablonski, "Biomass feedstocks for renewable fuel production: a review of the impacts of feedstock and pretreatment on the yield and product distribution of fast pyrolysis bio-oils and vapors," *Green Chemistry*, vol. 16, pp. 384-406, 2014.

[300] D. Howe, T. Westover, D. Carpenter, D. Santosa, R. Emerson, S. Deutch, *et al.*, "Field-to-Fuel Performance Testing of Lignocellulosic Feedstocks: An Integrated Study of the Fast Pyrolysis–Hydrotreating Pathway," *Energy & Fuels*, vol. 29, pp. 3188-3197, 2015/05/21 2015.

[301] M. Hinchee, W. Rottmann, L. Mullinax, C. Zhang, S. Chang, M. Cunningham, *et al.*, "Short-rotation woody crops for bioenergy and biofuels applications," *In Vitro Cellular & Developmental Biology*, vol. 45, pp. 619-629, 08/2604/12/received07/24/accepted 2009.

[302] S. Njakou Djomo, A. Ac, T. Zenone, T. De Groote, S. Bergante, G. Facciotto, *et al.*, "Energy performances of intensive and extensive short rotation cropping systems for

woody biomass production in the EU," *Renewable and Sustainable Energy Reviews,* vol. 41, pp. 845-854, 1// 2015.

[303] G. Berhongaray, O. El Kasmioui, and R. Ceulemans, "Comparative analysis of harvesting machines on an operational high-density short rotation woody crop (SRWC) culture: One-process versus two-process harvest operation," *Biomass and Bioenergy,* vol. 58, pp. 333-342, 11// 2013.

[304] S. Njakou Djomo, O. El Kasmioui, T. De Groote, L. S. Broeckx, M. S. Verlinden, G. Berhongaray, *et al.*, "Energy and climate benefits of bioelectricity from low-input short rotation woody crops on agricultural land over a two-year rotation," *Applied Energy,* vol. 111, pp. 862-870, 11// 2013.

[305] A. A. Rentizelas, A. J. Tolis, and I. P. Tatsiopoulos, "Logistics issues of biomass: The storage problem and the multi-biomass supply chain," *Renewable and Sustainable Energy Reviews,* vol. 13, pp. 887-894, 5// 2009.

[306] I. Bonner, M. Delwiche, L. Wendt, W. Smith, and K. Kenney, "A Laboratory Scale Reactor for Simulating Biomass Storage for Bioenergy," p. 1.

[307] J. Tumuluru, C. Lim, X. Bi, X. Kuang, S. Melin, F. Yazdanpanah, *et al.*, "Analysis on Storage Off-Gas Emissions from Woody, Herbaceous, and Torrefied Biomass," *Energies,* vol. 8, p. 1745, 2015.

[308] A. Roedl, "Production and energetic utilization of wood from short rotation coppice—a life cycle assessment," *The International Journal of Life Cycle Assessment,* vol. 15, pp. 567-578, 2010// 2010.

[309] T. W. Hertel, A. A. Golub, A. D. Jones, M. O'Hare, R. J. Plevin, and D. M. Kammen, "Effects of US Maize Ethanol on Global Land Use and Greenhouse Gas Emissions: Estimating Market-mediated Responses," *BioScience,* vol. 60, pp. 223-231, 2010.

[310] D. I. Dickmann, "Silviculture and biology of short-rotation woody crops in temperate regions: Then and now," *Biomass and Bioenergy,* vol. 30, pp. 696-705, 2006.

[311] A. Plus, "V8.4," *Aspen Technology Inc., Cambridge, MA,* 2013.

[312] D. E. Resasco and S. P. Crossley, "Implementation of concepts derived from model compound studies in the separation and conversion of bio-oil to fuel," *Catalysis Today,* 2014.

[313] H. Y. Zhao, D. Li, P. Bui, and S. T. Oyama, "Hydrodeoxygenation of guaiacol as model compound for pyrolysis oil on transition metal phosphide hydroprocessing catalysts," *Applied Catalysis A: General,* vol. 391, pp. 305-310, 2011.

[314] Daniel E. Resasco, Steven P. Crossley, and L. Lobban, "Carbon Hydrogen And Separation Efficiency (CHASE) Project," U. S. D. o. Enegry, Ed., ed. University of Oklahoma, OK., 2015.

[315] A. Corma, O. de la Torre, and M. Renz, "Production of high quality diesel from cellulose and hemicellulose by the Sylvan process: catalysts and process variables," *Energy & Environmental Science,* vol. 5, pp. 6328-6344, 2012.

[316] Q. Deng, P. Han, J. Xu, J.-J. Zou, L. Wang, and X. Zhang, "Highly controllable and selective hydroxyalkylation/alkylation of 2-methylfuran with cyclohexanone for synthesis of high-density biofuel," *Chemical Engineering Science,* vol. 138, pp. 239-243, 12/22/ 2015.

[317] J. Donnelly, R. Horton, K. Gopalan, C. D. Bannister, and C. J. Chuck, "Branched Ketone Biofuels as Blending Agents for Jet-A1 Aviation Kerosene," *Energy & Fuels,* vol. 30, pp. 294-301, 2016/01/21 2016.

[318] D. Santhanaraj, M. R. Rover, D. E. Resasco, R. C. Brown, and S. Crossley, "Gluconic acid from biomass fast pyrolysis oils: specialty chemicals from the thermochemical conversion of biomass," *ChemSusChem,* vol. 7, pp. 3132-3137, 2014.

[319] M. L. Cayuela, M. A. Sánchez-Monedero, A. Roig, K. Hanley, A. Enders, and J. Lehmann, "Biochar and denitrification in soils: when, how much and why does biochar reduce N2O emissions?," *Scientific Reports,* vol. 3, p. 1732, 04/25/online 2013.

[320] D. L. Jones, J. Rousk, G. Edwards-Jones, T. H. DeLuca, and D. V. Murphy, "Biochar-mediated changes in soil quality and plant growth in a three year field trial," *Soil Biology and Biochemistry,* vol. 45, pp. 113-124, 2// 2012.

[321] J. M. Novak, W. J. Busscher, D. L. Laird, M. Ahmedna, D. W. Watts, and M. A. S. Niandou, "Impact of Biochar Amendment on Fertility of a Southeastern Coastal Plain Soil," *Soil Science,* vol. 174, 2009.

[322] L. Van Zwieten, S. Kimber, S. Morris, K. Y. Chan, A. Downie, J. Rust, *et al.*, "Effects of biochar from slow pyrolysis of papermill waste on agronomic performance and soil fertility," *Plant and Soil,* vol. 327, pp. 235-246, 2009// 2009.

[323] J. Lehmann, M. C. Rillig, J. Thies, C. A. Masiello, W. C. Hockaday, and D. Crowley, "Biochar effects on soil biota – A review," *Soil Biology and Biochemistry,* vol. 43, pp. 1812-1836, 9// 2011.

[324] D. D. Warnock, J. Lehmann, T. W. Kuyper, and M. C. Rillig, "Mycorrhizal responses to biochar in soil – concepts and mechanisms," *Plant and Soil,* vol. 300, pp. 9-20, 2007// 2007.

[325] A. Enders, K. Hanley, T. Whitman, S. Joseph, and J. Lehmann, "Characterization of biochars to evaluate recalcitrance and agronomic performance," *Bioresource Technology,* vol. 114, pp. 644-653, 6// 2012.

[326] P. Grammelis, G. Skodras, and E. Kakaras, "An economic and environmental assessment of biomass utilization in lignite-fired power plants of Greece," *International Journal of Energy Research,* vol. 30, pp. 763-775, 2006.

[327] F. ter Veld, "Beyond the Fossil Fuel Era: On the Feasibility of Sustainable Electricity Generation Using Biogas from Microalgae," *Energy & Fuels*, vol. 26, pp. 3882-3890, 2012/06/21 2012.

[328] S. Siegl, M. Laaber, and P. Holubar, "Green Electricity From Biomass, Part I: Environmental Impacts of Direct Life Cycle Emissions," *Waste and Biomass Valorization*, vol. 2, pp. 267-284, 2011// 2011.

[329] D. Dressler, A. Loewen, and M. Nelles, "Life cycle assessment of the supply and use of bioenergy: impact of regional factors on biogas production," *The International Journal of Life Cycle Assessment*, vol. 17, pp. 1104-1115, 2012// 2012.

[330] S. Muench and E. Guenther, "A systematic review of bioenergy life cycle assessments," *Applied Energy*, vol. 112, pp. 257-273, 12// 2013.

[331] T. F. Stocker, D. Qin, G. K. Plattner, M. Tignor, S. K. Allen, J. Boschung, *et al.*, "IPCC, 2013: climate change 2013: the physical science basis. Contribution of working group I to the fifth assessment report of the intergovernmental panel on climate change," 2013.

[332] Cumulative Energy Demand, "Terms, definitions, methods of calculation," *Association of German Engineers*, 1997.

[333] U. S. Uslci, "Life Cycle Inventory Database," *National Renewable Energy Laboratory*, 2012.

[334] E. Center, "Ecoinvent data v2. 2," *Swiss Centre for Life Cycle Inventories*, vol. 529, 2014.

[335] A. B. Bindwal and P. D. Vaidya, "Kinetics of Aqueous-Phase Hydrogenation of Levoglucosan over Ru/C Catalyst," *Industrial & Engineering Chemistry Research*, vol. 52, pp. 17781-17789, 2013/12/18 2013.

[336] M. Wang, H. Huo, and S. Arora, "Methods of dealing with co-products of biofuels in life-cycle analysis and consequent results within the U.S. context," *Energy Policy*, vol. 39, pp. 5726-5736, 10// 2011.

[337] EPA, "Regulation of Fuels and Fuel Additives: Changes to Renewable Fuel Standard Program; Final Rule," vol. EPA–HQ–OAR–2005–01612010, U. S. E. P. Agency, Ed., ed, pp. 14669–15320.

[338] P. Parthasarathy and K. S. Narayanan, "Hydrogen production from steam gasification of biomass: Influence of process parameters on hydrogen yield–A review," *Renewable Energy*, vol. 66, pp. 570-579, 2014.

[339] G. G. Zaimes, N. Vora, S. S. Chopra, A. E. Landis, and V. Khanna, "Design of Sustainable Biofuel Processes and Supply Chains: Challenges and Opportunities," *Processes*, vol. 3, pp. 634-663, 2015.

[340] J. J. Bozell and G. R. Petersen, "Technology development for the production of biobased products from biorefinery carbohydrates-the US Department of Energy's "Top 10" revisited," *Green Chemistry,* vol. 12, pp. 539-554, 2010.

[341] I. T. Horvath, H. Mehdi, V. Fabos, L. Boda, and L. T. Mika, "[gamma]-Valerolactone-a sustainable liquid for energy and carbon-based chemicals," *Green Chemistry,* vol. 10, pp. 238-242, 2008.

[342] B. G. Hermann, K. Blok, and M. K. Patel, "Producing Bio-Based Bulk Chemicals Using Industrial Biotechnology Saves Energy and Combats Climate Change," *Environmental Science & Technology,* vol. 41, pp. 7915-7921, 2007/11/01 2007.

[343] M. J. Biddy, R. Davis, D. Humbird, L. Tao, N. Dowe, M. T. Guarnieri, *et al.*, "The Techno-Economic Basis for Coproduct Manufacturing To Enable Hydrocarbon Fuel Production from Lignocellulosic Biomass," *ACS Sustainable Chemistry & Engineering,* 2016/04/27 2016.

[344] M. Lapuerta, M. Villajos, J. R. Agudelo, and A. L. Boehman, "Key properties and blending strategies of hydrotreated vegetable oil as biofuel for diesel engines," *Fuel Processing Technology,* vol. 92, pp. 2406-2411, 2011.

[345] D. Darnoko and M. Cheryan, "Kinetics of palm oil transesterification in a batch reactor," *Journal of the American Oil Chemists' Society,* vol. 77, pp. 1263-1267, 2000.

[346] L. Nie and D. E. Resasco, "Kinetics and mechanism of m-cresol hydrodeoxygenation on a Pt/SiO2 catalyst," *Journal of Catalysis,* vol. 317, pp. 22-29, 8// 2014.

[347] J. Guretzky, J. Biermacher, B. Cook, M. Kering, and J. Mosali, "Switchgrass for forage and bioenergy: harvest and nitrogen rate effects on biomass yields and nutrient composition," *Plant and Soil,* vol. 339, pp. 69-81, 2011/02/01 2011.

[348] G. Vicente, A. Coteron, M. Martinez, and J. Aracil, "Application of the factorial design of experiments and response surface methodology to optimize biodiesel production," *Industrial crops and products,* vol. 8, pp. 29-35, 1998.

[349] S. Surendran Nair, S. Kang, X. Zhang, F. E. Miguez, R. C. Izaurralde, W. M. Post, *et al.*, "Bioenergy crop models: descriptions, data requirements, and future challenges," *GCB Bioenergy,* vol. 4, pp. 620-633, 2012.

[350] Y. Yin, X. Zhang, D. Lin, H. Yu, J. a. Wang, and P. Shi, "GEPIC-V-R model: A GIS-based tool for regional crop drought risk assessment," *Agricultural Water Management,* vol. 144, pp. 107-119, 10// 2014.

[351] A. Plus, "Aspen Technology," *Inc., version,* vol. 11, 2009.

[352] R. P. Anex, A. Aden, F. K. Kazi, J. Fortman, R. M. Swanson, M. M. Wright, *et al.*, "Techno-economic comparison of biomass-to-transportation fuels via pyrolysis,

gasification, and biochemical pathways," *Fuel*, vol. 89, Supplement 1, pp. S29-S35, 11/1/ 2010.

[353] D. J. Garcia and F. You, "Supply chain design and optimization: Challenges and opportunities," *Computers & Chemical Engineering*, 2015.

[354] G. C. Daily, S. Polasky, J. Goldstein, P. M. Kareiva, H. A. Mooney, L. Pejchar, *et al.*, "Ecosystem services in decision making: time to deliver," *Frontiers in Ecology and the Environment*, vol. 7, pp. 21-28, 2009.

[355] B. Neupane, A. Halog, and R. J. Lilieholm, "Environmental sustainability of wood-derived ethanol: a life cycle evaluation of resource intensity and emissions in Maine, USA," *Journal of Cleaner Production*, vol. 44, pp. 77-84, 4// 2013.

[356] G. G. Zaimes and V. Khanna, "Assessing the Critical Role of Ecological Goods and Services In Microalgal Biofuel Life Cycles," *RSC Advances*, 2014.

[357] R. Costanza, R. d'Arge, R. de Groot, S. Farber, M. Grasso, B. Hannon, *et al.*, "The value of the world's ecosystem services and natural capital," *Nature*, vol. 387, pp. 253-260, 05/15/print 1997.

[358] R. Costanza, R. d'Arge, R. de Groot, S. Farber, M. Grasso, B. Hannon, *et al.*, "The value of ecosystem services: putting the issues in perspective," *Ecological Economics*, vol. 25, pp. 67-72, 4// 1998.

[359] S. C. Farber, R. Costanza, and M. A. Wilson, "Economic and ecological concepts for valuing ecosystem services," *Ecological Economics*, vol. 41, pp. 375-392, 6// 2002.

[360] R. C. Izaurralde, W. B. McGill, and J. R. Williams, "Development and application of the EPIC model for carbon cycle, greenhouse-gas mitigation, and biofuel studies," Pacific Northwest National Laboratory (PNNL), Richland, WA (US)2012.

[361] P. W. Gassman, M. R. Reyes, C. H. Green, and J. G. Arnold, "Soil and Water Assessment Tool: Historical Development, Applications, and Future Research Directions, The," 2007.

[362] X. Wang, P. W. Gassman, J. R. Williams, S. Potter, and A. R. Kemanian, "Modeling the impacts of soil management practices on runoff, sediment yield, maize productivity, and soil organic carbon using APEX," *Soil and Tillage Research*, vol. 101, pp. 78-88, 2008.

[363] H. T. Tallis, T. Ricketts, A. D. Guerry, S. A. Wood, R. Sharp, E. Nelson, *et al.*, "InVEST 2.2. 0 user's guide," *The Natural Capital Project, Stanford*, 2011.

[364] B. R. Bakshi, "Methods and tools for sustainable process design," *Current Opinion in Chemical Engineering*, vol. 6, pp. 69-74, 11// 2014.

[365] B. R. Bakshi, G. Ziv, and M. D. Lepech, "Techno-Ecological Synergy: A Framework for Sustainable Engineering," *Environmental Science & Technology*, vol. 49, pp. 1752-1760, 2015/02/03 2015.

[366] Y. Yang, J. Bae, J. Kim, and S. Suh, "Replacing gasoline with corn ethanol results in significant environmental problem-shifting," *Environmental science & technology*, vol. 46, pp. 3671-3678, 2012.

[367] G. E. Merva, *Physio-engineering Principles*. Westport,CT: AVI Publishing Company, 1975.

[368] J. G. Cogley, "The Albedo of Water as a Function of Latitude," *Monthly Weather Review*, vol. 107, pp. 775-781, 1979/06/01 1979.

[369] D. Krassen. GreenFuel Technologies: A Case Study for Industrial Photosynthetic Energy Capture. Available: http://www.ecolo.org/documents/documents_in_english/biofuels-Algae-CaseStudy-09.pdf

[370] Farm and Rach Irrigation Survey (2008), "2007 Census of Agriculture," U.S. Department of Agriculture, Ed., ed.

[371] O. W. Golueke CG, "Harvesting and processing sewage gorwn plaktonic algae," 1965.

[372] P. k. Swamee, Jain, A.K., "Explicit equations for pipe-flow problems," *Journal of the Hydraulics Division*, 1976.

[373] A. Converti, A. A. Casazza, E. Y. Ortiz, P. Perego, and M. Del Borghi, "Effect of temperature and nitrogen concentration on the growth and lipid content of Nannochloropsis oculata and Chlorella vulgaris for biodiesel production," *Chemical Engineering and Processing: Process Intensification*, vol. 48, pp. 1146-1151, 2009.

[374] A. M. Illman, A. H. Scragg, and S. W. Shales, "Increase in Chlorella strains calorific values when grown in low nitrogen medium," *Enzyme and Microbial Technology*, vol. 27, pp. 631-635, 2000.

[375] K. J. Flynn, J. L. Garrido, M. Zapata, H. Öpik, and C. R. Hipkin, "Changes in fatty acids, amino acids and carbon/nitrogen biomass during nitrogen starvation of ammonium- and nitrate-grownIsochrysis galbana," *Journal of Applied Phycology*, vol. 4, pp. 95-104, 1992/06/01 1992.

[376] L. Lardon, A. Helias, B. Sialve, J.-P. Steyer, and O. Bernard, "Life-Cycle Assessment of Biodiesel Production from Microalgae," *Environmental Science & Technology*, p. 7, 2009.

[377] A. A. Acquaye, T. Wiedmann, K. S. Feng, R. H. Crawford, J. Barrett, J. Kuylenstierna, *et al.*, "Identification of 'carbon hot-spots' and quantification of GHG intensities in the biodiesel supply chain using hybrid LCA and structural path analysis," *Environmental Science & Technology*, vol. 45, pp. 2471-2478, Mar 2011.

[378] A. Baral and B. R. Bakshi, "Thermodynamic Metrics for Aggregation of Natural Resources in Life Cycle Analysis: Insight via Application to Some Transportation Fuels," *Environmental Science & Technology*, vol. 44, pp. 800-807, 2010/01/15 2009.

[379] Energy Information Agency. *Average Price by State by Provider (EIA-861)*. Available: http://www.eia.gov/electricity/data/state/

[380] Energy Information Agency. *United States Natural Gas Industrial Price*. Available: http://www.eia.gov/dnav/ng/hist/n3035us3a.htm

[381] United States Environmental Protection Agency. (2000). *Wastewater Technology Fact Sheet Chemical Precipitation*. Available: http://water.epa.gov/scitech/wastetech/upload/2002_06_28_mtb_chemical_precipitation.pdf

[382] U.S. Department of Agriculture. *National agricultural statistics service, agricultural prices*. Available: http://usda.mannlib.cornell.edu/MannUsda/viewDocumentInfo.do?documentID=1002

[383] N. M. Stone, *Renovating leaky ponds*: Southern Regional Aquaculture Center, 1999.

[384] E. Molina Grima, E.-H. Belarbi, F. Acién Fernández, A. Robles Medina, and Y. Chisti, "Recovery of microalgal biomass and metabolites: process options and economics," *Biotechnology Advances,* vol. 20, pp. 491-515, 2003.

[385] Y. Gao, C. Gregor, Y. Liang, D. Tang, and C. Tweed, "Algae biodiesel-a feasibility report," *Chemistry Central Journal*, vol. 6, pp. 1-16, 2012.

[386] M. M. Wright, D. E. Daugaard, J. A. Satrio, and R. C. Brown, "Techno-economic analysis of biomass fast pyrolysis to transportation fuels," *Fuel,* vol. 89, pp. S2-S10, 2010.

[387] A. Baral, B. R. Bakshi, and R. L. Smith, "Assessing resource intensity and renewability of cellulosic ethanol technologies using Eco-LCA," *Environmental Science & Technology*, 2012.

[388] Energy Information Agency. *U.S. Weekly Heating Oil and Propane Prices*. Available: http://www.eia.gov/dnav/pet/pet_pri_wfr_dcus_nus_m.htm

[389] J. Szargut, D. R. Morris, and F. R. Steward, "Energy analysis of thermal, chemical, and metallurgical processes," 1988.

[390] W. A. Hermann, "Quantifying global exergy resources," *Energy,* vol. 31, pp. 1685-1702, 2006.

[391] J. Szargut, *Exergy method: technical and ecological applications* vol. 18: WIT press, 2005.

[392] P. Nixon and M. Bullard, "Planting and growing Miscanthus, best practice guidelines," ed: Department for Environmental, Food & Rural Affairs (DEFRA) Publications, 2001.

[393] D. Styles and M. B. Jones, "Miscanthus and willow heat production—An effective land-use strategy for greenhouse gas emission avoidance in Ireland?," *Energy Policy,* vol. 36, pp. 97-107, 1// 2008.

[394] E. M. W. Smeets, I. M. Lewandowski, and A. P. C. Faaij, "The economical and environmental performance of miscanthus and switchgrass production and supply chains in a European setting," *Renewable and Sustainable Energy Reviews,* vol. 13, pp. 1230-1245, 8// 2009.

[395] S. Fazio and A. Monti, "Life cycle assessment of different bioenergy production systems including perennial and annual crops," *Biomass and Bioenergy,* vol. 35, pp. 4868-4878, 12// 2011.

[396] Y. Bai, L. Luo, and E. van der Voet, "Life cycle assessment of switchgrass-derived ethanol as transport fuel," *The International Journal of Life Cycle Assessment,* vol. 15, pp. 468-477, 2010/06/01 2010.

[397] D. J. Parrish and J. H. Fike, "The Biology and Agronomy of Switchgrass for Biofuels," *Critical Reviews in Plant Sciences,* vol. 24, pp. 423-459, 2005/09/01 2005.

[398] A. D. Halvorson and S. J. Del Grosso, "Nitrogen Source and Placement Effects on Soil Nitrous Oxide Emissions from No-Till Corn," *J. Environ. Qual.,* vol. 41, pp. 1349-1360, 2012/9 2012.

[399] A. F. Bouwman, L. J. M. Boumans, and N. H. Batjes, "Modeling global annual N2O and NO emissions from fertilized fields," *Global Biogeochemical Cycles,* vol. 16, p. 1080, 2002.

[400] M. A. A. Adviento-Borbe, M. L. Haddix, D. L. Binder, D. T. Walters, and A. Dobermann, "Soil greenhouse gas fluxes and global warming potential in four high-yielding maize systems," *Global Change Biology,* vol. 13, pp. 1972-1988, 2007.

[401] M. H. Chantigny, P. Rochette, D. A. Angers, S. Bittman, K. Buckley, D. Massé, *et al.*, "Soil Nitrous Oxide Emissions Following Band-Incorporation of Fertilizer Nitrogen and Swine Manure " *J. Environ. Qual.,* vol. 39, pp. 1545-1553, 2010/9 2010.

[402] A. D. Halvorson, S. J. Del Grosso, and C. A. Reule, "Nitrogen, Tillage, and Crop Rotation Effects on Nitrous Oxide Emissions from Irrigated Cropping Systems " *J. Environ. Qual.,* vol. 37, pp. 1337-1344, 2008/7 2008.

[403] A. D. Halvorson, S. J. Del Grosso, and F. Alluvione, "Tillage and Inorganic Nitrogen Source Effects on Nitrous Oxide Emissions from Irrigated Cropping Systems " *Soil Sci. Soc. Am. J.,* vol. 74, pp. 436-445, 2010/3 2010.

[404] A. D. Halvorson, S. J. Del Grosso, and C. P. Jantalia, "Nitrogen Source Effects on Soil Nitrous Oxide Emissions from Strip-Till Corn," *J. Environ. Qual.,* vol. 40, pp. 1775-1786, 2011/11 2011.

[405] C. Wagner-Riddle, A. Furon, N. L. McLaughlin, I. Lee, J. Barbeau, S. Jayasundara, *et al.*, "Intensive measurement of nitrous oxide emissions from a corn–soybean–wheat rotation under two contrasting management systems over 5 years," *Global Change Biology,* vol. 13, pp. 1722-1736, 2007.

[406] R. T. Venterea, M. Bijesh, and M. S. Dolan, "Fertilizer Source and Tillage Effects on Yield-Scaled Nitrous Oxide Emissions in a Corn Cropping System," *J. Environ. Qual.*, vol. 40, pp. 1521-1531, 2011/9 2011.

[407] S. J. Del Grosso, A. D. Halvorson, and W. J. Parton, "Testing DAYCENT Model Simulations of Corn Yields and Nitrous Oxide Emissions in Irrigated Tillage Systems in Colorado " *J. Environ. Qual.*, vol. 37, pp. 1383-1389, 2008/7 2008.

[408] K. R. Sistani, M. Jn-Baptiste, N. Lovanh, and K. L. Cook, "Atmospheric Emissions of Nitrous Oxide, Methane, and Carbon Dioxide from Different Nitrogen Fertilizers," *J. Environ. Qual.*, vol. 40, pp. 1797-1805, 2011/11 2011.

[409] S. Haile-Mariam, H. P. Collins, and S. S. Higgins, "Greenhouse Gas Fluxes from an Irrigated Sweet Corn (Zea mays L.)–Potato (Solanum tuberosum L.) Rotation " *J. Environ. Qual.*, vol. 37, pp. 759-771, 2008/5 2008.

[410] M. J. Eichner, "Nitrous Oxide Emissions from Fertilized Soils: Summary of Available Data," *J. Environ. Qual.*, vol. 19, pp. 272-280, 1990 1990.

[411] W. Seiler and R. Conrad, "Field Measurements of Natural and Fertilizer-Induced N2O Release Rates from Soils," *Journal of the Air Pollution Control Association*, vol. 31, pp. 767-772, 1981/07/01 1981.

[412] F. C. Thornton and R. J. Valente, "Soil Emissions of Nitric Oxide and Nitrous Oxide from No-till Corn," *Soil Sci. Soc. Am. J.*, vol. 60, pp. 1127-1133, 1996 1996.

[413] U. Skiba, K. J. Hargreaves, I. J. Beverland, D. H. O'Neill, D. Fowler, and J. B. Moncrieff, "Measurement of Field Scale N2O Emission Fluxes from a Wheat Crop Using Micrometeorological Techniques," in *Progress in Nitrogen Cycling Studies*. vol. 68, O. Van Cleemput, G. Hofman, and A. Vermoesen, Eds., ed: Springer Netherlands, 1996, pp. 627-632.

[414] G. Benckiser, R. Eilts, A. Linn, H. J. Lorch, E. Sümer, A. Weiske, *et al.*, "N2O emissions from different cropping systems and from aerated, nitrifying and denitrifying tanks of a municipal waste water treatment plant," *Biology and Fertility of Soils*, vol. 23, pp. 257-265, 1996/10/01 1996.

[415] G. Hutchinson and E. Brams, "NO versus N2O emissions from an NH4+-amended Bermuda grass pasture," *Journal of Geophysical Research: Atmospheres (1984–2012)*, vol. 97, pp. 9889-9896, 1992.

[416] E. Williams, G. Hutchinson, and F. Fehsenfeld, "NOx and N2O emissions from soil," *Global Biogeochemical Cycles*, vol. 6, pp. 351-388, 1992.

[417] A. R. Mosier, W. D. Guenzi, and E. E. Schweizer, "Soil Losses of Dinitrogen and Nitrous Oxide from Irrigated Crops in Northeastern Colorado," *Soil Sci. Soc. Am. J.*, vol. 50, pp. 344-348, 1986 1986.

[418] A. R. Mosier and G. L. Hutchinson, "Nitrous Oxide Emissions From Cropped Fields," *J. Environ. Qual.*, vol. 10, pp. 169-173, 1981 1981.

[419] J. M. Bremner, G. A. Breitenbeck, and A. M. Blackmer, "Effect of Anhydrous Ammonia Fertilization on Emission of Nitrous Oxide from Soils1," *J. Environ. Qual.*, vol. 10, pp. 77-80, 1981 1981.

[420] J. H. Qian, J. W. Doran, K. L. Weier, A. R. Mosier, T. A. Peterson, and J. F. Power, "Soil Denitrification and Nitrous Oxide Losses under Corn Irrigated with High-Nitrate Groundwater," *J. Environ. Qual.*, vol. 26, pp. 348-360, 1997 1997.

[421] A. Vermoesen, C.-J. de Groot, L. Nollet, P. Boeckx, and O. van Cleemput, "Effect of ammonium and nitrate application on the NO and N2O emission out of different soils," in *Progress in Nitrogen Cycling Studies*. vol. 68, O. Van Cleemput, G. Hofman, and A. Vermoesen, Eds., ed: Springer Netherlands, 1996, pp. 645-654.

[422] M. F. Shepherd, S. Barzetti, and D. R. Hastie, "The production of atmospheric NOx and N2O from a fertilized agricultural soil," *Atmospheric Environment. Part A. General Topics*, vol. 25, pp. 1961-1969, // 1991.

[423] A. Bouwman, K. Van der Hoek, and J. Olivier, "Uncertainties in the global source distribution of nitrous oxide," *Journal of Geophysical Research: Atmospheres (1984–2012)*, vol. 100, pp. 2785-2800, 1995.

[424] I. C. Anderson and J. S. Levine, "Simultaneous field measurements of biogenic emissions of nitric oxide and nitrous oxide," *Journal of Geophysical Research: Atmospheres (1984–2012)*, vol. 92, pp. 965-976, 1987.

[425] D. K. Lee, S. D. S. University, and S. G. Initiative, *Composition of Herbaceous Biomass Feedstocks*: North Central Sun Grant Center, South Dakota State University, 2007.

[426] Phyllis2. *Database for biomass and waste, Energy research Centre of the Netherlands.* Available: www.ecn.nl/phyllis2

[427] F. Melligan, R. Auccaise, E. Novotny, J. Leahy, M. Hayes, and W. Kwapinski, "Pressurised pyrolysis of Miscanthus using a fixed bed reactor," *Bioresource technology*, vol. 102, pp. 3466-3470, 2011.

[428] S. Oh, H. Hwang, H. S. Choi, and J. W. Choi, "The effects of noble metal catalysts on the bio-oil quality during the hydrodeoxygenative upgrading process," *Fuel*, vol. 153, pp. 535-543, 8/1/ 2015.

[429] P. M. Mortensen, J. D. Grunwaldt, P. A. Jensen, K. G. Knudsen, and A. D. Jensen, "A review of catalytic upgrading of bio-oil to engine fuels," *Applied Catalysis A: General*, vol. 407, pp. 1-19, 11/4/ 2011.

[430] J. Wildschut, F. H. Mahfud, R. H. Venderbosch, and H. J. Heeres, "Hydrotreatment of Fast Pyrolysis Oil Using Heterogeneous Noble-Metal Catalysts," *Industrial & Engineering Chemistry Research*, vol. 48, pp. 10324-10334, 2009/12/02 2009.

[431] W. Baldauf, U. Balfanz, and M. Rupp, "Upgrading of flash pyrolysis oil and utilization in refineries," *Biomass and Bioenergy*, vol. 7, pp. 237-244, // 1994.

[432] Y.-H. E. Sheu, R. G. Anthony, and E. J. Soltes, "Kinetic studies of upgrading pine pyrolytic oil by hydrotreatment," *Fuel Processing Technology*, vol. 19, pp. 31-50, 7// 1988.

[433] A. Gutierrez, R. K. Kaila, M. L. Honkela, R. Slioor, and A. O. I. Krause, "Hydrodeoxygenation of guaiacol on noble metal catalysts," *Catalysis Today*, vol. 147, pp. 239-246, 10/15/ 2009.

[434] R. H. Venderbosch, A. R. Ardiyanti, J. Wildschut, A. Oasmaa, and H. J. Heeres, "Stabilization of biomass-derived pyrolysis oils," *Journal of Chemical Technology & Biotechnology*, vol. 85, pp. 674-686, 2010.

[435] D. C. Elliott, H. Wang, M. Rover, L. Whitmer, R. Smith, and R. Brown, "Hydrocarbon Liquid Production via Catalytic Hydroprocessing of Phenolic Oils Fractionated from Fast Pyrolysis of Red Oak and Corn Stover," *ACS Sustainable Chemistry & Engineering*, vol. 3, pp. 892-902, 2015/05/04 2015.

[436] D. R. Parapati, V. K. Guda, V. K. Penmetsa, P. H. Steele, and S. K. Tanneru, "Single stage hydroprocessing of pyrolysis oil in a continuous packed-bed reactor," *Environmental Progress & Sustainable Energy*, vol. 33, pp. 726-731, 2014.

[437] O. D. Mante, F. A. Agblevor, S. T. Oyama, and R. McClung, "The influence of recycling non-condensable gases in the fractional catalytic pyrolysis of biomass," *Bioresource Technology*, vol. 111, pp. 482-490, 5// 2012.